DETERMINATION OF ACCEPTANCE CRITERIA FOR PRESTRESSING STRAND IN PRE-TENSIONED APPLICATIONS

by

THOMAIDA POLYDOROU

B.S., Kansas State University, 2009
M.S., Kansas State University, 2011

AN ABSTRACT OF A DISSERTATION

submitted in partial fulfillment of the requirements for the degree

DOCTOR OF PHILOSOPHY

Department of Civil Engineering
College of Engineering

KANSAS STATE UNIVERSITY
Manhattan, Kansas

2014

Abstract

ASTM recently adopted the Standard Test Method for Evaluating Bond of Seven-Wire Steel Prestressing Strand as ASTM A1081, a pull-out test procedure developed for verifying the ability of steel strands to bond to cementitious materials prior to their use as tensile reinforcement in prestressed concrete sections. The required by ASTM International precision and bias statement has not been developed for this test method. In addition, a minimum threshold value that will ensure only adequately bonding strand sources will be accepted has not yet been applied to ASTM A1081. The test method was developed after findings that prestressing steel strand sources of identical type and grade vary significantly as far as their bonding capacity. Bond is a crucial aspect of the prestressing force being transferred into the concrete, and insufficient bonding action can result in the prestressed concrete section lacking in capacity to sustain the loads that it was designed for. After an initial survey of the pull-out strength of North American Strand in mortar, three strands of differing pull-out strengths were selected for inclusion in further testing. A precision and bias statement for ASTM A1081 was developed by first performing ruggedness testing to determine how the results are affected by allowable variations in methods and materials, and followed by an inter-laboratory study to determine the reproducibility of the test method. Once the precision and bias statement for the standard test method was developed, the same strand sources were tested for their performance in concrete beams. Statistical analysis of the flexural beam testing data and correlation with the prestressing strand sources' ASTM A1081 test results was performed, and the industry was provided with minimum acceptance criteria for prestressing strand tested by ASTM A1081, along with recommendations regarding the standard test method and aspects of prestressed concrete design.

DETERMINATION OF ACCEPTANCE CRITERIA FOR PRESTRESSING STRAND IN PRE-TENSIONED APPLICATIONS

by

THOMAIDA POLYDOROU

B.S., Kansas State University, 2009
M.S., Kansas State University, 2011

A DISSERTATION

submitted in partial fulfillment of the requirements for the degree

DOCTOR OF PHILOSOPHY

Department of Civil Engineering
College of Engineering

KANSAS STATE UNIVERSITY
Manhattan, Kansas

2014

Approved by:

Major Professor
Kyle A. Riding

Copyright

Abstract

ASTM recently adopted the Standard Test Method for Evaluating Bond of Seven-Wire Steel Prestressing Strand as ASTM A1081, a pull-out test procedure developed for verifying the ability of steel strands to bond to cementitious materials prior to their use as tensile reinforcement in prestressed concrete sections. The required by ASTM International precision and bias statement has not been developed for this test method. In addition, a minimum threshold value that will ensure only adequately bonding strand sources will be accepted has not yet been applied to ASTM A1081. The test method was developed after findings that prestressing steel strand sources of identical type and grade vary significantly as far as their bonding capacity. Bond is a crucial aspect of the prestressing force being transferred into the concrete, and insufficient bonding action can result in the prestressed concrete section lacking in capacity to sustain the loads that it was designed for. After an initial survey of the pull-out strength of North American Strand in mortar, three strands of differing pull-out strengths were selected for inclusion in further testing. A precision and bias statement for ASTM A1081 was developed by first performing ruggedness testing to determine how the results are affected by allowable variations in methods and materials, and followed by an inter-laboratory study to determine the reproducibility of the test method. Once the precision and bias statement for the standard test method was developed, the same strand sources were tested for their performance in concrete beams. Statistical analysis of the flexural beam testing data and correlation with the prestressing strand sources' ASTM A1081 test results was performed, and the industry was provided with minimum acceptance criteria for prestressing strand tested by ASTM A1081, along with recommendations regarding the standard test method and aspects of prestressed concrete design.

Table of Contents

List of Figures x
List of Tables xix
Acknowledgements xxii
Dedication xxiv
Chapter 1 - Introduction 1
1.1 Background 1
1.2 Problem Statement 1
1.3 Project Objectives 2
1.4 Thesis Organization 2
Chapter 2 - Literature Review 4
2.1 Introduction to Prestressing 4
2.2 History of Prestressing 5
2.3 Strand Manufacturing 7
2.4 Transfer/Development Length Equations 11
2.5 Strand Testing 31
Chapter 3 - Material Selection 43
3.1 Initial Strand Selection 43
3.2 Mortar Mixture Design Procedure 45
Chapter 4 - Ruggedness Testing 50
4.1 Investigation of Factors Affecting the Test 50
4.1.1 Sand 50
4.1.2 Cement 50
4.1.3 Central Wire Slip during Test 53
4.2 ASTM Ruggedness 54
4.2.1 Ruggedness Testing Introduction 54
4.2.2 Ruggedness Testing Materials 54
4.2.3 Ruggedness Testing Methodology 56
4.2.4 Ruggedness Testing Results 59

4.2.5 Ruggedness Testing Conclusion 63
Chapter 5 - Inter-Laboratory Study 65
5.1 Inter-Laboratory Study Introduction 65
5.2 Inter-Laboratory Study Materials 65
5.3 Inter-Laboratory Study Methodology 68
5.4 Inter-Laboratory Study Results 69
5.5 Inter-Laboratory Study Conclusions 76
Chapter 6 - Strand Testing by NCHRP 621 77
6.1 Weight Loss on Ignition (QC-I) 77
6.2 Contact Angle Measurement after Lime Dip (QC-I) 78
6.3 Change in Corrosion Potential (QC-I) 79
6.4 Organic Residue Extraction with FTIR Analysis (QC-II) 80
Chapter 7 - Discussion of ASTM A1081 83
7.1 Summary of Factors that Affected the Test 83
7.2 Summary of Precision and Bias Statement for ASTM A1081 84
7.3 Strand Pullout Test Values to Consider in Phase II 85
Chapter 8 - Sensitivity Analysis 86
8.1 Analysis Using Bentley Software Leap Presto and Microsoft Excel 86
8.1.1 Sections Analyzed 86
8.1.2 Conditions Analyzed 88
8.2 Sensitivity Analysis Results 88
8.3 Sensitivity Analysis Conclusions and Recommendations 96
Chapter 9 - Rectangular Beam Specimens at Stresscon 97
9.1 Introduction 97
9.2 Beam Specimen Design and Fabrication 97
9.2.1 Rectangular Beam Specimen Design 97
9.2.1.1 Beam Dimensions and Strand Location 97
9.2.1.2 Shear Reinforcement Details 98
9.2.2 Concrete Mixture Design Specifications 99
9.2.3 Beam Fabrication Procedure 100
9.2.3.1 Beam Casting Schedule 100

9.2.3.2 Crack Formers and Beam Notching 101
9.2.3.3 Concrete Mixture Placement 106
9.2.3.4 Beam Specimen Curing Conditions 108
9.2.4 Transfer Length Measurements 109
9.2.4.1 Methodology 109
9.2.4.1.1 End Slip Readings 110
9.2.4.1.2 Laser Speckle Imaging 111
9.2.4.2 Instrumentation Setup for Laser Speckle Imaging Device 113
9.2.4.3 Transfer Length Measurements at Release 114
9.2.4.4 Transfer Length Measurements at Test 115
9.2.5 Flexural Beam Testing 116
9.2.5.1 Instrumentation Setup and Testing Procedures 116
9.2.5.2 Beam Loading Procedures 119
9.2.5.3 Test Results 120
Chapter 10 - Determination of ASTM A1081 Threshold Value 124
10.1 Statistical Analysis of Data 124
10.2 Transfer Length Measurements 124
10.3 Beam Specimen Experimental Moment 126
10.3.1 Ultimate Tensile Strength of Strand 126
10.4 Threshold Value Determination 127
Chapter 11 - Simple Quality Assurance Test for Strand Bond 133
11.1 Introduction 133
11.2 Beam Specimen Design and Fabrication 134
11.3 Test Methodology 134
11.4 Test Results 137
11.5 Simple Quality Assurance Test for Strand Bond Conclusions 140
Chapter 12 - Conclusions 141
12.1 Summary of Work Done and Conclusions 141
12.2 Recommendations for Implementation 143
12.3 Future Research 144
Bibliography 146

Appendix A - Rectangular Beam Specimens' Accompanying Concrete Cylinder Split Tensile Test Results 150
Appendix B - Rectangular Beam Specimen Transfer Lengths at Time of Prestress Release 152
Appendix C - Rectangular Beam Specimen Transfer Lengths at Time of Flexural Testing 155
Appendix D - Flexural Beam Specimen End Slip Values 158
Appendix E - Rectangular Beam End Actual Dimensions 161
Appendix F - Moment Capacity Calculation Example 164
Appendix G - Flexural Beam Testing Failure Analysis 167
Appendix H - Flexural Beam Test Results Summary Charts 170
Appendix I - Simple Quality Assurance Test for Strand Bond Summary Charts 289

List of Figures

Figure 2.1 Prestressed Concrete Beam 4
Figure 2.2 Raw Steel Coils used for Prestressing Strand Manufacturing 7
Figure 2.3 Wire Drawing Process during Strand Manufacturing 8
Figure 2.4 Cut Wire Die Cross Section (4a) and Top View (4b) 9
Figure 2.5 Variation of Steel Stress along Development Length 12
Figure 2.6 Adopted and Proposed Transfer Length Expressions by Year 30
Figure 2.7 Adopted and Proposed Development Length Equations by Year 31
Figure 3.1 Average Strand Force (lb) vs. Displacement (in) per Strand Source (Polydorou, Riding, Peterman, & Murray, 2013) 44
Figure 3.2 Pullout Force (lb) for 6 Specimens Tested per Strand Source for (Polydorou, Riding, Peterman, & Murray, 2013) 44
Figure 3.3 Interpolation Procedure used to Select w/c for Cement 1 (Riding, Peterman, Polydorou, & Ren, 2012) 46
Figure 3.4 Interpolation Procedure use to select s/c for Cement 1 (Riding, Peterman, Polydorou, & Ren, 2012) 47
Figure 4.1 Initial and Final Setting Times for Cements 1, 2, and 4, determined by ASTM C403 52
Figure 4.2 Specimen Setup (Polydorou, Riding, Peterman, & Murray, 2013) 56
Figure 4.3 Tensile Testing Frame (Polydorou, Riding, Peterman, & Murray, 2013) 58
Figure 4.4 LVDT Setup on Specimen (Polydorou, Riding, Peterman, & Murray, 2013) 59
Figure 5.1 Inter-Laboratory Study Results, Method A-Strand A (Polydorou, Riding, & Peterman, 2014) 72
Figure 5.2 Inter-Laboratory Study Results, Method B- Strand A (Polydorou, Riding, & Peterman, 2014) 72
Figure 5.3 Inter-Laboratory Study Results, Method A- Strand I (Polydorou, Riding, & Peterman, 2014) 73
Figure 5.4 Inter-Laboratory Study Results, Method B- Strand I (Polydorou, Riding, & Peterman, 2014) 73
Figure 5.5 Inter-Laboratory Study Results, Method A- Strand G (Polydorou, Riding, & Peterman, 2014) 74

Figure 5.6 Inter-Laboratory Study Results, Method B- Strand G (Polydorou, Riding, & Peterman, 2014) 74
Figure 8.1 7T264 Section Details 86
Figure 8.2 Highcore 8-1000 Section Details 87
Figure 8.3 Percent of ACI Moment Capacity per Case Analyzed for 7T264 89
Figure 8.4 Percent of ACI Shear Capacity per Case Analyzed for 7T264 89
Figure 8.5 Percent of ACI Moment Capacity per Case Analyzed for 10DT24 90
Figure 8.6 Percent of ACI Shear Capacity per Case Analyzed for 10DT24 90
Figure 8.7 Percent of ACI Moment Capacity per Case Analyzed for HC 8-1000 91
Figure 8.8 Percent of ACI Shear Capacity per Case Analyzed for HC 8-1000 91
Figure 8.9 Percent of ACI Moment Capacity per Case Analyzed for HC 12 92
Figure 8.10 Percent of ACI Shear Capacity per Case Analyzed for HC 12 92
Figure 8.11 Shear Diagrams for 30 ft. long HC 12 94
Figure 8.12 Moment Diagrams for 40ft. long 7T264 95
Figure 9.1 Beam Section Dimensions 97
Figure 9.2 Short End (60% ACI L_d) Loading Configuration 98
Figure 9.3 Long End (80% ACI L_d) Loading Configuration 98
Figure 9.4 Welded Wire Fabric Shear Reinforcement 99
Figure 9.5 Concrete Mixing Plant at Stresscon, Inc. 99
Figure 9.6 Beam Casting Setup and Schedule Details 101
Figure 9.7 Crack Inducer Setup 102
Figure 9.8 Crack Former 103
Figure 9.9 Saw Cut on Bottom Surface of Beam 103
Figure 9.10 Saw Cut on Bottom and Side Surfaces of Beam 104
Figure 9.11 Saw Cutting of Flexural Beam Sections 108
Figure 9.12 Taking End Slip Readings 111
Figure 9.13 Surface Strain Profile 113
Figure 9.14 Laser Speckle Imaging Device and Digital Speckle Patterns 113
Figure 9.15 LSI Device Mounting Instrumentation 114
Figure 9.16 Beam Testing Setup: Loading Setup 117
Figure 9.17 Beam Testing Setup: Load Cell, Load Point LVDTs, End Slip LVDT 118

Figure 9.18 Beam Testing Setup: Load Application Point on Steel Plate, LVDTs 119
Figure 9.19 Beam Testing Setup: Roller Support Configuration 119
Figure 9.20 Moment, Deflection, End Slip Plot for Beam End G9-S 120
Figure 10.1 Ultimate Tensile Strength of Strand Test Specimen after Failure 126
Figure 10.2 Graphic Representation of Linear Analysis of Data for ASTM A1081 Threshold Determination 128
Figure 10.3 Graphic Representation of Polynomial Analysis of Data for ASTM A1081 Threshold Determination 129
Figure 10.4 Strand Averaging Effects to Moment Ratio Standard Deviation Values 130
Figure 10.5 Threshold Value vs Number of Strands Combined- Polynomial Analysis 131
Figure 11.1 Simple Quality Assurance Test for Strand Bond Specimen Dimensions 133
Figure 11.2 Simple Quality Assurance Test for Strand Bond Loading Configuration 133
Figure 11.3 Simple Quality Assurance Test for Strand Bond Loading Setup 135
Figure 11.4 Beam A1 Setup for Simple Quality Assurance Test for Strand Bond 135
Figure 11.5 Beam A1 Loaded at 85% of its Nominal Moment Capacity during the Simple Quality Assurance Test for Strand Bond 136
Figure 11.6 Beam A1 Loaded at 100% of its Nominal Moment Capacity during the Simple Quality Assurance Test for Strand Bond 137
Figure 11.7 Beam A1 Simple Quality Assurance Test for Strand Bond Results 138
Figure 11.8 Mid span Deflection (in) vs Applied Load (lb) for all Specimens Tested by the Simple Quality Assurance Test for Strand Bond 139
Figure H.1 Beam End A1-L Flexural Test Results Summary Chart A 170
Figure H.2 Beam End A1-L Flexural Test Results Summary Chart B 170
Figure H.3 Beam End A1-L Failure 171
Figure H.4 Beam End A2-L Flexural Test Results Summary Chart A 172
Figure H.5 Beam End A2-L Flexural Test Results Summary Chart B 172
Figure H.6 Beam End A2-L Failure 173
Figure H.7 Beam End A3-L Flexural Test Results Summary Chart A 174
Figure H.8 Beam End A3-L Flexural Test Results Summary Chart B 174
Figure H.9 Beam End A3-L Failure 175
Figure H.10 Beam End A4-L Flexural Test Results Summary Chart A 176

Figure H.11 Beam End A4-L Flexural Test Results Summary Chart B 176
Figure H.12 Beam End A4-L Failure 177
Figure H.13 Beam End A5-L Flexural Test Results Summary Chart A 178
Figure H.14 Beam End A5-L Flexural Test Results Summary Chart B 178
Figure H.15 Beam End A5-L Failure 179
Figure H.16 Beam End A6-L Flexural Test Results Summary Chart A 180
Figure H.17 Beam End A6-L Flexural Test Results Summary Chart B 180
Figure H.18 Beam End A6-L Failure 181
Figure H.19 Beam End A7-L Flexural Test Results Summary Chart A 182
Figure H.20 Beam End A7-L Flexural Test Results Summary Chart B 182
Figure H.21 Beam End A7-L Failure 183
Figure H.22 Beam End A8-L Flexural Test Results Summary Chart A 184
Figure H.23 Beam End A8-L Flexural Test Results Summary Chart B 184
Figure H.24 Beam End A8-L Failure 185
Figure H.25 Beam End A9-L Flexural Test Results Summary Chart A 186
Figure H.26 Beam End A9-L Flexural Test Results Summary Chart B 186
Figure H.27 Beam End A9-L Failure 187
Figure H.28 Beam End A10-L Flexural Test Results Summary Chart A 188
Figure H.29 Beam End A10-L Flexural Test Results Summary Chart B 188
Figure H.30 Beam End A10-L Failure 189
Figure H.31 Beam End A1-S Flexural Test Results Summary Chart A 190
Figure H.32 Beam End A1-S Flexural Test Results Summary Chart B 190
Figure H.33 Beam End A1-S Failure 191
Figure H.34 Beam End A2-S Flexural Test Results Summary Chart A 192
Figure H.35 Beam End A2-S Flexural Test Results Summary Chart B 192
Figure H.36 Beam End A2-S Failure 193
Figure H.37 Beam End A3-S Flexural Test Results Summary Chart A 194
Figure H.38 Beam End A3-S Flexural Test Results Summary Chart B 194
Figure H.39 Beam End A3-S Failure 195
Figure H.40 Beam End A4-S Flexural Test Results Summary Chart A 196
Figure H.41 Beam End A4-S Flexural Test Results Summary Chart B 196

Figure H.42 Beam End A4-S Failure 197
Figure H.43 Beam End A5-S Flexural Test Results Summary Chart A 198
Figure H.44 Beam End A5-S Flexural Test Results Summary Chart B 198
Figure H.45 Beam End A5-S Failure 199
Figure H.46 Beam End A6-S Flexural Test Results Summary Chart A 200
Figure H.47 Beam End A6-S Flexural Test Results Summary Chart B 200
Figure H.48 Beam End A6-S Failure 201
Figure H.49 Beam End A7-S Flexural Test Results Summary Chart A 202
Figure H.50 Beam End A7-S Flexural Test Results Summary Chart B 202
Figure H.51 Beam End A7-S Failure 203
Figure H.52 Beam End A8-S Flexural Test Results Summary Chart A 204
Figure H.53 Beam End A8-S Flexural Test Results Summary Chart B 204
Figure H.54 Beam End A8-S Failure 205
Figure H.55 Beam End A9-S Flexural Test Results Summary Chart A 206
Figure H.56 Beam End A9-S Flexural Test Results Summary Chart B 206
Figure H.57 Beam End A9-S Failure 207
Figure H.58 Beam End A10-S Flexural Test Results Summary Chart A 208
Figure H.59 Beam End A10-S Flexural Test Results Summary Chart B 208
Figure H.60 Beam End G1-L Flexural Test Results Summary Chart A 209
Figure H.61 Beam End G1-L Flexural Test Results Summary Chart B 209
Figure H.62 Beam End G1-L Failure 210
Figure H.63 Beam End G2-L Flexural Test Results Summary Chart A 211
Figure H.64 Beam End G2-L Flexural Test Results Summary Chart B 211
Figure H.65 Beam End G2-L Failure 212
Figure H.66 Beam End G3-L Flexural Test Results Summary Chart A 213
Figure H.67 Beam End G3-L Flexural Test Results Summary Chart B 213
Figure H.68 Beam End G3-L Failure 214
Figure H.69 Beam End G4-L Flexural Test Results Summary Chart A 215
Figure H.70 Beam End G4-L Flexural Test Results Summary Chart B 215
Figure H.71 Beam End G4-L Failure 216
Figure H.72 Beam End G5-L Flexural Test Results Summary Chart A 217

Figure H.73 Beam End G5-L Flexural Test Results Summary Chart B 217
Figure H.74 Beam End G5-L Failure 218
Figure H.75 Beam End G6-L Flexural Test Results Summary Chart A 219
Figure H.76 Beam End G6-L Flexural Test Results Summary Chart B 219
Figure H.77 Beam End G6-L Failure 220
Figure H.78 Beam End G7-L Flexural Test Results Summary Chart A 221
Figure H.79 Beam End G7-L Flexural Test Results Summary Chart B 221
Figure H.80 Beam End G7-L Failure 222
Figure H.81 Beam End G8-L Flexural Test Results Summary Chart A 223
Figure H.82 Beam End G8-L Flexural Test Results Summary Chart B 223
Figure H.83 Beam End G8-L Failure 224
Figure H.84 Beam End G9-L Flexural Test Results Summary Chart A 225
Figure H.85 Beam End G9-L Flexural Test Results Summary Chart B 225
Figure H.86 Beam End G9-L Failure 226
Figure H.87 Beam End G10-L Flexural Test Results Summary Chart A 227
Figure H.88 Beam End G10-L Flexural Test Results Summary Chart B 227
Figure H.89 Beam End G10-L Failure 228
Figure H.90 Beam End G1-S Flexural Test Results Summary Chart A 229
Figure H.91 Beam End G1-S Flexural Test Results Summary Chart B 229
Figure H.92 Beam End G1-S Failure 230
Figure H.93 Beam End G2-S Flexural Test Results Summary Chart A 231
Figure H.94 Beam End G2-S Flexural Test Results Summary Chart B 231
Figure H.95 Beam End G2-S Failure 232
Figure H.96 Beam End G3-S Flexural Test Results Summary Chart A 233
Figure H.97 Beam End G3-S Flexural Test Results Summary Chart B 233
Figure H.98 Beam End G3-S Failure 234
Figure H.99 Beam End G4-S Flexural Test Results Summary Chart A 235
Figure H.100 Beam End G4-S Flexural Test Results Summary Chart B 235
Figure H.101 Beam End G4-S Failure 236
Figure H.102 Beam End G5-S Flexural Test Results Summary Chart A 237
Figure H.103 Beam End G5-S Flexural Test Results Summary Chart B 237

Figure H.104 Beam End G5-S Failure 238
Figure H.105 Beam End G6-S Flexural Test Results Summary Chart A 239
Figure H.106 Beam End G6-S Flexural Test Results Summary Chart B 239
Figure H.107 Beam End G6-S Failure 240
Figure H.108 Beam End G7-S Flexural Test Results Summary Chart A 241
Figure H.109 Beam End G7-S Flexural Test Results Summary Chart B 241
Figure H.110 Beam End G7-S Failure 242
Figure H.111 Beam End G8-S Flexural Test Results Summary Chart A 243
Figure H.112 Beam End G8-S Flexural Test Results Summary Chart B 243
Figure H.113 Beam End G8-S Failure 244
Figure H.114 Beam End G9-S Flexural Test Results Summary Chart A 245
Figure H.115 Beam End G9-S Flexural Test Results Summary Chart B 245
Figure H.116 Beam End G9-S Failure 246
Figure H.117 Beam End G10-S Flexural Test Results Summary Chart A 247
Figure H.118 Beam End G10-S Flexural Test Results Summary Chart B 247
Figure H.119 Beam End G10-S Failure 248
Figure H.120 Beam End I1-L Flexural Test Results Summary Chart A 249
Figure H.121 Beam End I1-L Flexural Test Results Summary Chart B 249
Figure H.122 Beam End I1-L Failure 250
Figure H.123 Beam End I2-L Flexural Test Results Summary Chart A 251
Figure H.124 Beam End I2-L Flexural Test Results Summary Chart B 251
Figure H.125 Beam End I2-L Failure 252
Figure H.126 Beam End I3-L Flexural Test Results Summary Chart A 253
Figure H.127 Beam End I3-L Flexural Test Results Summary Chart B 253
Figure H.128 Beam End I3-L Failure 254
Figure H.129 Beam End I4-L Flexural Test Results Summary Chart A 255
Figure H.130 Beam End I4-L Flexural Test Results Summary Chart B 255
Figure H.131 Beam End I4-L Failure 256
Figure H.132 Beam End I5-L Flexural Test Results Summary Chart A 257
Figure H.133 Beam End I5-L Flexural Test Results Summary Chart B 257
Figure H.134 Beam End I5-L Failure 258

Figure H.135 Beam End I6-L Flexural Test Results Summary Chart A 259
Figure H.136 Beam End I6-L Flexural Test Results Summary Chart B 259
Figure H.137 Beam End I6-L Failure 260
Figure H.138 Beam End I7-L Flexural Test Results Summary Chart A 261
Figure H.139 Beam End I7-L Flexural Test Results Summary Chart B 261
Figure H.140 Beam End I7-L Failure 262
Figure H.141 Beam End I8-L Flexural Test Results Summary Chart A 263
Figure H.142 Beam End I8-L Flexural Test Results Summary Chart B 263
Figure H.143 Beam End I8-L Failure 264
Figure H.144 Beam End I9-L Flexural Test Results Summary Chart A 265
Figure H.145 Beam End I9-L Flexural Test Results Summary Chart B 265
Figure H.146 Beam End I9-L Failure 266
Figure H.147 Beam End I10-L Flexural Test Results Summary Chart A 267
Figure H.148 Beam End I10-L Flexural Test Results Summary Chart B 267
Figure H.149 Beam End I10-L Failure 268
Figure H.150 Beam End I1-S Flexural Test Results Summary Chart A 269
Figure H.151 Beam End I1-S Flexural Test Results Summary Chart B 269
Figure H.152 Beam End I1-S Failure 270
Figure H.153 Beam End I2-S Flexural Test Results Summary Chart A 271
Figure H.154 Beam End I2-S Flexural Test Results Summary Chart B 271
Figure H.155 Beam End I2-S Failure 272
Figure H.156 Beam End I3-S Flexural Test Results Summary Chart A 273
Figure H.157 Beam End I3-S Flexural Test Results Summary Chart B 273
Figure H.158 Beam End I3-S Failure 274
Figure H.159 Beam End I4-S Flexural Test Results Summary Chart A 275
Figure H.160 Beam End I4-S Flexural Test Results Summary Chart B 275
Figure H.161 Beam End I4-S Failure 276
Figure H.162 Beam End I5-S Flexural Test Results Summary Chart A 277
Figure H.163 Beam End I5-S Flexural Test Results Summary Chart B 277
Figure H.164 Beam End I5-S Failure 278
Figure H.165 Beam End I6-S Flexural Test Results Summary Chart A 279

Figure H.166 Beam End I5-S Flexural Test Results Summary Chart B 279
Figure H.167 Beam End I5-S Failure 280
Figure H.168 Beam End I7-S Flexural Test Results Summary Chart A 281
Figure H.169 Beam End I7-S Flexural Test Results Summary Chart B 281
Figure H.170 Beam End I7-S Failure 282
Figure H.171 Beam End I8-S Flexural Test Results Summary Chart A 283
Figure H.172 Beam End I8-S Flexural Test Results Summary Chart B 283
Figure H.173 Beam End I8-S Failure 284
Figure H.174 Beam End I9-S Flexural Test Results Summary Chart A 285
Figure H.175 Beam End I9-S Flexural Test Results Summary Chart B 285
Figure H.176 Beam End I9-S Failure 286
Figure H.177 Beam End I10-S Flexural Test Results Summary Chart A 287
Figure H.178 Beam End I10-S Flexural Test Results Summary Chart B 287
Figure H.179 Beam End I10-S Failure 288
Figure I.1 Simple Quality Assurance Test for Strand Bond Specimen A1 Summary Chart 289
Figure I.2 Simple Quality Assurance Test for Strand Bond Specimen A2 Summary Chart 290
Figure I.3 Simple Quality Assurance Test for Strand Bond Specimen A3 Summary Chart 291
Figure I.4 Simple Quality Assurance Test for Strand Bond Specimen G1 Summary Chart 292
Figure I.5 Simple Quality Assurance Test for Strand Bond Specimen G2 Summary Chart 293
Figure I.6 Simple Quality Assurance Test for Strand Bond Specimen G3 Summary Chart 294
Figure I.7 Simple Quality Assurance Test for Strand Bond Specimen I1 Summary Chart..... 295
Figure I.8 Simple Quality Assurance Test for Strand Bond Specimen I2 Summary Chart..... 296
Figure I.9 Simple Quality Assurance Test for Strand Bond Specimen I3 Summary Chart..... 297

List of Tables

Table 2-1 Code Adopted and Proposed Equations for Transfer and Development Length 27
Table 2-2 Equation Symbol Description and Assumed Values for Numerical Representation of Adopted and Proposed Transfer and Development Length Equations 29
Table 3-1 Mortar Strength and Flow Results per Cement (Riding, Peterman, Polydorou, & Ren, 2012) 49
Table 4-1 Dolese Sand Gradations (Polydorou, Riding, Peterman, & Murray, 2013) 50
Table 4-2 Cement Chemical Composition and Physical Properties (Riding, Peterman, Polydorou, & Ren, 2012) 53
Table 4-3 Cement 1 Chemical and Physical Properties (Polydorou, Riding, Peterman, & Murray, 2013) 55
Table 4-4 Ruggedness Testing Matrix 57
Table 4-5 Mortar Compressive Strength Before and After Testing, Mortar Flow, Test Loading Rate, and Average Pullout Force Values per Test (Polydorou, Riding, Peterman, & Murray, 2013) 60
Table 4-6 Average Difference (5) between Pullout Test Results of Test Groups per Factor Investigated (Polydorou, Riding, Peterman, & Murray, 2013) 61
Table 4-7 Two-Sided Tail Probability Values per Effect by ASTM E1169-07 Procedures for Each Strand Source 62
Table 4-8 Two-Sided Probability Values per Effect for Each ANOVA Model Used to Analyze the Data (Strand A) 63
Table 5-1 Mixture Proportions and Mixture Flow for Mortar Samples Made with 5 Different Cement Sources (Polydorou, Riding, & Peterman, 2014) 66
Table 5-2 Average ASTM A1081 Test Results per Strand and Cement Source Tested at KSU . 66
Table 5-3 Average Modified ASTM A1081 Test Results per Strand and Cement Source Tested at KSU (w/c= 0.45 for all mixtures) 67
Table 5-4 Method A and Method B Specifications (Polydorou, Riding, & Peterman, 2014) 69
Table 5-5 Inter-Laboratory Study Data- Method A (ASTM A1081) (Polydorou, Riding, & Peterman, 2014) 70

Table 5-6 Inter-Laboratory Study Data- Method B (Modified ASTM A1081) (Polydorou, Riding, & Peterman, 2014) 71
Table 5-7 Average Pullout Test Result, Standard Deviation and Coefficient of Variation for Strands A, G and I, Method A vs Method B (Polydorou, Riding, & Peterman, 2014) 75
Table 6-1 Loss on Ignition Test Data 78
Table 6-2 Contact Angle Measurement Test Data 79
Table 6-3 Change in Corrosion Potential Test Data 80
Table 6-4 Organic Residue Extraction with FTIR Analysis Test Results 81
Table 8-1 Summary of ACI Capacities Reduced per Section and Case Analyzed 93
Table 9-1 Concrete Mixture Design Specifications 100
Table 9-2 Crack Inducing Techniques per Beam End 105
Table 9-3 Concrete Placement Conditions and Mixture Properties per Cast Day 106
Table 9-4 Day 1 Concrete Mixture Maturity Details (Beams A1-5, I1-5) 106
Table 9-5 Day 2 Concrete Mixture Maturity Details (Beams G1-5, A6-10) 107
Table 9-6 Day 3 Concrete Mixture Maturity Details (Beams G6-10, I6-10) 107
Table 9-7 Time Between Mixture Placement and Specimen Tested per Beam Group 109
Table 9-8 Average Transfer Length Values at Release for Strands A, G, and I by 95% AMS and ZL Method Analysis 115
Table 9-9 Average Transfer Length Values at Time of Flexural Beam Testing for Strands A, G, and I by ZL Method Analysis 116
Table 9-10 Average Transfer Length, Experimental to Nominal Moment Ratio, and End Slip During Test Values per Beam End Group 122
Table 9-11 Beam End Group Failure Mode Summary 122
Table 10-1 ASTM A1081 Pullout Force Values Corresponding to ACI 318 Transfer Length Values at Release and at Time of Test 125
Table 10-2 Ultimate Tensile Strength (ksi) per Strand Source 127
Table 10-3 Average Moment Ratios per Beam End Group Calculated Using Strand Ultimate Strength 127
Table 10-4 Strand Averaging Procedure Example 130
Table 10-5 Recommended ASTM A1081 Threshold Values 132
Table 11-1 Simple Quality Assurance Test for Strand Bond Results Summarized 139

Table A-1 Placement Day 1 (7-16-13): Rectangular Beam Specimens A 1-5, I 1-5 Accompanying Cylinders' Split Tensile Test Results 150
Table A-2 Placement Day 2 (7-18-13): Rectangular Beam Specimens A 5-10, G 1-5 Accompanying Cylinders' Split Tensile Test Results 150
Table A-3 Placement Day 3 (7-19-13): Rectangular Beam Specimens I 5-10, G 5-10 Accompanying Cylinders' Split Tensile Test Results 151
Table B-1 Strand G Transfer Lengths at Time of Prestress Release 152
Table B-2 Strand A Transfer Lengths at Time of Prestress Release 153
Table B-3 Strand I Transfer Lengths at Time of Prestress Release 154
Table C-1 Strand G Transfer Lengths at Time of Flexural Testing 155
Table C-2 Strand A Transfer Lengths at Time of Flexural Testing 156
Table C-3 Strand I Transfer Lengths at Time of Flexural Testing 157
Table D-1 Strand G End Slip Values 158
Table D-2 Strand A End Slip Values 159
Table D-3 Strand I End Slip Values 160
Table E-1 Strand A Beam Ends- Actual Dimensions 161
Table E-2 Strand G Beam Ends- Actual Dimensions 162
Table E-3 Strand I Beam Ends- Actual Dimensions 163
Table G-1 Flexural Beam Testing Failure Analysis for Strand A Beam Ends 167
Table G-2 Flexural Beam Testing Failure Analysis for Strand G Beam Ends 168
Table G-3 Flexural Beam Testing Failure Analysis for Strand I Beam Ends 169

Acknowledgements

I would like to thank my major professors Dr. Kyle A. Riding and Dr. Robert J. Peterman for their guidance with this research project, their patience, and understanding. I want to take this opportunity to express my respect to these two outstanding researchers, as well as my gratitude for being given the opportunity to work on this project. I want to also acknowledge my committee chairperson and Distinguished Professor from the Department of Physics, Dr. Itzik Ben-Itzhak, as well as my advisory committee members Dr. Asad Esmaeily, and Dr. B. Terry Beck, expressing my appreciation for their time, precious advice and constructive remarks on my work.

I would like to thank the Prestressed Concrete Institute (PCI), the major funding agency of this project, as well as Kansas State University's University Transportation Center (UTC) for supporting my research financially.

I would like to express my gratitude to Dolese Brothers Co., Oklahoma, for donating 2 truckloads of sand, as well as the prestressing strand manufacturing plants and cement manufacturing plants that donated the materials necessary to make this research project possible:

American Spring Wire, Ash Grove Cement Company, Bekaert Canada, Buzzi Unicem USA, Essroc Italicementi Group, Holcim (US) Inc., Insteel Wire Products, Lafarge Cement, The Monarch Cement Company, Rettco Steel, Strand Tech Martin Inc., Sumiden Wire Products Corporation. I also want to thank Bentley for providing me with a temporary license key to their product Leap Presto, and acknowledge Mr. Tim Cullen for his guidance on the analysis.

I would also like to acknowledge the laboratories that participated in our Inter-Laboratory Study, and thank them for their cooperation:

Florida Department of Transportation, Kansas Department of Transportation, Louisiana Department of Transportation, Missouri Department of Transportation, Ohio Department of Transportation, Sumiden Wire Products Corporation, Texas Department of Transportation, Turner Fairbank Highway Research Center. I would like to also thank co-project investigator Dr. Leigh Murray for her help with the statistical interpretation of the data.

I want to express my deep appreciation to the group of Stresscon, Inc., and the significant effort they put into our Flexural Beam Study, and acknowledge Stresscon founder Mr. Donald R. Logan for accommodating this study, and inspiring me with his passion for research on strand

bond. I would also like to thank our research technologist Ryan Benteman, my fellow graduate students for their help, as well as my undergraduate research assistants whose hard work made this research feasible; Thank you! Matt Arnold, Naga Bodapati, Brandon Bortz, Ben Brabec, Nick Clow, Brandon Heavener, Dr. Joey Holste, Dustin Hoyt, Jerry Hulsing, Amir Farid Momeni, Austin Muck, Dr. GengFeng Ren, Noura Saadi, Robert Schweiger, Garrett Sharpe, Andy Shearrer, and Luke Spaich.

Finally, I want to thank my father, my mother, my sisters, and all the supportive friends and loving family that I am blessed with; thank my grandmothers, former teachers and Track and Field coaches for the inspiration, but most importantly my son, who brought true joy to this rollercoaster ride!

Dedication

Σ' εσένα, που χαμογελάς..!

Chapter 1 - Introduction

The Prestressed Concrete Institute (PCI) hired researchers from Kansas State University to investigate the repeatability and reproducibility of the North American Strand Producers (NASP) test method, and establish appropriate threshold criteria for prestressing strand to be used in pre-tensioned applications. The NASP method is a pull-out test procedure developed for verifying the bonding ability of steel strands to cementitious materials, and is now accepted by ASTM as the "Standard Test Method for Evaluating Bond of Seven-Wire Steel Prestressing Strand".

The methodology, procedures, and presentation of the findings from the extensive research project "Determination of Acceptance Criteria for Prestressing Strand in Pre-Tensioned Applications" funded by PCI will be presented and discussed in this doctoral dissertation.

1.1 Background

The bonding performance of prestressing strand in pre-tensioned applications is crucial, since it is through the bond between the two materials that the tensile stresses are transferred from the strand tendons to the concrete material. In prestressed concrete, a section relies on the bond between concrete and steel strands, in order to provide it with the necessary flexural and shear capacity to withstand the loading it was designed for. Recently it was observed that strands of the same grade and type vary in their bonding capacity, turning the prestressing industry's attention to strand bond research.

1.2 Problem Statement

It is necessary to establish minimum acceptance criteria for the "Standard Test Method for Evaluating Bond of Seven-Wire Steel Prestressing Strand" in order to ensure adequate bonding capacity of prestressing strand samples to be used in pre-tensioned applications, and therefore provide prestressed concrete members that will meet code requirements.

1.3 Project Objectives

The purpose of this research project was first of all to determine the reproducibility and repeatability of the "Standard Test Method for Evaluating Bond of Seven-Wire Steel Prestressing Strand", and then provide a precision and bias statement for the test method. Following the investigation of the test method, this research project was geared towards correlating the pullout force capacity of three strand sources as tested by the standard test, with their performance in flexural concrete beam specimens. The objective was to determine an appropriate minimum threshold for the "Standard Test Method of Evaluating Bond of Seven-Wire Steel Prestressing Strand" to ensure adequate performance of strand in prestressed concrete applications.

1.4 Thesis Organization

This doctoral dissertation is divided into 12 chapters, with Chapter 1 introducing the research project and providing the scope of this dissertation.

Chapter 2 presents an extensive Literature Review of the subjects studied, and the following 10 chapters describe the experimental tasks completed during the course of this research project.

Chapter 3 is a discussion of the material selection process, employed during the preliminary testing rounds.

Chapter 4 describes the ruggedness investigation of ASTM A1081.

Chapter 5 follows, presenting the Inter-Laboratory study conducted on the ASTM A1081 test.

Chapter 6 reports the strand surface characteristics tested by NCHRP 621 methods.

Chapter 7 is a discussion of the ASTM A1081 test method investigation findings.

Chapter 8 presents an analysis of the sensitivity of pre-tensioned applications to the transfer and development length criteria of ACI 318.

Chapter 9 explains and discusses the rectangular beam testing study.

Chapter 10 describes the methods of analysis conducted in order to determine the test method threshold value.

Chapter 11 presents the Peterman Beam Test program procedures and findings.

Chapter 12 is an overall summary and conclusion, with recommendations for implementation and future research.

Chapter 2 - Literature Review

2.1 Introduction to Prestressing

In prestressed concrete applications, steel tendons are inserted at preselected locations in forms where a concrete section will be fabricated, and are tensioned to a desired stress prior to the placing of fresh concrete. As the concrete gains compressive strength during the curing process, it also bonds to the prestressing steel strands. Once the concrete mixture reaches a specified compressive strength, the steel strands are released from their anchorages. The tensile stress is transferred into the concrete as the prestressed tendons react upon release, aiming to return to their original length, and therefore compress the concrete section. A perfect balance between prestress and load generated stresses is the ideal application of the prestressing theory.

The principle of prestressing is to reduce the tensile stresses that are applied to concrete as a result of external loading. Achieving this provision delivers a prestressed concrete section with fewer cracks compared to the equivalent traditionally reinforced concrete section, and also offers alternative design possibilities that can ease the construction and maximize the economy and functionality of structures. The schematic of a rectangular prestressed concrete beam and the effects of prestressing in balancing out the applied stresses is illustrated in Figure 2.1.

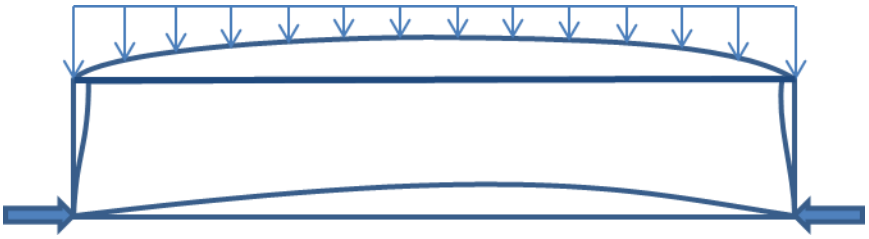

Figure 2.1 Prestressed Concrete Beam

Prestressing allows greater span-to-length ratios, and therefore the construction of cable-stayed bridges, segmental bridges and other large span sections, which are quite uneconomical, if not impossible to reinforce with traditional reinforcement alone.

In conventional construction, the use of prestressing instead of traditional reinforcement allows decreasing of the concrete section depth; accounting for less concrete material as well as less reinforcing material required. In buildings, prestressing minimizes the number of column supports required to support a structure, and therefore maximizes open space areas. Prestressing

will also contribute to structure longevity, since it limits the amount of contaminants entering the concrete, by reduced cracking of the section.

2.2 History of Prestressing

As a relatively new concept, it was not until the 1950s that the prestressing industry began to rise in the United States. The construction of the Walnut Lane Memorial Bridge in Philadelphia, Pennsylvania is believed to have been the breakthrough of the prestressed concrete industry in North America. Before then, P.H. Jackson was the first engineer to introduce prestressing in 1872, with C.W. Doehring to follow in 1888. Both of the engineers' attempts were unsuccessful at that time, since neither one accounted for long-term prestress losses. It was during the 1920s that the prestressing principles started to develop in both the United States and Europe (Nawy, 2010).

In France in the early 1900s, Eugène Freyssinet was the first engineer who attempted the construction of pre-compressed bridges, setting successive world records for span length, and also discovering concrete creep while riding his bicycle across one of his first built bridges. Freyssinet had to repair his bridges, and did so by replacing the original jacks and raising the vaults. After studying the phenomena of creep and shrinkage which brought his bridges near collapse, he concluded that higher quality concrete and higher strength steel was required for successful prestressing applications. By the 1930s, Freyssinet had grasped his prestressing vision; he was then using concrete of 4000-5000 psi compressive strength, prestressed with steel of strength in the range of 190,000-200,000 psi (Xercavins, Demarthe, & Sushkewich, 2008).

During World War II, Belgian engineer and academic Gustave Magnel studied Freyssinet's principles and also conducted his own research on full scale sections; his findings making significant embellishments to the developing technology of prestressed concrete (Dinges, 2009). Through his research, Magnel had discovered that creep in prestressed concrete is not the effect of concrete material alone as Freyssinet had assumed; it is in fact the prestressing steel that contributes a large amount of the stress relaxation in a prestressed concrete application. With this finding, Magnel was able to make more accurate calculations in determining the loss of prestress in a prestressed concrete section. In addition to his experimental research aptitude,

Gustave Magnel was also a gifted educator, able to simplify concepts and communicate

his findings to other engineers and students. Magnel's book Le Béton Précontraint (Prestressed Concrete) was translated to English and published in the United States. American engineers turned to him when planning to construct the first major prestressed concrete structure in the United States (Dinges, 2009). The first prestressing materials catalogue was published in America in 1951 by John A. Roebling and Sons Company, named "Roebling- Strands and Fittings for Prestressed Concrete" (Dinges, 2009).

The completion of the Walnut Lane Memorial Bridge in Philadelphia in 1951 was a landmark in the history of American prestressing. The challenging design of the long spans of the bridge and its successful design using prestressing had turned the attention of American engineers to prestressed concrete, inspiring them to improve prestressing techniques and materials.

The Prestressed Concrete Institute was established in 1954, during the decade when significant industry innovations were also developing, and prestressing techniques were becoming standardized (www.pci.org).

Charles Sunderland led extensive research on prestressing materials at John A. Roebling and Sons, and he was the inventor of the cold drawn stress relieved wire, which later led to the development of the stress relieved strand (Dinges, 2009). The prestressing industry continued to thrive with the development of the 7-wire strand, the introduction of the method of pre-casting, and usage of long-line beds.

In 1963, T.Y. Lin introduced the innovative Load Balancing Method, a design approach that simplified the design process considerably, making prestressed concrete projects less intimidating to the structural engineer. The Load Balancing Method relies on simply balancing the moment provided by the prestressing force at a certain location with the moment developed due to the loading condition, allowing analysis by conventional methods. Lin's Load Balancing Method is commonly used today in prestressed concrete design (Dinges, 2009).

The revolutionary invention of the low relaxation strand came towards the end of the 1970s, a key development for the prestressing industry. Low relaxation strand is the material that is most commonly used in prestressed concrete today, allowing for longer spans and also smaller sections, as it experiences highly reduced losses of prestress due to strand creep, compared to the conventional stress-relieved or normal relaxation prestressing strand.

2.3 Strand Manufacturing

Prestressing strands are manufactured daily at wire and strand manufacturing plants in the United States, to supply the American prestressed concrete industry. The raw material specified for the production of prestressed concrete wire and strand is a high carbon steel, AISI/SAE 1080 (Osborn, Lawler, & Connolly, 2008). Wire rods of nominal diameter between 3/8" and 1/2" are commonly used as the initial raw material in the strand manufacturing process, and arrive at the plants in coils, supplied by steel mills. Figure 2.2 shows several coils of raw steel, stored at a strand manufacturing plant as received from steel mills.

Figure 2.2 Raw Steel Coils used for Prestressing Strand Manufacturing

Since mill scale and rust is abundant on the surface of the wire rods initially, the first step at a strand manufacturing plant is either mechanical or chemical cleaning of the raw steel. The chemical removal of iron oxides from the surface of the wire rods is the most common

procedure, and it starts with a process called the pickling, beginning with dipping the steel in hydrochloric or sulfuric acid, and followed by rinsing it with water. The steel is then pre-treated with a textured carrier coating that will promote lubricant adherence during the drawing process that will follow (Hawkins & Ramirez, 2010).

Pre-treating is done by submerging the wire rod into a zinc phosphate solution, or other less commonly used coating materials like specialized polymers, borax, or lime, and then proceeding with rinsing of the rod in water and drying. After they are treated with phosphate, multiple wires of raw steel are welded together to form a longer coil before they enter a wiredrawing machine (Osborn, Lawler, & Connolly, 2008).

Once it enters the wiredrawing machine, the rod stock will be drawn down the eight or nine successively smaller carbide dies that the machine consists of, the cold-working process generating wire of diameter reduced by two-thirds, compared to the original raw steel rod diameter. Lubricants are introduced to the wire surface during this process as the wire is drawn through a lubricant box before each die. Part of the wiredrawing process is shown in Figure 2.3, a photograph taken at one of the North American strand manufacturing plants.

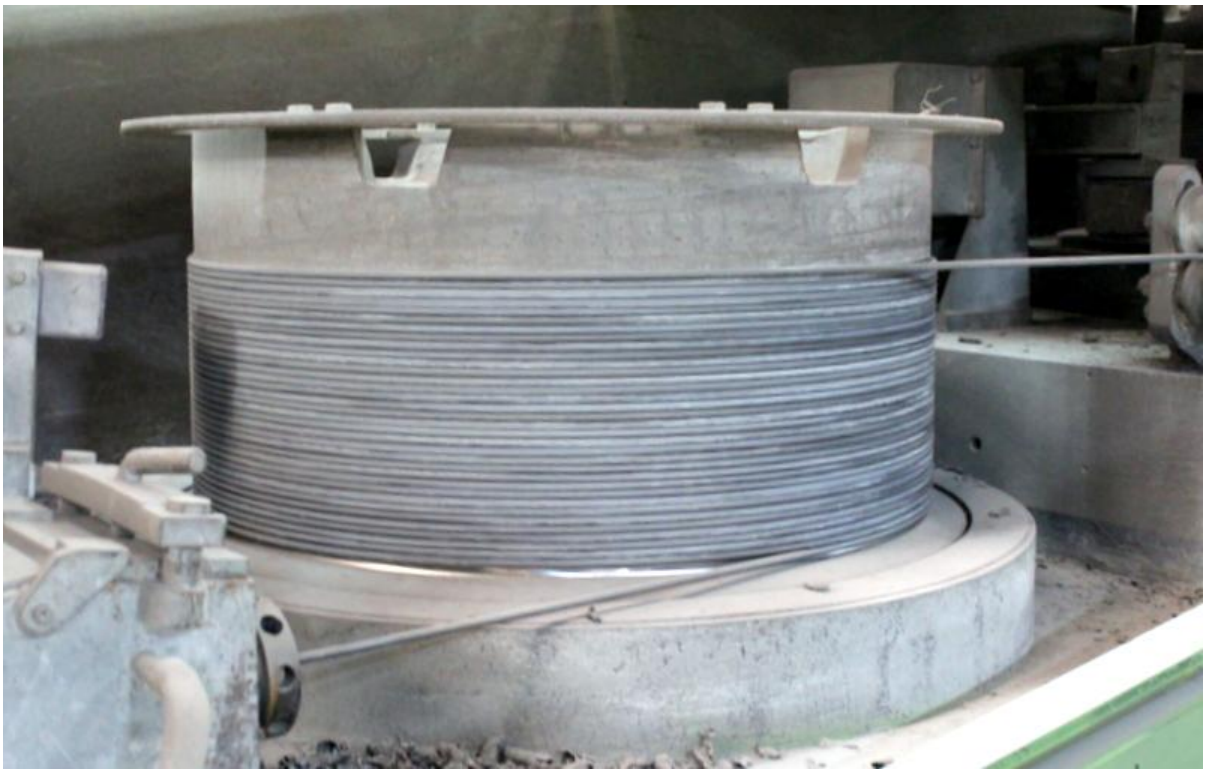

Figure 2.3 Wire Drawing Process during Strand Manufacturing

The wire-drawing lubricants used during this process are usually sodium stearate or calcium stearate, and might differ from plant to plant and even between successive dies of a wiredrawing machine, allowing the wire to go through multiple wiredrawing lubricants before it exits the machine (Hawkins & Ramirez, 2010). The lubricants act as barriers between the wire surface and the carbide drawing dies and therefore can postpone die wear-out, and at the same time control the frictional heat on the wire surface. A capstan exists for each die in order to pull the wire through the die, and both capstans and dies are water-cooled during the wiredrawing process, in order to protect the wire and wiredrawing lubricants, as both can be greatly affected by high temperatures (Osborn, Lawler, & Connolly, 2008). Figure 2.4 shows a wiredrawing die that was cut in half for illustration purposes, displaying the cross section of the die in figure 4a) and the top view of the die in figure 4b).

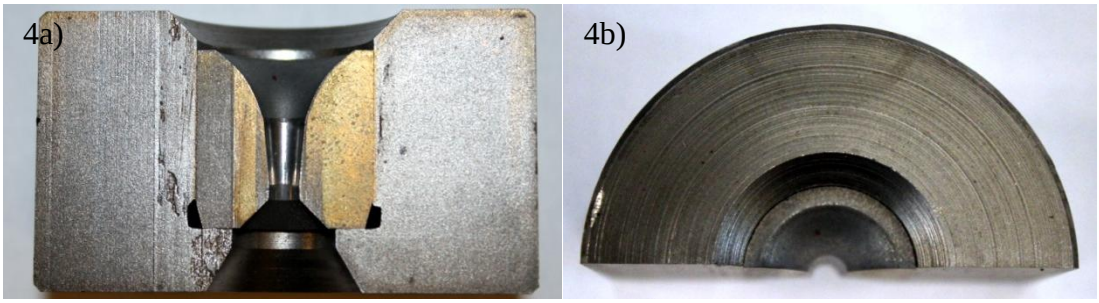

Figure 2.4 Cut Wire Die Cross Section (4a) and Top View (4b)

The wire rod that enters the wire drawing machine is typically 170 ksi ±5 ksi tensile strength, and after it gets drawn through the successive dies and has its diameter reduced to the standard diameter specified for its final use, the wire comes out with a tensile strength of 270 ksi ± 20 ksi, for grade 270 low-relaxation strand wires, which is a tensile strength increase of greater than 50% as a result of work hardening. For the case of ½" diameter, 7-wire strand, the specified diameter for the king wire is 0.174" ± 0.002", and has to be a minimum of 0.003" greater than the diameter of the 6 outer wires (Hawkins & Ramirez, 2010), (ASTM A416, 2010). Each individual wire is spooled at the end of the wire drawing machine, and once the seven spools of wire are produced, they are loaded into a skip strander, to proceed with stranding.

The stranding machine wraps the 6 outer wires helically around the king wire at a specified rate according to the final strand diameter, as specified by ASTM A416 (Osborn,

Lawler, & Connolly, 2008), (Hawkins & Ramirez, 2010). When the 7-wire strand is shaped, it will undergo a thermo-mechanical process, the critical step for the strand's stress relaxation properties.

During this step, the strand is drawn through an induction furnace at 700°F ± 80°F, continuously heating the strand while it's also under tension, relieving the residual wire drawing stresses and elongating the strand, to increase the strand's yield strength and convey it with low relaxation properties. Any remaining residual lubricants are then washed off; the strand is cooled and later looped back into a coil (Osborn, Lawler, & Connolly, 2008), (Hawkins & Ramirez, 2010).

Even though the mechanical properties of prestressed concrete strand and wires are controlled at wire manufacturing plants as prescribed by the corresponding specifications, the ability of prestressing steel reinforcement to bond to concrete has been of great concern to the industry during the last decades. The issue of prestressing strand not having uniform bonding capabilities was highlighted by a near failure of a structure in Texas in 1997, where thorough investigation concluded that the severe cracking on the prestressed double tees of the parking garage had occurred due to inadequate prestressing force at the ends of the members (Wiss, Janney, Elstner, & Associates).

Prestressing material of the same type and grade, with the only disparity among them being their plant of manufacture, were identified to have highly variable bonding performance in identical cementitious mixtures (Russell & Paulsgrove, NASP Strand Bond Testing Round I, 1999), (Russell & Paulsgrove, NASP Strand Bond Testing Round II, 1999), (Russell B. W., NASP Strand Bond Testing Round III), (Russell B. , NASP Round IV Strand Bond Testing, 2006), (Logan, 1997).

Dissimilar chemicals used as lubricants during the wire drawing process was one of the differences observed between strand manufacturing plants, and a possible influence on the strand bonding behavior. Another method that varies between manufacturing plants is heating during the stress relieving process, as the temperature ranges used vary between plants, affecting the degree of lubricant removal from the strand surface; and finally, the speed of winding the wires together varies according to the stranding machine that each plant is using, and that can affect the mechanical tightness of the strand and assembly of the king wire to the outer wires, affecting the

bonding capacity of the strand as a whole (Hawkins & Ramirez, 2010), (Osborn, Lawler, & Connolly, 2008).

It is widely accepted that the bond between steel and concrete is affected by the residual films of any lubricant and other contaminants not adequately removed from the strand surface during the final stages of the strand manufacturing process. The use of lubricants is essential to the wiredrawing process during strand manufacturing, and other contaminants cannot be controlled since the surface condition of the raw steel material will vary. The North American Strand Producers Association (NASPA) had suggested using the water soluble lubricant sodium stearate instead of calcium stearate in order to reduce the residual films remaining on the strand surface after manufacture, but strand bond problems were not eliminated (Osborn, Lawler, & Connolly, 2008).

The adequacy of strand bond is critical to the transferring of prestressing force into concrete members, and current codes include a distance called the transfer length, as well as a development length, depending on the characteristics of the strand utilized in the section. A structural engineer will design according to the code, assuming that the strand is fully bonded by the prescribed lengths, and therefore that the strand will develop its effective prestress by the transfer length, and achieve additional stress increase by the development length, as the structural member reaches its nominal strength. In the case where there is no sufficient bonding action between the strand and concrete material, the prestressing force will not be able to transfer into the concrete, and therefore the section will be lacking in capacity to sustain the loads it was designed for.

2.4 Transfer/Development Length Equations

In a prestressed concrete member, the prestressing force is transferred from the prestressing steel to the prestressed concrete member as the strands adhere to the concrete material along the length of the member. Analytical equations are provided in the American Concrete Institute (ACI) Building Code, which are intended to predict the distance it takes to fully transfer and develop the prestressing force from the prestressing strands into the concrete. The variation in steel stress along the development length of a prestressing strand is illustrated in Figure 2.5.

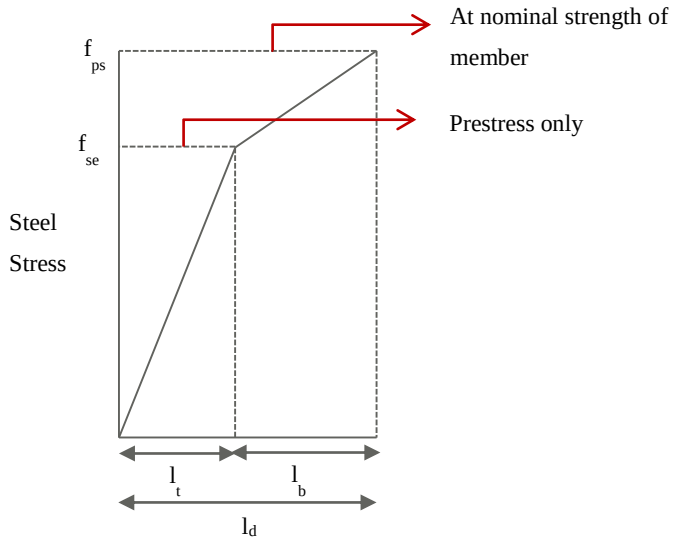

Figure 2.5 Variation of Steel Stress along Development Length

The transfer length, l_t, is defined as the distance from the edge of the concrete member to the point where the effective prestressing force is fully established into the concrete. The development length, l_d, is defined as the distance from the edge of the member to the point into the member where the strand stress can achieve additional increase at the ultimate capacity of the member. The development length consists of the transfer length and an additional distance called the flexural bond length, l_d.

It would be conservative to assume greater transfer lengths and greater development lengths, but this will only be a conservative assumption if the loads on the member are evenly distributed. For the cases where a point load is applied near the end of a prestressed member, it is very important to know exactly where the prestressing force is developed to ultimate stress level, and also where the prestressing force is fully transferred into the concrete. Predicting the bonding behavior of prestressing strand might be challenging, but inaccurate assumptions can be detrimental to structures and possibly life threatening.

It is therefore necessary to develop accurate expressions that will be reliable in calculating the transfer and development length required for prestressing forces to be transferred into cementitious materials by strands of known properties. The strands' ability to bond with the material will be a crucial factor in transferring prestressing forces, and even though some strand

samples share identical ASTM A416 properties, their bonding capabilities vary as shown by strand bond tests.

The expressions in the current ACI code provided for predicting the transfer length and development length are as shown in Equation 2-1 and Equation 2-2 respectively (ACI 318, 2011):

$$L_t = \left(\frac{f_{se}}{3}\right) d_b \qquad \textbf{Equation 2-1}$$

$$L_d = \left(\frac{f_{se}}{3}\right) d_b + \left(f_{ps} - f_{se}\right) d_b \qquad \textbf{Equation 2-2}$$

where f_{se} = effective stress in prestressing strand, ksi

f_{ps} = stress in prestressing strand at nominal strength, ksi

d_b = nominal strand diameter, in

The equations originate from the research findings of an experimental program conducted by Hanson and Kaar, published in 1959. In their report, Hanson and Kaar had recommended minimum embedment lengths per strand diameter; the actual equations were derived later by Dr. Alan H. Mattock, based on Hanson and Kaar's test results (Tabatabai & Dickson, 1995). The forty seven beams tested by Hanson and Kaar were prestressed with 1⁄4, 3⁄8 and 1⁄2 inch diameter strands. Eighteen of the beams were included in series 1 of the test program, where the effect of strand diameter and embedment length on bond performance was evaluated. Series 2 included nine beams, all prestressed with 3⁄8 inch diameter strand, but having variable concrete compressive strengths at roughly 3700 psi, 5400 psi, and 7200 psi, aiming to evaluate the effects of concrete compressive strength on strand bond performance (Hanson & Kaar).

The third series of the testing program was targeted towards determining the effect of varying the percentage of reinforcement used in a section, by comparing beams that included two, four, or six strands. Series 4 was geared towards indicating any effects of strand surface condition to beam performance, thus four pairs of beams were casted, each pair having one

section prestressed with a clean, smooth strand and the other section prestressed with a rusted strand of equal diameter (Hanson & Kaar).

The researchers found that the strand diameter and strand embedment length had significant influence on the value of bond stress where strand slipping occurred. It was also observed that when increasing the percentage of steel reinforcement by prestressing equivalent beam sections with two, four, and six strands, the occurrence of general bond slip was reduced even for embedment lengths that were lower than the required critical length. Hanson and Kaar indicated that with higher percentage of reinforcement, we have lower steel stresses as well as lower bond stresses at failure for a given embedment length (Hanson & Kaar).

The equation that Dr. Mattock had derived for the transfer length is the expression currently used and shown in equation 1, but in the case of the development length, Dr. Mattock had derived an equation which was modified by the ACI Committee in 1962, before it appeared in the code. Dr. Mattock originally proposed Equation 2-3 for development length (Tabatabai & Dickson, 1995).

$$L_d = (1.11\, f_{su} - 0.77\, f_{se})\, D \qquad \textbf{Equation 2-3}$$

where f_{se} = effective stress in prestressing strand, ksi

f_{su} = average stress in prestressing strand at ultimate load, ksi

$D = d_b$ = nominal strand diameter, in

The expression that Dr. Mattock had derived was modified by ACI to Equation 2-4 (Tabatabai & Dickson, 1995):

$$L_d = \left(\frac{f_{se}}{3}\right) D + (f_{su} - f_{se})\, D \qquad \textbf{Equation 2-4}$$

Since ACI adopted these equations in 1963, and the American Association of State Highway and Transportation Officials (AASHTO) followed in 1973 (Tabatabai & Dickson, 1995), numerous modifications have been proposed by researchers, in attempts to improve the accuracy of the equations, and account for the higher compressive strengths of the concrete used

in pre-tensioned applications, as well as the strand stress adjustments due to an evolving industry of strand manufacturing.

In 1976, and after studying a bond related failure of a pre-tensioned application, Martin and Scott noted that the adopted equations had to be reexamined. In Hanson and Kaar's study, on which the code equations were based, the strands were released slowly instead of the commonly used saw cut or flame cut methods that lead to sudden release of the prestress force. Because of this slow release method, the strand bonding behavior was not representative of the industry practice (Martin & Scott, 1976).

Martin and Scott also noted that the equations required reconsideration since the 270 ksi ultimate strength prestressing strand was becoming more popular at the time. The researchers also discussed the results obtained during series three of Hanson and Kaar's experimental program, where the percentage of prestressing reinforcement was varied, and had significant effects on the performance of the specimens. Strand bond slip had occurred at 90 percent of the average calculated design strength for the beams with the lowest percentage of steel used in the study, at an average of 0.31. This group of beams was the only one out of the three included in the study that would be of concern, since the percentage of reinforcement included in the other two groups was over the maximum percentage of steel allowed by code, considering typical concrete compressive strength of 5 ksi and prestressing strand of 270 ksi ultimate strength (Martin & Scott, 1976).

The researchers noted that it would be more common to have structural members with less than 0.31 percent steel, and thus implying that strand bond slip would occur before the section reaches 90 percent of its calculated design strength, according to Hanson and Kaar's findings (Martin & Scott, 1976).

Martin and Scott reevaluated existing test results from prior transfer and development length studies, and then proposed their code provisions, which implied a much more conservative expression for the transfer length, set to be equal to 80 times the diameter of prestressing strand, as seen in Equation 2-5.

$$L_t = 80\,D \qquad \textbf{Equation 2-5}$$

The original expression for the transfer length can be estimated as 50 times the strand diameter, assuming an effective steel prestress of 150 ksi. Martin and Scott's recommendation was based on the transfer length study published by Kaar, LaFraugh, and Mass in 1963, where the strands were released by flame cutting (Martin & Scott, 1976).

Researchers Zia and Mostafa had also published their recommended equations for the transfer length and flexural bond length, which were developed based on a linear regression analysis of the data that was available before 1977. Zia and Mostafa's equation for the transfer length allows for different concrete compressive strengths at release, initial prestressing forces and strand diameters to be accounted for, which was reviewed later in a study conducted by Cousins et al., and was found to be a more conservative expression than the equation adopted by ACI when it came to larger strand diameters.

$$L_t = 1.5\left(\frac{f_{si}}{f'_{ci}}\right)D - 4.6 \qquad \textbf{Equation 2-6}$$

Zia and Mostafa based their flexural bond length expression on experimental data from Hanson and Kaar's study, and recommended a 25 percent increase to the flexural bond expression of the development length equation adopted by ACI. Zia and Mostafa's recommended transfer and development length equations are shown in Equation 2-6 and Equation 2-7 (Cousins, Johnston, & Zia, Transfer and Development Length of Epoxy Coated and Uncoated Prestressing Strand, 1990).

$$L_d = 1.5\left(\frac{f_{si}}{f'_{ci}}\right)D - 4.6 + 1.25\,(f_{su} - f_{se})\,D \qquad \textbf{Equation 2-7}$$

Cousins et al. (1986) conducted a study that was specifically geared towards comparing the transfer lengths of epoxy-coated prestressing strands to transfer lengths observed for uncoated strands. It was conducted soon after epoxy-coated strands appeared in the market as a solution to steel strand corrosion. Single strand beam sections were tested, using 3⁄8, 1⁄2 and 0.6 inch diameter prestressing strands of various surface coating conditions. Transfer length readings were taken on 13 square beam sections which were prestressed with one concentric

strand. Transfer length readings were also taken on the 38 rectangular beams that were prestressed with a single strand at the lower kern point of the section. The beams were designed so that the maximum stress level in the concrete after transfer was approximately equal for the various configurations. The concrete compressive strength of these beams had an average of 4340 psi at release, and an average strength of 5580psi at 28-days from casting (Cousins, Johnston, & Zia, Transfer Length of Epoxy-Coated Prestressing Strand, 1990). This study showed that three types of uncoated prestressing strands tested required transfer lengths that were greater than the lengths predicted by the code equations (Cousins, Johnston, & Zia, Transfer Length of Epoxy-Coated Prestressing Strand, 1990), agreeing with the previous studies of Zia and Mostafa, and Martin and Scott (Cousins, Johnston, & Zia, Transfer Length of Epoxy-Coated Prestressing Strand, 1990) that the current ACI transfer length equation tends to underestimate the transfer length.

A controversy arose in the Precast/Prestressed Concrete Institute due to Cousins et al.'s findings, with some of the technical committee members insisting that the ACI code equation was adequate for all strands, and that the bond failures experienced were due to contaminants on the strand surface, that simply required cleaning. The rest of the committee members were in agreement with Cousins et al.'s findings, and as soon as the research material was published, the strand producers became alarmed. The situation gave birth to Saad Moustafa's Large Block Pullout Test (Jurakev, 2004).

In addition, the FHWA was alarmed, and went on to place strict limitations on prestressing strand (Tabatabai & Dickson, 1995). The memorandum published by FHWA in 1988 banned the use of 0.6 inch diameter strand in pre-tensioned applications, imposed a minimum strand spacing distance of 4 times the strand diameter, as well as a multiplier of 1.6 to the development length of fully bonded strands, and a factor of 2.0 to the development length of de-bonded strands (Akhnoukh, 2008), (Russell & Burns, Design Guidelines for Transfer, Development and Debonding of Large Diameter Seven Wire Strands in Pretensioned Concrete Girders, 1993). The restrictions imposed by FHWA required design revisions and equipment reformatting to the prestressing industry, causing inconvenience and additional expenses to precast companies at the time. Further investigation of the code equations followed in order to resolve the issues, and provide better recommendations for the use of 0.6 inch diameter strand.

Cousins et al.'s (1986) transfer length study observed that for both uncoated and epoxy-coated strands the transfer lengths increased with time, with the epoxy-coated strand transfer lengths experiencing slightly greater rates of increase. Epoxy-coated strands still never reached the longer transfer lengths of their equivalent uncoated strands. It was also found that the method used to release the prestressing force affects the beam transfer lengths. In Cousins et al.'s study, it was observed that the beam ends that were flame-cut for a sudden release of the prestressing force experienced transfer lengths 8 percent longer than their opposite beam ends that were saw-cut for gradual release of the force.

Cousins, Johnston and Zia develop analytical models for the transfer and development length equations, based on an elastic-plastic model. The analysis was made after extensive review of the existing equations and data from their own experimental program as well as previous studies; to propose new expressions in 1990, which applied to both uncoated and epoxy coated strands (Cousins, Johnston, & Zia, Transfer and Development Length of Epoxy Coated and Uncoated Prestressing Strand, 1990). The equations proposed by Cousins et al. were developed assuming that bond stress is proportional to slip for small displacements of the strand during the elastic zone, and also assuming that the bond stress will maintain a maximum yield value in what is called the plastic zone. The effects of the concrete compressive strength at the time of prestress transfer were incorporated into the transfer length expression since a review of prior research findings was indicating that bond strength is proportional to the square root of concrete compressive strength. The flexural bond length was also idealized in a similar way, but in this case assuming that the entire bond length is composed of a plastic zone since their data analysis showed that the elastic region could be neglected. The equation for the flexural bond length was derived based on the fact that over the plastic bond stress will be resisting the increase in strand force at the event of failure. The concrete compressive strength at the time of development length test was incorporated in the flexural bond length expression (Cousins, Johnston, & Zia, Transfer and Development Length of Epoxy Coated and Uncoated Prestressing Strand, 1990).

Cousins et al.'s 1990 model was first verified using the experimental data that the research group had obtained during their previous research program, where they compared the performance of uncoated and epoxy coated strand of 0.375, 0.5, and 0.6 inch diameter. The idealized bond stress, bond modulus, and strand stress factors included in the derived equations

were determined based on the experimental concrete strain data, and therefore the transfer and development lengths were calculated for the several specimens of Cousins et al.'s research program. The concrete compressive strengths for the transfer length specimens one day after transfer were consistently between 4100-4200 psi. Transfer lengths were also calculated for the specimens that were specifically fabricated for development length tests, using the average bond modulus obtained from the transfer length specimens. In this category, the compressive strength of the specimens one day after transfer ranged from 3890 psi up to 6720 psi. The researchers also applied their model to data from experimental studies conducted by other researchers in the past, including tests on 250 ksi as well as 270 ksi strands of 0.375, 0.5, and 0.6 inch diameter. The compressive strength at time of transfer is noted for every case, and the values vary between 3400 psi and 5500 psi. It should be noted that the model proposed by Cousins et al. was able to predict the transfer lengths obtained by other researchers, typically overestimating them by an average of about 20 percent. The equation proposed for the development length was not as accurate or consistent in predicting experimental data. The researchers explained that development length parameters should be verified with additional experimental data, and recommended the expressions shown in Equation 2-8 and Equation 2-9 for the transfer length and development length respectively (Cousins, Johnston, & Zia, Transfer and Development Length of Epoxy Coated and Uncoated Prestressing Strand, 1990).

$$L_t = 0.5\left(\frac{U'_t}{B}\right)\sqrt{f'_{ci}} + \left(\frac{f_{se}\,A_{ps}}{\pi D U'_t \sqrt{f'_{ci}}}\right) \qquad \textbf{Equation 2-8}$$

$$L_d = 0.5\left(\frac{U'_t}{B}\right)\sqrt{f'_{ci}} + \left(\frac{f_{se}\,A_{ps}}{\pi D U'_t \sqrt{f'_{ci}}}\right) + \left(\frac{(f_{ps} - f_{se})^* A_{ps}}{\pi D U'_d \sqrt{f'_{ci}}}\right) \qquad \textbf{Equation 2-9}$$

In a comparison of the existing experimental data and proposed transfer and development length expressions in the literature, Cousins et al. showed that the adopted ACI code equations, as well as the expression proposed by Zia and Mostafa, are not conservative for uncoated strands. It was also noted that Martin and Scott's transfer length equation was the most conservative for uncoated strand (Cousins, Johnston, & Zia, Transfer and Development Length of Epoxy Coated and Uncoated Prestressing Strand, 1990).

Shahawy et al. (1992) developed a transfer length equation after evaluation of their experimental findings from three research programs funded by the Florida Department of Transportation (FDOT) (Akhnoukh, 2008). Their equation proposed changing the ACI 318 transfer length equation by replacing the effective prestress stress term by the initial stress that the strands experience before prestress losses, as shown in Equation 2-10:

$$L_t = \frac{1}{3} f_{si} D \qquad \textbf{Equation 2-10}$$

Equations were proposed by researchers at Purdue, McGill University, and the University of Texas at Austin in 1993, and they were followed by a proposal published in the PCI Journal in 1994, made after experimental research was conducted by Deatherage et al. at the University of Tennessee at Knoxville, originally published in 1991 (Akhnoukh, 2008).

During the extensive study conducted at the University of Texas at Austin, and published by Russell and Burns in 1993, both 0.5 inch and 0.6 inch diameter strands were tested, and experimental data were compared to the ACI and AASHTO expressions, Shahawy's proposed equations, as well as to results from related studies performed during the early 1990s at other institutions. The authors had indicated that the expression previously proposed by Shahawy ($f_{si}/3*d_b$) was successful at predicting the behavior of strand embedded in the rectangular sections tested by Russell and Burns, but not for the rest of the specimens in the study (Russell & Burns, Design Guidelines for Transfer, Development and Debonding of Large Diameter Seven Wire Strands in Pretensioned Concrete Girders, 1993).

Russell and Burns tested strand in rectangular beam sections, as well as AASHTO-type beams and Texas Type C girders utilizing various strand configurations. The strands in Russell and Burns' study were initially tensioned to 202.5 ksi, and for most of the specimens, release of prestressing was accomplished 48 hours after casting, at concrete compressive strengths ranging between 3853 and 4792 psi (Russell & Burns, Design Guidelines for Transfer, Development and Debonding of Large Diameter Seven Wire Strands in Pretensioned Concrete Girders, 1993).

The first 18 single strand specimens were flame cut at full tension, but since this procedure caused damage to the specimens, the multiple strand specimens were flame cut after being de-tensioned gradually down to 70 percent of their full tension, and the transfer length readings from these specimens were closely correlated with the AASHTO-type beams and Texas

Type C girders which were also flame cut at 100% tension like the single strand specimens. The effects of strand diameter, strand spacing, de-bonding, size of cross section, and confining reinforcement on beam transfer lengths were investigated during Russell and Burns' study (Russell & Burns, Design Guidelines for Transfer, Development and Debonding of Large Diameter Seven Wire Strands in Pretensioned Concrete Girders, 1993).

During their transfer length study, Russell and Burns tested 65 specimens, including rectangular sections, AASHTO-type cross sections and also Texas type C girders. The authors did not investigate the effects of concrete compressive strength based on the conclusions made by Kaar, LaFraugh, and Mass that concrete compressive strength will not affect transfer length, even though they noted that preliminary findings from other research projects indicated that higher concrete compressive strengths result in shorter transfer lengths. Russell and Burns actually mentioned that for the few specimens included in their study that were below their specified concrete compressive strength, the transfer lengths were consistently longer than their equivalent beams that reached specified strengths (Russell & Burns, Design Guidelines for Transfer, Development and Debonding of Large Diameter Seven Wire Strands in Pretensioned Concrete Girders, 1993).

A very important finding from Russell and Burns' transfer length study was that for larger cross sections prestressed with greater number of strands, the transfer lengths were significantly shorter than specimens prestressed with fewer strands. The researchers determined that strand surface condition was the most effective variable on the transfer lengths (Russell & Burns, Design Guidelines for Transfer, Development and Debonding of Large Diameter Seven Wire Strands in Pretensioned Concrete Girders, 1993).

AASHTO-type girders as well as rectangular sections were tested during the development length study by Russell and Burns. Some of these specimens were prestressed with 0.5 inch diameter strands while others were prestressed with 0.6 inch diameter strands. The concrete compressive strengths for the beams prestressed with 0.5 inch diameter strands were between 5110 and 6790 psi, and for the beams prestressed with 0.6 inch diameter strands between 6260 and 7440 psi. The researchers determined the transfer lengths for their specimens using the 95% Average Maximum Strain method, a procedure that was established during Russell and Burns' research project 3-5-89-1210, "Influence of Debonding Strands on Behavior of Composite Prestressed Concrete Girders" (Russell & Burns, Design Guidelines for Transfer,

Development and Debonding of Large Diameter Seven Wire Strands in Pretensioned Concrete Girders, 1993).

The 95% Average Maximum Strain method is a transfer length determination procedure that is based on averaging the concrete strain readings that fall in or near the plateau of a fully effective prestress force, and taking the 95% of that average. The method might have been criticized because it doesn't take into consideration the fully effective concrete strain, but holds the advantage of predicting values that will be relatively free of arbitrary interpretation, and also provides the security that the projected value will not be significantly different in the case of including or excluding 1-2 points in error. The average transfer length reported for the 0.5 inch diameter strands tested during this study was 30 inches; and 40.9 inches for the 0.6 inch diameter strands (Russell & Burns, Design Guidelines for Transfer, Development and Debonding of Large Diameter Seven Wire Strands in Pretensioned Concrete Girders, 1993).

After comparing the behavior of 0.6 inch diameter strands that of 0.5 inch diameter strands tested in concrete specimens during Russell and Burn's experimental study, the authors reported similar transfer lengths as well as concrete strain profiles for the specimens prestressed with either size diameter strands, and concluded that the restrictions on the use of 0.6 inch diameter strands in pretensioned applications by the FHWA be reconsidered. The authors suggested that 0.6 inch diameter strands at 2 inch spacing be used with the same provisions as other size strands. Russell and Burns also found that strand bond failures will only occur when cracks propagate in the prestressing strand transfer zone. They concluded that the expression shown in Equation 2-11 should be used for the transfer length (Russell & Burns, Design Guidelines for Transfer, Development and Debonding of Large Diameter Seven Wire Strands in Pretensioned Concrete Girders, 1993).

$$L_t = \frac{1}{2} f_{se} D \qquad \textbf{Equation 2-11}$$

Development lengths were also determined during Russell and Burns' study, after static loading of both ends of each beam until failure. 28 tests were conducted on rectangular specimens as well as AASHTO type sections. The authors reported that the development lengths of 0.5 inch diameter strands in rectangular single strand specimens were much longer than

expected (Russell & Burns, Design Guidelines for Transfer, Development and Debonding of Large Diameter Seven Wire Strands in Pretensioned Concrete Girders, 1993).

By 1993, multiple proposals for transfer and development length equations were contradicting each other. The FHWA decided to review the existing data obtained from studies conducted across the United States, in an attempt to bridge the gap between the various recommended expressions for transfer and development length, in order to come up with a recommendation.

On behalf of the FHWA, Dr. Dale Buckner reviewed the existing expressions for the transfer length, and concluded that the equation that was proposed by Shahawy et al. after the FDOT studies was appropriate for estimating the transfer length. Dr. Buckner based his conclusion that the code equation was not conservative since the equation was derived based on the average bond stress of Grade 250 strands, and switching to Grade 270 meant a 6% increase in cross sectional area of strands compared to their equivalent Grade 250 strands of equal nominal diameter. The 6% larger cross sectional area of prestressing strands predicts 6% longer expected transfer lengths, and in addition to that, a 20% increase in transfer length would be expected for the case of low relaxation strands due to the higher strand stress that low relaxation strands experience after transfer (Buckner, 1995).

Dr. Buckner also reviewed the ACI code equation for the development length, as well as the major previously proposed development length expressions, and concluded by recommending an alternative equation based on his transfer length recommendations, and also Hanson and Kaar's variable bond stress approach. Dr. Buckner proposed a development length expression that is more conservative than the development length equation seen in ACI code, stating that the code expression was not adequately predicting the development length of prestressing strands, but failures were avoided since the development length does not prevail in prestressed concrete design. Dr. Buckner made a fair statement that a conservative expression for the development length is necessary, because sudden failures without adequate warning could occur in the possibility of shear related bond failures. Dr. Buckner added that both of his recommended expressions should be multiplied by a factor of 1.3 for any straight or draped strands that end up in the upper 1/3 of a member's depth and have 12 in. or more of concrete cast beneath them. Dr. Buckner's recommended expressions are shown in Equation 2-12 and Equation 2-13 respectively for the transfer and development length (Buckner, 1995).

$$L_t = \frac{1}{3} f_{si} D$$ **Equation 2-12**

$$L_d = \frac{1}{3} f_{si} D + \lambda (f_{su} - f_{se}) D$$ **Equation 2-13**

Following Dr. Buckner's report, the FHWA revisited their 1988 restrictions on 0.6 in diameter prestressing strand in pre-tensioned applications in a memorandum released in 1996. The use of 0.6 inch diameter strand was allowed at a spacing distance of 2 inches, while 0.5 inch diameter strands were specified to be spaced at 1.75 inches. The factor of 1.6 which was imposed on the code development length equation in 1988 was kept until further validation (Akhnoukh, 2008).

Gross and Burns reexamined the transfer and development length equations as they tested rectangular beams prestressed with 0.6 inch diameter strands. The strands were placed in rectangular beams that were14 inches wide by 42 inches deep, with six strands spaced at 2 inches in each beam. The beams were made using high performance concrete, and were designed for 6000 psi release strength, and 8000 psi 28-day strength (Gross & Burns, 1995). The average transfer length measured in this study was 14.3 inches, lower than the transfer lengths obtained by previous studies using high performance concrete. The average development length measured during Gross and Burns study was 78 inches. With experimental transfer and development lengths being lower than the lengths calculated by the code equations, the researchers concluded that the code expressions for both the transfer and development lengths were conservative. The short transfer lengths measured could be because the strand used had a rusty surface condition (Gross & Burns, 1995).

An experimental research program led by Susan Lane at the FHWA in 1998 was conducted in order to reevaluate the transfer and development length of prestressing strand. During this study, the effectiveness of multiple parameters was investigated, some of which were included into the transfer and development length expressions that they proposed. During the first phase of the study, 50 rectangular beam specimens were tested, containing either one or fours strands, and these were with 3/8 inch diameter, 0.5 inch, or 0.6 inch diameter strands, uncoated or epoxy-coated (Lane, 1998). The second phase of this study incorporated testing 270 ksi low relaxation strand in normal strength as well as high strength concrete AASHTO type II

girders. 0.5 inch or 0.6 inch diameter strands were used in the study, embedded in the girders in 3 patterns. Patterns R and T girders included 8 strands, while pattern S girders included 9 strands in a single row at the bottom flange of the beam. The study included 6 of each pattern R and T girders, and 4 pattern S girders. Flame cutting was used to de-tension all of the specimens in this study. A 30 percent increase in transfer length was observed between the strand release and 28 days for the beams prestressed with uncoated strands. This mirrors the transfer and development length increase also reported by Russell and Paulsgrove. The recommended expressions for the transfer length and development length from this study are shown in Equation 2-14 and Equation 2-15 (Lane, 1998).

$$L_t = \frac{4 f_{pt}}{f'_c} D - 5 \qquad \textbf{Equation 2-14}$$

$$L_d = \frac{4 f_{pt}}{f'_c} D - 5 + \frac{6.4 (f_{su} - f_{se}) D}{f'_c} + 15 \qquad \textbf{Equation 2-15}$$

A new development length expression was proposed in 2001 by Shahawy, and was based on the test results from previously led test programs that took place at the FDOT structures research center. Shahawy performed an evaluation of the development length tests conducted on solid and voided prestressed slabs, AASHTO Type II Girders, and prestressed concrete piles. The solid and voided slabs were tested under static loading conditions, with the incremental loads applied at varied locations up to failure. AASHTO Type II girders of 3 different strand configurations were tested at FDOT, by application of a single concentrated load also applied incrementally to failure. It was observed that shear cracking at the end regions of the girders affected the bond behavior of prestressing strand. Prestressed concrete piles of 6 different configurations were also tested up to failure by applying an incremental point load at various distances from the support (Shahawy, 1999). Shahawy recommended the development length expression shown in Equation 2-16 (Akhnoukh, 2008):

$$L_d = \frac{1}{3} f_{si} D + \frac{(f_{ps} - f_{se}) D}{1.2} + K \qquad \textbf{Equation 2-16}$$

An evaluation of the code requirements for 270 ksi, 0.6 inch diameter prestressing strand was made by Kose and Burkett. In this study, fully bonded as well as de-bonded 0.6 inch diameter strands was used in AASHTO-Type II beams of various concrete strengths, in order to investigate the effects of concrete compressive strength on the transfer and development lengths of prestressing strands. The research program goal was to establish a new basis for transfer and development length code requirements, taking into account that high strength concrete is more commonly utilized in the industry during recent years (Kose & Burkett, 2005).

In Kose and Burkett's study, three groups of beam specimens were tested at Texas Tech University, and t University of Texas at Austin. The 3 groups of beams were designed to range in the following categories; 5000-7000 psi, 9500-11500 psi, and 13000-15000 psi. Specimens were divided into subgroups according to the percentage of de-bonded reinforcement in the section, and whether the surface of the strands used in the member was bright or rusty. The experimental transfer and development lengths were compared to the ACI code equations, AASHTO LRFD standard, and also Buckner's and Lane's proposed expressions. In only one case, the short term transfer length (at release) was exceeding the ACI code value, and none exceeded the AASHTO LRFD requirements, Buckner's or Lane's predictions. It was observed that strand de-bonding increases the development length of the strand, and that the code equations overestimate the development length of fully bonded prestressing strands (Kose & Burkett, 2005). The equations proposed by Buckner and Lane were characterized as very conservative for the case of fully bonded strands but less conservative for the case of de-bonded strands (Kose & Burkett, 2005). Kose and Burkett went on to propose alternative expressions for both the transfer length and development length, based on their findings (Akhnoukh, 2008).

In 2008, a report for the National Cooperative Highway Research Program was published by Ramirez and Russell, after completion of the NCHRP Project 12-60. The authors were concerned that the current code expressions do not include the factor of concrete compressive strength, which was found to affect significantly the transfer and development lengths measured during the NCHRP Project 12-60, a finding that came to confirm the results published previously by researchers who conducted experimental programs before Ramirez and Russell's study (Ramirez & Russell, 2008).

Ramirez and Russell specified that the adopted transfer and development length equations are capable of predicting bonding behavior of prestressing strands embedded in normal

strength concrete of 4 ksi release strength. The authors tested both 0.5 inch and 0.6 inch diameter strands in concrete specimens with release strengths that varied from 4 ksi to 10 ksi. It was found that there was correlation between Ramirez and Russell's tests results and the NASP Bond Test, also developed by Russell before the NCHRP study, and just recently adopted by ASTM as ASTM A1081 (ASTM A1081, 2012).

For the purpose of this study, the NASP Bond Test was modified in order to utilize concrete instead of mortar, and the authors were able to develop relationships between the standard mortar NASP test and the modified concrete NASP test, and therefore conclude with expressions that are able to estimate the standard mortar NASP pullout test values for prestressing strands, according to the concrete strength of the specimen they are tested in. The transfer length data from the NCHRP Project 12-60 showed that the transfer lengths are inversely related to the concrete release strength, and concluded with a proposed expression for the transfer length which is shown in Equation 2-17 (Ramirez & Russell, 2008):

$$L_t = \frac{120\ \mathrm{D}}{\sqrt{\mathrm{f'_{ci}}}} \geq 40\ \mathrm{D} \qquad \textbf{Equation 2-17}$$

Ramirez and Russell's data analysis indicated that the development length also reduces with increasing concrete release strengths, and the authors proposed an expression for the development length as well, shown in Equation 2-18 (Ramirez & Russell, 2008).

$$\left[\frac{120}{\sqrt{\mathrm{f'_{ci}}}} + \frac{225}{\sqrt{\mathrm{f'_{c}}}}\right]\mathrm{D} \geq 100\ \mathrm{D} \qquad \textbf{Equation 2-18}$$

The original code equations as well as many of the expressions proposed throughout the years and some of the modifications adopted by ACI and AASHTO are listed in Table 2-1.

Table 2-1 Code Adopted and Proposed Equations for Transfer and Development Length

	Transfer Length, L_t	Development Length, L_d
Alan Mattock 1962	$\frac{1}{3} f_{se} D$ [2-1]	$(1.11 f_{su} - 0.77 f_{se}) D$ [2-3]
ACI 318 1963	$\frac{1}{3} f_{se} D$ [2-1]	$\frac{1}{3} f_{se} D + (f_{su} - f_{se}) D$ [2-4]
Martin and Scott 1976	$80 D$ [2-5]	
Zia and Mostafa 1977	$1.5 \left(\frac{f_{si}}{f'_{ci}} \right) D - 4.6$ [2-6]	$L_t + 1.25 (f_{su} - f_{se}) D$ [2-7]
FHWA 1988		$1.6 [\frac{1}{3} f_{se} D + (f_{su} - f_{se}) D]$
Cousins et al. 1990	$0.5 \left(\frac{U'_t}{B} \right) \sqrt{f'_{ci}} + \left(\frac{f_{se} A_{ps}}{\pi D U'_t \sqrt{f'_{ci}}} \right)$ [2-8]	$L_t + \left(\frac{(f_{ps} - f_{se}) * A_{ps}}{\pi D U'_d \sqrt{f'_{ci}}} \right)$ [2-9]
Shahawy 1992	$\frac{1}{3} f_{si} D$ [2-10]	
Abdalla et al. 1993		$\frac{1}{3} f_{se} + 1.7 (f_{ps} - f_{se}) D$
Mitchell et al. 1993		$0.33 f_{si} D \sqrt{\frac{3}{f'_{ci}}} + (f_{ps} - f_{se}) D \sqrt{\frac{4.5}{f'_c}}$
Russell and Burns1993	$\frac{1}{2} f_{se} D$ [2-11]	
Deatherage et al. 1994		$\frac{1}{3} f_{si} D + 1.5 (f_{ps} - f_{se}) D$
Buckner 1995	$\frac{1}{3} f_{si} D$ [2-12]	$L_t + \lambda (f_{su} - f_{se}) D$ [2-13]
Lane 1998	$\frac{4 f_{pt}}{f'_c} D - 5$ [2-14]	$L_t + \frac{6.4 (f_{su} - f_{se}) D}{f'_c} + 15$ [2-15]
Shahawy 2001		$\frac{1}{3} f_{si} D + \frac{(f_{ps} - f_{se}) D}{1.2} + K$ [2-16]
Ramirez and Russell2008	$\frac{120 D}{\sqrt{f'_{ci}}} \geq 40 D$ [2-17]	$\left[\frac{120}{\sqrt{f'_{ci}}} + \frac{225}{\sqrt{f'_c}} \right] D \geq 100 D$ [2-18]

The transfer and development length for a common set of assumed conditions was calculated for each of the equations given in Table 2-1. The assumed values for these equation factors were selected based on the beam study conducted by Kansas State University at Stresscon Inc., with the exception of the values for the expressions U'_t, U'_d and B, which are taken as suggested by Cousins et al (Cousins, Johnston, & Zia, Transfer and Development Length of Epoxy Coated and Uncoated Prestressing Strand, 1990). Table 2-2 lists the symbol, description, and assumed value substituted for each of the equation factors, in order to calculate the transfer and development length expressions.

Table 2-2 Equation Symbol Description and Assumed Values for Numerical Representation of Adopted and Proposed Transfer and Development Length Equations

Symbol	Description	Assumed value
D	nominal diameter of prestressing strand	0.5 in
A_{ps}	cross-sectional area of prestressing strand	0.153 in^2
f_{se}	effective stress in prestressing strand after losses	184 ksi
f_{su}	ultimate strength of prestressing strand	270 ksi
f_{ps}	stress in prestressed reinforcement at nominal strength	263 ksi
$f_{pi}= f_{si}$	initial stress in strand before losses	198 ksi
f'_{ci}	concrete compressive strength at transfer	3500 psi
f'_c	28-day concrete compressive strength	6000 psi
U'_t	plastic transfer bond stress	6.7
U'_d	plastic bond stress for development	1.32
B	bond modulus	300 psi/in
$\lambda=0.72+(0.102*\beta_1* f'_c*b*d_e)/(f_{ps} * A_{ps})$, where:	multiplying factor applied to flexural bond length	
β_1	ratio of depth of equivalent rectangular stress block to depth of neutral axis	0.75 for f'_c= 6000 psi
B	width of compression face of member	6.5in
d_e	effective depth from compression face to center of gravity of prestressed reinforcement in tension zone	10 in

The listed transfer and development length equations are summarized in Figure 2.6 and Figure 2.7 respectively, where the actual lengths are plotted according to the year that the corresponding expression was proposed or adopted by code. The last column represents the average of all the proposed/adopted equation values shown.

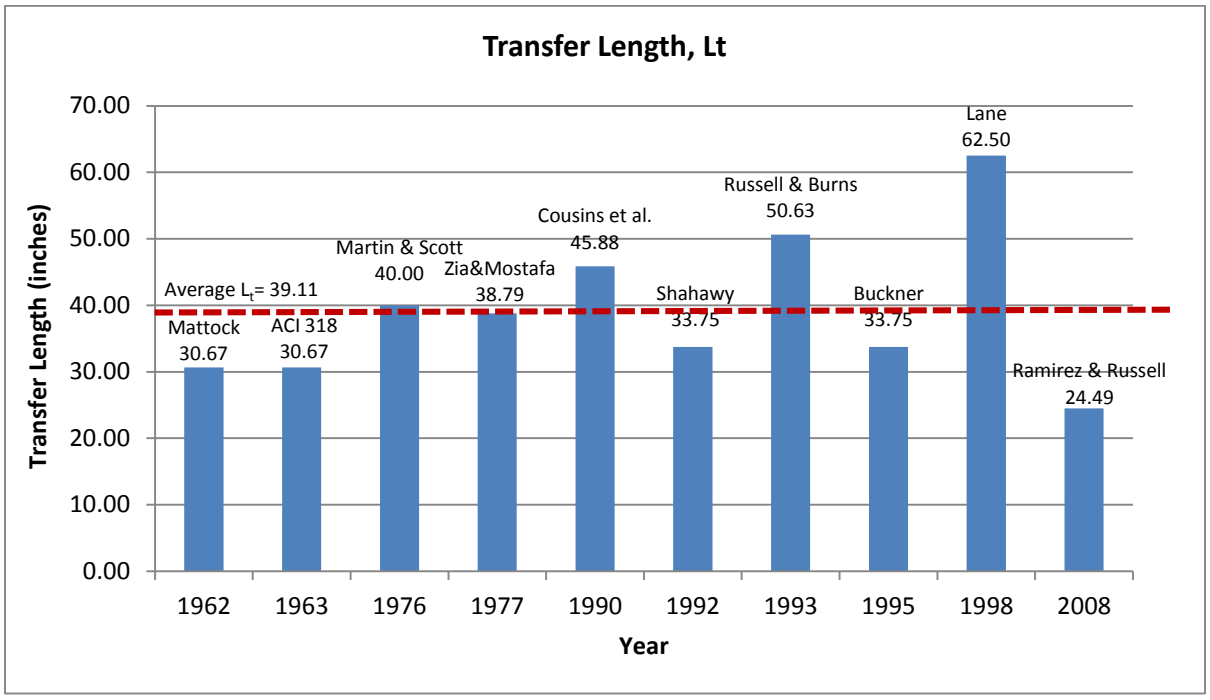

Figure 2.6 Adopted and Proposed Transfer Length Expressions by Year

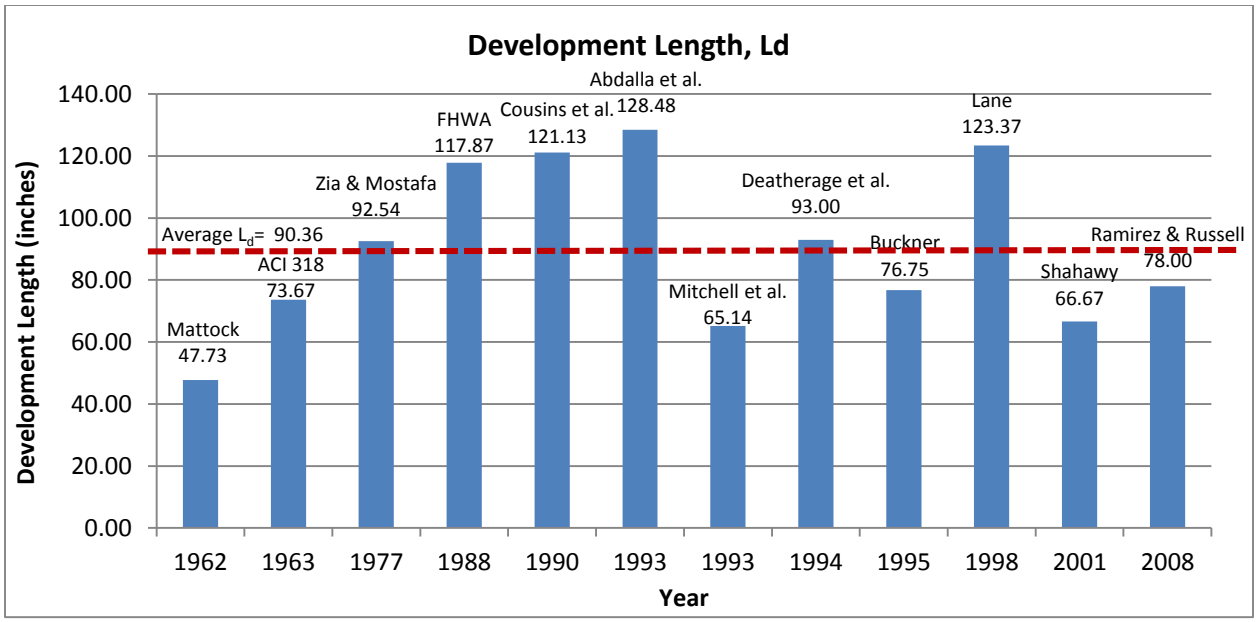

Figure 2.7 Adopted and Proposed Development Length Equations by Year

2.5 Strand Testing

The most accurate way to evaluate strand bond performance is through testing a beam's transfer length, but since this is not a cost or time effective method, various pull-out test procedures have been suggested throughout the years, with the latest method being accepted by ASTM International in 2012 as the "Standard Test Method for Evaluating Bond of Seven-Wire Steel Prestressing Strand", and designated ASTM A1081/A1081M-12 (ASTM A1081, 2012). There have been concerns that with simple pullout testing of un-tensioned strand it is not possible to predict bonding performance in a pre-tensioned beam, but experimental programs have shown correlation between simple pullout test results and beam transfer lengths. Pullout testing of un-tensioned strand is actually a conservative way to evaluate strand bond, since the frictional bonding benefits observed in tensioned applications due to the Hoyer's effect are not encountered.

The oldest pullout test proposed as a 7-wire strand bond acceptance test was performed by Dr. Saad Moustafa in 1974 at Concrete Technology Corporation (CTC), and therefore named the Moustafa test. This un-tensioned strand pullout test was performed on 0.5 in diameter strands, to determine if they had enough capacity to be used as lifting loops. The test incorporated pulling strand specimens that were embedded into a concrete block, utilizing a

hydraulic jack, which was driven by an electric powered hydraulic pump. An 18-inch length of the strand specimens was embedded into the hardened concrete, and pulled during a process that lasted less than 2 minutes. CTC and Dr. Saad Moustafa conducted a second round of Moustafa pullout tests in 1992, this time to address a lifting loop failure that took place at CTC, and also the anchorage failures observed abundant in the rock anchor industry at the time (Rose & Russell, 1997).

In the meantime, tensioned pullout tests were performed by Brearly and Johnston, the results published in the Journal of Structural Engineering in 1990. These tensioned pullout tests involved having 12 inches of strand samples embedded into single strand specimens, pulled at a much slower rate compared to the Moustafa test; and even allowing for complete strand slipping between pulling load increments. The tensioned pullout test was slightly altered by Cousins, Bateaux and Moustafa for their series of tests that was reported in the PCI Journal in 1992, while another series of tensioned pullout test results was published in the ACI journal in 1993, by Abrishami and Mitchell, who also slightly altered the original procedure for the tensioned pullout test. All three versions of the tensioned pullout test had a strand embedment length of 12 inches, and conducted using the slow pulling approach. The results from the three tensioned pullout test versions revealed that slower pullout rates implied lower ultimate pullout forces (Rose & Russell, 1997).

In 1997, Rose and Russell published their findings from an experimental program that was aiming to identify the method that could predict strand bond behavior most accurately, by comparing the simple or un-tensioned pullout test method known as the Moustafa test, and the tensioned pullout test, along with the measured strand end slip method. It was concluded that the tensioned pullout test proposed was not able to predict prestressing bond, and the researchers recommended further testing towards development of a simple pullout test procedure based on the Moustafa test, which proved to predict the bond performance of strand in a previous study conducted by Logan in 1994 (Rose & Russell, 1997).

Succeeding these findings, an extensive study was funded by the North American Strand Producers (NASP), the main objective of which was to evaluate three existing untensioned strand test methods, and determine the most reliable method to be adapted for testing ½ inch diameter 7 wire prestressing strand bond. Along with the Moustafa test, the investigation included the PTI pullout test, as well as the Friction Bond test.

What is known as the PTI pullout test or the Prestressing Strand Bond Capacity Test is the procedure used by the Post-Tensioning Institute (PTI) to test the bonding capabilities of 0.6 inch diameter prestressing strand in grout, which is used in prestressed ground anchors. This procedure is now established as ASTM A981 or the Standard Test Method for Evaluating Bond Strength for 0.6 inch Diameter Steel Prestressing Strand, Grade 270, Un-coated, used in Prestressed Ground Anchors. The PTI pullout test incorporated testing individual strand samples casted in 5 inch outer diameter steel grout cylinders, with force applied on the specimens at a rate of 0.1 inch/minute by a hydraulic or mechanical jack at the lower end of the specimen. The outcome of this procedure was the force reading that produced a displacement of 0.01 inches at the unloaded end of the specimen, which indicated the strand's bond strength (Russell & Paulsgrove, NASP Strand Bond Testing Round I, 1999).

The third pullout test procedure evaluated by the NASP study was the Friction Bond Pullout Test. In the case of the Friction Bond Test, the strand specimens are pulled in tension without being casted into cementitious material. Two bare lengths of a strand sample are mechanically spliced together, and put under tension as a hydraulic cylinder moves the upper cross head of the testing setup until failure of the mechanical splice. The test outcome is the maximum tensile load applied on the specimen (Russell & Paulsgrove, NASP Strand Bond Testing Round I, 1999).

The first round of the NASP study was completed in 1999 at the University of Oklahoma, led by Professor Bruce Russell. During the first round of the study, 11 strand samples were tested, with one round of the Moustafa pullout tests performed at Stresscon Corporation in Colorado Springs, CO, and two rounds of the Moustafa pullout test performed in Jacksonville, FL by Florida Wire and Cable (FWC). The PTI pullout tests were also performed by FWC, and finally the steel to steel friction bond tests were performed at the University of Oklahoma. Analysis of the Moustafa test results indicated that the results were highly biased by their test location, since there was inconsistency between the two laboratories with the Stresscon results being consistently higher than the FWC results (Russell & Paulsgrove, NASP Strand Bond Testing Round I, 1999).

The Moustafa pullout test method proved to be generally effective in ranking the strands' bond performance relative to one another, but was considered to be improper for strand acceptance as some samples would be inconsistently accepted or rejected depending on their

testing laboratory. The PTI pullout test method was also characterized as reliable in ranking the strands' relative bond performance, but the Friction Bond Test was found to be unable to differentiate the strands' bond performance properly (Russell & Paulsgrove, NASP Strand Bond Testing Round I, 1999).

In conclusion, the authors identified that all three tests were unable to adequately measure the prestressing strands' bonding capacities, and recommended an ongoing investigation in order to improve the Moustafa test, and generate alternative procedures so that the variability of the existing Moustafa test method and the PTI test method would be diminished (Russell & Paulsgrove, NASP Strand Bond Testing Round I, 1999).

A second round of the NASP study followed, where the existing Moustafa and PTI tests were investigated along with a new proposed version of the test called the NASP pullout test. The NASP pullout test procedure is similar to that of the PTI pullout test, but instead of using grout to cast the strands in, sand-cement mortar is used for the NASP pullout test. Additionally, for the NASP pullout tests the load on the strand specimen was recorded not only at 0.01 inch strand slip, but also at 0.1 inches strand slip, as well as maximum load.

Nine different strand samples were tested overall during the second round of the NASP study, with testing taking place at the following sites; Moustafa pullout tests were run at Stresscon Corp., Colorado Springs, Colorado; at Florida Wire and Cable, Inc., Jacksonville, Florida, and also at the University of Oklahoma, Norman, Oklahoma. The PTI pullout tests were performed at Florida Wire and Cable, Inc., Jacksonville, Florida, and at the University of Oklahoma, Norman, Oklahoma; the two locations were the NASP pullout test series were also performed.

The researchers found that all three of the test methods were able to differentiate between strands of good quality bond and those of poor quality bond. The NASP pullout test method performed more consistently than the Moustafa and PTI test methods, where the PTI method presented the greatest variability within the three. It was also noted that for both the NASP and PTI test methods, variability increased significantly when measurements were taken at 0.01 inch end slip instead of 0.1 inch. Russell and Paulsgrove recommended that the NASP test method be advanced further for the development of a strand acceptance test for measurements at 0.1 inch (Russell & Paulsgrove, NASP Strand Bond Testing Round II, 1999).

A third round of the NASP study followed, aiming to investigate the repeatability and reproducibility of the three pullout test methods, as well as to define a minimum threshold for bond as tested by the pullout methods. The study involved running the three pullout test methods at multiple laboratories, and also correlating the test results to transfer and development length tests as a basis for determining the threshold.

Ten strand groups were used in the third round of the NASP study, and were tested by the three pullout test methods. Four out of the ten strand groups were selected based on their pullout test performance, and used in prestressed concrete beams to implement transfer and development length testing.

Four beams per strand group were cast for the execution of the concrete beam testing program. Strand end slip readings were taken at various ages, and therefore transfer lengths were calculated accordingly. The beams were later loaded to failure and tested at various embedment lengths, thus flexural bond and strand development were investigated.

The Moustafa pullout tests, PTI bond tests, and the NASP pullout tests were performed at Florida Wire and Cable (FWC), as well as at the University of Oklahoma. For both the PTI and NASP pullout test series, the researchers had analyzed data at 0.01 inch and 0.1 inch end slip, along with the maximum pullout force case for each strand source.

Russell and Paulsgrove reported that the strand source that performed the most poorly in the pullout testing series had the longest end slips and therefore transfer lengths at 28 days, and as expected, the strand source the performed the best during the pullout testing series was the one with the shortest end slips measured and therefore the shortest transfer lengths at 28 days.

The Moustafa test data and the PTI bond test data at 0.01 inches indicated that the two methods are not capable of ranking strand sources consistently amongst multiple laboratories, while the NASP test at 0.1 inches was the most consistent in ranking the ten strand sources between the two testing sites. The results from the third round of the NASP study had confirmed the researchers' findings during the second round; the NASP pullout test was shown to be the most reliable method in ranking strand sources consistently at multiple laboratories.

In addition to the inconsistent ranking of strands between laboratories, low correlation of the pullout test results to the calculated transfer lengths for the four strand sources that were tested in beams had shown that the Moustafa pullout test was not a reliable method in predicting strand bond performance.

For the case of the PTI bond test, correlation was evaluated between results from the pullout tests at 0.1 inch end slip and beam transfer lengths. The data indicated strong correlation when transfer lengths were correlated to PTI bond test results from Florida Wire and Cable, and weak correlation when compared to PTI bond test results from the University of Oklahoma. The researchers concluded that the overall correlation of the PTI test values to the transfer lengths was not significant, and therefore the test proved unreliable in predicting strand bond performance as well.

The NASP pullout test results had the highest correlation to the transfer length values, when compared to the other two strand bond predicting methods. The NASP test at 0.1 inch end slip was also more consistent amongst test sites, therefore the researchers concluded that it was the most reliable method to predict strand bond performance, and recommended further exploration of the new pullout testing method before adaptation.

The development length testing conducted on beams during the third round of the NASP study revealed that the beams that met their nominal flexure capacities when tested at 100% of the development length were prestressed with strands that tested at a minimum of 7,300 lb NASP pullout test load at 0.1 inch displacement as an average of six specimens, and at 5,500 lb NASP pullout test load at 0.1 inch displacement as a result for individual strand specimens (Russell B. W., NASP Strand Bond Testing Round III).

Before the NASP study proceeded with a fourth round of testing, another study was conducted at the University of Arkansas, and was focused on comparing the repeatability and practicality of the NASP test method to the Moustafa or Large Block Pullout Test (LBPT), and findings were published in August 2005. During this research program, six strand types were tested using the two pullout test methods, and conclusions were drawn that both test methods were able to reliably distinguish between high, middle, and low bond performing strands, and noted that the two methods showed similar coefficients of variation. Furthermore, it was discussed that the Large Block Pullout Test involves the use of heavy equipment and therefore it will be difficult to perform at many laboratories, and was considered a less practical procedure (Sobin, 2005).

Succeeding these conclusions, results from the fourth round of the NASP study were published by Russell in 2006. The last round of the study was focused on developing the NASP

bond test, and performing round robin test trials at three laboratories; those of Oklahoma State University, Purdue University, and the University of Arkansas.

During the first part of the fourth round of the NASP study, the effects of the mortar compressive strength, testing with load control versus displacement control, mortar mixture flow, loading rate of displacement controlled tests, as well as the effects of curing temperature were investigated as part of the test protocol refinement process.

The results from Oklahoma State University revealed that using a different cement source, even at consistent mix proportions can alter the mortar mixture compressive strength values, therefore it was added that trial batches should be made every time a new cement source is introduced. Furthermore, it was shown that the mortar compressive strength is inversely related to the water to cement ratio. It was also indicated that the mortar mixture flow increases with increasing water to cement ratios, and decreases significantly over time which proved that for consistent mixture flows the measurements should be completed as soon as possible after mortar mixing.

Specimen curing temperature increase was able to raise the compressive strength of the samples as expected, therefore maintaining a consistent curing environment in the laboratory is crucial. Another finding, the fact that fresh unit weight did not assist in predicting mortar mixture properties, encouraged the author to avoid setting any limits regarding mortar unit weight to the NASP test protocols.

The mortar mixture compressive strength was indeed a critical factor to the NASP test results. The higher the compressive strengths, the higher the pullout test results, especially for the better bonding strand samples. It was reported that various types of strands can be differentiated and ranked more easily when the samples obtain higher compressive strengths.

As far as the testing methods are concerned, it was recommended to keep testing the NASP specimens by displacement controlled loading. The effect of different loading rates as a result of variable testing frame stiffness was also investigated, but no significant correlation was observed.

A third version of the test was published; the “official version” of the bond test which was adopted in 2006 by the North American Strand Producers. The test protocol had undergone sample preparation and testing procedure modifications since the initial protocol of 2001, but the basic testing procedure remains unchanged.

The second part of this fourth round of the NASP study was basically a round robin test series where test results from Oklahoma State University were compared to results from Purdue University and the University of Arkansas. Data analysis showed that the NASP test is a reproducible strand bond test amongst testing sites and materials (Russell B. , NASP Round IV Strand Bond Testing, 2006).

The final version of the test protocol was recommended by the author to be adopted as the Standard Test for Strand Bond, and it was finally accepted by ASTM in 2012 as ASTM 1081, the "Standard Test Method for Evaluating Bond of Seven-Wire Steel Prestressing Strand" (ASTM A1081, 2012).

Soon after the final NASP study report was released, Russell along with Julio Ramirez of Purdue jointly worked for the National Cooperative Highway Research Program to publish NCHRP report 603, where they recommended the addition of the NASP test method to the AASHTO LRFD bridge design guide, as a standard test for prestressing steel strand bonding properties. The authors had also introduced and recommended new transfer and development length equations, which included factors to account for concrete compressive strength, a property that was found to affect the bonding behavior of strands in previous research.

In the NCHRP report 603, Russell and Ramirez also reported minimum threshold values to be taken into consideration when qualifying prestressing strand by the NASP test method. It was recommended that the minimum pullout test average result of 10,500 lb should be reached by any set of six 0.5 inch diameter strand samples for the strand to be qualified. At the same time, the minimum individual strand sample threshold was set at 9000 lb for 0.5 inch diameter strands. When 0.6 inch diameter strand samples are tested for bond properties by the NASP test, the researchers recommended that a minimum threshold for acceptance should be at 12,600 lb as an average of the 6 individual strand samples tested, and at 10,800 lb for any individual 0.6 inch diameter sample (Russell & Ramirez, NCHRP Report 603, 2008).

In the meantime, a due diligence review of the NASP Strand Bond Test was performed by Hawkins and Ramirez, who were hired by the Prestressed Concrete Institute Committee on Research and Development shortly after the NASP Study was completed. In addition to the due diligence review of the test method, an objective of the study was to provide a minimum NASP test value for strand acceptance.

The researchers performed an intensive assessment of the NASP study rounds three and four, as well as the results from Bruce Russell's NASP tests which were performed subsequently to the study for the benefit of strand producers. In addition, they reviewed the work that was included in NCHRP report 603 and NCHRP report 621.

Within their conclusions, the authors reported that the NASP test method was proven by the NASP and NCHRP studies to be a reliable test method for the bonding properties of prestressing strand; as the final NASP test method version was able to differentiate strands in their ability to meet the ACI development length requirements.

The researchers added that the stress-strain properties of the strand should be reported in order for the yield and post-yield behavior of strand to be explored before concluding that strands will develop additional development length under these conditions after reaching their transfer lengths. They also recommended that additional testing should be performed in order to determine the ability of strands to attain increase in their transfer lengths with time.

Regarding the development length testing of beams reported in the NASP round three and NCHRP 603 reports, the authors noted that the resulting numbers were not adequate to support reasonable minimum criteria for NASP strand strengths. They recommended additional testing so that a statistically legitimate threshold can be established.

The authors also added that since the NASP values are sensitive to machine stiffness, there should be a specified range of stiffness for the testing frames used to run the test. It was also noted that the NASP values can be affected by mortar compressive strength and mortar mixture flow, therefore the authors suggested that the cohesiveness and workability of mortar should be controlled by specifying an acceptable range of angularity and gradation of the sand used in mortar.

The researchers recommended that further round robin testing should be endorsed by the Precast/Prestressed Concrete Institute and be run at a minimum of four testing sites before the NASP test protocol is accepted. A ruggedness testing study was also suggested, as a requirement for ASTM specification approval, since the authors believe that the test should be standardized for testing the bonding behavior of strands. It was highlighted that for quality assurance of the strand samples tested in the round robin and ruggedness studies, the recommended tests in NCHRP report 621 should be done on each strand type.

The authors also recommended that additional NASP testing along with development length testing should be conducted, so that a statistically reasonable minimum threshold value for NASP test results can be specified. They noted that before testing, the PCI Bond Task Force needs to agree on the maximum acceptable value of end slip in order to assure adequate bond between the strand and concrete before the nominal flexural capacity of the member is reached.

Based on the ongoing testing, the authors calculated a five percent fractal minimum acceptance value for the NASP test to be at 12,000 lb, and noted that the values reported in the final NASP test protocol were not statistically justifiable.

In the due diligence report for the NASP test, it was also stated that the precast concrete manufacturers should not solely rely on the strand pullout test to determine the bonding capability of a given strand, but also run a simple quality assurance test using the concrete mixture and product details in order to determine if the bond between the strand and that specific product will be adequate. The authors recommended using Moustafa specimens or Peterman Beam Test specimens for that purpose; unless the precast concrete suppliers have come up with a different quality assurance test they can rely on (Hawkins & Ramirez, 2010).

Recently, two other studies were conducted with main objective the investigation of prestressing strand bond, and both were published in 2012. One study came from the University of Arkansas, while the other one was performed by the Missouri University of Science and Technology.

The study conducted at Missouri S&T was focused on prestressing strand bonding behavior in self-consolidated concrete, but one of the objectives was to evaluate different strand bond tests, and specifically to evaluate the consistency and make a comparison of the two most widely used pullout tests for the qualification of prestressing steel strand by its bonding capacity, the Moustafa or Large Block pullout test, and the NASP pullout test. The research program also aimed to determine the correlation between measured transfer lengths and pullout test values, as well as to evaluate the effect of the compressive strength of the cementitious material that the strand is casted in to the bonding performance of the strand.

The research program findings revealed that the two pullout test methods are equally consistent in evaluating strand bond performance, as the coefficients of variation obtained by the pullout test results of the two test methods were very close. The disagreement between the test methods came when considering acceptance of the strand as adequate bonding, since all three

strand types passed the NASP test, but only one out of the three passed the Large Block pullout test. This issue raised concerns that the minimum acceptance criteria set for one or both of the test methods might not be realistic. It should be mentioned that the water to cement ratios reported for the 2 mortar mixtures utilized at Missouri S&T during their NASP test series were 0.38 and 0.395, while the mortar compressive strengths of the mixtures during the test were ranging between 4770psi and 5000 psi, and the mortar mixture flows were between 100.2 and 116 %. The strand specimens tested at Missouri S&T had average NASP pullout values between 11700 lb and 21600 lb. The author suggested a minimum acceptance value for the NASP pullout test to be set at 16,000 lb for the average of six specimens, and at 14,000 lb for any individual strand specimen.

The author also recommended that additional refinement of the minimum values for acceptance of strand bond be made, and suggested that focusing on testing strands of pullout values in the ranges of 12,000 – 18,000 lb for the NASP test, and 33- 36 k for the Large Block pullout test will assist in establishing reasonable thresholds. Another suggestion that came from this study was that the effects of mortar mixture proportioning on the NASP test should be further investigated, and recommended that limits should be set on the mortar mix proportions in addition to the strength and flow limits. It was also noted that the load versus slip curve contours could possibly indicate bond quality and that additional research should investigate this pattern.

The Missouri S&T research program also concluded that higher compressive strengths result in lower transfer lengths, and that the transfer length equation should be a function of concrete compressive strength, and in agreement with Ramirez and Russell's as well as other researchers' findings, it was shown that the transfer length is related to the square root of the concrete compressive strength. The study findings also confirmed the relationship found by Russell and Ramirez that correlates the NASP test results, concrete compressive strength, and initial transfer lengths (Porterfield, 2012).

In the study conducted at the University of Arkansas, the main objective was to determine how the mortar mixture compressive strength affects the NASP test values. Prestressing strands of 0.5 inch and 0.6 inch diameters were tested in mortar mixtures with low compressive strengths, high compressive strengths, and compressive strengths within the NASP test protocol allowable range. While the NASP protocol requires mixture compressive strengths between 4500 and 5000 psi, the lowest average mortar compressive strength observed during the

University of Arkansas' study was 3780 psi, and the highest compressive strength was 6540 psi (Murray, 2012).

When comparing the pullout test results, it was found that the low mortar compressive strength samples always resulted in low NASP pullout test values, and that the high mortar compressive strength samples always observed higher NASP pullout test values. The author suggested that when samples of compressive strengths lower than the NASP protocol specified range meet the minimum pullout test threshold, they should be considered valid; and noted that higher mortar compressive strength samples could be over representative of the actual bonding abilities of the strand tested by the NASP pullout test (Murray, 2012).

Chapter 3 - Material Selection

3.1 Initial Strand Selection

Eight sets of samples of 0.5-inch diameter, seven-wire, 270 ksi, low relaxation steel strands conforming to ASTM A416 (ASTM A416, 2010) were tested according to ASTM A1081. The samples were supplied by six of the major strand manufacturers in North America, and were designated as strands A, B, C, E, F, G, H, and I. All of the strands except strand I were market condition strand. Strand I was a known lower-bonding strand that was supplied by one of the strand producers in order to assist the researchers in identifying a low bond source.

The purpose of the initial strand selection process was to identify one strand source with a pull-out force in each of the following ranges:

a) 10,500-12,500 lb
b) 12,500-15,000 lb
c) 15,000-17,500 lb

Figure 3.1 shows the average pull-out strengths versus free end displacement for each strand source tested. Figure 3.2 shows the pull-out strengths at 0.1 in. free end displacement for the six specimens tested and average value for each strand source. Strand A was determined to have an average pull-out force value at 0.1-inch displacement of 14,100 lb during the initial strand selection process, and was therefore chosen as the b) 12,500-15,000 lb range representative strand. Strand I was indeed the only representative of the low pull-out force range a) 10,500-12,500 lb, with an average pull-out force of 10,900 lb during the initial selection process. Strand G had an average pull-out force of 17,800 lb during the initial round of testing, and was chosen as the higher pull-out force value representative for range c) 15,000-17,500 lb. Although strand E had an average pull-out force of 16,700 lb and inside range c, the strand E free-end displacement vs. force curve was not typical, as shown in Figure 3.1 (Polydorou, Riding, Peterman, & Murray, 2013).

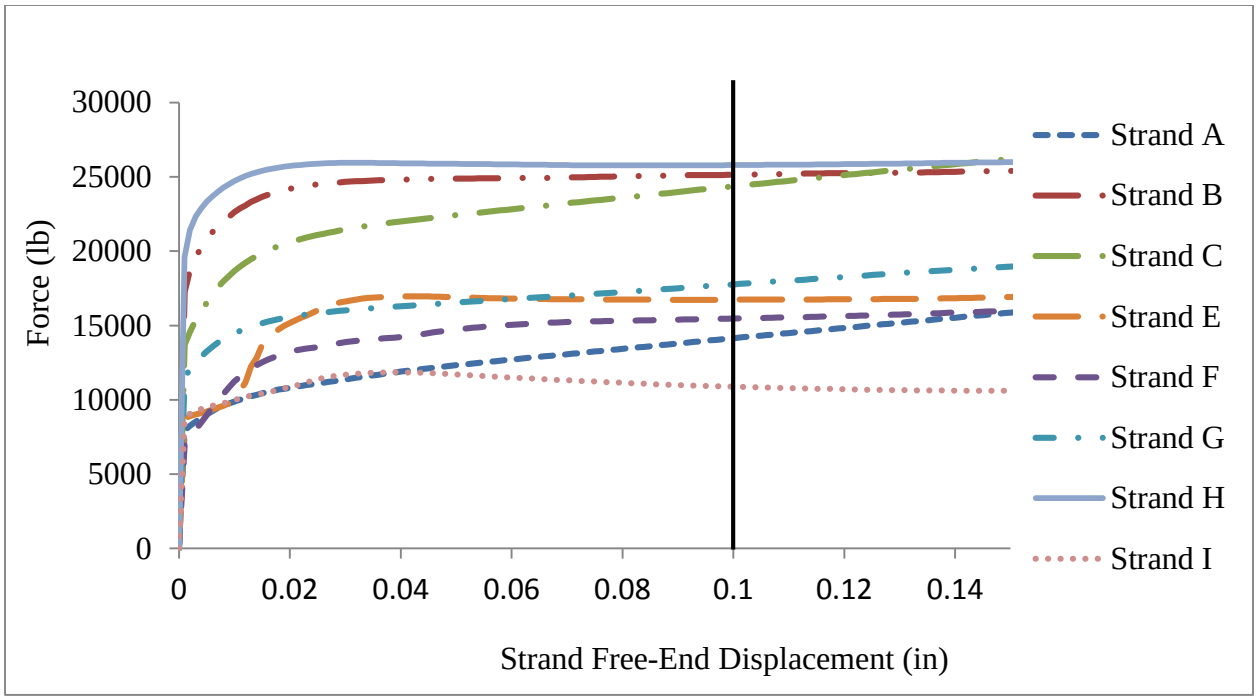

Figure 3.1 Average Strand Force (lb) vs. Displacement (in) per Strand Source (Polydorou, Riding, Peterman, & Murray, 2013)

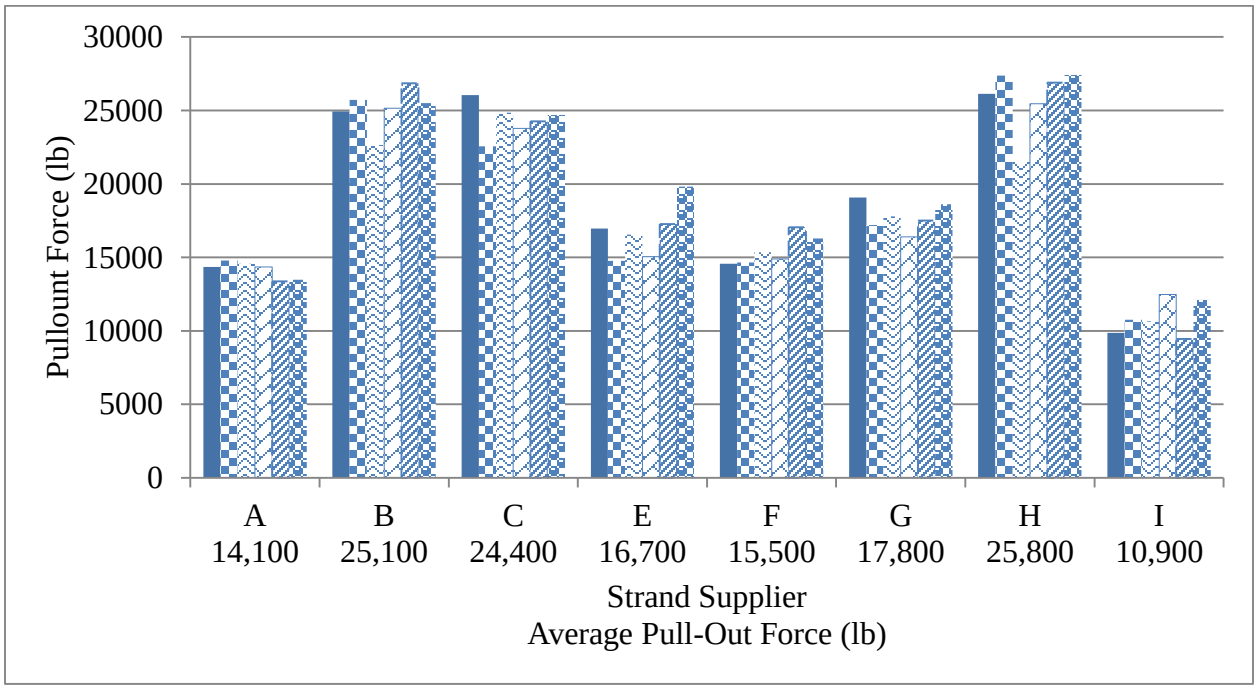

Figure 3.2 Pullout Force (lb) for 6 Specimens Tested per Strand Source for (Polydorou, Riding, Peterman, & Murray, 2013)

At least 3000 ft. of strand A, G, and I were obtained from the corresponding strand manufacturers. The longer coils received were retested according to ASTM A 1081 to verify that the strand received was the same as that tested during the selection process. The pull-out test results obtained from testing the coil samples were in agreement with the results obtained by the initial strand selection testing (Polydorou, Riding, Peterman, & Murray, 2013).

3.2 Mortar Mixture Design Procedure

The Standard Test Method for evaluating bond of 7-wire, 0.5 inch diameter prestressing strand (ASTM A1081) allows any ASTM C33 sand source and any ASTM C150 type III cement source to be used when designing the mortar mixture for the pullout tests (ASTM A1081, 2012).

The standard specification for the pullout test requires that strand be tested within a time window of 24 ± 2 hours since the time of mixing, and that the mortar mixture is at a compressive strength between 4500 and 5000 psi at that time (ASTM A1081, 2012). After taking several trial and error mortar mixtures to accommodate this requirement with one of the cement samples, a simple method was developed which greatly assisted with determining the mixture proportions of mortar mixtures made with the rest of the cement sources, complying with ASTM A1081 requirements.

The procedure was a simple, three step method based on the fact that mortar compressive strength is controlled by the water to cement ratio of the mix. Even though it is generally accepted that the relationship between water to cement ratio and compressive strength is non-linear, a linear relationship was assumed in this case; a valid approximation due to the small range of values taken into consideration (Riding, Peterman, Polydorou, & Ren, 2012).

As a first step, two mortar mixtures with pre-selected water to cement ratios are mixed, and three cubes' compressive strengths per batch are tested at 24 hours from mixing. A linear fit of the results helped identify the water to cement ratio that corresponded to a mortar mixture with compressive strength at 4500 psi, 24 hours after mixing. Figure 3.3 illustrates an example of this procedure (Riding, Peterman, Polydorou, & Ren, 2012).

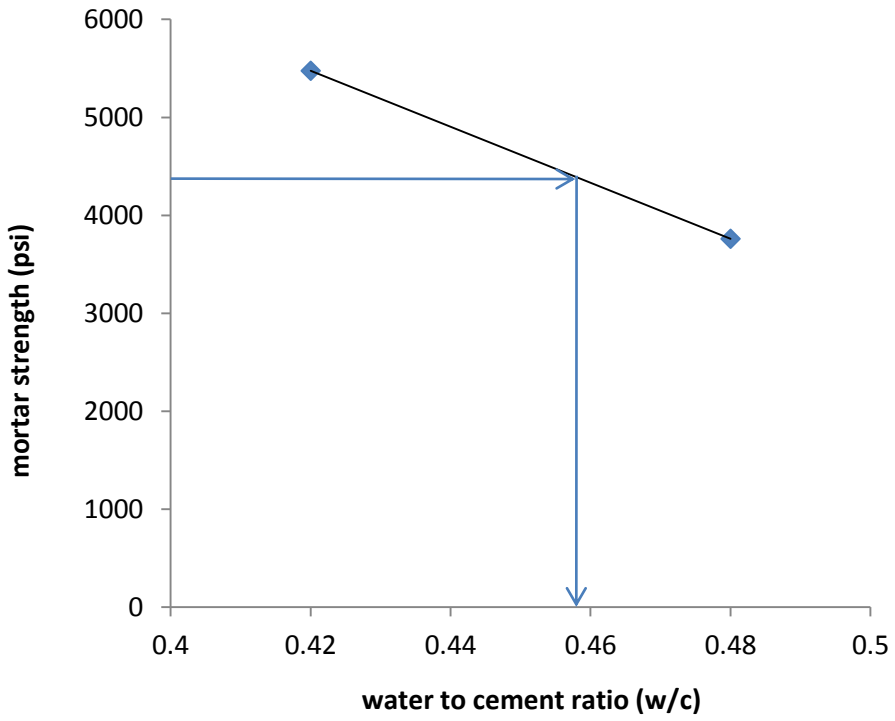

Figure 3.3 Interpolation Procedure used to Select w/c for Cement 1 (Riding, Peterman, Polydorou, & Ren, 2012)

Once the water to cement ratio is selected, the second step is to choose the sand to cement ratio of the mixture, which in combination with the selected water to cement ratio will provide a mortar mixture flow within the specification requirements. Following the same procedure, 2 small mortar batches are mixed at the pre-selected w/c ratio and at 2 different s/c ratios. The mixture flow is then determined according to ASTM C1437, and the sand to cement ratio vs flow values are plotted. In a similar fashion, a linear fit indicates the s/c ratio value that will output an acceptable mortar mixture flow. An example is shown in Figure 3.4 (Riding, Peterman, Polydorou, & Ren, 2012).

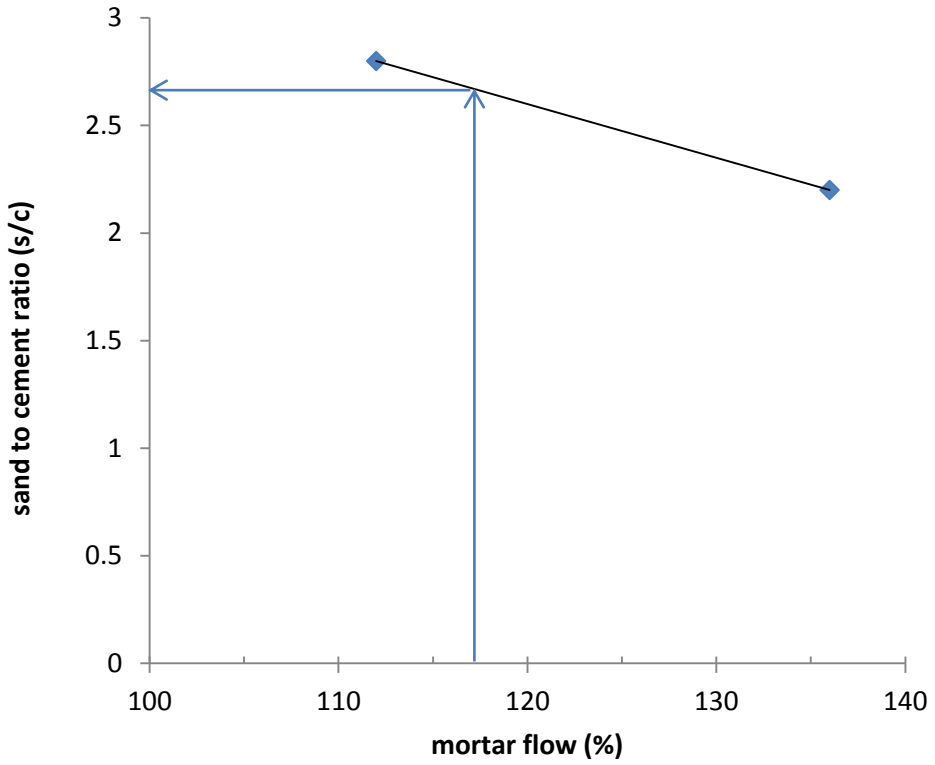

Figure 3.4 Interpolation Procedure use to select s/c for Cement 1 (Riding, Peterman, Polydorou, & Ren, 2012)

The third step in this procedure was the mixing of a large scale mortar batch in order to confirm the compressive strength and mortar flow of the mixture with the selected proportions. Slight difference in both mixture characteristics were observed, due to the different mixing action between the small laboratory mortar mixer and the $12ft^3$ commercial grade concrete mixer that was used for the large scale batches in this project (Riding, Peterman, Polydorou, & Ren, 2012).

A summary of the mortar mixtures developed using this method is presented in Table 3-1, listing the mixture proportions used per cement trial batch, along with their corresponding compressive strengths and mixture flows. A variety of w/c ratios had to be used in order to create mixtures that will reach compressive strengths between 4500-5000 psi at 24 hours for the 5 cements used. Based on the resulting strengths, it is recommended to start with the first step using w/c ratios of 0.42 and 0.46 at a s/c ratio of 2.6 for every new cement source to be used (Riding, Peterman, Polydorou, & Ren, 2012).

The predicted and measured compressive strengths and flows are compared for the case of the large scale mixtures, and we can see that the maximum difference between a predicted and a measure strength value is at 170 psi or 3.8%, which is lower than the maximum threshold of the difference between two tests specified by ASTM C109 (8.7%). Another interesting finding is that when adjusting the w/c ratio only in order to adjust the compressive strength of a mortar mixture, the flow was only affected slightly. Therefore when adjustments need to be made in order to accommodate for different compressive strengths between small scale and large scale batches, we can change the w/c ratio without having to worry about adjusting the s/c ratio; assuming that the predicted mixture flow is not at the two extremes of the allowable range. Instead, it was observed during the first few rounds of testing that the mortar mixture flow was affected much more by improper oiling of the flow table shaft, therefore it was recommended that ASTM C1437 be followed strictly, especially when developing mortar mixtures using this methodology (Riding, Peterman, Polydorou, & Ren, 2012).

Table 3-1 Mortar Strength and Flow Results per Cement (Riding, Peterman, Polydorou, & Ren, 2012)

			Cement				
	Batch	Property	1	2	3	4	5
Strength Trial Batches	1	w/c	0.42	0.45	0.4	0.4	0.4
		s/c	2	2	2.5	2	2.5
		Compressive Strength	5480	5040	5590	6290	5120
	2	w/c	0.48	0.5	0.45	0.45	0.45
		s/c	2	2	2.5	2	2.5
		Compressive Strength	3760	4420	4500	5200	4160
Flow Trial Batches	3	w/c	0.455	0.48	0.45	0.475	0.45
		s/c	2.2	1.8	2.5	2.5	2.5
		Flow	136	128	117	128	114
	4	w/c	0.455	0.48	0.45	0.475	0.45
		s/c	2.8	2.5	2	2.8	2
		Flow	112	113	129	116	139
Large Trial Batch	5	w/c	0.455	0.47	0.45	0.475	0.425
		s/c	2.6	2.2	2.65	2.9	2.5
		Predicted Flow	120	119	113	112	114
		Measured Flow	116	120	116	124	109
		Predicted Strength @ 24hr	4470	4800	4500	4650	4640
		Measured Strength (psi)	4640	4870	4570	4600	4800

Chapter 4 - Ruggedness Testing

4.1 Investigation of Factors Affecting the Test

4.1.1 Sand

There was some concern that the sand gradation, hardness, and angularity could affect the test results. To eliminate this concern, a specific sand source at a specified gradation was used for the mortar mixtures that were included in the initial testing rounds, ruggedness study, and also in half of the Inter-laboratory study mixtures, where testing was ran using Method A and Method B; with Method A following the standard procedure as specified in ASTM A1081, and Method B was a modified procedure which required the use of a specific source of sand at a specified gradation along with other modifications.

The sand source utilized in the initial testing rounds, ruggedness testing mixtures and Method B mixtures was supplied by Dolese Brothers Co, Oklahoma, the suppliers of the sand utilized during the NASP study, where the standard test method was developed. The sand gradations used for all Method B mixtures are shown in Table 4-1 (Polydorou, Riding, Peterman, & Murray, 2013).

Table 4-1 Dolese Sand Gradations (Polydorou, Riding, Peterman, & Murray, 2013)

Sieve	% Total	% Passing
#4	0.5	99.5
#8	4.8	94.7
#16	15.9	78.8
#30	33.5	45.3
#50	31.8	13.5
#100	12	1.5
#200	1.5	0.0

4.1.2 Cement

There were also concerns that the pullout test results are affected by the chemical composition and physical properties of type III cement sources; therefore 5 type III cement

samples were obtained from multiple states of America for the purpose of this investigation. In order to provide uniformity during the initial testing rounds where the variability in strand sources was the main concern, a single cement source was used. Similarly, the same cement source was used throughout the ruggedness testing rounds, where other parameters of the test method were being investigated. The 5 cement sources were compared in mixtures that met the ASTM A1081 specification per cement source, and also in mixtures with common water to cement ratios for all sources.

Large scale mortar mixtures were made for each case, and along with the pullout test specimens and mortar cubes which were cured as prescribed in ASTM A1081, an extra steel canister was included with no strand embedded in it, but instead a thermocouple was placed in the canister in order to keep track of the temperature variation of the mortar with time. In addition, 2 extra sets of mortar cubes were made, which were matched cured to follow the temperature of the extra can specimen.

The 2 sets of 3 match cured mortar cubes were tested for their compressive strength along with the moist cured mortar cubes, in order to compare the values. As it was expected, the match cured mortar cubes experienced higher compressive strengths than their equivalent moist cured cubes. The difference in compressive strength is explained by the difference in temperature between the matched cured and standard moist cured cubes; and this is due to the fact that the match cured cubes are following the temperature curve of a can specimen, which includes a larger volume of mortar and therefore cement, accounting for higher heat generation in the specimen.

The mortar mixture temperature vs curing time was plotted for each cement source, using the data obtained from the thermocouple in the additional can specimen of each batch. The curves indicated that cement 1 mixtures were starting to set much sooner than cement 2 and cement 4 mixtures, and therefore the mortar setting test was conducted on samples of the 3 cement sources. The initial and final setting times were determined for the 3 type III cement sources, and are illustrated in Figure 4.1.

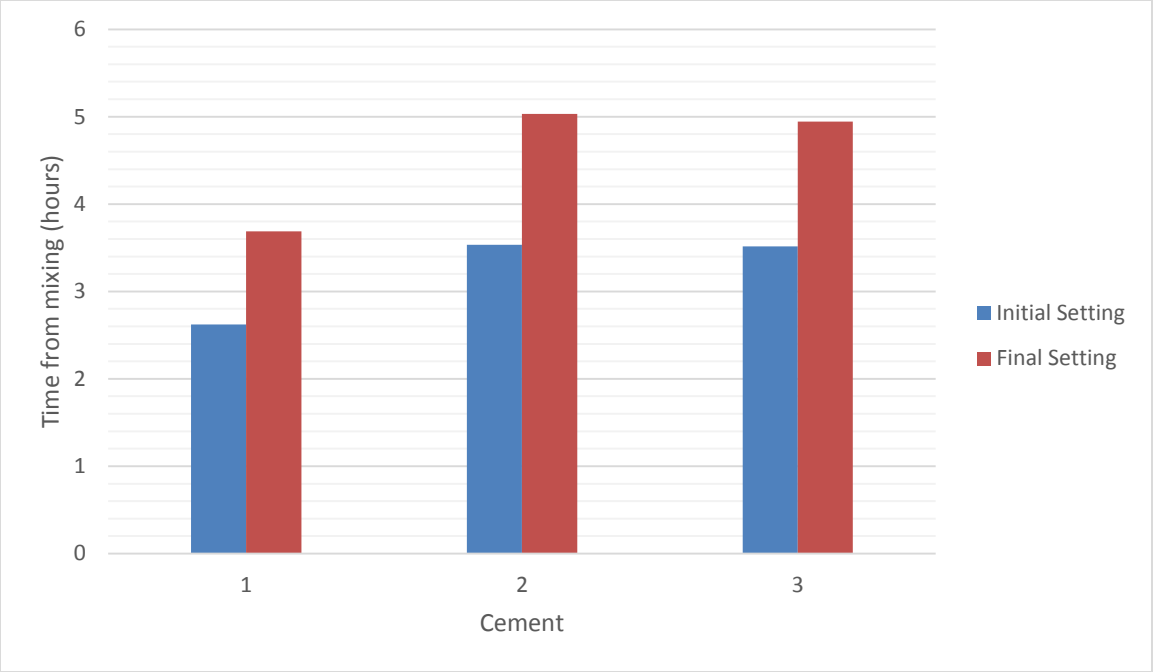

Figure 4.1 Initial and Final Setting Times for Cements 1, 2, and 4, determined by ASTM C403

Another aspect that was investigated in an attempt to differentiate between the 5 cement sources was the amount of bleed water generated on the bottom of each pullout test specimen. A plastic cup was placed under each strand where the mortar mixture bleed water was dripping, and was later weighed to compare the bleed water amounts per cement. Unfortunately the results did not conclude to a noteworthy finding in this case. Table 4-2 shows the variability in chemical composition and physical properties of the 5 type III cement sources used in this project.

Table 4-2 Cement Chemical Composition and Physical Properties (Riding, Peterman, Polydorou, & Ren, 2012)

Cement	1	2	3	4	5
SiO2 (%)	21.8	21.0	19.6	18.9	20.4
Al2O3 (%)	4.3	4.4	5.1	5.3	3.9
Fe2O3 (%)	3.3	3.7	2.3	3.0	3.7
CaO (%)	63.3	63.4	62.3	62.8	63.4
MgO (%)	1.9	2.4	3.1	3.2	2.5
SO3 (%)	3.3	3.2	4.7	4.1	3.4
Na2Oeq (%)	0.	0.6	0.9	0.8	0.5
Blaine Fineness (m^2/kg)	577	660	522	577	536
Potential Composition					
C3S (%)	49	54	54	61	61
C2S (%)	25	19	16	8	12
C3A (%)	6	5	10	9	4
C4AF (%)	10	11	7	9	11

4.1.3 Central Wire Slip during Test

Another factor that was suspected for affecting the pullout test was the requirement by ASTM A1081 that the displacement measuring device be placed on the central wire of the strand, therefore strictly measuring the displacement of that one wire, instead of the strand as a whole. After the initial testing rounds, it was observed that the central wire was slipping independently from the other 6 wires in the case of strand I. In order to investigate how this affects the test results, aluminum caps were fabricated and placed on the top surface of the strand specimen to be tested. The results of the pullout tests ran with the LVDT set on the center of the aluminum caps were plotted versus the results of the standard test method where the LVDT was set on the central wire. Comparison of the test results and the resulting average curves of the two cases indicated that the central wire slipping did not impose significant effects to the pullout test results.

4.2 ASTM Ruggedness

4.2.1 Ruggedness Testing Introduction

With the conclusion of the strand selection rounds and after studying the findings from the mixture development process, an official ruggedness testing study was conducted. The ruggedness testing study was an initial step in developing the precision and bias statement for the "Standard Test Method for Evaluating Bond of Seven-Wire Steel Prestressing Strand", or ASTM A1081/A1081M-12. During this study, the mortar flow, compressive strength at testing, and test loading rate were varied in order to determine their effect on the test results (Polydorou, Riding, Peterman, & Murray, 2013).

4.2.2 Ruggedness Testing Materials

The sand source used in this study was the sand obtained from Dolese Brothers Co, Oklahoma, at the gradations presented in Table 4-1. The ASTM C33 concrete sand had an absorption content of 0.26%, specific gravity of 2.59, and fineness modulus of 2.67. The sand was oven dried for 24 hours and then sieved to ensure that there would be no variability in the pull-out test results due to inconsistent aggregate moisture content between the mortar batches (Polydorou, Riding, Peterman, & Murray, 2013).

Cement 1 was used for all the ruggedness testing study mixtures, to provide uniformity. The chemical and physical properties of this cement source are shown in Table 4-3 (Polydorou, Riding, Peterman, & Murray, 2013).

Table 4-3 Cement 1 Chemical and Physical Properties (Polydorou, Riding, Peterman, & Murray, 2013)

Property	Value
SiO_2 (%)	21.8
Al_2O_3 (%)	4.3
Fe_2O_3 (%)	3.3
CaO (%)	63.3
MgO (%)	1.9
SO_3 (%)	3.3
Na_2O (%)	0.2
K_2O (%)	0.5
Na_2O_{eq} (%)	0.5
Free lime (%)	1.4
Loss on ignition (LOI) (%)	1.6
Insoluble residue (%)	0.4
Blaine Surface Area (m^2/kg)	577
POTENTIAL CALCULATED COMPOUNDS:	
C_3S (%)	49.2
C_2S (%)	25.4
C_3A (%)	5.7
C_4AF (%)	10.2

4.2.3 Ruggedness Testing Methodology

Two rounds of testing were performed in June and July 2012 at KSU in Manhattan, KS. The mortar mixtures were mixed in a 12 cubic ft. capacity commercial horizontal shaft hydraulic mortar mixer located in a climate controlled room following ASTM C305 (ASTM C305, 99). Sample preparation took place before mixing. The 5-inch diameter steel pipes were welded on to 6-inch square plates and sealed before mortar mixing. The specimens were placed on a wooden cart on wheels before mortar placement (Polydorou, Riding, Peterman, & Murray, 2013).

Strand samples were cut to 32 inches. Following the application of 2-inch wide foam bond breaker material where the strand sits on the 6-inch square plate, strand samples were secured in steel cylinders as shown in Figure 4.2. Painter's tape was used to keep the top surface of the strand clean from any mortar during mortar placement (Polydorou, Riding, Peterman, & Murray, 2013).

Figure 4.2 Specimen Setup (Polydorou, Riding, Peterman, & Murray, 2013)

After mixing, the mortar flow was immediately measured. The mortar was placed in two approximately equal lifts. An immersion vibrator was used to vibrate the samples after each lift. After vibration, specimens were filled to the top with mortar, finished with trowels, and then wheeled into a 100% humidity room at 73°F for curing. A plastic tarp shielded the top surface of the specimens from any water dripping onto the mortar while curing (Polydorou, Riding, Peterman, & Murray, 2013).

While the specimens were being made, 2-inch mortar cubes were prepared according to ASTM C109 (ASTM C109, 2012). The mortar cubes were covered to protect them from dripping water and cured in the same 100% humidity room as the steel specimens. The mortar compressive strength was tested prior to and immediately after the pull-out testing of the samples.

The 4500 psi and 5000 psi compressive strength targets were achieved by testing at approximately 23 and 28 hours after batch time, respectively. The testing matrix shown in Table 4-4 was repeated twice (Polydorou, Riding, Peterman, & Murray, 2013).

Table 4-4 Ruggedness Testing Matrix

Test #	Mortar Cube Strength (psi)	Loading Rate (in/min)	Mortar Flow (%)
1	5000	0.12	125
2	5000	0.12	100
3	5000	0.08	125
4	5000	0.08	100
5	4500	0.12	125
6	4500	0.12	100
7	4500	0.08	125
8	4500	0.08	100

The pull-out tests were performed on a tensile testing frame with a 70,000 lb load capacity. The testing frame which is identified in Figure 4.3 was fabricated at KSU and uses a thrust bearing to provide torsion-free test conditions, by allowing the specimen to rotate without restrictions (Polydorou, Riding, Peterman, & Murray, 2013).

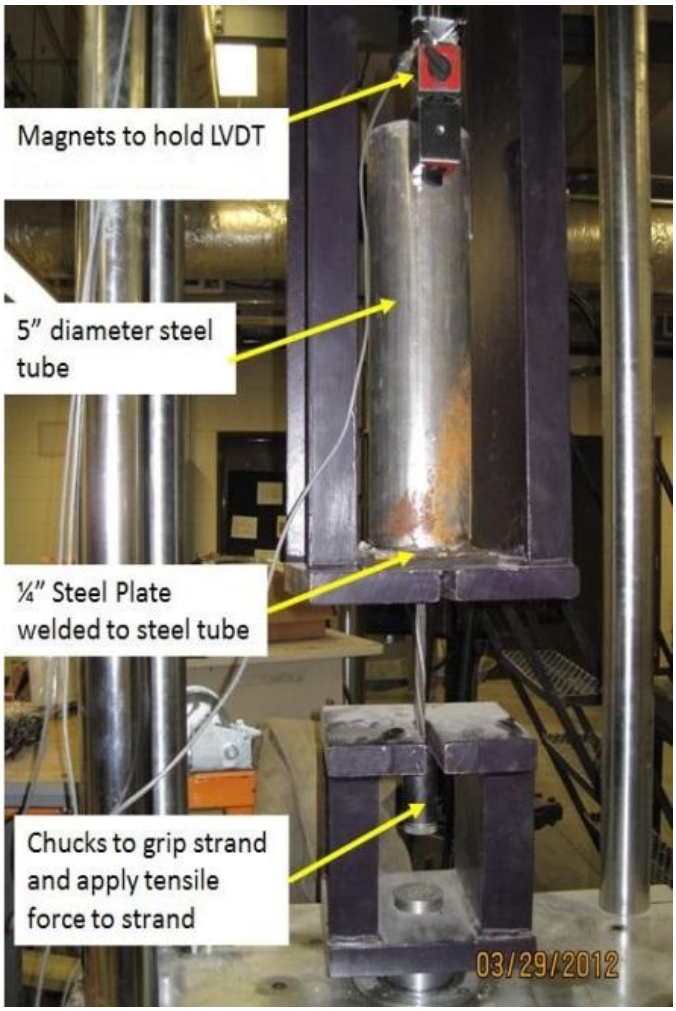

Figure 4.3 Tensile Testing Frame (Polydorou, Riding, Peterman, & Murray, 2013)

The strand free-end displacement was measured using a linear variable differential transformer (LVDT). The LVDTs were attached to the steel specimens with the use of 2 magnetic bases as shown is Figure 4.4, allowing for quick setup of the LVDT's tip on the top surface of the center wire of each strand sample (Polydorou, Riding, Peterman, & Murray, 2013).

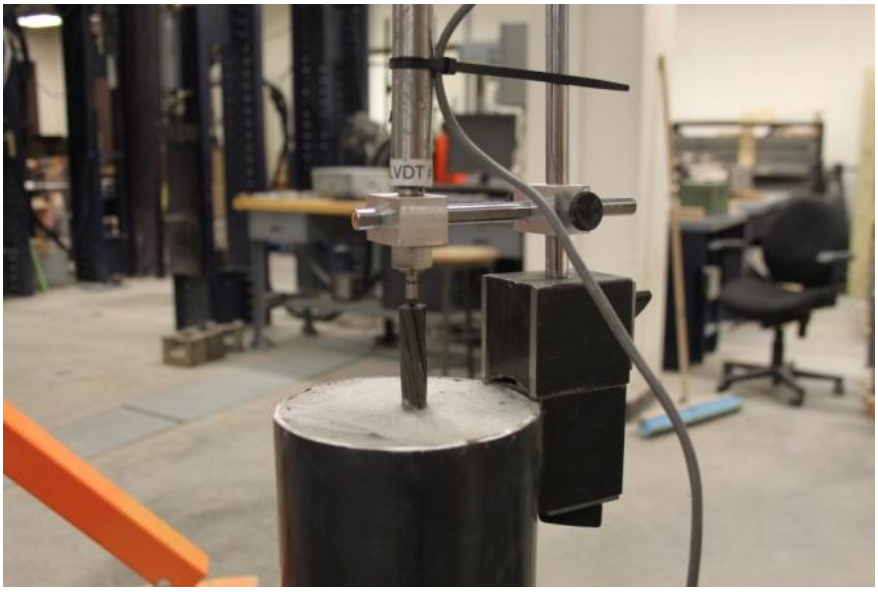

Figure 4.4 LVDT Setup on Specimen (Polydorou, Riding, Peterman, & Murray, 2013)

Processing of the test results was executed with the use of spreadsheets, including an analysis of the findings performed as directed by ASTM E1169-07 (ASTM E1169, 2007). Additional statistical analysis of the ruggedness study results was completed utilizing the statistical analysis software SAS, in order to confirm the ASTM E1169 results and provide a more accurate representation of the study findings. The results of the study were modeled by three statistical models as part of an analysis of variance (ANOVA) (Polydorou, Riding, Peterman, & Murray, 2013).

4.2.4 Ruggedness Testing Results

After the two rounds of testing were completed, the resultant pull-out force average values for each strand supplier were compared in an attempt to identify the effects of each of the three factors on the test results. The testing matrix shown in Table 4-4 included eight factor combinations tested twice; therefore four groups per factor were comparable in terms of the one factor they had in variance, and since the other two factors were identical for each specific group (Polydorou, Riding, Peterman, & Murray, 2013).

The actual compressive strength values before and after the pull-out tests, along with the actual mortar flow rates obtained for each mixture, and the average pull-out force values are

given in Table 4-5, where the letters A and B designate the first and second rounds of each test respectively (Polydorou, Riding, Peterman, & Murray, 2013).

Table 4-5 Mortar Compressive Strength Before and After Testing, Mortar Flow, Test Loading Rate, and Average Pullout Force Values per Test (Polydorou, Riding, Peterman, & Murray, 2013)

Test #	Mortar Compressive Strength Before Test (psi)	Mortar Compressive Strength After Test (psi)	Mortar Flow (%)	Test Loading Rate (in/min)	Average Pull-out value (lb) Strand A	Average Pull-out value (lb) Strand G	Average Pull-out value (lb) Strand I
1A	5065	4958	123	0.12	14,194	17,381	12,435
1B	4932	5063	120	0.12	15,410	18,218	12,844
2A	4808	4974	101	0.12	15,065	19,489	12,959
2B	5018	5074	101	0.12	14,763	18,784	13,019
3A	4921	5065	121	0.08	14,577	18,435	10,434
3B	5080	5089	121	0.08	14,489	16,969	11,625
4A	4898	4988	104	0.08	13,931	18,635	11,529
4B	5059	5029	102	0.08	14,336	17,672	12,885
5A	4566	4667	121	0.12	13,952	17,649	10,722
5B	4568	4699	123	0.12	14,312	16,512	12,277
6A	4566	4703	100	0.12	14,313	19,880	12,858
6B	4654	4713	102	0.12	14,783	18,148	11,664
7A	4536	4674	123	0.08	13,657	16,984	11,220
7B	4607	4722	122	0.08	13,336	17,474	11,538
8A	4631	4834	101	0.08	14,737	18,516	12,139
8B	4460	4656	101	0.08	13,875	17,231	12,189

Test groups 1 vs. 5, 2 vs. 6, 3 vs. 7, and 4 vs. 8 were compared to investigate the effect of the compressive strength on the test results, since the mortar flows and test loading rates are consistent per group. As shown in Table 4-5, varying the mortar compressive strength between

the two limits set by the standard test specification resulted in a 3.4% difference in the pull-out test values of strand A, a 2.2% difference in the values obtained with strand G, and a 3.0% difference for strand I (Polydorou, Riding, Peterman, & Murray, 2013).

In order to examine the effect of varying the test loading rate, groups 1 vs. 3, 2 vs. 4, 5 vs. 7, and 6 vs. 8 were compared. Each group shares identical compressive strength and mortar flow but different loading rates, with 1, 2, 5, and 6 tested by the higher loading rate of 0.12 in. /min. and 3, 4, 7 and 8 tested at the lower rate of 0.08 in. /min. The results indicate that a variation of the test loading rate by 0.04 lb/in. reflected a difference of 3.4% in the pull-out test results for strand A, 2.8% difference for strand G, and 5.6% difference for strand I (Polydorou, Riding, Peterman, & Murray, 2013).

Test groups 1 vs. 2, 3 vs. 4, 5 vs. 6, and 7 vs. 8 were compared for the purpose of investigating the effect on the pull-out strengths of a mortar mixture flow varying between the two extremes allowed by the standard test specification. The results revealed a 1.6% difference in the test results for strand A, a 5.9% difference for strand G, and a 6.2% difference for strand I. The average difference between the pull-out test results obtained by varying the three factors per strand are summarized in Table 4-6 (Polydorou, Riding, Peterman, & Murray, 2013).

Table 4-6 Average Difference (5) between Pullout Test Results of Test Groups per Factor Investigated (Polydorou, Riding, Peterman, & Murray, 2013)

Factor	Strand A	Strand G	Strand I
Compressive Strength	3.4	2.2	3.0
Loading Rate	3.4	2.8	5.6
Mortar Flow	1.6	5.9	6.2

The test method error, calculated after comparing the results from the two rounds of testing, turned out to be 0.7% in the case of strand A, 4.5% for strand G, and 4.2% for strand I. Half-normal plots were created for each of the three strands, following the procedures of ASTM E1169-07. The two-sided tail probabilities (p-values) for each of the factors were calculated for

the purpose of developing a half-normal probability plot for each strand. The statistical significance of a factor was evaluated from the p-values, as an effect is considered significant when its p-value is equal to or less than 0.05 (Polydorou, Riding, Peterman, & Murray, 2013).

The p-values calculated for the three investigated effects in accordance with ASTM E1169-07 are shown in Table 4-7 for each of the three strand suppliers. A probability value below 0.05 corresponds to a significant factor in this analysis. None of the factors studied for strand A were found significant according to the ASTM E1169 analysis. For strands G and I however, the analysis showed that the mortar mixture flow was significant (Polydorou, Riding, Peterman, & Murray, 2013).

Table 4-7 Two-Sided Tail Probability Values per Effect by ASTM E1169-07 Procedures for Each Strand Source

Factor	Strand A	Strand G	Strand I
Compressive Strength	0.073	0.263	0.257
Loading Rate	0.070	0.158	0.078
Mortar Flow Rate	0.333	0.013	0.046

Additional statistical analysis using ANOVA models was completed utilizing statistical analysis software. The results were analyzed by three General Linear Models (GLM), with the first one utilizing the mean of the two replicates, and setting the residual sum of squares (residual error) as simply a lack of fit sum of squares (lack of fit), with 4 degrees of freedom (Polydorou, Riding, Peterman, & Murray, 2013).

The second as well as the third GLM utilized all replicate measurements individually instead. GLM#2 modeled the residual error as a combination of lack of fit and pure error having 12 degrees of freedom, and the third model or GLM#3 modeled the residual error as simply pure error with 8 degrees of freedom (Polydorou, Riding, Peterman, & Murray, 2013).

The GLM models yielded a p-value for each case, and these p-values are the indication for the significance of a factor to the test method. If an outputted p-value is equal to or less than 0.05, then we can conclude that the factor is significant, but if the resulting p-value is greater than 0.05, that indicates non-significance of the factor. Since the analysis proved that the error due to lack of fit was present but not significant, it was concluded that GLM#2 represented the

data best. The p-values of the three factors by model are shown in Table 4-8 for the case of strand A (Polydorou, Riding, Peterman, & Murray, 2013).

Table 4-8 Two-Sided Probability Values per Effect for Each ANOVA Model Used to Analyze the Data (Strand A)

Strand	Factor	GLM#1	GLM#2	GLM#3
A	Compressive Strength	0.0992	0.0490	0.0575
	Loading Rate	0.0958	0.0463	0.0547
	Mortar Flow Rate	0.3505	0.3008	0.3056
G	Compressive Strength	0.2463	0.3037	0.3528
	Loading Rate	0.1526	0.1879	0.2357
	Mortar Flow Rate	0.0206	0.0123	0.0270
I	Compressive Strength	0.2745	0.2588	0.2831
	Loading Rate	0.1021	0.0711	0.0908
	Mortar Flow Rate	0.0676	0.0379	0.0534

Even though GLM#2 classifies the effects of the compressive strength and the loading rate as significant in the case of strand A, their representative p-values are very close to 0.05, therefore we can say that the effects of the compressive strength and the loading rate were borderline significant to the pull-out test results for strand A. In the case of strand G, all three ANOVA models showed that the only significant effect to the pull-out test values was the variance of the mortar flow. Similarly in the case of strand I, varying the mortar mixture flow proved to be a significant factor for the difference in pull-out test values obtained.

After the analysis of the results from this study, it is recommended that the mortar mixture flow rate requirements of ASTM A1081 be adjusted to a tighter permissible range in order to improve the repeatability and reproducibility of the test method (Polydorou, Riding, Peterman, & Murray, 2013).

4.2.5 Ruggedness Testing Conclusion

A ruggedness study was conducted to investigate the influence of loading rate, mortar compressive strength, and mortar flow rate on the results of ASTM A1081 “Standard Test

Method for Evaluating Bond of Seven-Wire Steel Prestressing Strand". In the ruggedness testing, the loading rate was varied to be 120% and 80% of the specified 0.1 in/minute loading rate. The mortar flow was varied to be at the low and high end of the allowable range of 100% to 125%. The mortar compressive strength was varied to be at the low and high end of the 4500-5000 psi range. Statistical analysis of the results indicated that the mortar mixture flow is a significant factor on the ASTM A1081 pull-out test results. The current specification allows a range of mortar mixture flows between 100 and 125. It is recommended that the mortar flow allowable range is confined between 105 and 120, in order to reduce the variability of this test method. Varying the mortar compressive strength between 4500 and 5000 psi was found to not be a significant factor to the test results. The test loading rate was found to be a significant factor in two out of the three strand cases; therefore no modifications can be applied to the specification regarding the loading rate (Polydorou, Riding, Peterman, & Murray, 2013).

Chapter 5 - Inter-Laboratory Study

5.1 Inter-Laboratory Study Introduction

An Inter-Laboratory investigation followed, in order to determine the precision and bias of the newly adopted ASTM. After evaluating the findings of the ruggedness testing study and observations while altering different variables of the test method and studying the related effects, KSU researchers defined a modified ASTM A1081 pullout test procedure (Method B) which was incorporated in the Inter-Laboratory study, along with the standard test method (Method A) as specified by ASTM.

5.2 Inter-Laboratory Study Materials

ASTM A1081 allows any ASTM C33 sand source and any ASTM C150 type III cement source to be used when designing the mortar mixture (ASTM A1081, 2012). There was some concern that the sand gradation, hardness, and angularity could affect the test results. To eliminate this concern, Method B required the use of a specific source of sand at a specified gradation for all testing laboratories (Polydorou, Riding, & Peterman, 2014).

The sand source utilized for the Method B mortar mixtures was supplied by Dolese Brothers Co, Oklahoma, the suppliers of the sand utilized during the NASP study, where the standard test method was developed. The sand was sieved by KSU and sent to the participating research labs for Method B testing. The sand gradations used for all Method B mixtures are shown in Table 4-1 (Polydorou, Riding, Peterman, & Murray, 2013). The requirements regarding the cement source were kept as specified by the ASTM standard for Method B also, allowing the use of any ASTM C150 (ASTM C150, 2012) Type III cement source.

This study was conducted using 0.5 inch diameter, seven-wire steel strand samples that were supplied by three different manufacturers. The strands used in this study were all designated as 270 ksi minimum ultimate tensile strength, low relaxation; uncoated steel strands meeting ASTM A416 (ASTM A416, 2010), and were preselected out of the 8 strand sources supplied during the initial strand selection round. The participating strand sources were labeled strand A, strand G, and strand I (Polydorou, Riding, & Peterman, 2014).

The three strands were initially tested at KSU Civil Engineering laboratories, using a simple mixture proportioning method developed to quickly design a mortar mixture made with any given Type III cement source that will meet ASTM A1081 requirements and is described elsewhere (Riding, Peterman, Polydorou, & Ren, 2012). The mixture characteristics for the 5 mortar mixtures developed using the different cement sources available at KSU are summarized in Table 5-1 (Polydorou, Riding, & Peterman, 2014).

Table 5-1 Mixture Proportions and Mixture Flow for Mortar Samples Made with 5 Different Cement Sources (Polydorou, Riding, & Peterman, 2014)

	w/c ratio	s/c ratio	Mixture flow (%)
cement 1	0.455	2.60	123
cement 2	0.480	2.00	121
cement 3	0.475	2.85	124
cement 4	0.450	2.50	123
cement 5	0.452	2.50	123

An average maximum difference of over 21% was obtained when comparing the pullout test results of identical strand sources tested in mortar mixtures that meet ASTM A1081 standards but utilized different ASTM C150 type III cement sources. The actual test results per strand source and cement source are listed in Table 5-2 (Polydorou, Riding, & Peterman, 2014).

Table 5-2 Average ASTM A1081 Test Results per Strand and Cement Source Tested at KSU

	Strand A	Strand G	Strand I
cement 1	12,800 lb	17,400 lb	11,500 lb
cement 2	13,500 lb	17,500 lb	11,300 lb
cement 3	15,300 lb	20,500 lb	11,900 lb
cement 4	16,600 lb	20,900 lb	11,700 lb
cement 5	15,700 lb	21,500 lb	13,400 lb
Max. Difference	23%	24 %	17%

The work proceeded with testing the three strands in 5 additional mortar mixtures which were prepared with the same 5 cements, but this time the water to cement ratio was kept consistent, at 0.45, for all 5 mixtures. In this case, some of the mortar mixtures did not meet the test time specification set by ASTM A1081, but all samples were tested while their mortar compressive strength was between the specified range of 4500-5000 psi, ignoring the specified test time window. The results per strand and also per cement are listed in Table 5-3 (Polydorou, Riding, & Peterman, 2014).

Table 5-3 Average Modified ASTM A1081 Test Results per Strand and Cement Source Tested at KSU (w/c= 0.45 for all mixtures)

	Strand A	Strand G	Strand I
cement 1	14,300 lb	17,000 lb	11,600 lb
cement 2	14,900 lb	17,300 lb	13,000 lb
cement 3	13,400 lb	17,000 lb	11,000 lb
cement 4	13,500 lb	16,800 lb	10,400 lb
cement 5	15,300 lb	17,500 lb	11,200 lb
Max. Difference	14 %	4%	25%

Using a consistent w/c ratio for all 5 cement mortar mixtures reduced the variability of the pullout test results down to an average maximum difference of just over 14%. It was decided to further investigate eliminating the test time window requirement and instead imposing a set water to cement ratio of 0.45 to the standard ASTM A1081 test method. Considering this finding, Method B was included as an alternate method in the Inter-laboratory study to determine if these modifications could reduce the test variability.

At Kansas State University, mortar mixtures were developed using the uniform sand source supplied by Dolese Brothers Co, Oklahoma, which was oven dried, sieved and graded for every mixture, in order to reduce variability due to inconsistent moisture content and sand gradation. This sand was sieved and supplied by KSU to the participating laboratories for testing the strand bond using Method B (Polydorou, Riding, & Peterman, 2014).

5.3 Inter-Laboratory Study Methodology

Two methods of testing strand bond were performed during the round robin study investigating the "Standard Test Method for Evaluating Bond of Seven-Wire Steel Prestressing Strand", designated ASTM A1081. The first method, called hereafter Method A, recommends testing strand samples exactly as prescribed by the ASTM standard. A second method was defined by the project investigators, hereafter called Method B, which was also a version of the standard ASTM A1081 test method, modified to reduce variability based on the ruggedness test results (Polydorou, Riding, & Peterman, 2014).

No requirements are imposed on mixture proportioning by the ASTM standard as long as the flow and mortar strength requirements are met. For Method B, a water-cement ratio (w/c) of 0.45 was specified. Because different cements would give different strength gain rates at a constant w/c, the time window requirement was deleted for Method B. The standard test method allows for a range of mortar flow between 100-125 %, as determined by ASTM C1437 (ASTM C1437, 2007). Because the ruggedness study determined that mortar flow was a significant variable in bond testing (Polydorou, Riding, Peterman, & Murray, 2013), this requirement was modified for Method B. The mortar mixture flow allowable range for Method B was tightened to 105-120 % (Polydorou, Riding, & Peterman, 2014).

The standard ASTM A1081 test method specifies that samples be tested at 24 ± 2 hours after mortar mixing takes place. The test also requires that the mortar mixture compressive strength of the samples be between 4500 and 5000 psi at the time of testing. In the case of Method B, the project investigators omitted the requirement of keeping the tests within the time frame of 24 ± 2 hours, and required only that the mortar mixture compressive strength is kept between 4500 and 5000 psi. The time frame requirement was omitted after initial testing revealed that it was not possible for all 5 cement source mixtures used at KSU to reach the specified compressive strength of 4500-5000 psi within 22-26 hours from mixing time at the Method B specified water-cement ratio (w/c) of 0.45 (Polydorou, Riding, & Peterman, 2014). Table 5-4 shows a comparison of the key specification differences between Method A (ASTM A1081) and Method B (Polydorou, Riding, & Peterman, 2014).

Table 5-4 Method A and Method B Specifications (Polydorou, Riding, & Peterman, 2014)

	Method A	Method B
Time of test	24 ± 2 hours after mixing	No constraint
w/c ratio	No constraint	0.45
Mortar mixture flow	100-125 %	105-120 %
Compressive Strength at time of test	4500-5000 psi	4500-5000 psi
Sand Source	ASTM C33 sand	Dolese sand, specified gradations
Cement Source	ASTM C 150 type III cement	ASTM C 150 type III cement

A webinar was shared with the participating laboratories, where they were guided on testing procedures and general test setup since most of the participating laboratories had not previously run this test as a first step in preparing for the Inter-laboratory study. A detailed guide was sent to all participating laboratories in order to assist with their mixture development process; however laboratories were not required to follow this mixture development process as long as the mortar mixtures they developed met the test requirements. As soon as a participating laboratory had successfully developed their trial mixtures for both Method A and Method B, a researcher from KSU traveled to each laboratory to observe testing and record data (Polydorou, Riding, & Peterman, 2014).

5.4 Inter-Laboratory Study Results

The average mortar compressive strength of each sample, mortar mixture flow, sample curing conditions, testing conditions, and pullout test results were gathered from 8 external participating laboratories during the months of the Inter-laboratory study. Data from the 5 cement mixtures tested at KSU laboratories were included in the study, to total 13 sets of data, but since not all of the specifications were met by 2 of the external participating laboratories, their data was not taken into consideration during the final round of analysis, and therefore will not be presented in the data summary tables in this report (Polydorou, Riding, & Peterman, 2014).

The average mortar compressive strength during testing, average mortar mixture flow, and average pullout force per strand group from the remaining 6 laboratories and also from the 5 sets of data obtained by KSU labs are summarized in Table 5-5 for Method A, and Table 5-6 for Method B (Polydorou, Riding, & Peterman, 2014).

Table 5-5 Inter-Laboratory Study Data- Method A (ASTM A1081) (Polydorou, Riding, & Peterman, 2014)

	Average Mortar Compressive Strength before test (psi)	Average Mortar Compressive Strength after test (psi)	Average Mortar Mixture Flow (%)	Strand A Average Pullout Force (lb)	Strand I Average Pullout Force (lb)	Strand G Average Pullout Force (lb)
KSU 1	4554	4701	122.5	12803	14739	16921
KSU 2	4655	4762	122.4	13534	11446	17534
KSU 3	4589	4736	118	15250	12036	20548
KSU 4	4654	4675	124	16564	11652	20423
KSU 5	4619	4641	122	15711	13441	21503
LAB 1	4630	4785	115	14163	10114	20725
LAB 2	4535	4668	120	10947	10515	16722
LAB 3	4634	4814	117.5	14634	12681	17127
LAB 4	4630	4995	111	11103	10682	13832
LAB 5	4699	4896	120.7	10687	8966	12715
LAB 6	4511	4522	123.5	13201	10955	16695

Table 5-6 Inter-Laboratory Study Data- Method B (Modified ASTM A1081) (Polydorou, Riding, & Peterman, 2014)

	Average Mortar Compressive Strength before test (psi)	Average Mortar Compressive Strength after test (psi)	Average Mortar Mixture Flow (%)	Strand A Average Pullout Force (lb)	Strand I Average Pullout Force (lb)	Strand G Average Pullout Force (lb)
KSU 1	4525	4485	114.5	14267	11585	17060
KSU 2	4525	4443	112	14890	12981	17307
KSU 3	4516	4731	116	13510	10373	16807
KSU 4	4579	4728	112.7	15343	11163	17495
KSU 5	4578	4794	116	13397	11027	16993
LAB 1	4648	4709	116	15250	9581	19037
LAB 2	4707	4884	113.5	13437	10331	20570
LAB 3	4551	4799	107.5	19367	13876	20591
LAB 4	4475	4820	115	12653	12445	17338
LAB 5	4359	4475	115.3	11886	10582	15046
LAB 6	4010	4115	114.5	13813	11589	17735

The mortar compressive strengths from Lab 6 during Method B tests were lower than expected because some of the mortar cubes tested had visible imperfections on the surface, indicating poor consolidation. The pullout tests were still performed as some of the cubes indicated adequate strength and the time from casting was similar to that seen for companion mixtures made with the same materials and proportions. The pullout test results from the Inter-Laboratory study are illustrated in Figure 5.1- Figure 5.6, in a more detailed representation that includes the high and low values for each group of 6 specimens tested. Each figure illustrates a chart showing the pullout test values obtained per strand group, per method of testing, by the 8 external laboratories that participated in the study, and the 5 sets of data obtained by KSU labs utilizing a different cement source per set of data. The minimum and maximum pullout force values of the six strand samples tested per laboratory are shown in each chart. This also

illustrates the range of values obtained by each laboratory, highlighting the variability of data within a single test site (Polydorou, Riding, & Peterman, 2014).

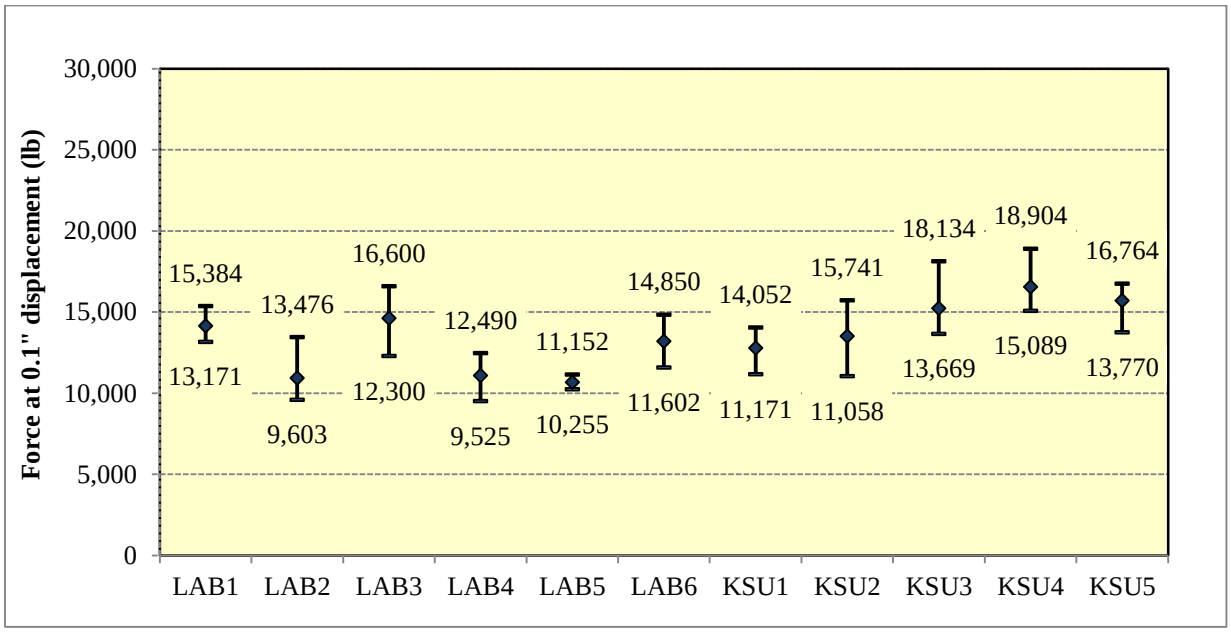

Figure 5.1 Inter-Laboratory Study Results, Method A-Strand A (Polydorou, Riding, & Peterman, 2014)

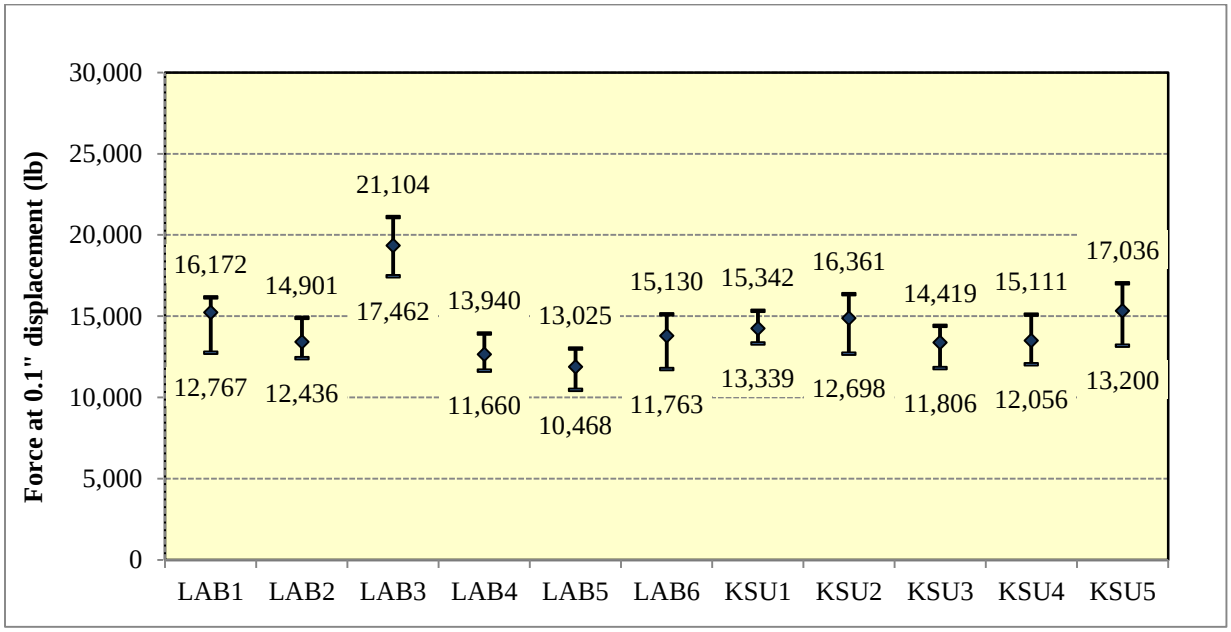

Figure 5.2 Inter-Laboratory Study Results, Method B- Strand A (Polydorou, Riding, & Peterman, 2014)

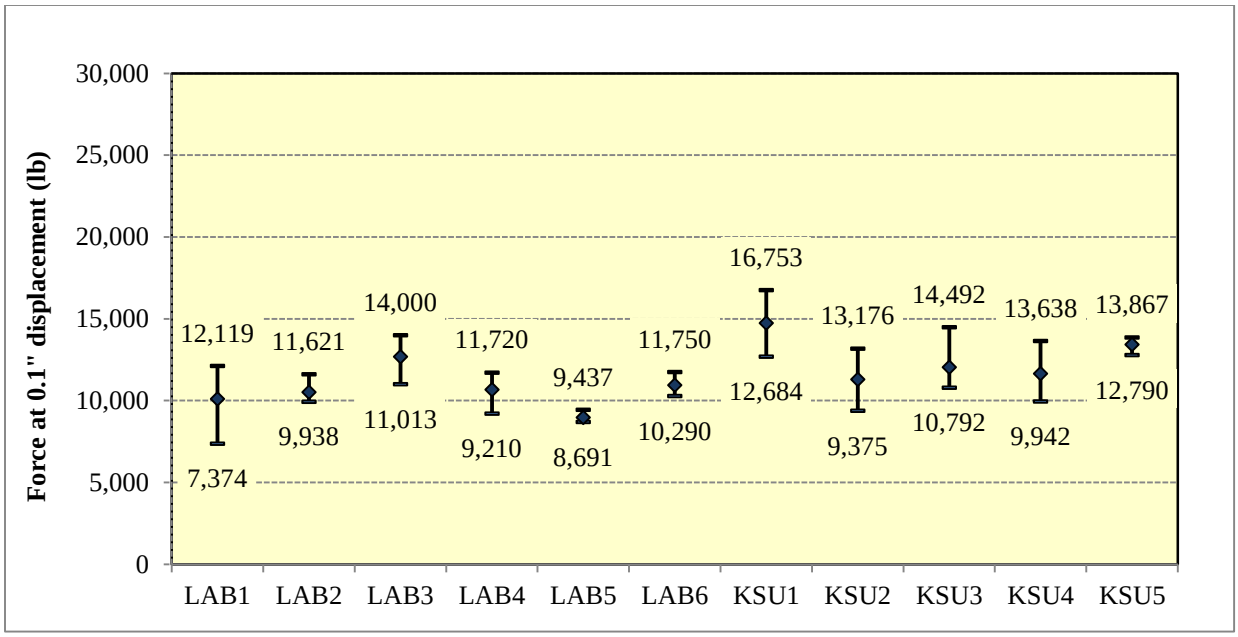

Figure 5.3 Inter-Laboratory Study Results, Method A- Strand I (Polydorou, Riding, & Peterman, 2014)

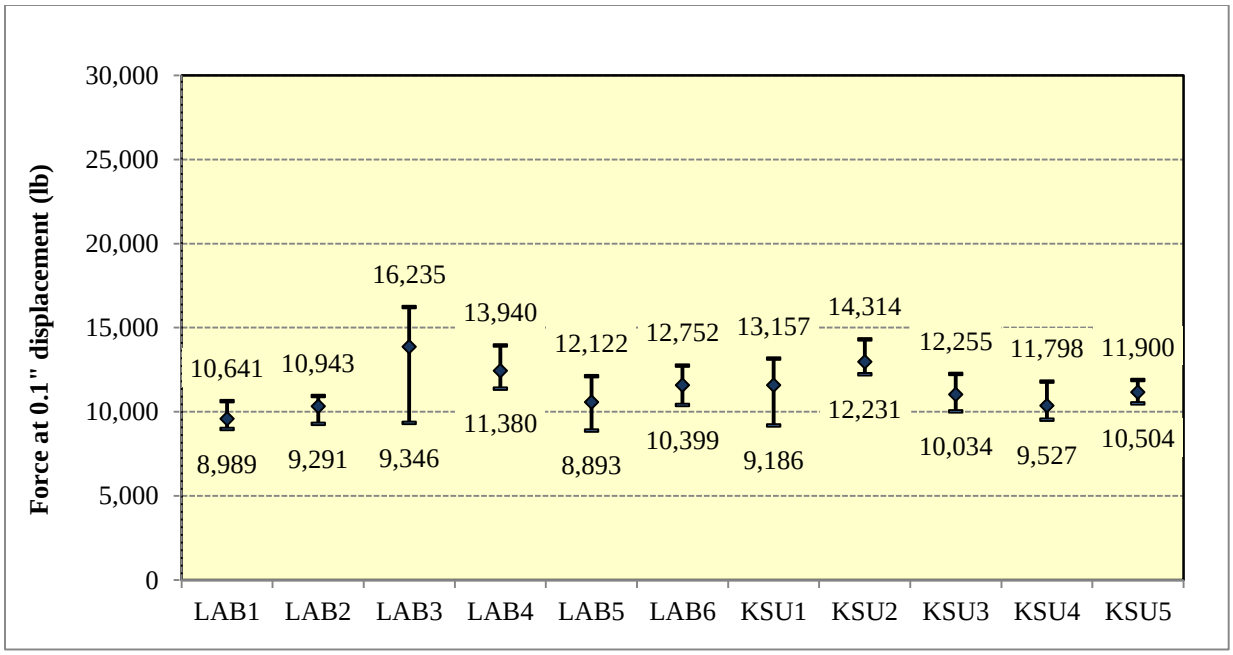

Figure 5.4 Inter-Laboratory Study Results, Method B- Strand I (Polydorou, Riding, & Peterman, 2014)

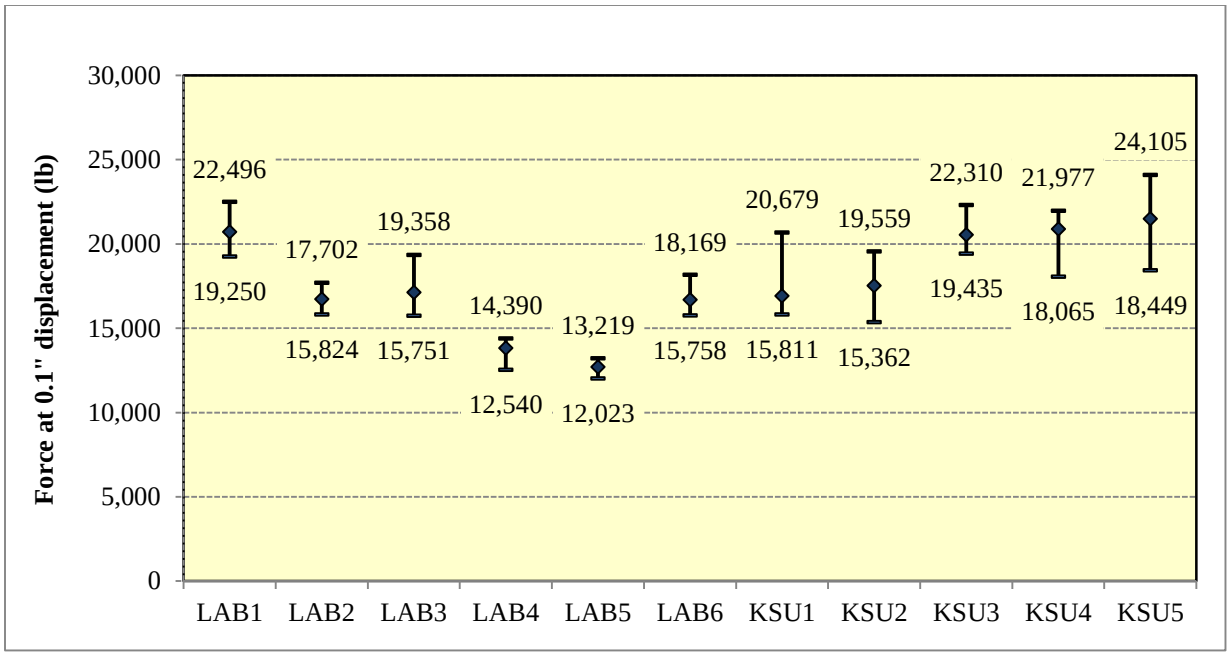

Figure 5.5 Inter-Laboratory Study Results, Method A- Strand G (Polydorou, Riding, & Peterman, 2014)

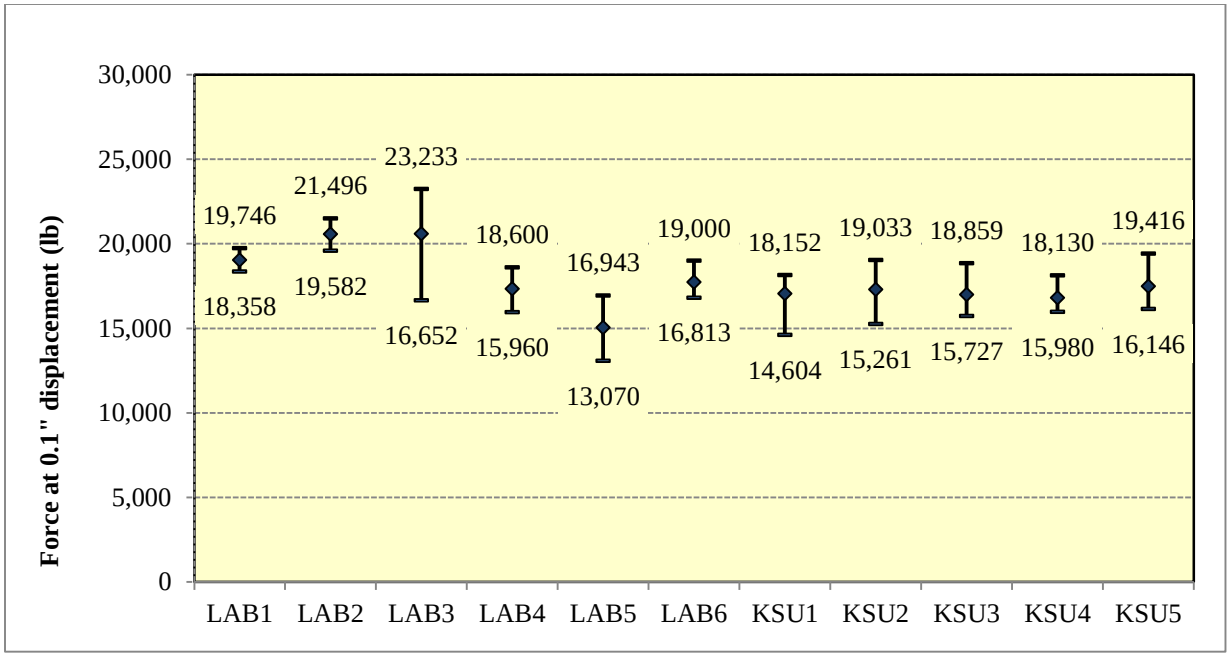

Figure 5.6 Inter-Laboratory Study Results, Method B- Strand G (Polydorou, Riding, & Peterman, 2014)

Switching to Method B reduced the variability of the test results within laboratories, as well as total variability when considering the Inter-Laboratory study as a whole. The standard deviations and coefficients of variability per strand are shown in Table 5-7 (Polydorou, Riding, & Peterman, 2014).

Table 5-7 Average Pullout Test Result, Standard Deviation and Coefficient of Variation for Strands A, G and I, Method A vs Method B (Polydorou, Riding, & Peterman, 2014)

	Strand A Method A	Strand A Method B	Strand G Method A	Strand G Method B	Strand I Method A	Strand I Method B
Average Pullout Force (lb)	13,500	14,300	17,700	17,800	11,600	11,400
Standard Deviation	1903	1882	2728	1576	1543	1212
Coefficient of Variation	0.14	0.13	0.15	0.09	0.13	0.11

As observed in Table 5-7, the average test results for strands G and I when comparing Method A to Method B only vary by 100 lb and 200 lb respectively. In the case of strand A, the average pullout test result that was obtained when utilizing Method B was 800 lb higher that the average pullout test result obtained by Method A. The standard deviation of the data samples was reduced in every case when Method B results were considered, especially for Strand G, where Method B was able to reduce the variability from a coefficient of variation of 0.15 down to a 0.09. This reduction in variability was expected since the ruggedness study results suggested that reducing the mortar mixture flow allowable range would also reduce the test variability (Polydorou, Riding, & Peterman, 2014).

Enforcing a water to cement ratio of 0.45 was also found to reduce the variability when KSU researchers first attempted this method modification, but the outliers obtained during the

Inter-Laboratory study from specific laboratories raise the question of how the duration of sample curing affects specimen performance, while they are at equal compressive strengths. This could be because the mortar cubes were cured at a constant laboratory temperature. The specimens containing strand were stored in moist rooms kept at a constant temperature. Because the specimens have a considerable amount of cement, their heat of hydration can raise the temperature of the specimens significantly, raising the maturity of the samples. This could explain why mixtures with significantly faster or slower reacting cements at the same w/c gave different pullout strengths, even when companion mortar strengths were similar (Polydorou, Riding, & Peterman, 2014).

5.5 Inter-Laboratory Study Conclusions

By using different type III cement sources at the different ILS laboratories and also within KSU, it was noticed that it was not possible for all cement sources to reach the specified mortar compressive strength of 4500-5000 psi within 22-26 hours from mixing time when using a prescribed water-cement ratio of 0.45. For this reason, the modified ASTM A1081 method proposed imposed no constraints when it came to curing time. This modification to the test method resulted in curing times that varied substantially among laboratories, leading to wariness that differences in mortar maturity at the time of test could cause some strength discrepancies (Polydorou, Riding, & Peterman, 2014).

The ASTM A1081 test method was found to have a coefficient of variation of 14%. Modifications to the test that include using a standard graded sand source at all laboratories, using mortar mixtures of a consistent water-cement ratio (w/c) of 0.45 at all sites, and reducing the allowable mortar mixture flow range reduced the average coefficient of variation to 11%. While it was found that the modifications proposed did reduce the test variability, the use of a standard graded sand source would also raise the cost of performing the test substantially (Polydorou, Riding, & Peterman, 2014).

Using different cements affected the test results. Further investigation of cement source chemical composition and properties might lead to further recommendations about cement source selection to reduce test variability (Polydorou, Riding, & Peterman, 2014).

Chapter 6 - Strand Testing by NCHRP 621

Samples of the three strand sources A, G, and I were shipped to Wiss, Janney, Elstner Associates, Inc. (WJE), for their surface characteristics to be determined in accordance with the testing procedures described in NCHRP Report 621 (Osborn, Lawler, & Connolly, 2008). The four test methods used in this study were recommended for qualifying strand for bond quality by the NCHRP program and are given as follows:

- Weight Loss on Ignition (QC-I),
- Contact Angle Measurement after Lime Dip (QC-I),
- Change in Corrosion Potential (QC-I), and
- Organic Residue Extraction with FTIR Analysis (QC-II) (Osborn, Lawler, & Connolly, 2008).

The four tests were performed on 3 samples of each strand source that were cut and shipped to WJE by KSU. The results are summarized in this chapter.

6.1 Weight Loss on Ignition (QC-I)

Three nine-inch long strand samples per strand source were cut and tested for weight loss on ignition. This test method provided the strand loss on ignition in mg/cm^2, after recording the change in strand weight, and calculating the strand surface area. The calculated weight burned off the strand surface at high temperatures is considered to consist of organic components of residues, for example drawing lubricants, which are known to affect the bonding capacity of strands. It should be noted that the initial and final strand weights reported were the average of 3 measurements per sample; and that the strand surface areas were calculated using the formula shown in **Equation 6-1**, where D is the nominal strand diameter and L is the length of the strand sample. The test results are summarized in Table 6-1.

$$A=\left(\frac{4}{3}\right)*\pi*D*L \qquad \textbf{Equation 6-1}$$

Table 6-1 Loss on Ignition Test Data

Strand Sample	Strand Length (cm)	Nominal Strand Diameter (cm)	Average Initial Weight (g)	Average Final Weight (g)	Change in weight (mg)	Surface Area of Strand (cm^2)	Loss on Ignition (mg/cm^2)
A 1 (LOI)	23.0	1.3	175.8154	175.8248	-9.4	125.2	-0.075
A 2 (LOI)	23.0	1.3	176.4379	176.4294	8.5	125.2	0.068
A 3 (LOI)	23.0	1.3	175.9624	175.9667	-4.2	125.2	-0.034
G 1 (LOI)	22.9	1.3	176.6762	176.6701	6.1	124.7	0.049
G 2 (LOI)	22.9	1.3	176.2935	176.2966	-3.1	124.7	-0.025
G 3 (LOI)	22.9	1.3	176.1889	176.1845	4.4	124.7	0.035
I 1 (LOI)	23.1	1.3	176.0243	176.0180	6.3	125.8	0.050
I 2 (LOI)	23.0	1.3	175.5060	175.4869	19.1	125.2	0.153
I 3 (LOI)	23.0	1.3	176.0478	176.0284	19.3	125.2	0.154

Compared to the NASP pullout test, the NCHRP study revealed that lower bond applies to higher Loss on Ignition values, and this study can agree with the trend, since the lower bonding strand I experienced much higher Loss on Ignition values that the other two sources. Even though strand G is the highest bonding source in this study as far as pullout test values as considered, 2 out of 3 strand A samples experienced a Loss on Ignition that was lower than all 3 strand G samples in this study.

6.2 Contact Angle Measurement after Lime Dip (QC-I)

NCHRP 621 prescribes that the surface tension of steel strand be determined by contact angle measurement (CAM), which is performed by a modified half-angle technique. The contact angles were calculated for three foot-long samples of each strand source. The average of 6 readings per strand was reported to KSU. The 3 strand I samples had the smallest contact angles and the 3 strand G samples shared the largest contact angles. The results are shown in Table 6-2.

Table 6-2 Contact Angle Measurement Test Data

Strand Source	Sample #	Contact Angle (degrees)
A	1	76.7
A	2	80.2
A	3	82.0
G	1	82.2
G	2	82.8
G	3	81.5
I	1	75.1
I	2	70.0
I	3	67.6

The NCHRP study revealed that strands of a contact angle of 73° or lower will give 90% confidence of adequate bond through correlation of the Contact Angle Measurement test results with the NASP pullout test results. This applies to strand I of our study which averaged a 70.9° Contact Angle, but surprisingly strand I is the lowest bonding strand source of this study. Looking at all three sources, the exact opposite trend is observed in our study compared to the NCHRP.

In this study we see the highest bonding strand by the pullout test (Strand G) to obtain the highest Contact Angles at an average of 80.3°, the in between performer under pullout test strand A to experience an average Contact Angle Measurement of 79.6°, and the lowest bonding strand I to experience a very low average Contact Angle at 70.9°.

6.3 Change in Corrosion Potential (QC-I)

The change in corrosion potential of steel strand was determined by sealing one end of each strand sample with epoxy, and partially submerging it in deionized water. This test is performed in order to reveal the coating of residue amounts per strand, since it was revealed in prior studies that strands with a coating of residue are less likely to corrode. The initial corrosion potential and potential change were measured using a potentiostat. The initial corrosion potential

and change after 1 hour and 6 hours are reported in Table 6-3. The NCHRP study revealed that a Change in Corrosion Potential of -0.175 V or higher (less negative) provides good confidence for adequate bond.

Table 6-3 Change in Corrosion Potential Test Data

Strand Sample	Initial Corrosion Potential (V)	Corrosion Potential Change after 1 hour (V)	Corrosion Potential Change after 6 hour (V)
A 1 (CCP)	-0.232	-0.126	-0.262
A 2 (CCP)	-0.163	-0.167	-0.311
A 3 (CCP)	-0.159	-0.181	-0.304
G 1 (CCP)	-0.254	-0.144	-0.199
G 2 (CCP)	-0.254	-0.139	-0.209
G 3 (CCP)	-0.261	-0.115	-0.180
I 1 (CCP)	-0.205	-0.141	-0.255
I 2 (CCP)	-0.192	-0.168	-0.291
I 3 (CCP)	-0.203	-0.151	-0.283

All of the strand samples tested for our study experienced corrosion potential changes that are less negative than -0.175 V, but still following the trend obtained in the NCHRP study with Strand G experiencing the least negative corrosion potential change out of the 3 sources, but strand I slightly outperforming strand A in this test, even though strand I was the lowest performer in the pullout testing rounds.

6.4 Organic Residue Extraction with FTIR Analysis (QC-II)

Using solvent extraction procedures, as well as gravimetric and Fourier Transform Infrared (FTIR) spectroscopy, the organic drawing-compound residues of 3 samples from each strand source were identified and quantified, and the extracted residue concentrations were reported along with the FTIR spectrum plots for each sample tested. This procedure allows for identification of the type of residue as well as determination of the amount of residue on a strand

surface, and therefore can help in identifying the potential cause of inadequate bond. A summary of the test results is shown in Table 6-4.

Table 6-4 Organic Residue Extraction with FTIR Analysis Test Results

Strand Sample	Nominal Strand Diameter (cm)	Mass of residue (mg)	Surface Area (cm^2)	Residue (mg/cm^2)	FTIR Interpretation
A 1 (OR)	1.3	1.4	166.1	0.008	Stearic Acid
A 2 (OR)	1.3	4.8	166.1	0.029	Stearic Acid
A 3 (OR)	1.3	4.9	166.1	0.030	Stearic Acid
G 1 (OR)	1.3	4.4	166.1	0.026	Stearic Acid plus ester
G 2 (OR)	1.3	3.2	166.1	0.019	Stearic Acid plus ester
G 3 (OR)	1.3	2.2	166.1	0.013	Stearic Acid plus ester
I 1 (OR)	1.3	13.0	166.1	0.078	Stearic Acid
I 2 (OR)	1.3	4.8	166.1	0.029	Stearic Acid
I 3 (OR)	1.3	10.5	166.1	0.063	Stearic Acid

Better correlation was observed during the NCHRP study when the FTIR analysis identified only stearate residue on the samples, but overall, higher concentrations of residue were matched with lower pullout test values. In the case of our 3 strand sources A, G and I, the test results match the NCHRP trend exactly, with higher concentrations of residue corresponding to lower ASTM A1081 pullout force values.

After testing by the 4 recommended Quality Control procedures was concluded, an analysis of the prediction intervals and thresholds was conducted, following the procedures outlined in NCHRP Report 621, and taking into consideration the strand source average pullout force values reported by KSU in June 2012; which were 14,983 lb for Strand A, 19,617 lb for Strand G, and 12,167 lb for Strand I. The threshold value applied to the data analysis was 10,500 lb, or 0.313 ksi; the same value used for NCHRP Report 621. Based on that information, the data from this study was analyzed separately, and also in combination with the data from the NCHRP Report 621. It was observed that even though the values obtained for the Strand Sources

A, G, and I for the purpose of this study by all 4 tests conducted fell within the ranges of test result values obtained for the 9 strand sources tested in 2006 during the NCHRP study, the Contact Angle Measurement results did not follow the trend seen in the NCHRP study, but instead revealed an opposite trend that disagrees with the NCHRP Report 621 findings.

Chapter 7 - Discussion of ASTM A1081

7.1 Summary of Factors that Affected the Test

During this investigation of ASTM A 1081, "Standard Test Method for Evaluating Bond of Seven-Wire Steel Prestressing Strand", a few factors were identified that can affect the test method and test results.

Great caution should be taken in maintaining the equipment required to run the test, especially for the sensitive brass table used to measure the mortar mixture flow. ASTM C1437 should be followed strictly in order to avoid inconsistency in mortar mixture flow measurements. It was seen that improper oiling of the flow table shaft had significant effects on the flow values, affecting the test method repeatability (Riding, Peterman, Polydorou, & Ren, 2012).

Through the ruggedness testing study, where the effects of the mortar compressive strength, mortar mixture flow, and test loading rate were investigated, it was determined that the mortar mixture flow was the only factor that affected the test results significantly (Polydorou, Riding, Peterman, & Murray, 2013). It is therefore crucial that accurate mortar flow measurements are taken consistently. Consistency in sand gradations was found to reduce the variability of the results, since uniformly graded sand will provide uniform mortar mixture flows, however using graded sand may not be practical (Polydorou, Riding, & Peterman, 2014). The compressive strength range allowed by the standard test is small enough so that the range of mortar compressive strength allowed during the test (4500psi to 5000psi) should not be reduced further because of the variability in mortar compressive strength tests and difficulty in meeting the test time window specification (Polydorou, Riding, Peterman, & Murray, 2013).

When 5 different cement sources were used at Kansas State University, the average maximum difference obtained for the three strands tested by the standard method was 21%. When the test was performed using mortar mixtures that all shared the same water to cement ratio of 0.45, the average maximum difference was reduced down to 14%. In this case, the test time window requirement was ignored, in order to accommodate mortar mixtures with all 5 cement sources at this w/c ratio (Polydorou, Riding, & Peterman, 2014).

It was observed that the pullout test results were greatly affected when using ASTM C150 type III cements coming from different manufacturers. The results experienced higher variability when performed at multiple testing sites using cements from a wider spectrum of

manufacturers. The results obtained that were far away from the mean during the inter-Laboratory study when all mortar mixtures were made with a w/c ratio of 0.45 raised a concern that the time required for a mortar mixture to reach the required compressive strength might have an effect on the test results, and it was recommended that further investigation on the cement sources' chemical composition and physical properties be done (Polydorou, Riding, & Peterman, 2014). Setting some limits on the cement source chemistry is expected to reduce the variability of the ASTM A1081 test results substantially. It is recommended that further investigation of the cement source chemical composition and properties can lead to a prescribed cement composition range to be used in this test, in order to reduce its variability.

7.2 Summary of Precision and Bias Statement for ASTM A1081

As part of the Inter-Laboratory study, 5 sets of data from KSU, 1 set per cement source, plus the data from 6 additional laboratories which participated in the Inter-Laboratory study were analyzed in order to define the precision and bias statements for ASTM A1081/A1081M-12: "Standard Test Method for Evaluating Bond of Seven-Wire Steel Prestressing Strand." Samples of 0.5 inch diameter strands from the 3 manufacturing plants labeled A, G, and I were tested at every laboratory according to ASTM A1081-12, with the result of the test method taken as the average of six individual test determinations.

The single operator coefficient of variation has been found to be 9.0 %. It was also determined by ASTM C670 that two properly conducted tests (each consisting of the average of six single determinations) by the same operator on the same material are not expected to differ by more than 12.1 %. The range (difference between highest and lowest) of the six single determinations used in calculating the average is not expected to exceed 24.9 %, as determined by ASTM C670.

The multi-laboratory coefficient of variation was calculated as 14.5 %. The results of two properly conducted tests in different laboratories on the same material are not expected to differ by more than 40.2 %, as determined following ASTM C670. It was not possible to make a justifiable statement on the bias of this test method, since an appropriate accepted reference value does not exist at this time.

7.3 Strand Pullout Test Values to Consider in Phase II

In conclusion of the first phase of this project, the average pullout test values per strand were finalized. For Strand A, the average pullout force from the Inter-Laboratory study was determined to be 13,500 lb. Strand G averaged a pullout force of 17,700 lb, and Strand I averaged 11,600 lb. These ASTM A1081 values are to be taken into consideration in the analysis of Phase II, where rectangular beam sections were prestressed with a single strand specimen coming from the coils of either strand A, strand G, or strand I.

Chapter 8 - Sensitivity Analysis

8.1 Analysis Using Bentley Software Leap Presto and Microsoft Excel

An independent analytical study was conducted in order to determine the sensitivity of specific prestressed concrete sections to transfer length and development length. The study included prestressed Double Tee sections and Hollow Core sections which were suggested by Professional Engineer Tim Cullen, as examples of shapes that could be of concern if ACI 318 Code transfer and development length requirements are not met.

8.1.1 Sections Analyzed

Double Tee (DT) sections are used most commonly in parking garages and floors, but also in roof and wall construction. In this study, 2 Double Tee sections were analyzed, the section referred to as 7T264, and the section referred to as 10DT24. The section details for 7T264 are shown in Figure 8.1. The two Double Tee sections were analyzed for 2 cases of section lengths, at 40 foot long as well as 60 foot long.

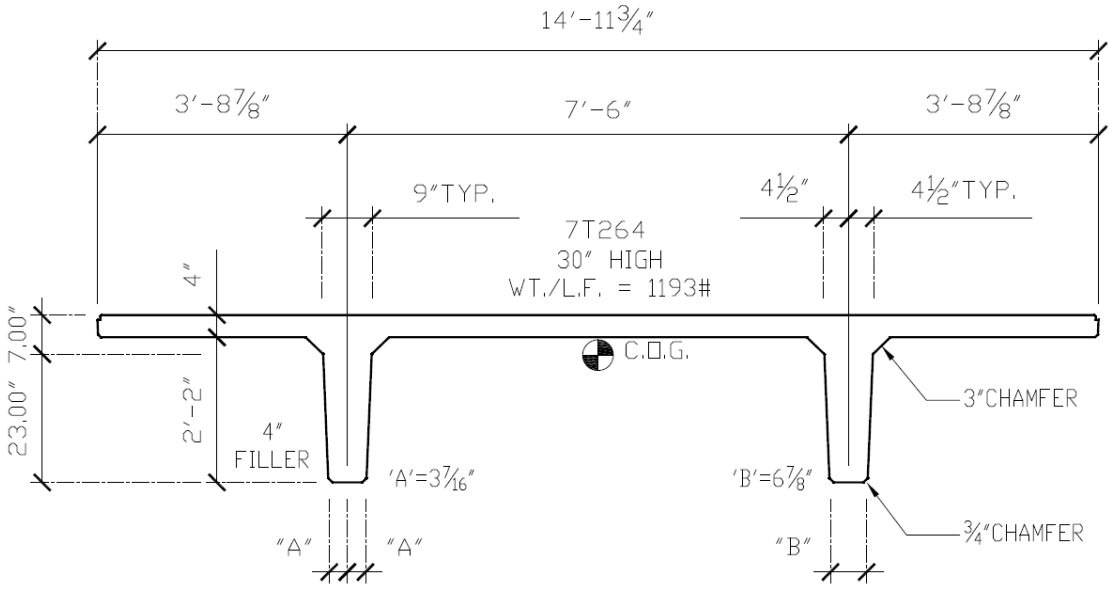

Figure 8.1 7T264 Section Details

Hollow Core sections are also very common in the prestressing industry, used in floor, roof and wall construction, preferred due to their shallow depths for occasions where floor-to-floor heights are limited. Hollow Core sections are also preferred in some cases order for accommodation of HVAC, plumbing and electrical equipment. Two Hollow Core sections were considered in this analysis, and they are referred to as Highcore 8-1000 and Highcore 12. The Hollow Core sections were analyzed at 3 different lengths each. Highcore 8-1000 was analyzed as a 12 foot, 24 foot, and 36 foot long member, and Highcore 12 was analyzed as a 20 foot, 30 foot, and 40 foot member. The details for section Highcore 8-1000 are shown in Figure 8.2.

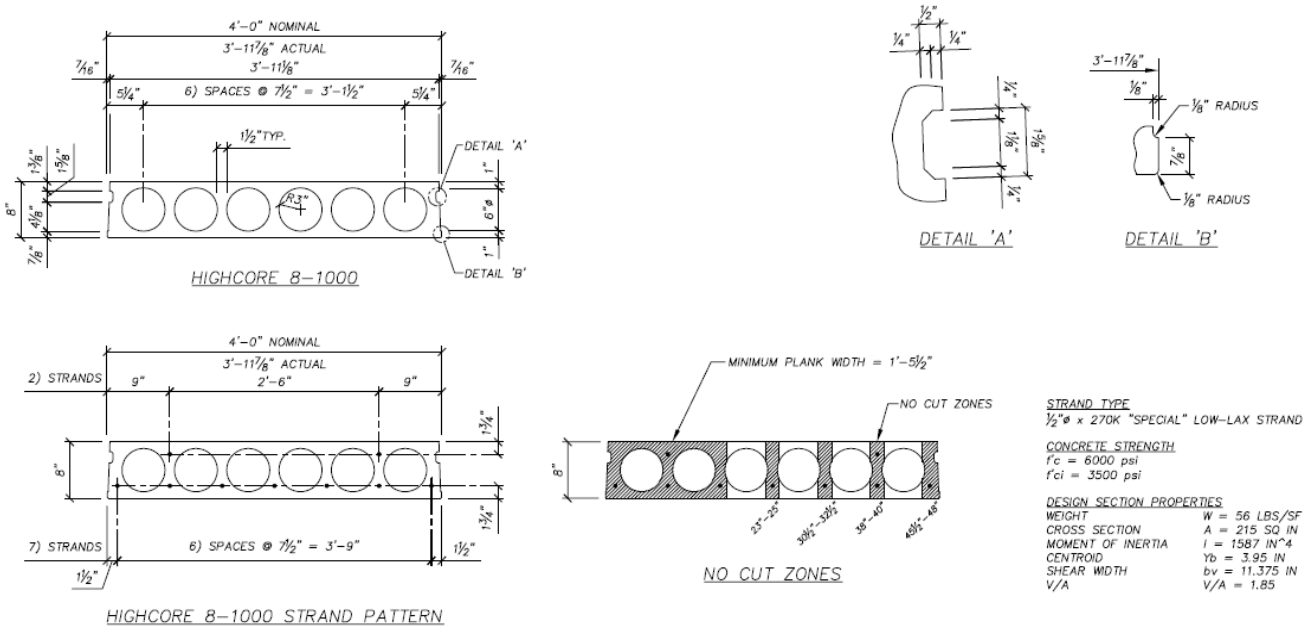

Figure 8.2 Highcore 8-1000 Section Details

Analysis was performed using the comprehensive software LEAP PRESTO of Bentley Systems, Inc., as well as Microsoft Excel. The specific section properties, strand reinforcement patterns and material properties considered in the study were suggested by Mr. Cullen. All sections were prestressed with 0.5 inch diameter, 270 ksi strands.

8.1.2 Conditions Analyzed

The sections were analyzed for the uniform loading condition of 40 lb per square foot live load and and 25.2 lb per square foot snow load. The analysis was based on varying the design transfer length and development length values per section case, first by applying the exact actual code suggested values, and then applying a factor of 1.4 as well as a factor of 2.0 to the code suggested values. The purpose of this analysis was to study how the moment capacity as well as the shear capacity varies for each member under these specific loading conditions, and determine the effects of having prestressing strands of transfer and development lengths that are longer than the values recommended by ACI 318 code.

8.2 Sensitivity Analysis Results

As expected, the effects of changing the assumed transfer and development length values were evident near the members' ends, reducing the moment as well as shear capacities at the ends of every member analyzed, as the ACI code values' multipliers were increased from 1.0 to 1.4 and then 2.0. Analysis of the results revealed reduction in moment as well as shear capacity of all the sections considered, as the transfer and development length factors increased. The nominal moment and shear capacity values at 6 inch increments through the mid span of each section were extracted from the software. The values for the case where the ACI transfer and development lengths are multiplied by 1.0 were considered as the 100% capacities and were compared to the capacities obtained for the cases where the transfer and development lengths were multiplied by 1.4 and 2.0, and graphical representations of the specific points that reflected the maximum capacity reductions, or critical section per case, were prepared. The examples considered for the Double Tee section 72T64 are shown in Figure 8.3 and Figure 8.4 considering moment and shear capacities respectively. The moment and shear capacities for the cases analyzed are shown in Figure 8.5 and Figure 8.6 for section 10DT24, Figure 8.7 and Figure 8.8 for Highcore 8-1000, and Figure 8.9 and Figure 8.10 for Highcore 12. A summary of the remaining moment and shear capacities at the critical section per case analyzed is shown in Table 8-1.

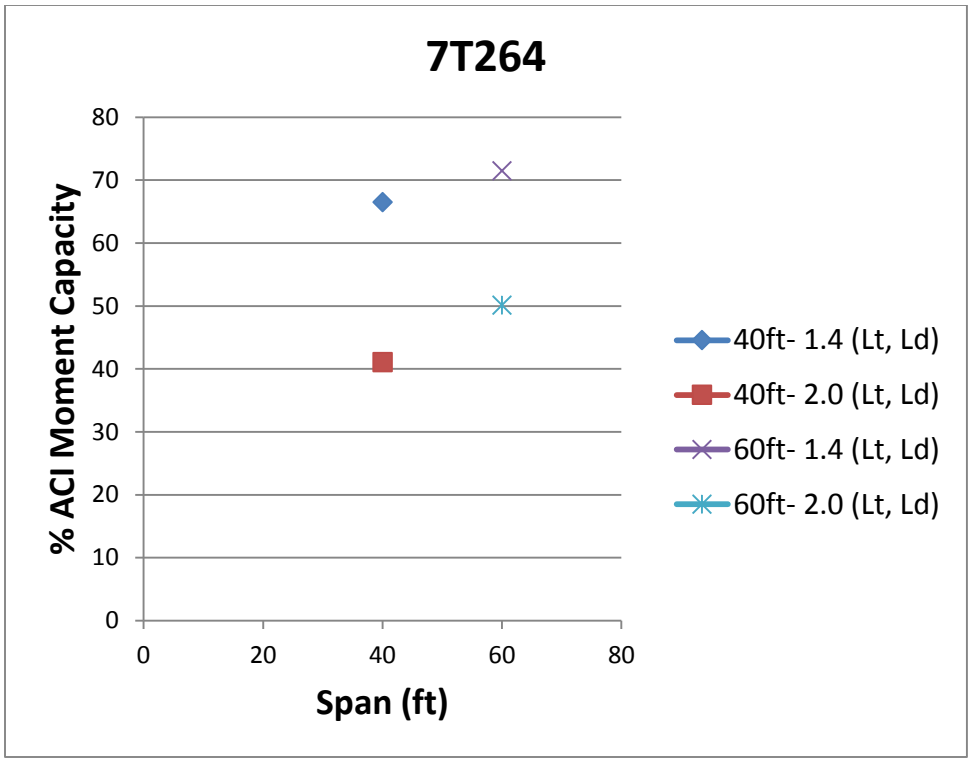

Figure 8.3 Percent of ACI Moment Capacity per Case Analyzed for 7T264

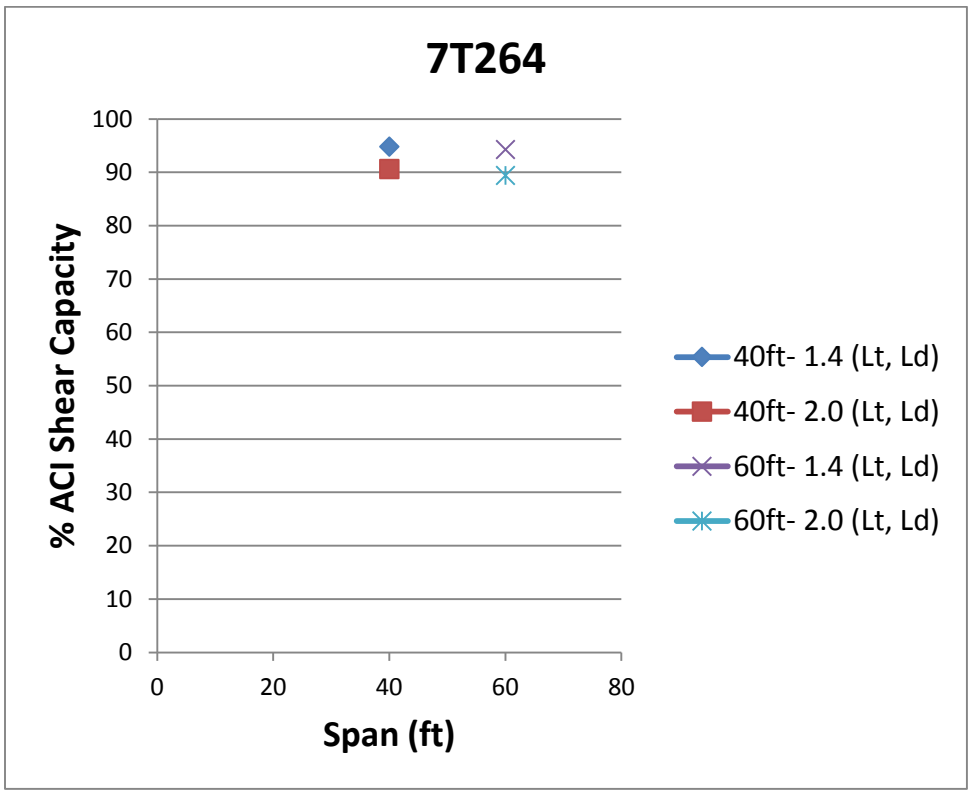

Figure 8.4 Percent of ACI Shear Capacity per Case Analyzed for 7T264

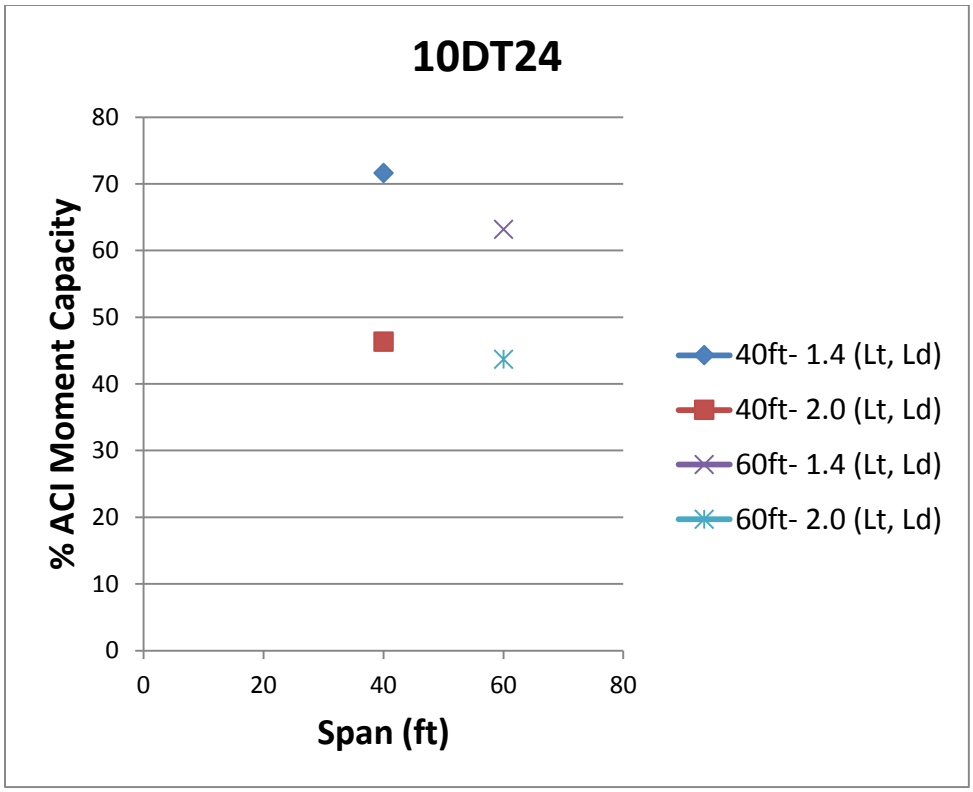

Figure 8.5 Percent of ACI Moment Capacity per Case Analyzed for 10DT24

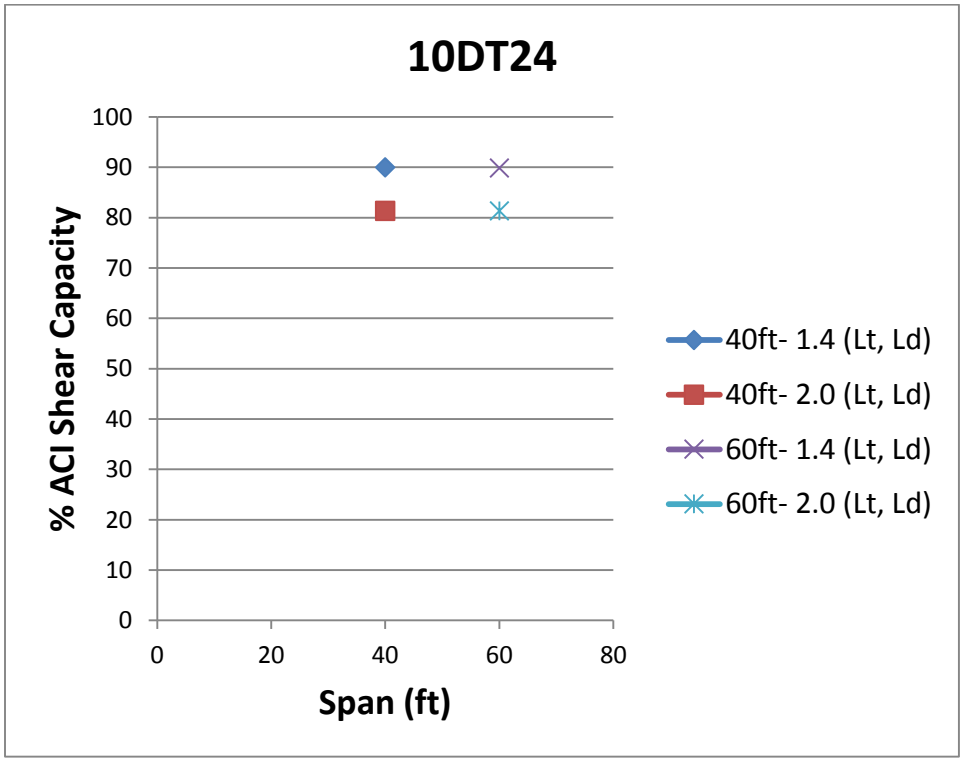

Figure 8.6 Percent of ACI Shear Capacity per Case Analyzed for 10DT24

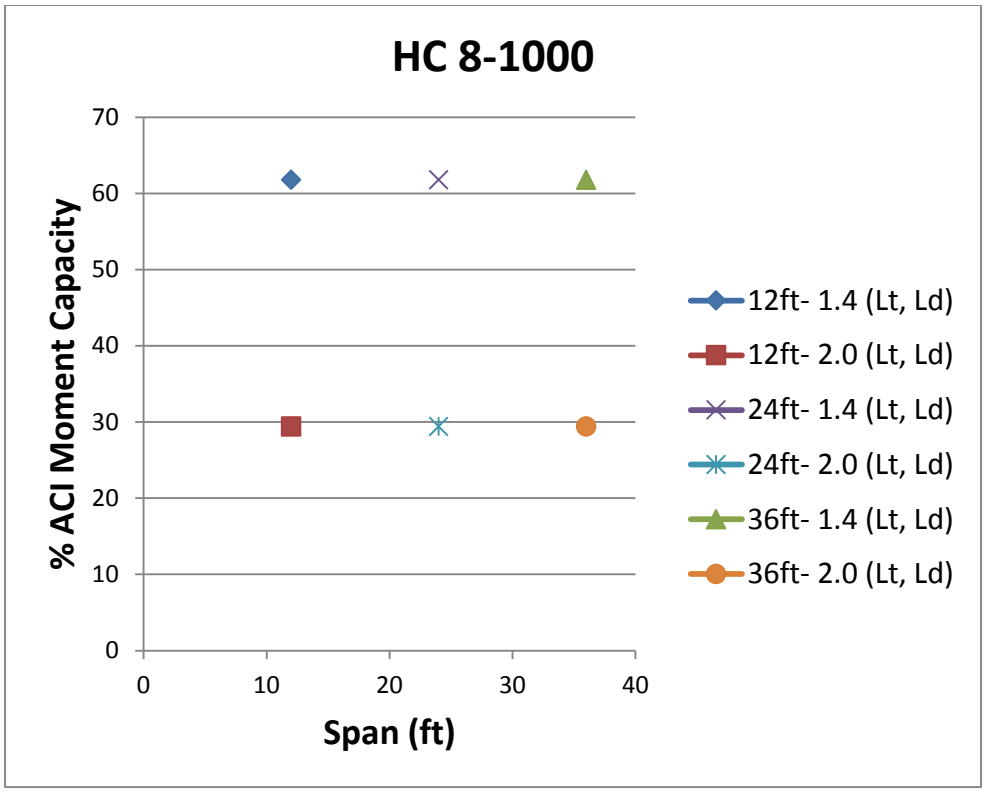

Figure 8.7 Percent of ACI Moment Capacity per Case Analyzed for HC 8-1000

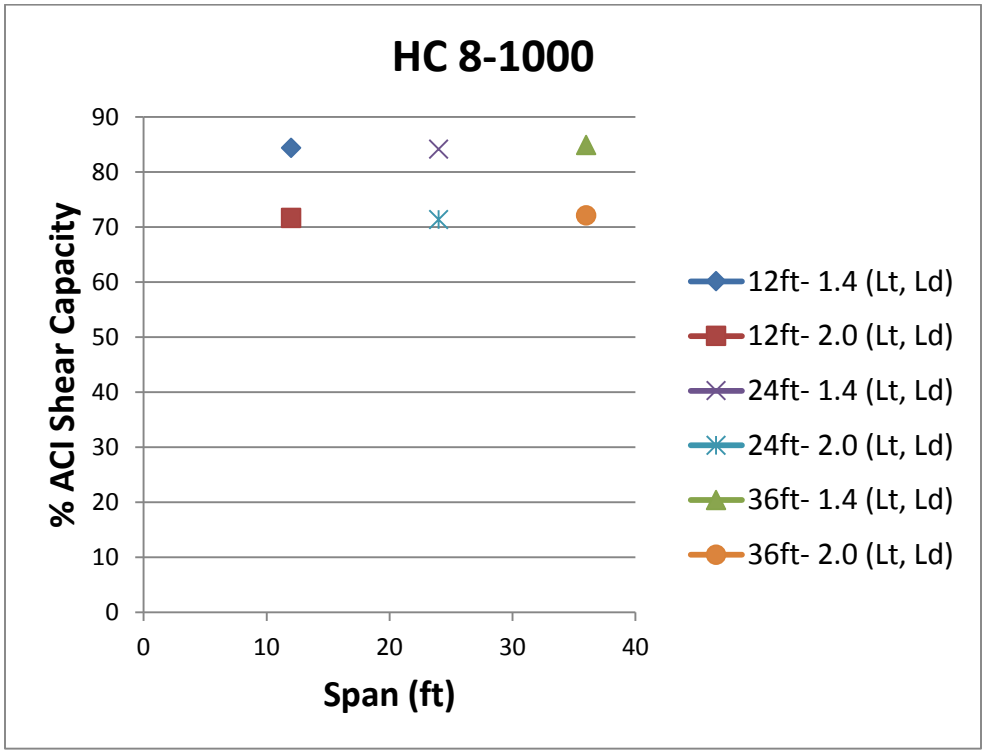

Figure 8.8 Percent of ACI Shear Capacity per Case Analyzed for HC 8-1000

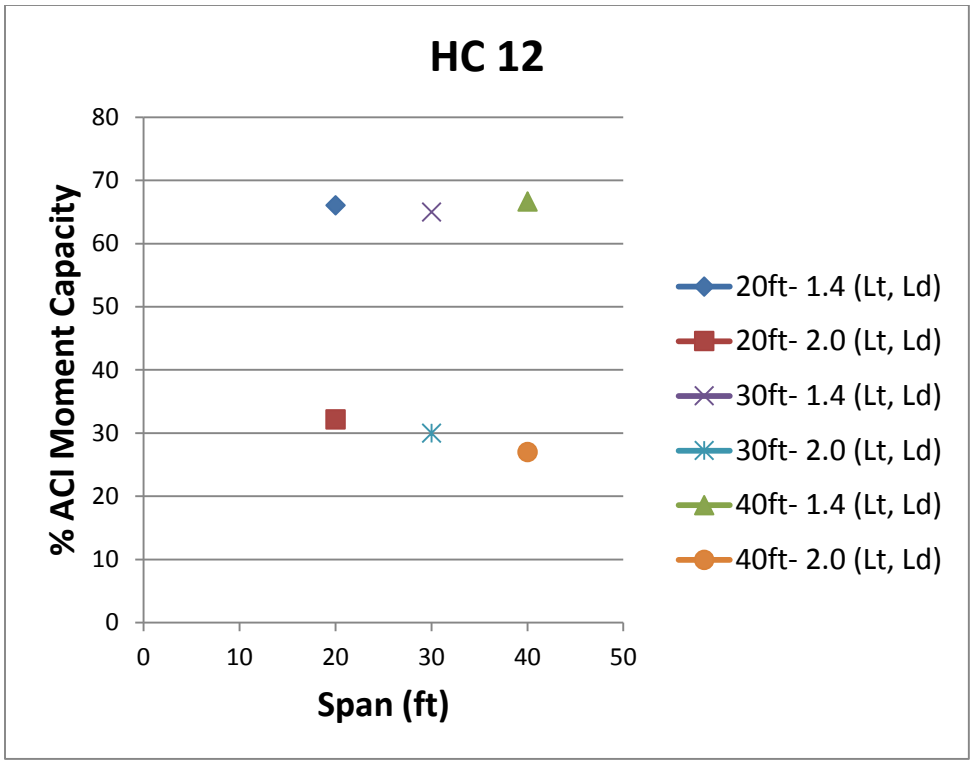

Figure 8.9 Percent of ACI Moment Capacity per Case Analyzed for HC 12

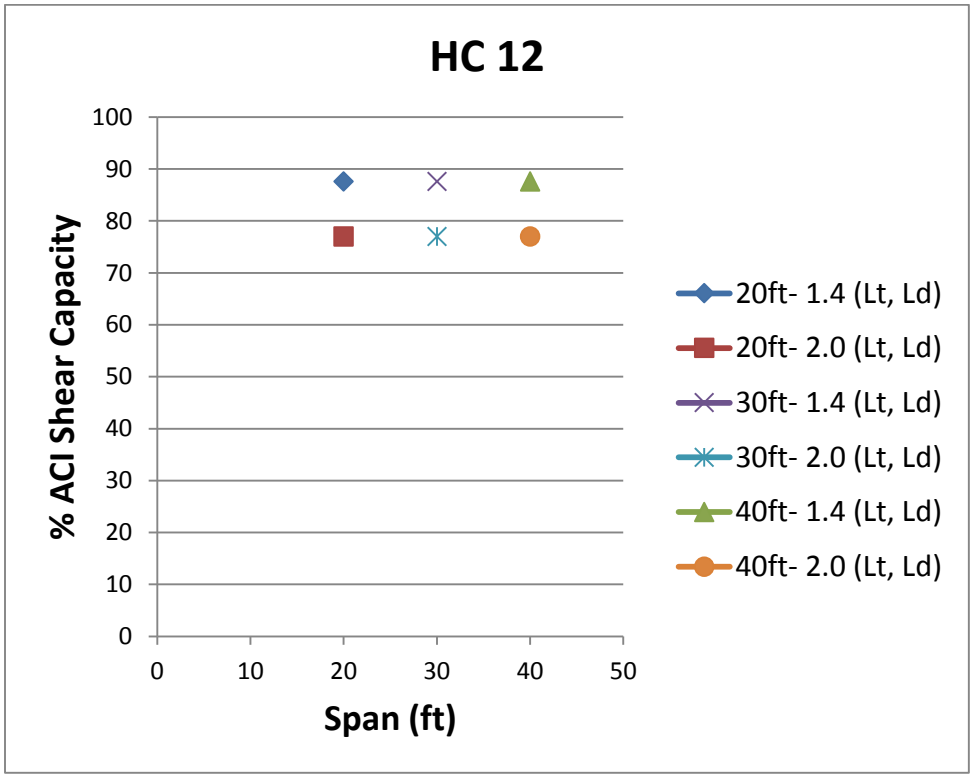

Figure 8.10 Percent of ACI Shear Capacity per Case Analyzed for HC 12

Table 8-1 Summary of ACI Capacities Reduced per Section and Case Analyzed

Section	Length (ft)	TL/DL factor	% ACI Moment Capacity	% ACI Shear Capacity
7T264	40	1.4	66.5	94.9
		2.0	41.1	90.6
	60	1.4	71.5	94.3
		2.0	50.1	89.4
10DT64	40	1.4	71.6	90.0
		2.0	46.3	81.3
	60	1.4	63.2	89.9
		2.0	43.7	81.4
HC 8-1000	12	1.4	61.8	84.4
		2.0	29.4	71.7
	24	1.4	61.8	84.2
		2.0	29.4	71.4
	36	1.4	61.8	86.7
		2.0	29.4	73.9
HC 12	20	1.4	66.0	87.6
		2.0	32.2	77.0
	30	1.4	65.0	87.6
		2.0	30.0	77.0
	40	1.4	66.7	87.6
		2.0	27.0	77.0

Table 8-1 reveals that applying a factor of 1.4 to the ACI transfer and development length equations can reduce the moment capacity of a section down to 61.8%, and shear capacity down to 84.2% of ACI values, as determined for the case of the Hollow Core section “HC 8-1000”.

Applying a factor of 2.0 was able to reduce the moment capacity down to 27% of ACI capacity for the 40ft long Highcore 12 example analyzed in this study. Doubling the transfer/development lengths assumed by the ACI 318 code was able to reduce the shear capacity down to 71.4% of ACI capacity for the Hollow Core “HC 8-1000”.

In a telephone discussion, design engineer Mr. Tim Cullen agreed that hollow core sections are of high sensitivity to poor bond, especially when shear requirements are not met, since most of the time no shear reinforcement is provided in hollow core sections. Mr. Cullen also added that it is always assumed that the specimen will meet ACI 318 transfer length provisions, and no consideration for longer transfer lengths is taken in design practice. Unlike for Hollow Core members, Mr. Cullen mentioned that at least 5 feet of stem mesh is provided for shear reinforcement in Double Tee members, providing additional capacity at the ends.

The shear diagrams for the Hollow Core section "HC 12" are shown in Figure 8.11 for the 30 ft. long section, where we can see the 3 shear capacity curves, and notice that the curve corresponding to the 2.0 factor applied to the ACI 318 code equations for the transfer and development length does not meet the requirements for shear.

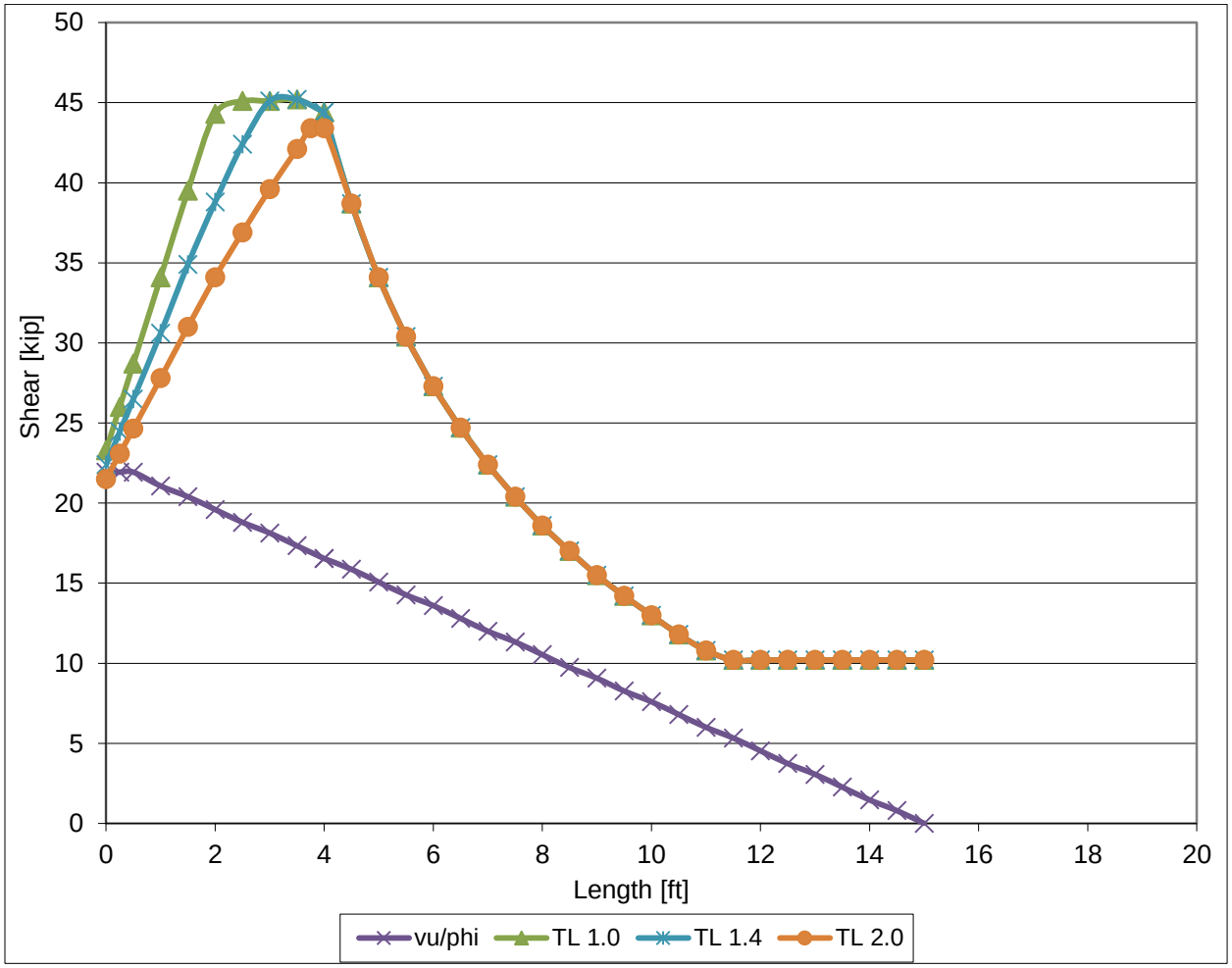

Figure 8.11 Shear Diagrams for 30 ft. long HC 12

An example of moment capacity diagrams is presented in Figure 8.12, where the comparison between the 3 factors applied to the transfer/development length equations is shown for the 40ft. long Double Tee section 7T264.

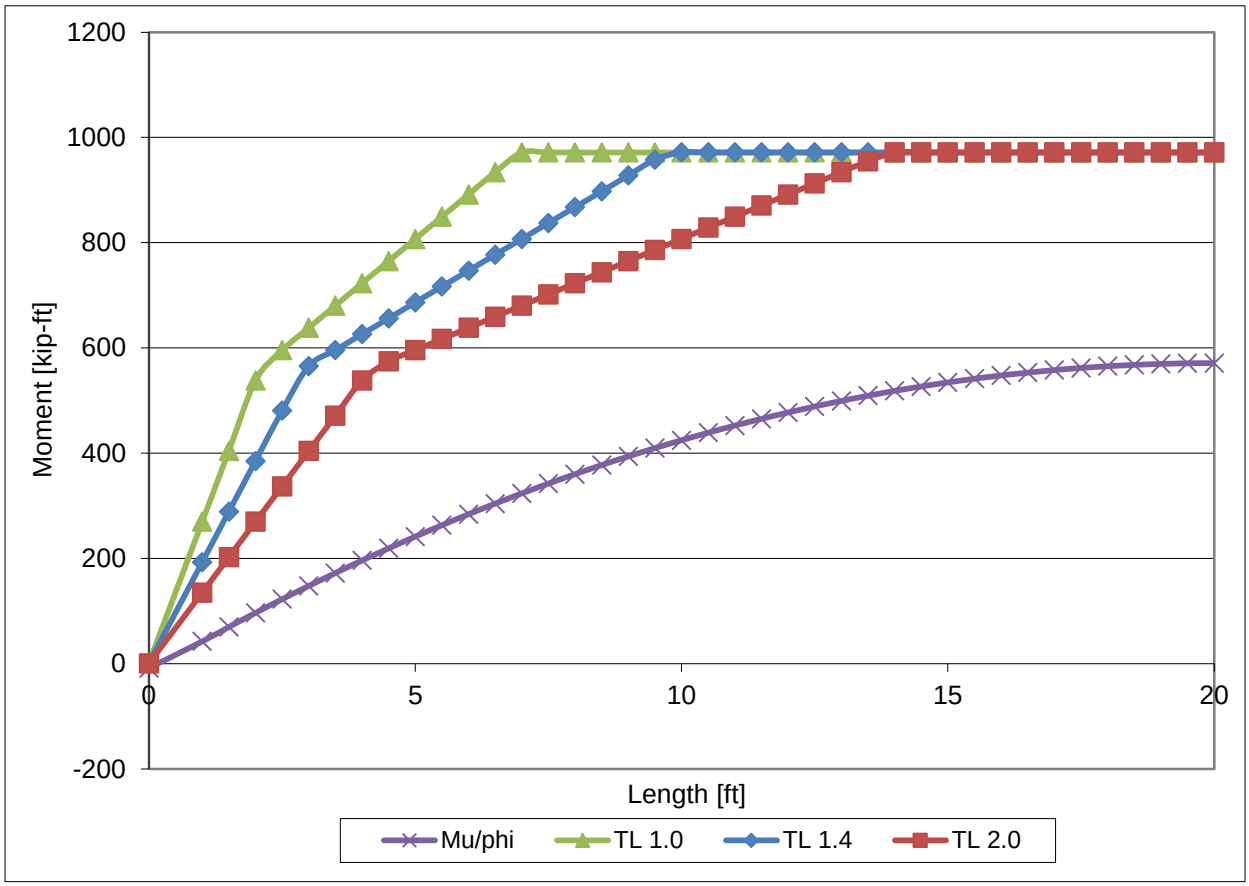

Figure 8.12 Moment Diagrams for 40ft. long 7T264

The effects of using lightweight concrete instead of normal weight concrete were also investigated during the Sensitivity Analysis Study. The results simply revealed that the lightweight factor, λ, reduces the shear capacities; but the percentages when comparing the 3 cases of transfer and development lengths considered are equal to the percentages obtained with normal weight concrete, since all the values are affected by the same factor. It was also observed that the lightweight factor, λ, does not affect moment capacity, therefore the percentages in this case are also equal to the values obtained when considering normal weight concrete.

8.3 Sensitivity Analysis Conclusions and Recommendations

The results obtained per beam section investigated in this study are specific to the section's case and cannot be generalized. The general trend observed in all cases was the reduction in moment as well as shear capacity near the beam ends, with an increase in transfer length.

The effects of longer transfer and development lengths are more pronounced in the flexural capacity than shear capacity of the sections analyzed.

For the uniformly loaded Double Tee and Hollow Core sections analyzed, the reduced capacities due to the considered longer transfer and development lengths were still higher than the factored load demand, indicating that uniformly loaded members may still perform well with increased transfer and development lengths. However, these results could be misleading as many Double Tee and Hollow Core members are subjected to heavy point loads near the end of their span, due to wall loading. The most sensitive cases were determined to be those of hollow core sections. Additional analysis is recommended, with distributed loading as well as concentrated loads considered.

Chapter 9 - Rectangular Beam Specimens at Stresscon

9.1 Introduction

In order to test the performance of the 3 strand samples A, G, and I in concrete beam sections, rectangular beams were made using the strands and loaded until failure at Stresscon, Inc. Stresscon Inc. is a prestressed concrete manufacturer located in Colorado Springs, CO. Beams were made and tested at Stresscon, Inc. in order to fabricate the beams using the same aggregates and similar mixture proportions used in a previous study on strand bond (Logan, 1997).

9.2 Beam Specimen Design and Fabrication

9.2.1 Rectangular Beam Specimen Design

9.2.1.1 Beam Dimensions and Strand Location

The rectangular beam specimens made at Stresscon, Inc. had design dimensions of 6.5 inches wide and 12 inches deep, as shown in Figure 9.1. The sections were reinforced with a single strand specimen placed in the middle of the beam's width and at a distance of 10 inches from the top face of the section. Ten 18 foot long beams were cast for each of the strand sources A, G and I.

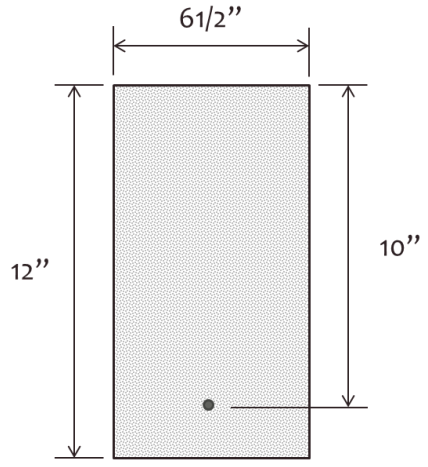

Figure 9.1 Beam Section Dimensions

9.2.1.2 Shear Reinforcement Details

Every beam section was tested on both sides, at pre-determined distances from the ends of each beam. Every beam was loaded on one side at a distance of 80% of the prescribed ACI 318 code development length from its end, and on the opposite side at a distance of 60% of the prescribed ACI 318 code development length from the beam's end.

The loading point selections were made in agreement with the project advisory committee, aiming to determine approximate development lengths. The loading configuration details for the short ends as well as the long ends of each beam are illustrated in Figure 9.2 and Figure 9.3 respectively. One side of each beam was loaded first, and then the beams were moved and prepared for their opposite end to be tested.

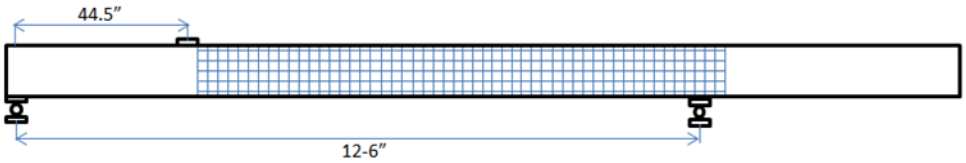

Figure 9.2 Short End (60% ACI L_d) Loading Configuration

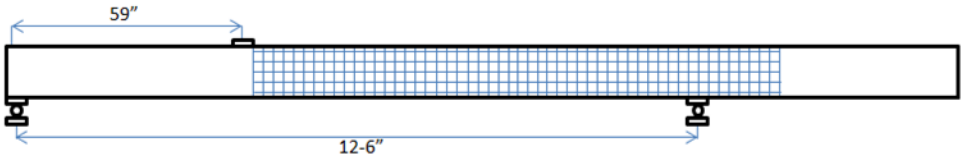

Figure 9.3 Long End (80% ACI L_d) Loading Configuration

Flexural beam sections were reinforced with welded wire fabric for shear between the two load application points to force beam failure between the beam load application point and the beam end. The welded wire fabric used for shear reinforcement of the Stresscon beams is shown in Figure 9.4. Similarly to Mr. Logan's study, 2 layers of 9 inch deep stem mesh were used (Logan, 1997), at 9ft and 7 ½ inches long. The shear reinforcement was used in order to avoid any interactions between the two beam ends, since flexural testing for development length was conducted on both sides of each beam. Figure 9.2 and Figure 9.3 show the shear reinforcement configuration details.

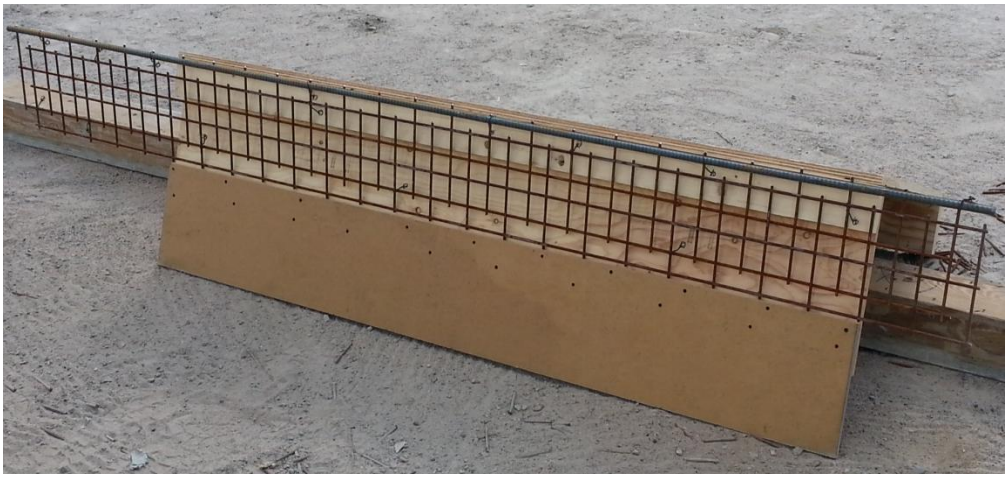

Figure 9.4 Welded Wire Fabric Shear Reinforcement

9.2.2 Concrete Mixture Design Specifications

The concrete mixture used during the beam study at Stresscon, Inc., was designed to match the low slump concrete mixture that was used by Mr. Logan during his 1996 strand bond study, also conducted at Stresscon, Inc. Figure 9.5 shows the concrete mixing plant used at Stresscon, Inc. The concrete mixture was designed for a concrete compressive strength at the time of initial prestress (f'_{ci}) of 3500 psi, and a 28-day compressive strength (f'_c) of 6000 psi. The mixture composition is shown in Table 9-1.

Figure 9.5 Concrete Mixing Plant at Stresscon, Inc.

Table 9-1 Concrete Mixture Design Specifications

Material	Quantity	Unit
Type III Cement	658	lb/yd^3
Water	322	lb/yd^3
Fine Aggregate	1081	lb/yd^3
Coarse Aggregate	1876	lb/yd^3
Delvo (admixture)	4	oz/cwt

9.2.3 Beam Fabrication Procedure

9.2.3.1 Beam Casting Schedule

The beams were fabricated on a single prestressed concrete bed at Stresscon, Inc. over three days. Two wooden beam forms were used, in which the strands were placed and tensioned before concrete placement. Each form was made long enough to include 5 beam sections and two dummy blocks, one on each end. The dummy blocks were 4 foot-long and were cast on both ends in order to accommodate de-tensioning by saw cutting. This ensured that all beam ends experienced the same type of strand release mechanism: saw cutting.

On the first day of concrete placement, the first five strand A and the first five strand I beams were fabricated. On the second day of concrete placement, the second set of 5 strand A beams were cast along with the first 5 strand G beams. The second sets of strand G and strand I beams were fabricated on the third day of concrete placement. The beam casting setup and schedule details are shown in Figure 9.6.

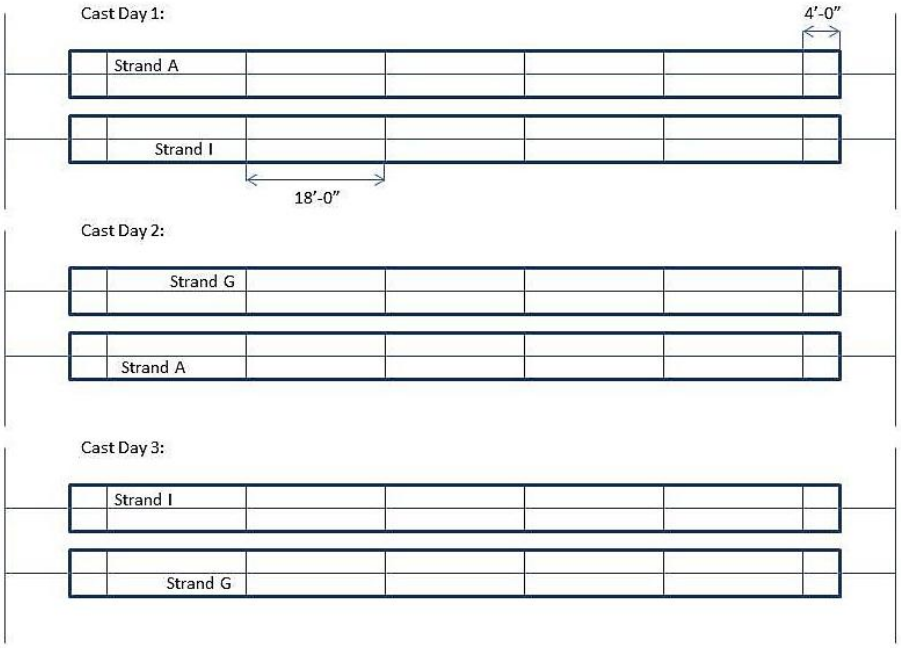

Figure 9.6 Beam Casting Setup and Schedule Details

9.2.3.2 Crack Formers and Beam Notching

It was originally planned to provide 4-inch tall galvanized steel crack inducers at the lower part of every beam below both locations of loading in order to control stress concentration and cracking in the concrete. The galvanized crack formers, which were wrapped with tape to assist with de-bonding from the concrete material, are illustrated in Figure 9.7.

The purpose of the crack formers was to force flexural cracking in the bond region, increasing the bond stress on the strand at that location. It was believed that this would result in more bond slip failures.

Figure 9.7 Crack Inducer Setup

Unfortunately after cast day 1, it was observed that the much higher strains experienced by the compressible tape on the crack former in the concrete were causing disturbances in the surface strain readings. Because of this issue, no crack inducers were placed in the beam forms on cast days 2 and 3. Instead, cracking was induced by saw cutting the beams at the desired locations. A single 1 in. deep saw cut was applied to 5 strand G long ends and 5 strand G short ends, to match the effects of the crack formers placed in the strand A and I beams that were fabricated on cast day 1. Except for the fact that no crack formers were placed in any of the strand G beams, the crack inducing techniques were kept consistent between strand groups. Table 9-2 shows the different crack inducing technique used per beam end. The table lists the numbered (1-10) beam ends, indicating with the letter "L" the ends which were loaded at a distance of 80% of the ACI development length (long ends), and with the letter "S" the ends that were loaded at a distance of 60% of the ACI development length, or short ends. For some of the sections there was only one, 1 inch deep saw cut implemented on the bottom face of the beam, but for others there were multiple saw cuts implemented at 2 or 3 locations on the bottom face and for others also on the sides of the beam. Post-test pictures of sections displaying 3 different crack induction techniques are shown in Figure 9.8, Figure 9.9, and Figure 9.10.

Figure 9.8 Crack Former

Figure 9.9 Saw Cut on Bottom Surface of Beam

Figure 9.10 Saw Cut on Bottom and Side Surfaces of Beam

Saw cuts in four beams were made under the load application point and at a distance d from the load towards the beam end on the beam ends tested at 60% of the ACI calculated development length. For these beam sides tested as short ends, the saw cuts were located at 33 in. and 43 in. from the ends. Similarly, saw cuts in four beams were made under the load application point and at a distance d and 2d from the load towards the beam end on the beam ends tested at 80% of the ACI calculated development length. For these beam sides tested as long ends, the saw cuts were located at distances of 37.5 in., 47.5 in., and 57.5 in. from the beam ends. This was done with the purpose of investigating the effects of cracking within the development length, since it is expected that flexural cracking will reduce the average flexural bond stress as the cracking disturbs the bonding action between the strands and the concrete material (Russell & Burns, 1993).

No saw cuts in any case made within the ACI transfer length, in order to avoid any bond slip and anchorage failure due to reduction in strand diameter immediately adjacent to the cracks, which is caused by the increased tension due to the cracking action. When cracking within the transfer zone can be avoided, the strands should be expected to develop to their full tension (Russell & Burns, 1993).

Table 9-2 Crack Inducing Techniques per Beam End

Crack Inducing Technique	Beam End (s):						Estimated Cracking Moment, M_{cr} (kip-in)
	A-L:	A-S:	G-L:	G-S:	I-L:	I-S:	
4" crack former	1-5	1-4			1-4	1-5	209
4" crack former + (1 or 2) 1.375" saw cuts and side cuts		5			5		215
One 1" saw cut		6	1-5	1-4, 6	6		250
(2 or 3) 1.375" saw cuts	8-10	8-10	8-10	8-10	8-10	8-10	247
(2 or 3) 1.375" saw cuts + 1" side cuts	6		6	5		6	238
NONE	7	7	7	7	7	7	260

The different crack inducing techniques imply different cracking moments (M_{cr}) per beam end. These moments were approximated for every case, and considered when comparing the experimental moment values that caused the first crack to appear on each section. The cracking moments were calculated assuming a modulus of rupture of 581 psi, which corresponds to a 6000 psi 28-day compressive strength as the concrete mixture was designed. The split tensile strengths of accompanying concrete cylinders were also determined experimentally, in order to compare to the modulus of rupture. The split tensile strengths are listed in Appendix A.

The cracking moment calculated for a standard beam of this study, assuming no crack inducing technique was determined to be 260 kip-in. For the cases where 4 in. crack formers were placed in the beams, the cracking moment was estimated at 209 kip-in. Adjustments were made to the cracking moment calculated for the standard plain concrete beam, in order to account for the reduced capacity due to the crack former taking up 4 inches of the section height, and the assumed zero stress on the bottom surface of the beam.

For the beams which were saw cut, the cracking moment was estimated at 250 kip-in. for the case of 1 in. tall saw cuts and 247 kip-in. where the cuts were 1 3/8" tall. For the case where there were additional 1 in. saw cuts on the sides of the beams, the cracking moment was estimated at 238 kip-in. These values were calculated by assuming reduced concrete surface capacities according to the saw cut dimensions per case. The beam end cracking moments are listed in Table 9-2.

9.2.3.3 Concrete Mixture Placement

The 30 beams were fabricated in groups of 10 on 3 different days, with concrete being placed at approximately 5 am on placement days 1 and 2, and 9am on placement day 3. Each cast day's concrete mixture properties and placement conditions are summarized in Table 9-3. The concrete compressive strengths and mixture temperatures as they varied with time are presented in Table 9-4 for the mixture placed on day 1, Table 9-5 for the mixture placed on day 2, and Table 9-6 for the mixture placed on day 3.

Table 9-3 Concrete Placement Conditions and Mixture Properties per Cast Day

Property	Day 1	Day 2	Day 3
Air Content (%)	1.6	1.4	1.5
Slump (in)	3.25	3.25	3.5
Unit Weight (lb/ft^3)	145.6	145.6	146.0
Concrete Temperature (°F)	74	74	78
Ambient Temperature (°F)	53	57	69
Release Strength (psi)	3860	3680	3880
Compressive Strength at 21 days (psi)	6690	6270	5800

Table 9-4 Day 1 Concrete Mixture Maturity Details (Beams A1-5, I1-5)

Time of Concrete Placement: 5:25am – 6:10am			
Cylinder Test Specimen	Time of Test	Compressive Strength (psi)	Mixture Temperature (°F)
CS-D1-1	11:35am	552	105
CS-D1-2	1:06 pm	2268	128
CS-D1-3	2:04 pm	2760	136
CS-D1-4	3:00 pm	3133	136
CS-D1-5	3:30 pm	3345	136
CS-D1-6	4:00 pm	3625	136
CS-D1-7	4:47 pm	3864	-
CS-D1-8	6:00 pm	4134	-

Table 9-5 Day 2 Concrete Mixture Maturity Details (Beams G1-5, A6-10)

Time of Concrete Placement: 5:11am – 5:39am			
Cylinder Test Specimen	Time of Test	Compressive Strength (psi)	Mixture Temperature (°F)
CS-D2-1	11:07 am	547	107
CS-D2-2	12:03 pm	1394	125
CS-D2-3	12:30 pm	1927	132
CS-D2-4	1:00 pm	2290	137
CS-D2-5	2:00 pm	2563	136
CS-D2-6	3:10 pm	3129	133
CS-D2-7	3:30 pm	3281	132
CS-D2-8	4:03 pm	3242	131
CS-D2-9	4:55 pm	3543	-
CS-D2-10	5:43 pm	3823	-

Table 9-6 Day 3 Concrete Mixture Maturity Details (Beams G6-10, I6-10)

Time of Concrete Placement: 9:02am – 9:28am			
Cylinder Test Specimen	Time of Test	Compressive Strength (psi)	Mixture Temperature (°F)
CS-D3-1	3:20 pm	1403	126
CS-D3-2	4:10 pm	2210	135
CS-D3-3	7:16 pm	3351	-
CS-D3-4	8:45 pm	3892	123
CS-D3-5	9:18 pm	3979	120

9.2.3.4 Beam Specimen Curing Conditions

The beam specimens were covered and cured in their fabricating forms until their companion concrete cylinders reached the specified compressive strength of 3500 psi. The beams were fabricated in outdoor conditions. Saw cutting was the method used to release the prestressing strands, and it took place as soon as the equivalent concrete cylinders reached 3500 psi compressive strength, which was specified as the release compressive strength in order to match Mr. Logan's 1997 study. Each individual beam section was then saw cut from its strand line as shown in Figure 9.11, and moved to a nearby location where the initial end slip readings as well as transfer length readings were taken.

Figure 9.11 Saw Cutting of Flexural Beam Sections

The beams were let to cure for approximately 21 days before flexural testing, as was done in Mr. Logan's study (Logan, 1997). Since the specimens were fabricated in 3 different days from July 16th and until July 19th, and tested during the period of August 5th to August 9th, the concrete age varied per beam group, between ranging from 18 to 22 days. The concrete beams were stored outside at Stresscon, Inc. during these days. The exact number of days after mixture placement that each beam group was tested is listed in Table 9-7 per case.

Table 9-7 Time Between Mixture Placement and Specimen Tested per Beam Group

Specimen	Fabrication Day	Flexural Test Day	Time Elapsed (days)
A 1-2	1	1	20
I 1-2	1	1	20
G 1-2	2	1	18
A 3-4	1	2	22
I 3-4	1	2	22
G 3-4	2	2	19
A 5	1	3	22
A 6	2	3	20
I 5	1	3	22
I 6	3	3	19
G 5	2	3	20
G 6	3	3	19
A 7-8	2	4	21
I 7-8	3	4	20
G 7-8	3	4	20
A 9-10	2	5	22
I 9-10	3	5	21
G 9-10	3	5	21

9.2.4 Transfer Length Measurements

9.2.4.1 Methodology

Transfer lengths were determined immediately after prestress release (initial transfer lengths) and also before load testing at approximately 21 days after beam fabrication. Transfer lengths were determined by analysis of end slip readings and surface strain readings. End slip

readings were taken after the prestressing force was released and each individual beam section was saw-cut from its strand line, as well as immediately before flexural testing of each beam.

In addition to end slip readings, a rapid, non-contact laser speckle imaging (LSI) device was used to measure concrete surface strains and therefore determine the transfer lengths immediately after strand release (Zhao, 2011).

Attempts were made to read surface strains using the LSI device also at the time of test, but since the beams were stored outdoors, the concrete surface had weathered and despite the protective covers that were used to avoid this, the concrete surface of most of the beam ends did not allow reading strains with the imaging device. Instead, the transfer length values corresponding to the time of flexural beam testing were determined indirectly by adding the end slip growth to the initial transfer length values which were determined at the time of prestress release. The increase in end slip between the time of flexural beam testing and time of prestress release was multiplied by the appropriate factors recommended for generating transfer lengths from end slip readings (Logan, 1997). The relationship between transfer length and end slip is shown in Equation 9-1, where Δ represents the measured strand end slip. It should be noted that the Modulus of Elasticity of the prestressing strand, E_{ps}, was 28,500 ksi, and the initial stress in the strand before losses, f_{si}, was 198 ksi; approximately 98% of the jacking stress which was set to 75% of the assumed ultimate stress for the strand (270 ksi).

$$L_t = \Delta \left(\frac{2\, E_{ps}}{f_{si}} \right) \qquad \textbf{Equation 9-1}$$

9.2.4.1.1 End Slip Readings

Strand end slip readings were taken using a digital depth gauge as shown in Figure 9.12. The digital length indicator was fixed on 3 supports to ensure stability during measurements. The device consists of a needle that stretches into the examined depth for a range of 0 to 0.47 inches, and can be controlled by a lift lever, operated using one hand. The digital display presents depth measurements of 0.0005 in. resolution.

The end slip readings represent the distance into the section that each strand pulled in, measured from the flat concrete surface of the beam specimens after they were saw-cut from their strand line. Strands slip occurs when greater stresses than the bond strength at the steel and

concrete interface are experienced. At the time of prestress release, which was achieved by saw-cutting in this study, slip is expected to occur throughout the transfer length of all members.

Unfortunately, the end slip readings taken were found to not represent the total strand end slip, because the concrete surface was polished by the excessive wobbling of the saw blade during saw cutting. End slip values of 0.000 were obtained in some cases, which confirmed that the initial readings did not accurately reflect the initial end slip. The initial end slip readings were compared to the end slip readings taken at the time of test to give the growth in end slip. The growth in end slip was then used to calculate the growth in transfer length using Equation 9-1.

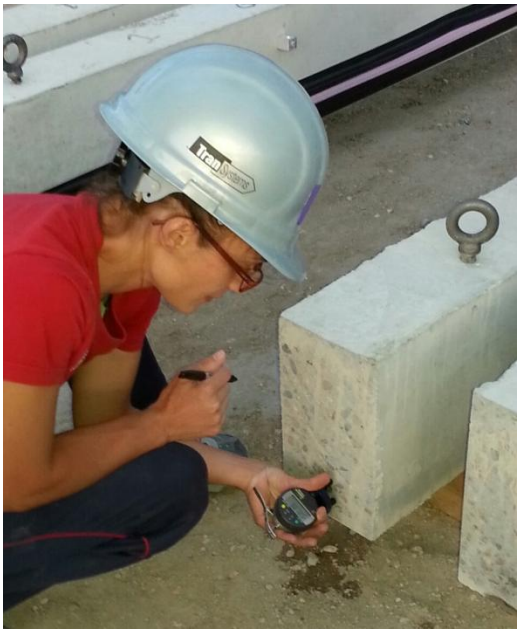

Figure 9.12 Taking End Slip Readings

9.2.4.1.2 Laser Speckle Imaging

An automated non-contact surface strain reading device was developed at Kansas State University. This study was the first occasion that the laser speckle device took surface strain measurements while being mounted on a vertical surface.

While the device moved along the concrete beam surface, it generated and recorded digital laser speckle images of the surface. Images were taken preceding as well as succeeding stress application to the surface, and with digital processing, the surface strains could be

determined through correlation of the surface roughness. The LSI device and its corresponding software while generating digital images are shown in Figure 9.14.

Transfer Length values were obtained by 2 methods of analysis of the surface strain readings. The first method is the 95% AMS method (Russell & Burns, 1993), which is commonly used in transfer length studies. The transfer lengths by 95% AMS were determined when smoothed surface strain data are plotted and the operator determines the strain profile plateau by observation and judgment, and takes the maximum strain value which is then multiplied by 0.95 to determine the "95% Average Maximum Strain (AMS)". The point where the 95% AMS line intersects the smoothed strain profile, which is a distance from the end of the beam, is thought to be the transfer length (Russell & Burns, Design Guidelines for Transfer, Development and Debonding of Large Diameter Seven Wire Strands in Pretensioned Concrete Girders, 1993). One of the surface strain profiles obtained during the flexural beam study is shown in Figure 9.13, where the transfer length was 45 inches.

The second method used in this study is a statistically-based process called the Zhao-Lee (ZL) method, which was proposed by the LSI device inventors at Kansas State University. The ZL method is an unbiased process of strain profile analysis, and was confirmed to provide faster, more accurate, and more reliable transfer length values when compared to the 95% AMS method (Zhao, Beck, Peterman, Murphy, Wu, & Lee, 2013). While the 95% AMS method requires manual implementation by the operator in order to yield transfer length values, the ZL method software generates the values automatically, taking the random error due to the strain sensor into account, and eliminating the bias or human error involved in manual determination of the strain profile plateau (Zhao, Beck, Peterman, Murphy, Wu, & Lee, 2013).

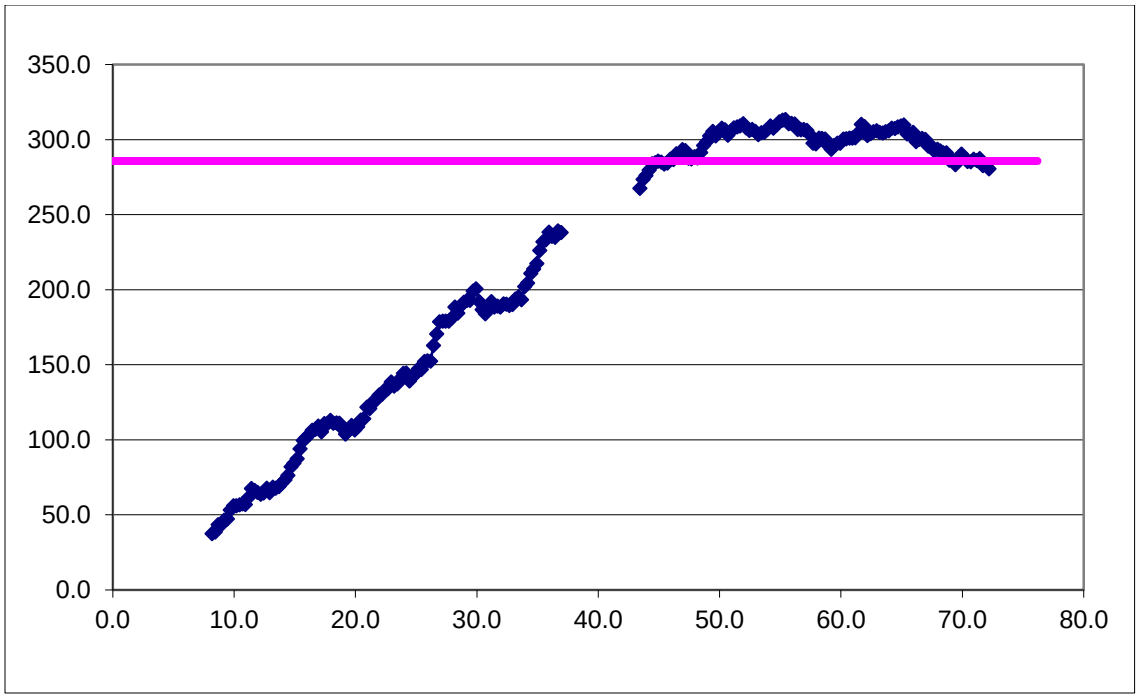

Figure 9.13 Surface Strain Profile

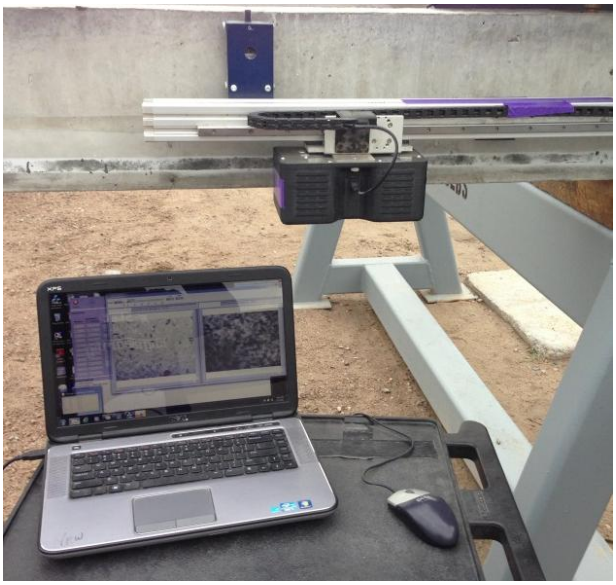

Figure 9.14 Laser Speckle Imaging Device and Digital Speckle Patterns

9.2.4.2 Instrumentation Setup for Laser Speckle Imaging Device

Aluminum mounting blocks were fabricated at Kansas State University prior to the research group's visit to Colorado Springs, in order to mount the laser speckle imaging (LSI)

device onto the beams. Bolt inserts were placed on the inside of the concrete beam forms before concrete placement, and the aluminum blocks were later bolted on the concrete surface once the wooden forms were removed at the time of prestress release. The aluminum blocks used to mount the LSI device on the vertical surface of the concrete beams are shown in Figure 9.15. This method of mounting the LSI device on the vertical surface of the beam sections allowed for consistent and accurate imaging, assuring that the laser speckle images will be taken at exactly the same locations before and after de-tensioning.

The black paint on the concrete beam surface seen in Figure 9.15 marks the part of the surface where laser speckle readings were taken. A textured paint was used in order to create an artificial speckle pattern for the LSI device to base its initial readings on, and return after de-tensioning to the same location to take readings on the same speckle pattern, in order to allow for correlation between the image pairs. The LSI device is sensitive to surface roughness characteristics, and factors like dust and water that alter the concrete surface can cause the LSI device to not recognize the strain surface analyzed initially. It is therefore unable to correlate the subsequent images taken before and after de-tensioning, and generate surface strain values.

Figure 9.15 LSI Device Mounting Instrumentation

9.2.4.3 Transfer Length Measurements at Release

Only the LSI device readings were used to determine transfer lengths at release, since the end slip readings were considered invalid. It was observed that the excessive wobbling of the

saw blade had ruined the concrete surface of the beams; therefore the end slip readings were not considered for determining the initial transfer lengths.

Analysis of the surface strain measurements obtained by the LSI device returned the average initial transfer length values shown in Table 9-8, including both the transfer lengths obtained manually by the 95% AMS method, and the values obtained by the ZL software method of surface strain measurement analysis. The transfer length values for each individual beam end at the time of release are listed in Appendix B.

Table 9-8 Average Transfer Length Values at Release for Strands A, G, and I by 95% AMS and ZL Method Analysis

Strand Source	Average Transfer Length at Release (in)	
	95% AMS method	ZL method
A	34.6	35.8
G	27.4	28.1
I	39.6	42.2

9.2.4.4 Transfer Length Measurements at Test

At the time of test, the LSI device was not able to take surface strain readings on all beam ends. Protective plastic covers were placed on the sides of the beams to prevent mud from splashing onto the areas where readings were being taken. Between the time of the initial surface strain readings after strand release and before testing, it was observed that the paint used to enhance the image definition delaminated. The plastic covers placed on the concrete side surfaces sealed in the moisture. Moisture from the beam interiors caused the paint to delaminate, changing the concrete surface. This made it difficult to obtain surface strain readings before load tests.

End slip readings were taken before flexural beam testing. The difference between these end slip readings and the initial end slip readings taken at the time of prestress release gave the growth in end slip. The transfer length growth calculated from the end slip growth values using Equation 9-1 were added to the transfer lengths at the time of release to give the beam transfer lengths at the time of load testing. The average transfer length values at the time of flexural beam testing are shown in Table 9-9. The transfer length values shown in Table 9-9 were generated by adding the transfer length growth calculated through the end slip growth values to

the values determined by the ZL method for the transfer lengths at the time of prestress release. The transfer length values for each individual beam end at the time of release are listed in Appendix C, and the individual end slip values per beam end are provided in Appendix D.

Table 9-9 Average Transfer Length Values at Time of Flexural Beam Testing for Strands A, G, and I by ZL Method Analysis

Strand Source	Average Transfer Length at Time of Test (in) (ZL method)
A	48.5
G	37.7
I	54.7

9.2.5 Flexural Beam Testing

9.2.5.1 Instrumentation Setup and Testing Procedures

A special testing frame was prepared by Stresscon, Inc. for this study. The frame was fabricated by bolting a steel beam onto two 7ft by 7ft concrete blocks, which served as gravity loads for the reaction load. The specimens were loaded using a hydraulic cylinder which was brought to Stresscon, Inc. by the project investigators from KSU. The load and stroke outputs of KSU's hydraulic cylinder which is implemented with a pressure transducer, load cell and cable potentiometer, were captured by a Keithley Model 2700 data acquisition system. Linear Variable Differential Transformers (LVDTs) were also brought to the testing site from KSU in order to measure beam deflection and strand end slip during the tests. The beam loading setup is shown in Figure 9.16, Figure 9.17, and Figure 9.18.

Steel plates were placed on the top surface of each beam section using the gypsum product "Hydrostone" in order to provide a consistent loading point, and distribute the load along the width of the beams. Steel plates were also placed on the bottom surface of each beam where pin and roller support configurations were placed for each beam. The plates are shown in Figure 9.16 - Figure 9.19. Figure 9.19 illustrates the roller support configuration system. Using pin and roller supports allowed for accurate measurements of the beam deflection at the loading point and ensured that the beam was statically determinate for analysis.

Figure 9.16 Beam Testing Setup: Loading Setup

Figure 9.17 Beam Testing Setup: Load Cell, Load Point LVDTs, End Slip LVDT

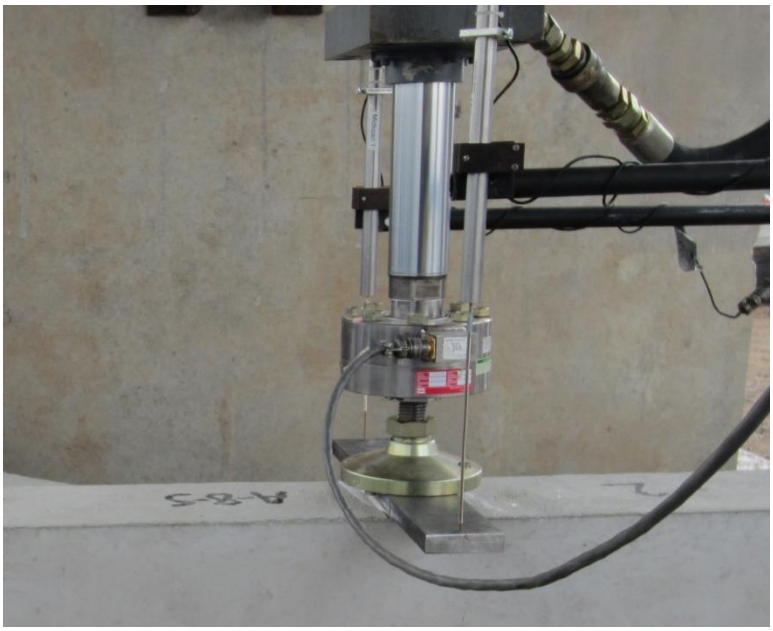

Figure 9.18 Beam Testing Setup: Load Application Point on Steel Plate, LVDTs

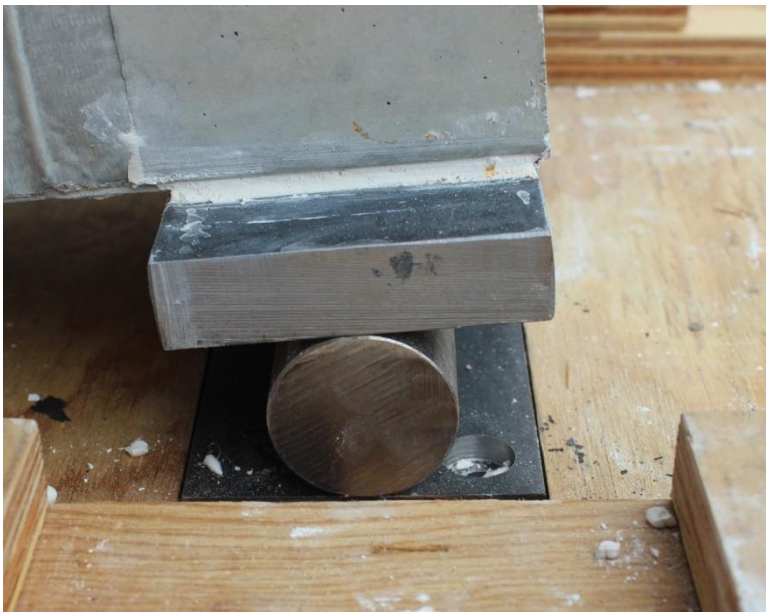

Figure 9.19 Beam Testing Setup: Roller Support Configuration

9.2.5.2 Beam Loading Procedures

The loading rate was set to 1000 lb/ minute, up to the 7000 lb limit. After that, loading proceeded at 250 lb/ minute until beam failure. It should also be noted that as directed by the advisory committee, during the first 2 days of testing the load was held once strand end slip

initiated and until the beams were stable again, or experienced no additional end slip for 1 minute.

9.2.5.3 Test Results

Data collected from the flexural beam testing included strand end slip, beam deflection, load, and time of first visual observation of cracking. Each test was video recorded, and a description of each failure mode was also made. The actual measured dimensions of each beam were also recorded after saw cutting, and the details are listed in Appendix E.

Graphs illustrating the measured moment, deflection, and end slip as well as a photo of the failure were prepared for every beam end tested, with the example of beam end G-9-S, which stands for strand G, beam 9, short end (60% L_d) is shown in Figure 9.20.

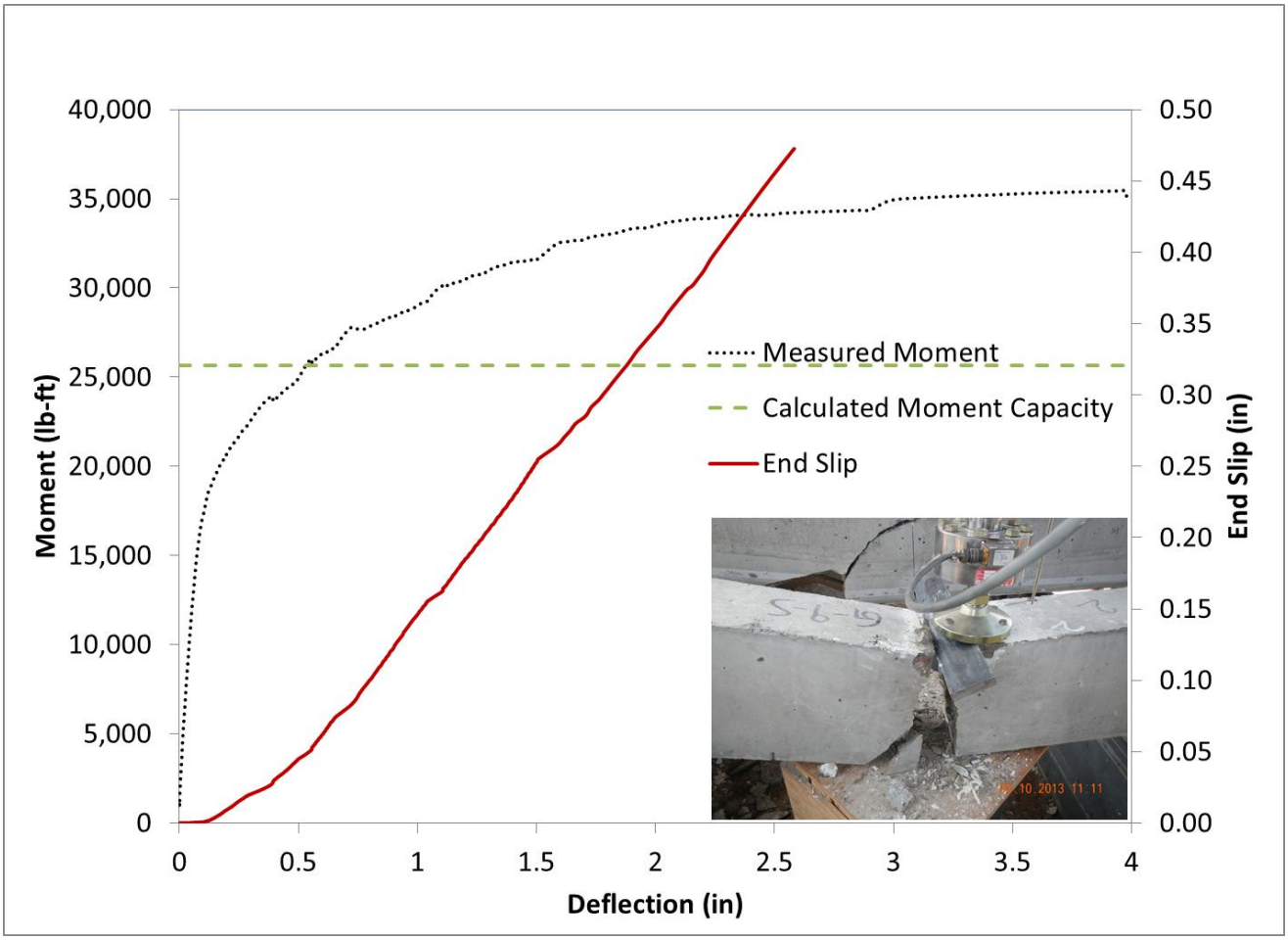

Figure 9.20 Moment, Deflection, End Slip Plot for Beam End G9-S

A summary of the results from the Flexural Beam Testing study is presented in Table 9-10, where the average transfer length at the time of test, the average ratio of experimental moment to nominal moment capacity and average end slip are listed by beam end group. The beam ends are grouped by strand source and length tested.

It should be noted that the nominal moment capacity of the beams tested at a distance of 80% of the ACI code development length was calculated to be 348 kip-in., and the nominal moment capacity of the beams tested at a distance of 60% of the ACI code development length was determined to be 308.3 kip-in., therefore each individual experimental moment value was compared to the nominal capacity of its particular end group. The nominal moment capacities were calculated as shown in Appendix F.

From the results we can see that the beam ends on which more saw cuts were applied reached lower experimental to nominal moment ratios compared to the beam ends where fewer saw cuts were made or no saw cutting was performed at all. In all 3 strand source cases, the lowest moment ratios were experienced by the longer beams ends. Within each long end category, the beam ends that reached the lowest ratios were those on which more saw cutting was applied. The lowest ratio overall was obtained by specimen I-5-L, which was the only beam in the study with 2 saw cuts applied in addition to its crack former.

Beam ends 8-10, both long and short for all 3 strand sources tested, we saw cut at 1.375 in., but where the short ends had 2 cuts; the long ends had 3 cuts applied to them. The additional saw cuts affected these ends by disrupting the bond between steel and concrete, and therefore causing early bond failures. This explains the fact that the short ends resulted in higher ratios than the long ends, as less saw cutting action on the short ends allowed them to outperform their calculated nominal capacity by higher percentage. The average experimental to nominal moment ratios per beam end group are shown in the third column of Table 9-10.

The failure mode experienced by every beam end that was tested was described as either Shear-Compression, or Strand Rupture. A summary of the failure modes is shown in Table 9-11, also organized by beam end group. A summary of the flexural beam testing results per beam end tested is provided in Appendix G. The moment, deflection and end slip charts as well as photographs of the beam ends after failure are provided in Appendix H.

Table 9-10 Average Transfer Length, Experimental to Nominal Moment Ratio, and End Slip During Test Values per Beam End Group

Beam End Group	Lt (in.)	M_{exp}/M_n	End Slip during Test (in.)
A-S	50.4	1.29	0.183
A-L	46.6	1.15	0.046
G-S	36.9	1.32	0.220
G-L	38.4	1.21	0.033
I-S	53.5	1.21	0.668
I-L	56.0	1.09	0.227

Table 9-11 Beam End Group Failure Mode Summary

Beam End Group	Number of Shear Compression Failures	Number of Strand Rupture Failures
A-S	5	5
A-L	9	1
G-S	7	3
G-L	4	6
I-S	5	5
I-L	6	4

Initial observations from the flexural beam testing rounds included the early cracking loads experienced by the beams, a fact that explains the long transfer lengths noted. It was also noticed that the beam ends that were characterized by "poor bond" did not experience typical flexural behavior during the tests, and developed only 1 crack at a single location before failure, where the beam ends associated with better quality bond were able to develop multiple cracks before failure. Slip is believed to occur at a location where higher stress is applied compared to the bond strength of the strand to the concrete at that location. Consequently, for lower bonding strands there was a longer range of locations where low bond strength was experienced, and slip had occurred before any cracking was able to form.

Another key observation from this study was that when the cracking strength of the beams was reduced by additional saw cuts, the beam ends were reaching lower moment capacities compared to their equivalent ends of less or no saw cutting applied to. There were 4 strand I failures and 1 strand A failure which occurred below nominal capacity, all in the case of beam ends tested at 80% of the ACI L_d, and all in the groups of beam ends with the highest number of saw cuts applied to.

In general, strand I specimens reached the lowest experimental to nominal moment ratios compared to their equivalent groups of strand A and strand G beam ends, and also experienced the highest values of end slips during testing. Strand G outperformed strand A as far as moment capacity ratios are concerned; which was expected after strand G tested as a higher bonding source in the ASTM A1081 testing rounds.

The transfer length values obtained per strand source follow the trend that the ILS study results revealed, with strand G experiencing the shortest transfer length values out of the 3, strand I experiencing the longest transfer length values out of the three and strand A specimens having transfer length values between those of I and G, similarly to being the middle performer when tested by ASTM A1081.

Chapter 10 - Determination of ASTM A1081 Threshold Value

10.1 Statistical Analysis of Data

The results from the Inter-Laboratory study (ILS) were analyzed in order to determine a fair pullout force value for each strand source A, G and I. The data included results from 6 laboratories other than KSU, plus the 5 sets of results from KSU labs where 5 different cement sources were used in the testing. Statistical analysis of the ASTM A1081 values obtained for each strand concluded with the numbers listed in
Table 5-7, where Method A represents the standard ASTM A1081 test method.

The average pullout force values from the Inter-Laboratory study are considered unbiased, since they were obtained at different testing sites while using dissimilar material and where testing was conducted under diverse conditions.

It was concluded that a simple statistical analysis of the average beam performance values will be the most applicable in order to determine an acceptable threshold value for ASTM A 1081 based on the flexural beam performance at Stresscon. Analysis was conducted considering the multiple sets of results obtained during the flexural beam testing study. The transfer length values at time of prestress release, transfer length values at the time of test, and moment performance ratios where some of the data sets the threshold statistics were based on.

Analysis was conducted for every case by plotting the average values per strand against the ILS study results, and also considering the 90% confidence interval with 5% fractal applied as well as the 90% interval with a 10% fractal applied.

10.2 Transfer Length Measurements

The transfer length values obtained during the flexural beam study at Stresscon were considered rather high in comparison with other recent studies, but the early cracking moments experienced by the beams during flexural testing confirmed the long transfer lengths. The concrete compressive strengths at release were selected to be as close as possible to 3500 psi because this is a lower-bound release strength expected for prestressed concrete plants.

Attempts were made in order to determine the ASTM test threshold value based on the transfer length values determined during the Stresscon study, but the analysis revealed that in

order to meet ACI code requirements for transfer length, the strands should have unreasonably high pullout force values when tested by ASTM A 1081. The threshold values resulting from the statistical analysis of the transfer lengths at release and also at the time of test are summarized in Table 10-1.

As agreed with the advisory committee, a 90% confidence interval on 10% fractal as well as a 90% confidence interval on 5% fractal was applied to the numbers, which brought the threshold values even higher. After review of the potential threshold values, the committee decided to consider other criteria for the basis of the ASTM A1081 threshold value.

Determining the 90% confidence values for ASTM A1081 was performed following the Experimental Statistics portion of the National Bureau of Standards Handbook. The document lists the factors corresponding to one-sided tolerance limits per sample size per case of confidence interval targeted and the related fractal values (Natrella, 1963).

For example in our case, for a 90% confidence that 90% of our values will be above the average value obtained during the ILS, or a 90% confidence that no more than 10% will be lower than the average ILS average value (10% fractal), the standard deviation of the ILS population was multiplied by a K factor of 2.012 as recommended by Mary Gibbons Natrella in the National Bureau of Standards Handbook, and then added to the average value obtained by the ILS population. Similarly, the 5% fractal values were determined, applying instead the recommended K factor of 2.503 for a sample size of 11 (Natrella, 1963). The values calculated following Natrella's recommendations were incorporated in the threshold determination analysis, obtaining potential acceptance criteria that will ensure adequate bond strength with high confidence.

Table 10-1 ASTM A1081 Pullout Force Values Corresponding to ACI 318 Transfer Length Values at Release and at Time of Test

Time of Transfer Length Measurement	Pullout force that corresponds to the ACI 318 calculated transfer length for the ASTM A1081 Inter-Laboratory study		
	Average Pullout Force (lb)	90% Confidence Interval on 10% Fractal (lb)	90% Confidence Interval on 5% Fractal (lb)
Strand Release	15,400	20,200	21,400
Time of Flexural Testing	21,700	29,500	31,500

10.3 Beam Specimen Experimental Moment

The experimental moment values were determined for all tests, and compared to the section's nominal moment capacity, resulting in ratios above or below unity, showing if the beams met or not their expected performance to be considered reliable for use in pretensioned applications. An ultimate strength of 270 ksi was assumed initially for all 3 strand sources, as they are all rated as 270 ksi minimum ultimate strength samples, but in reality, the strands are produced to reach higher ultimate strengths than their rated values, therefore the exact ultimate strengths per strand source A, G and I were determined experimentally at KSU laboratories, in order to determine the actual strength each strand source was able to reach before rupture.

10.3.1 Ultimate Tensile Strength of Strand

The ultimate tensile strength of each strand source was measured at Kansas State University after completion of the Flexural Beam Study. The specimens were secured by strand chucks, and epoxy-filled steel tubes were placed at both ends of each specimen in order to distribute the force evenly and avoid strand rupture at the chucks. Strand samples were loaded to failure on a tensile testing frame, and the ultimate force values were recorded. An example showing one of the test specimens after rupture is illustrated in Figure 10.1.

Figure 10.1 Ultimate Tensile Strength of Strand Test Specimen after Failure

The ultimate strength of each strand source was determined as the average of 5 strand tensile strength tests, and the values are summarized in Table 10-2. These values were used to calculate the experimental moment calculations for the flexural beams which had failed by strand rupture at Stresscon, Inc. The ratios of beam experimental moment capacity-to-calculated moment capacity using the strand measured ultimate strength are listed in Table 10-3.

Table 10-2 Ultimate Tensile Strength (ksi) per Strand Source

Strand Source	F_{ult} (ksi)
A	281
G	281
I	280

Table 10-3 Average Moment Ratios per Beam End Group Calculated Using Strand Ultimate Strength

Beam End Group	M_{exp}/M_n
A-S	1.25
A-L	1.15
G-S	1.29
G-L	1.17
I-S	1.20
I-L	1.07

10.4 Threshold Value Determination

After discussion with the committee, it was decided that the most reasonable basis for proposing a threshold value for ASTM A1081 test would be the experimental performance of the flexural beams in terms of the moment capacity reached compared to their nominal moment capacity. The average moment performance ratios per strand source were plotted and compared to the ILS pullout force average values, 90% confidence, 10% fractal values, as well as the 90% confidence, 5% fractal values calculated.

Initially, a linear fit of the data was considered to extrapolate and find the ASTM A1081 value for a strand that would have the calculated capacity match that of the experimental capacity. Figure 10.2 is a graphical explanation of the linear analysis assumption. A linear fit of the data however was problematic however because it assumes that the moment capacity can

increase indefinitely with higher bond. This cannot happen because the moment capacity is limited by the moment at which strand rupture occurs.

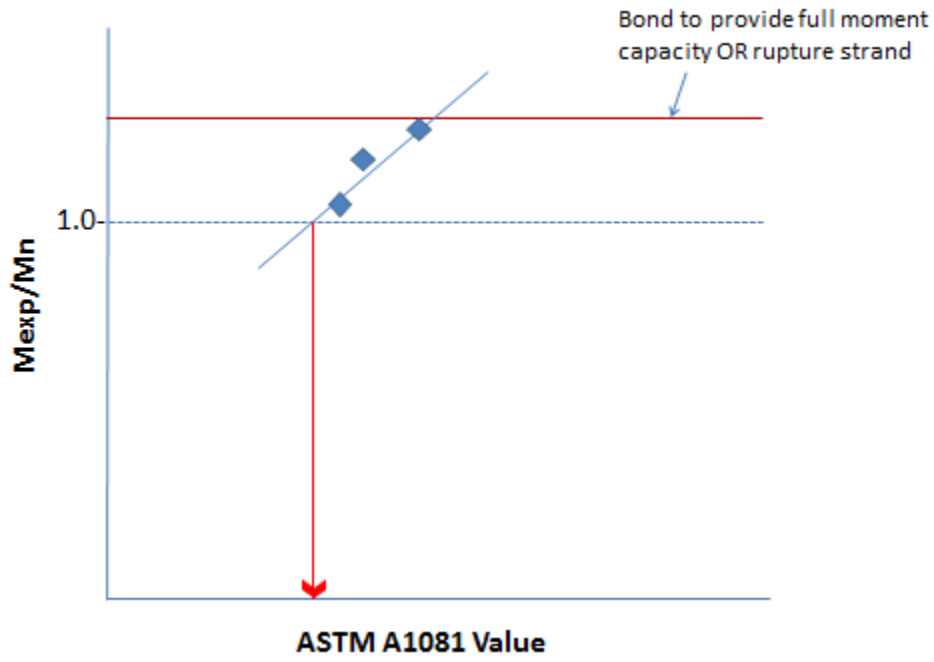

Figure 10.2 Graphic Representation of Linear Analysis of Data for ASTM A1081 Threshold Determination

A polynomial analysis of the data was used in the analysis and gives a more realistic fit. Figure 10.3 represents the polynomial fit analysis used during the ASTM A1081 threshold determination study.

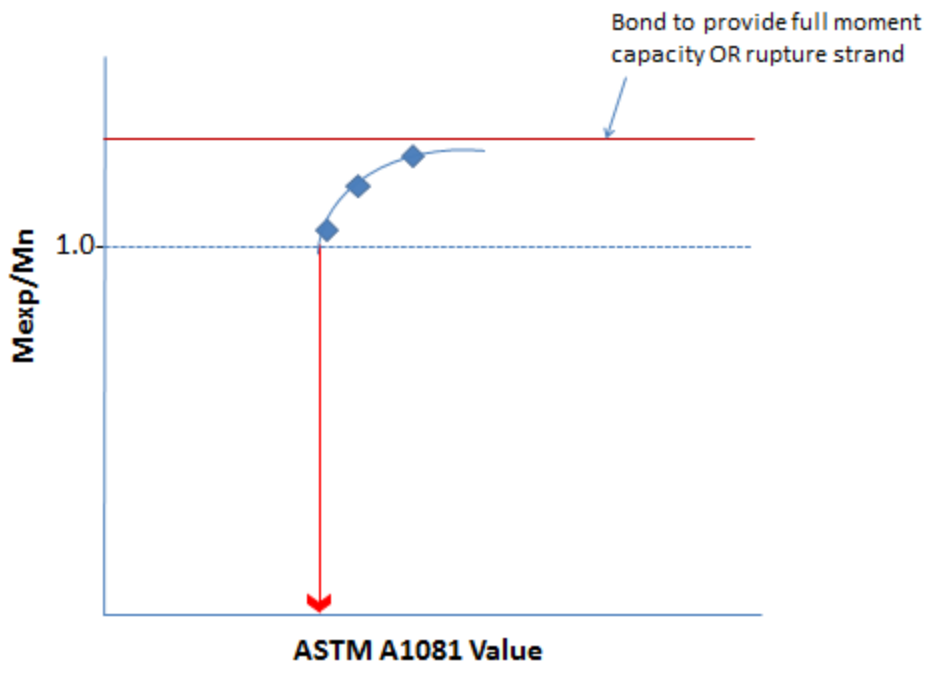

Figure 10.3 Graphic Representation of Polynomial Analysis of Data for ASTM A1081 Threshold Determination

Since prestressing a concrete beam with a single strand is a very rare occasion, it was decided to numerically investigate the consequences of using multiple strands in a beam on the strand moment capacity. For this analysis, it was assumed that the moment capacity of a beam prestressed with 2 strands instead of 1 will be the average of the moment capacity of 2 separate beams prestressed with 1 strand each. This method assumed no interactions between the strands.

The committee had advised the project investigators that a combination of 6 strands would be the minimum number of strands in a beam and was selected for use in the threshold determination. All combinations of strands up to 20 strands in a single beam were investigated however. Considering combinations of multiple strands, therefore averaging their performance, implied lower standard deviations, which resulted in decreasing threshold values with increasing number of strands combined. The procedure followed is explained in Table 10-4. The strand averaging effects to the standard deviations considered in this study are presented in Figure 10.4.

Table 10-4 Strand Averaging Procedure Example

Combination	Combined Value 1	Combined Value 2	Strand Average
1 & 2	1.300	1.310	1.305
1 & 3	1.300	1.380	1.340
1 & 4	1.300	1.351	1.326
2 & 3	1.310	1.380	1.345
2 & 4	1.310	1.351	1.331
3 & 4	1.380	1.351	1.366
Average			1.335
Standard Deviation			0.020

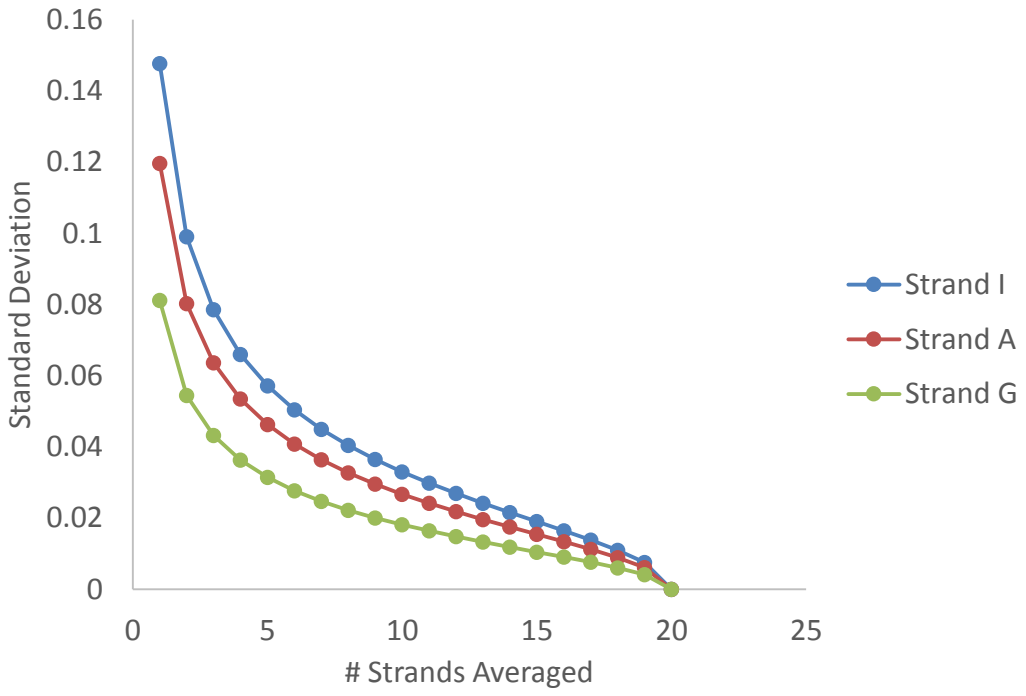

Figure 10.4 Strand Averaging Effects to Moment Ratio Standard Deviation Values

In order to complete the calculations in a timely manner, a macro was written in Visual Basic for Applications (VBA) in excel, which yielded an over 180,000 values when considering all possible combinations of 10 out of 20 strands. The combinations were made with all twenty strands, but were later reproduced after separating the ends among short and long, since the

moment ratios per case are based on different assumptions. Figure 10.5 is a plot of the threshold value variation as the number of strands in a single beam section increases, using the numbers generated during the first round of analysis where the ratios of all 20 beam ends tested per strand source were considered.

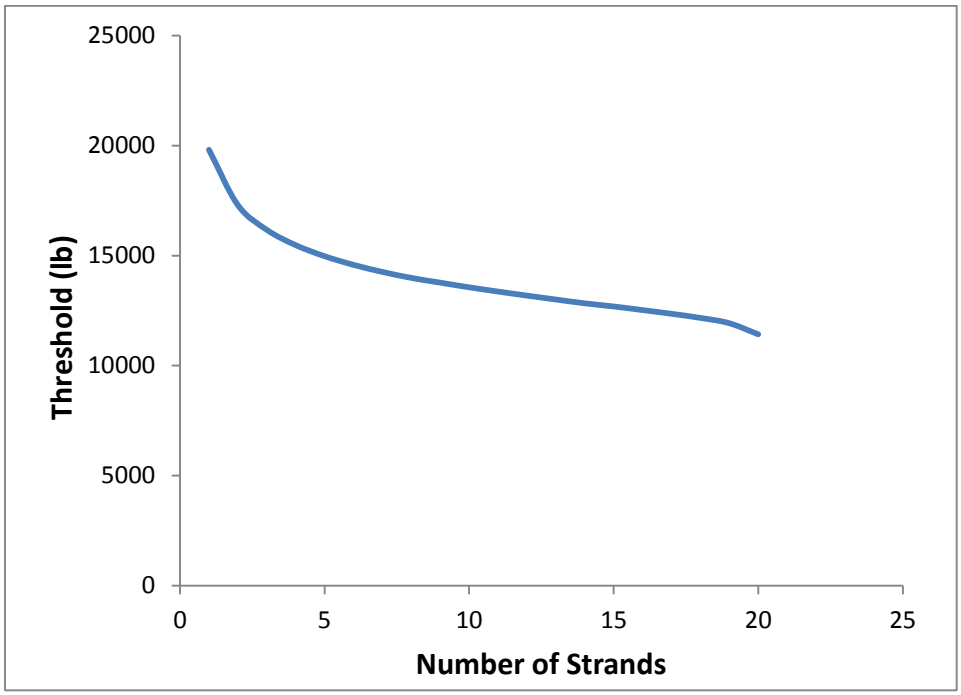

Figure 10.5 Threshold Value vs Number of Strands Combined- Polynomial Analysis

The analysis was repeated, with the ratios now considered separately for the short and long beam ends. Threshold values were calculated considering 6 strands per beam, the average pullout force values from all the valid sets of data obtained during the Inter-Laboratory study, as well as the 90% confidence intervals with 5% and 10% fractals applied.

The recommended threshold values are presented in Table 10-5, which lists the recommended threshold values by method of analysis, for the case of prestressing a beam section with only 1 strand just as it was incorporated in the Stresscon beam study, but also for the case of 6 strands prestressing a single beam section without any interaction between them.

Table 10-5 Recommended ASTM A1081 Threshold Values

Type of Analysis	Pullout force that corresponds to meeting Stresscon beam Moment Capacity for the ASTM A1081 Inter-Laboratory study		
	Average Pullout Force (lb)	90% Confidence Interval on 10% Fractal (lb)	90% Confidence Interval on 5% Fractal (lb)
1 Strand- 20 beam ends	14,400	18,800	19,800
1 Strand- 10 beam ends tested at 60% ACI L_d	13,400	17,400	18,400
1 Strand- 10 beam ends tested at 80% ACI L_d	14,800	19,300	20,500
6 Strands- 20 beam ends	10,900	13,900	14,600
6 Strands- 10 beam ends tested at 60% ACI L_d	10,100	12,700	13,400
6 Strands- 10 beam ends tested at 80% ACI L_d	11,400	14,500	15,300

Chapter 11 - Simple Quality Assurance Test for Strand Bond

11.1 Introduction

In addition to the flexural beams tested at Stresscon, Inc., 3 additional beams for each strand of smaller cross section were fabricated on cast day 3, and were shipped to be tested by RJ Peterman and Associates, under the Simple Quality Assurance Test for Strand Bond proposed by Robert J. Peterman (Peterman, 2009). The test method provides a simple procedure for verification of bond for the concrete mixture, strand being used, placement conditions, and de-tensioning conditions used at a particular prestressed concrete plant (Peterman, 2009).

The dimensions of the standard beam tested under the Simple Quality Assurance Test for Strand Bond are shown in Figure 11.1 and the test loading configuration in Figure 11.2.

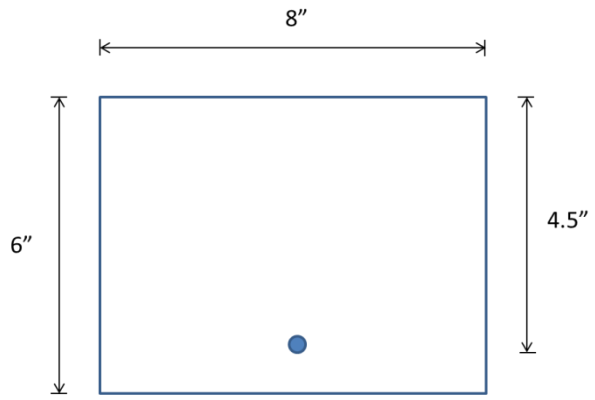

Figure 11.1 Simple Quality Assurance Test for Strand Bond Specimen Dimensions

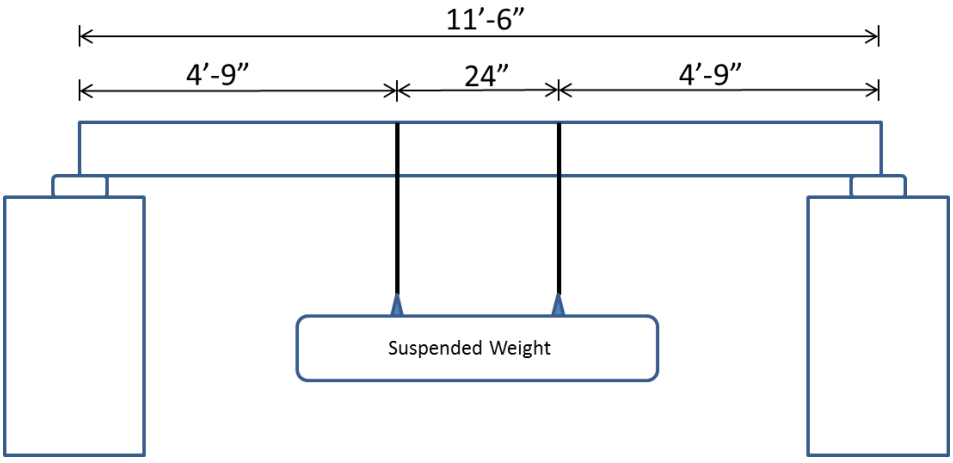

Figure 11.2 Simple Quality Assurance Test for Strand Bond Loading Configuration

11.2 Beam Specimen Design and Fabrication

The Peterman test beams were cast at Stresscon, Inc., with the same concrete mixture as the flexural beam test specimens. Three beams for each strand source A, G and I were fabricated. The quality assurance beams were dimensioned at the standard 8 in. by 6in. by 11 ft. 6 in. long, prestressed with a single strand in the beam center at 4.5 in. below the beam top surface. No shear reinforcement was provided for the specimens, as specified by the test protocol.

The beams were all fabricated in a single line, with splice chucks used in order to connect the 3 different strand sources. The 9 beam sections were saw cut to their specified length as soon as the companion concrete cylinder reached a compressive strength of 4040 psi, following the same de-tensioning procedures as the flexural beam specimens at Stresscon, Inc.

11.3 Test Methodology

The Simple Quality Assurance Test for Strand Bond was employed by setting each beam on simple supports and gradually loading each beam section to 85% of its calculated nominal moment capacity, (Peterman, 2009). The loading setup for the quality assurance test is shown in Figure 11.2 and Figure 11.3, and test specimen A1 is shown in Figure 11.4, as an example of the full test setup configuration.

Figure 11.3 Simple Quality Assurance Test for Strand Bond Loading Setup

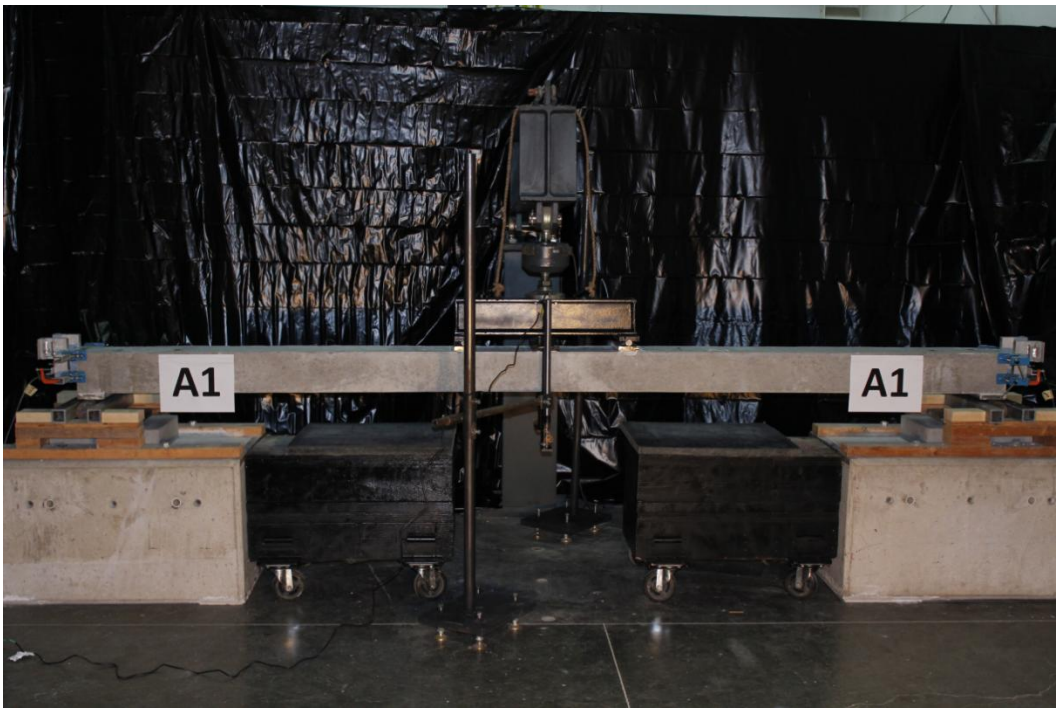

Figure 11.4 Beam A1 Setup for Simple Quality Assurance Test for Strand Bond

The specimens were then inspected for cracks and strand end slip, documenting the details. While the load was sustained for 24 hours, the beams were examined for additional signs of distress, like increased end slip, concrete cracking or crushing. Beam specimen A1 is represented in Figure 11.5, while sustaining 85% of its nominal moment capacity.

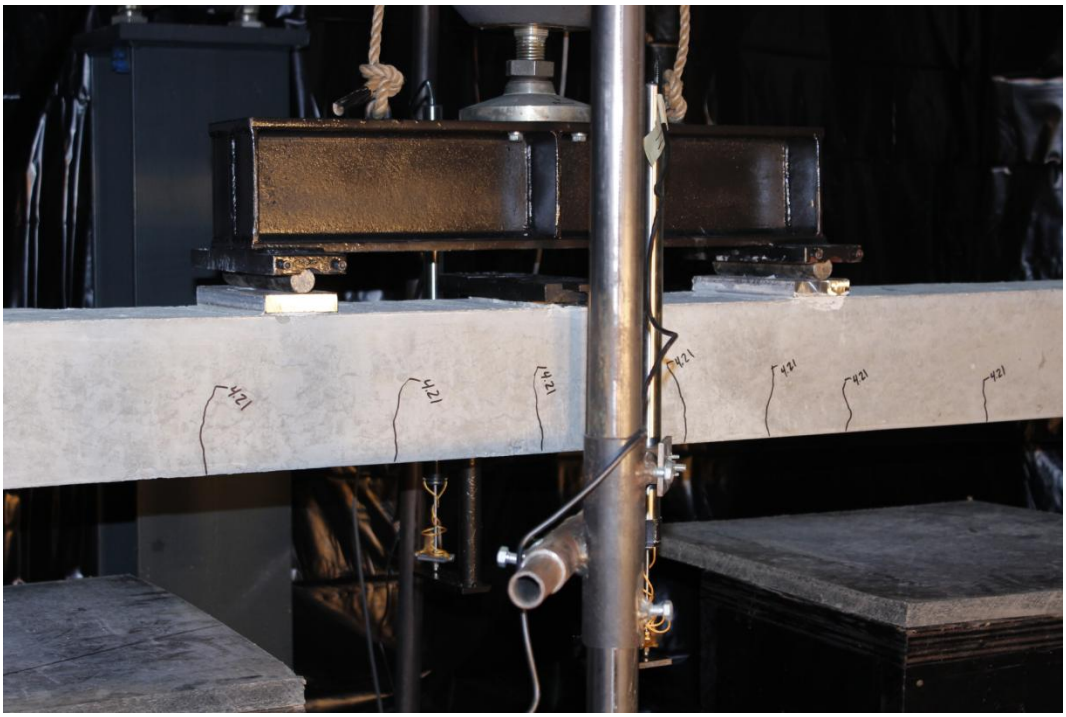

Figure 11.5 Beam A1 Loaded at 85% of its Nominal Moment Capacity during the Simple Quality Assurance Test for Strand Bond

After sustaining 85% of their nominal moment capacity for 24 hours, the beams were loaded to their full nominal capacity, and allowed to hold that load for 10 minutes, unless they failed previously. The beam specimens that were able to sustain their nominal moment capacity for 10 minutes passed the test, and were later loaded to failure. Figure 11.6 shows beam A1 while loaded at its full nominal moment capacity.

Figure 11.6 Beam A1 Loaded at 100% of its Nominal Moment Capacity during the Simple Quality Assurance Test for Strand Bond

The Simple Quality Assurance Test for Strand Bond results are simply determined as fail or pass, based on whether the beam collapses or not during the test. In other words, a beam passes the test if it can successfully hold its nominal moment capacity for 10 minutes, after being loaded for 24 hours at 85% of its nominal moment capacity. The nine beams tested in this project were loaded until failure after they held their nominal moment capacity for 10 minutes.

11.4 Test Results

The Simple Quality Assurance Test for Strand Bond specimens were load tested by RJ Peterman and Associates. The applied load, mid-span deflection and strand end slip during loading were plotted for each beam, and an example of the test results for the case of beam A1 is illustrated in Figure 11.7. The corresponding figures for all 9 beams tested are provided in Appendix I.

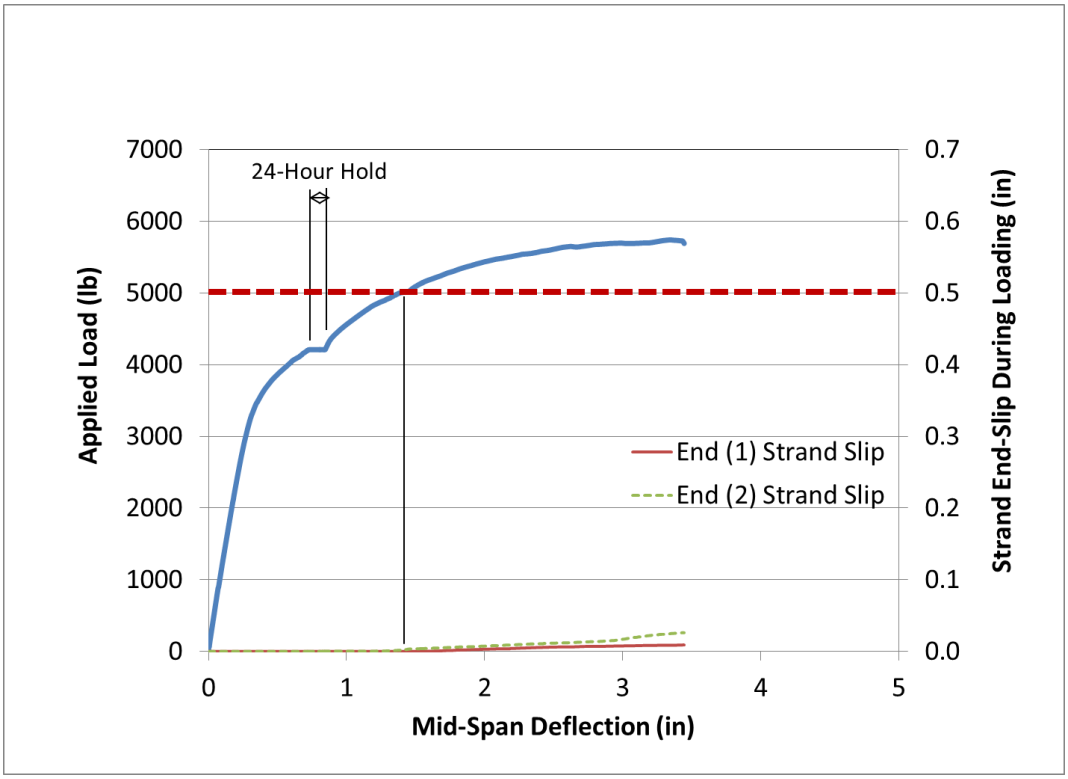

Figure 11.7 Beam A1 Simple Quality Assurance Test for Strand Bond Results

While 3 beam sections were tested per strand source during the Peterman Test Program, all of the specimens which were prestressed with strands A and G passed the test and held 100% of the calculated nominal load, but all 3 strand I specimens failed before reaching the calculated nominal load.

Table 11-1 presents a summary of the Quality Assurance Test Program, displaying the mid span deflection per beam after each load sustaining period, as well as the maximum load sustained by each section. Figure 11.8 also illustrates the performance of the beams, in a plot of their mid span deflection versus the load applied to them. It should be noted that the mid span deflection for the beams prestressed with strand I kept growing significantly while the beams were sustaining 85% of their nominal capacity, and while the 3 strand A and 3 strand G experienced similar deflections, the 3 strand I specimens averaged almost quadruple deflection compared to the average of the other two strand sources.

Table 11-1 Simple Quality Assurance Test for Strand Bond Results Summarized

Test Beam	Deflection (in) After 24 Hours at 85% Mn	Deflection (in) After 10 Minutes at 100% Mn	Maximum Load (lb)
A-1	0.85	1.45	5740
A-2	0.70	1.16	5978
A-3	0.74	1.17	6106
G-1	0.68	1.08	6143
G-2	0.82	1.30	5802
G-3	0.79	1.31	5778
I-1	3.73	Failed Prior	4659
I-2	2.38	Failed Prior	4774
I-3	2.92	Failed Prior	4607

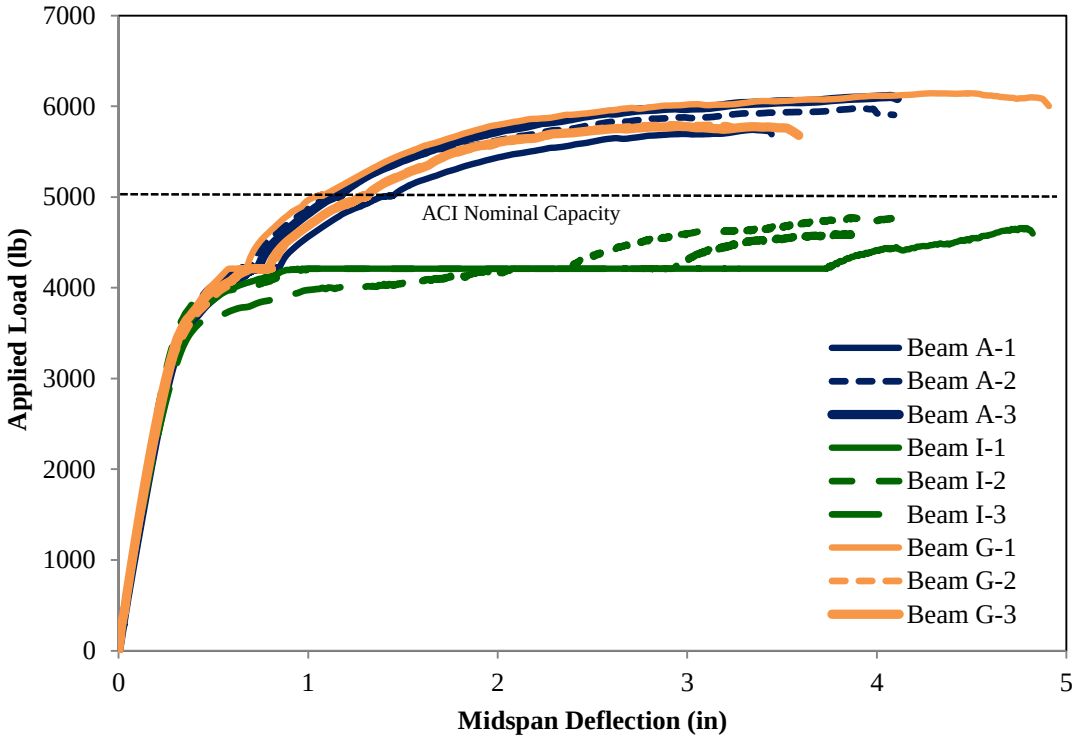

Figure 11.8 Mid span Deflection (in) vs Applied Load (lb) for all Specimens Tested by the Simple Quality Assurance Test for Strand Bond

11.5 Simple Quality Assurance Test for Strand Bond Conclusions

All strand A and strand G samples passed the Simple Quality Assurance Test for Strand Bond, but none of the three strand I specimens passed the test. The consistent outcome of these tests indicates that, for the concrete mixture and release strength used, both strands A and G met the ACI design assumptions for bond while strand I did not. If the strand acceptance value is established based on the concrete mixture and release strength used to fabricate these beams, the Simple Quality Assurance Test for Strand Bond results would indicate that the threshold value should be set such that strand I is excluded but strands A and G are allowed.

Chapter 12 - Conclusions

12.1 Summary of Work Done and Conclusions

During the progression of this research project, many aspects of the strand bond subject were considered. Research initiated with an extensive literature review of the previous studies conducted since the invention of prestressed concrete.

The first experimental step was the pullout testing of 0.5 inch diameter prestressing strand samples from 8 plants of the leading strand manufacturers of North America. Testing was conducted following the now standard pullout test procedure of ASTM A1081. The initial strand testing round included 7 market condition samples and a non-market condition strand which was supplied by one of the manufacturers in order to provide a low bonding sample to meet the specific requirements of the project proposal.

After the initial round of testing was concluded, three strand samples were selected to participate in the further experimental studies of the project, including the non-market condition sample labeled as strand I, which represented the lowest bonding strand of the three. Strand labeled as strand G was selected to represent the highest bonding sample and strand A was selected as the sample of intermediate bonding performance.

Once the three strand sources were selected, large coils of at least 3000 ft were ordered from the corresponding manufacturers and were verified once they arrived at KSU labs. Testing proceeded as the results were in agreement with the values obtained for the three samples during the initial round of strand testing.

The materials used to prepare the mortar mixture were investigated next. After concerns that different sand gradation, hardness and angularity could be affecting the mixture characteristics, a specific source was selected, and the sand was graded at specified gradations to ensure consistency during the following testing rounds.

Another concern was the fact that even though only Type III cements can be used for this test, it was suspected that the cement chemical composition could have effects on the mixture; therefore a specific cement source was obtained for the following testing rounds. In the meantime, Type III cement samples were obtained from 5 manufacturers, and were used to make mortar mixtures and test the 3 preselected strands at KSU labs. Significant variability was

observed on the pullout test results of the same strand source tested in mixtures created using different Type III cement sources.

The subsequent task involved investigation of the ASTM A1081 method for ruggedness. The Ruggedness Testing study was incorporated at Kansas State University, and involved varying certain test parameters which were suspected to have an influence on the test results. The mortar mixture flow, compressive strength of the samples at the time of testing, and the test loading rate were investigated in order to determine their effects numerically. Only the mortar mixture flow factor was determined significant after statistical analysis of the study results.

An Inter-Laboratory study (ILS) followed, in order to determine the reproducibility of the ASTM A1081 test method. The actual test as specified in ASTM A1081 (Method A) plus an alternative version of the test (Method B) were investigated during this study. The different aspects incorporated into Method B were based on the Ruggedness Testing study findings and also the application of fixed water to cement ratio in order to accommodate Type III cements of different fineness without implying significant discrepancy of the test results. The results obtained from 6 participating laboratories in addition to 5 sets of data from testing conducted at KSU using different cement sources and mortar mixture characteristics were analyzed to conclude to a coefficient of variation of 14% for ASTM A1081, which can be reduced to 11% if the test is modified by Method B specifications.

While test rounds for investigation of ASTM A1081 were taking place at KSU and the ILS participating laboratories, Wiss, Janney, Elstner Associates, Inc. (WJE) tested the three strands' surface characteristics under a quality control program defined in NCHRP Report 621. It was observed that for the Contact Angle Measurement test, the results for the 3 strand sources A, G and I followed the exact opposite trend compared to the results from the strands tested during the NCHRP study. Instead of having the highest bonding source experience the lowest contact angle, in this study, the lowest bonding source had by far the lowest contact angles determined.

These tasks concluded the first phase of the project and let to the precision and bias statement of the ASTM A1081 test method, and the final pullout test values for the three strand samples that were subsequently tested in beam sections during phases II and III.

The precision of the test method was determined as follows; the single operator coefficient of variation was 9 %, and multi laboratory coefficient of variation was 14.5 %.

The second phase of the project initiated with the design and fabrication of 30 rectangular beam sections, which later underwent flexural testing at Stresscon, Inc. in Colorado Springs, CO. The beam study was aiming to compare results to a similar study that was also conducted at Stresscon by Donald R. Logan; therefore the beam sections were fabricated to match Mr. Logan's samples, and the concrete mixture used was also designed to reach similar compressive strengths.

Ten beams per strand source were made to measure the flexural capacity. They were tested once for each of their two ends, for a total of 20 tests per strand source A, G, and I. The beams were tested with a single point load, with the load placed at a distance of 60% L_d from their end on one side (short end), and at a distance of 80% L_d from their end on the other side (long end).End slip readings and surface strain readings taken by a laser speckle imaging device were made for transfer length determination at release and before testing. Analysis of the flexural testing data followed with the transfer length readings compared to ACI code requirements, and experimental moments reached by the beam ends compared to their nominal moment capacities. The beam testing results were plotted against the pullout test values set for each strand and extrapolated in order to determine an acceptable ASTM A1081 threshold value for different confidence levels. A numerical analysis was done assuming that a beam section is prestressed using 6 strand specimens instead of one, assuming no interactions between the specimens and considering the average capacity of all 6 possible combinations per case, to represent the minimum amount of reinforcement expected in a prestressed concrete section used in the industry.

During the third phase of this research project, a quality assurance test was conducted on 9 additional beam sections that were also fabricated at Stresscon with the same concrete mixture as the flexural beam sections, but were of smaller cross sections. The specimens were tested by RJ Peterman and Associates under the Simple Quality Assurance Test for Strand Bond proposed by Robert J. Peterman. The test program concluded that strand I is unsafe to be used in pre-tensioned applications fabricated with the concrete mixture and release strength used.

12.2 Recommendations for Implementation

It is recommended to keep great caution in maintaining the equipment to run the ASTM A1081 test, since testing during this research project revealed that determining the mortar

mixture flow was very sensitive to equipment condition, as well as keeping procedures consistent. The mortar mixture flow was found during the ruggedness testing to be the parameter that had significant effects on the test results, when varied between the two extremes that the test method allows.

A recommendation to use a single sand source, sieved and graded to specified gradations, could be made for the cases where consistent mortar mixture flows and reduced variability of pullout test results are of importance beyond the cost and time intensity of sieving and grading the sand source.

The precision and bias statement for ASTM A1081 was also defined during this project. The coefficient of variation of the test method was determined to be 9.0% for a single operator, and 14.5% for multiple laboratory testing. It was determined that two properly conducted tests by a single operator on the same material should not differ by more than 12.1%, and that the range of the six single determinations used to calculate the average test result should not exceed 24.9%. When considering multi-laboratory testing, the difference between 2 properly conducted tests should not differ by more than 40.2%.

For a 90% confidence interval and 5% fractal, a threshold value of 14,600 lb is recommended for ASTM A1081, after data analysis from the flexural beam testing study and the Inter-Laboratory study, assuming that 6 strands will coexist in a beam section. This threshold would preclude the use of strand I, which was found to be unsafe in the Simple Quality Assurance Test for Strand Bond. Additionally, this criterion does not guarantee that the ACI 318 code transfer length requirements will be met.

12.3 Future Research

It was obvious during the course of this research project that difference in cement chemistry can affect the ASTM A1081 test results. Properties such as fineness were dictating the amount of water required to create mortar mixtures of the specified flow, and variability was also seen in the cements' setting times even though they were all Type III samples. It is recommended that further research on type III cement source chemistry be conducted, in order to specify the effects that different cement properties reflect on the test method results. It would be

helpful to provide certain requirements as far as cement chemical composition that will be applied to the standard method in order to reduce variability of the test results.

While making attempts to provide a reasonable threshold value for ASTM A1081 based on ACI 318 code transfer length requirements, it was considered that the current ACI 318 code equation underestimates the transfer length, and it is highly recommended to revisit the current code provisions.

Bibliography

ACI 318. (2011). *Building Code Requirements for Structural Concrete (ACI 318-11) and Commentary*. Farmington Hills: American Concrete Institute.

Akhnoukh, A. K. (2008). *Development of High Performance Precast/Prestressed Bridge Girders.* University of Nebraska, Lincoln.

ASTM A1081. (2012). Standard Test Method for Evaluating Bond of Seven-Wire Prestressing Strand. 5 pp. West Conshohocken, PA: ASTM International.

ASTM A416. (2010). Standard Specification for Steel Strand, Uncoated Seven-Wire for Prestressed Concrete. 5 pp. West Conshohocken, PA: ASTM International.

ASTM C109. (2012). Standard Test Method for Compressive Strength of Hydraulic Cement Mortars. 10 pp. West Conshohocken, PA: ASTM International.

ASTM C1437. (2007). Standard Test Method for Flow of Hydraulic Cement Mortar. 2 pp. West Conshohocken, PA: ASTM International.

ASTM C150. (2012). Standard Specification for Portland Cement. 9 pp. West Conshohocken, PA: ASTM International.

ASTM C305. (99). Standard Practice for Mechanical Mixing of Hydraulic Cement Pastes and Mortars of Plastic Consistency. 3 pp. West Conshohocken, PA: ASTM International.

ASTM E1169. (2007). Standard Practice for Conducting Ruggedness Tests. 9 pp. West Conshohocken, Penn.: ASTM International.

Buckner, C. D. (1995). A Review of Strand Development Length for Pretensioned Concrete Members.

Cousins, T. E., Johnston, D. W., & Zia, P. (1990). Transfer and Development Length of Epoxy Coated and Uncoated Prestressing Strand. *35*(4).

Cousins, T. E., Johnston, D. W., & Zia, P. (1990). Transfer Length of Epoxy-Coated Prestressing Strand. *ACI Materials Journal, 87*(3).

Dinges, T. (2009). *The History of Prestressed Concrete: 1888 to 1963.* Manhattan, KS: Kansas State University.

Gross, S. P., & Burns, N. H. (1995). *Transfer and Development Length of 15.2mm (0.6 in) Diameter Prestressing Strand in High Performance Concrete: Results of the Hoblitzell-Buckner Beam Tests.* The University of Texas at Austin, Center for Transportation Research.

Hanson, W. N., & Kaar, P. H. (n.d.). Flexural Bond Tests of Pretensioned Prestressed Beams. *Journal of the American Concrete Institute*.

Hawkins, N. M., & Ramirez, J. A. (2010). *Due Diligence Review of NASP Strand Bond Test Method.* Chicago, IL: Precast/Prestressed Concrete Institute (PCI).

Jurakev, Y. V. (2004). *Investigation of Development of Prestressing Strands and Deformed Bars.* University of Nebraska-Lincoln.

Kose, M. M., & Burkett, W. R. (2005). Evaluation of Code Requirement for 0.6 in. (15 mm) Prestressing Strand. *ACI Structural Journal, 3*(102).

Lane, S. N. (1998). *A New Development Length Equation for Pretensioned Strands in Bridge Beams and Piles.* McLean, VA: Federal Highway Administration.

Logan, D. R. (1997). Acceptance Criteria for Bond Quality of Strand for Pretensioned Prestressed Concrete Applications. *PCI Journal*.

Martin, L. D., & Scott, N. L. (1976). Development of Prestressing Strand in Pretensioned Members. *73*(8).

Murray, C. D. (2012). *The effect of Mortar Strength on the Standard Test for Strand Bond.* University of Arkansas, Civil Engineering, Fayetteville, Arkansas.

Natrella, M. G. (1963). Experimental Statistics. In *National Bureau of Standards Handbook 91* (pp. 2-13-2-15). Washington, D.C: United States Department of Commerce.

Nawy, E. G. (2010). *Prestressed Concrete: A fundamental Approach.* Upper Saddle River, NJ: Pearson Education, Inc.

Osborn, A. E., Lawler, J. S., & Connolly, J. D. (2008). *NCHRP Report 621.* Washington, D.C.: Transportation Research Board.

Peterman, R. J. (2009). A simple quality assurance test for strand bond. *PCI Journal, 54*(2), 143-161.

Polydorou, T., Riding, K. A., & Peterman, R. J. (2014). *Interlaboratory Study for ASTM A1081 Standard Test Method for Evaluating Bond of Seven-Wire Steel Prestressing Strand.* Manhattan, KS: Kansas State University.

Polydorou, T., Riding, K. A., Peterman, R. J., & Murray, L. (2013). *Effects of Setup and Material Parameters on the Standard Test for Strand Bond.* Manhattan, KS: Kansas State University.

Porterfield, K. B. (2012). *Bond, Transfer Length, and Development Length of Prestressing Strand in Self-Consolidating Concrete.* Missouri University of Science and Technology, Civil, Architectural and Environmental Engineering, Rolla, Missouri.

Ramirez, J. A., & Russell, B. W. (2008). *Transfer, Development, and Splice Length for Strand/Reinforcement in High-Strength Concrete.* Washington, D.C.: Transportation Research Board.

Riding, K. A., Peterman, R. J., Polydorou, T., & Ren, G. (2012). *Simple Mortar Mixture Proportioning Method for Meeting Minimum and Maximum Flow and Strength Requirements.* Manhattan, KS: Kansas State University.

Rose, D., & Russell, B. W. (1997). Investigation of Standardized Tests to Measure the Bond Performance of Prestressing Strand.

Russell, B. (2006). *NASP Round IV Strand Bond Testing.* Final Report.

Russell, B. W. (n.d.). *NASP Strand Bond Testing Round III.*

Russell, B. W., & Burns, N. H. (1993). *Design Guidelines for Transfer, Development and Debonding of Large Diameter Seven Wire Strands in Pretensioned Concrete Girders.* The University of Texas at Austin, Austin, TX.

Russell, B. W., & Paulsgrove, G. A. (1999). *NASP Strand Bond Testing Round I.* Norman, OK: The University of Oklahoma.

Russell, B. W., & Paulsgrove, G. A. (1999). *NASP Strand Bond Testing Round II.* Norman, OK: University of Oklahoma.

Russell, B. W., & Ramirez, J. A. (2008). *NCHRP Report 603.* Washington, DC: Transportation Research Board.

Shahawy, M. A. (1999). *Critical Evaluation of the Design Code Requirements for Development Length of Prestressing Tendons.* Tallahassee, FL: Structural Research Center Florida Department of Transportation.

Sobin, N. J. (2005). *Evaluation of Strand Bond Assurance Tests for Pretensioned Applications.* University of Arkansas, Civil Engineering, Fayeteville.

Tabatabai, H., & Dickson, T. J. (1995). *The History of the Prestressing Strand Development Length Equation.* McLean, Virginia: US Department of Transportation Federal Highway Administration.

Wiss, Janney, Elstner, & Associates. (n.d.). Retrieved October 17, 2013, from Wiss, Janney Elstner Associates, Inc.Web site: http://www.wje.com/projects/detail.php?pid=2003.2612.0

www.pci.org. (n.d.). Retrieved 2013, from Precast/Prestressed Concrete Institute.

Xercavins, P., Demarthe, D., & Sushkewich, K. (2008). *Eugene Freyssinet- The Invention of Presressed Concrete and Precast Segmental Construction.*

Zhao, W. (2011). *Development of a Portable Optical Strain Sensor with Applications to Diagnostic Testing of Prestressed Concrete.* Manhattan, KS: Kansas State University.

Zhao, W., Beck, B. T., Peterman, R. J., Murphy, R., Wu, C.-H. J., & Lee, G. (2013). A Direct Comparison of the Traditional Method and a New Approach in Determining Transfer Lengths in Prestressed Concrete Railroad Ties. *2013 Joint Railroad Conference.* Knoxville, TN.

Appendix A - **Rectangular Beam Specimens' Accompanying Concrete Cylinder Split Tensile Test Results**

Table A-1 Placement Day 1 (7-16-13): Rectangular Beam Specimens A 1-5, I 1-5 Accompanying Cylinders' Split Tensile Test Results

Cylinder Test Specimen	Date Tested	Split Tensile Strength (psi)	Time between Concrete Placement and Test (days)
ST-D1-1	8-5-13	677	20
ST-D1-2*	8-5-13	652	20
ST-D1-3	8-8-13	630	23
ST-D1-4*	8-8-13	647	23
ST-D1-5*	8-12-13	700	27

*Cylinder was tested for Modulus of Elasticity prior to Split Tensile Test

Table A-2 Placement Day 2 (7-18-13): Rectangular Beam Specimens A 5-10, G 1-5 Accompanying Cylinders' Split Tensile Test Results

Cylinder Test Specimen	Date Tested	Split Tensile Strength (psi)	Time between Concrete Placement and Test (days)
ST-D2-1	8-5-13	540	18
ST-D2-2*	8-5-13	502	18
ST-D2-3	8-12-13	574	25
ST-D2-4*	8-12-13	692	25

*Cylinder was tested for Modulus of Elasticity prior to Split Tensile Test

Table A-3 Placement Day 3 (7-19-13): Rectangular Beam Specimens I 5-10, G 5-10 Accompanying Cylinders' Split Tensile Test Results

Cylinder Test Specimen	Date Tested	Split Tensile Strength (psi)	Time between Concrete Placement and Test (days)
ST-D3-1	8-8-13	655	20
ST-D3-2*	8-8-13	645	20
ST-D3-3*	8-12-13	814	24

*Cylinder was tested for Modulus of Elasticity prior to Split Tensile Test

Appendix B - **Rectangular Beam Specimen Transfer Lengths at Time of Prestress Release**

Table B-1 Strand G Transfer Lengths at Time of Prestress Release

Specimen	ZL Method Transfer Length (in)	95% AMS Transfer Length (in)
G1-S	22.93	23.28
G2-S	27.71	28.56
G3-S	22.41	22.51
G4-S	33.79	32.03
G5-S	30.71	29.24
G6-S	18.43	18.29
G7-S	20.41	19.03
G8-S	36.48	36.71
G9-S	37.30	35.80
G10-S	22.36	19.65
G1-L	26.84	28.62
G2-L	28.99	31.20
G3-L	29.35	31.25
G4-L	35.21	33.70
G5-L	31.94	31.31
G6-L	23.71	23.14
G7-L	32.24	28.41
G8-L	31.44	28.56
G9-L	27.15	27.01
G10-L	21.60	19.88

Table B-2 Strand A Transfer Lengths at Time of Prestress Release

Specimen	ZL Method Transfer Length (in)	95% AMS Transfer Length (in)
A1-S	28.39	28.67
A2-S	45.08	40.54
A3-S	31.70	29.75
A4-S	35.09	33.70
A5-S	56.36	55.85
A6-S	34.65	35.09
A7-S	37.11	33.03
A8-S	34.80	32.15
A9-S	34.98	33.23
A10-S	40.61	39.70
A1-L	27.03	26.14
A2-L	31.45	31.32
A3-L	34.36	30.54
A4-L	17.13	24.82
A5-L	31.50	29.49
A6-L	33.13	38.37
A7-L	39.96	38.82
A8-L	38.46	36.44
A9-L	39.20	34.48
A10-L	44.69	40.15

Table B-3 Strand I Transfer Lengths at Time of Prestress Release

Specimen	ZL Method Transfer Length (in)	95% AMS Transfer Length (in)
I1-S	37.73	N/A
I2-S	30.93	29.78
I3-S	40.65	N/A
I4-S	61.60	57.14
I5-S	58.23	54.08
I6-S	28.69	27.44
I7-S	33.49	31.62
I8-S	56.79	48.60
I9-S	47.45	44.93
I10-S	23.91	21.01
I1-L	39.79	38.18
I2-L	32.85	31.03
I3-L	28.01	26.23
I4-L	54.69	64.04
I5-L	33.98	30.62
I6-L	38.93	36.74
I7-L	44.81	39.92
I8-L	44.34	38.61
I9-L	53.74	47.36
I10-L	52.49	45.74

Appendix C - **Rectangular Beam Specimen Transfer Lengths at Time of Flexural Testing**

Table C-1 Strand G Transfer Lengths at Time of Flexural Testing

Specimen	ZL Method Transfer Length (in)
G1-S	33.15
G2-S	35.63
G3-S	31.34
G4-S	42.43
G5-S	38.34
G6-S	29.09
G7-S	30.06
G8-S	47.28
G9-S	49.11
G10-S	32.58
G1-L	33.90
G2-L	37.20
G3-L	37.85
G4-L	42.84
G5-L	39.86
G6-L	31.49
G7-L	44.34
G8-L	41.81
G9-L	40.69
G10-L	34.27

Table C-2 Strand A Transfer Lengths at Time of Flexural Testing

Specimen	ZL Method Transfer Length (in)
A1-S	40.05
A2-S	55.59
A3-S	40.34
A4-S	47.62
A5-S	69.46
A6-S	46.89
A7-S	50.36
A8-S	50.93
A9-S	50.82
A10-S	51.55
A1-L	37.97
A2-L	42.83
A3-L	42.14
A4-L	34.55
A5-L	44.60
A6-L	46.09
A7-L	52.49
A8-L	49.98
A9-L	54.32
A10-L	61.39

Table C-3 Strand I Transfer Lengths at Time of Flexural Testing

Specimen	ZL Method Transfer Length (in)
I1-S	51.27
I2-S	47.20
I3-S	56.06
I4-S	71.82
I5-S	73.21
I6-S	33.87
I7-S	46.16
I8-S	65.14
I9-S	58.25
I10-S	32.12
I1-L	53.04
I2-L	49.27
I3-L	40.54
I4-L	65.78
I5-L	44.20
I6-L	48.43
I7-L	56.33
I8-L	53.56
I9-L	65.69
I10-L	83.02

Appendix D - **Flexural Beam Specimen End Slip Values**

Table D-1 Strand G End Slip Values

Specimen	Initial End Slip (in) and Date Taken (Immediately after Prestress Release)		1-Day End Slip (in) and Date Taken		End Slip Before Flexural Test (in) and Date Taken	
G1-S	0.0165	7/18/13	0.0385	7/19/13	0.0520	8/5/13
G2-S	0.0160	7/18/13	0.0320	7/19/13	0.0435	8/5/13
G3-S	0.0170	7/18/13	0.0335	7/19/13	0.0480	8/6/13
G4-S	0.0085	7/18/13	0.0295	7/19/13	0.0385	8/6/13
G5-S	0.0265	7/18/13	0.0425	7/19/13	0.0530	8/7/13
G6-S	0.0095	7/19/13	0.0370	7/20/13	0.0465	8/7/13
G7-S	0.0140	7/19/13	0.0395	7/20/13	0.0475	8/8/13
G8-S	0.0375	7/19/13	0.0695	7/20/13	0.0750	8/8/13
G9-S	0.0480	7/19/13	0.0640	7/20/13	0.0890	8/9/13
G10-S	0.0225	7/19/13	0.0480	7/20/13	0.0580	8/9/13
G1-L	0.0180	7/18/13	0.0380	7/19/13	0.0425	8/5/13
G2-L	0.0170	7/18/13	0.0315	7/19/13	0.0455	8/5/13
G3-L	0.0095	7/18/13	0.0230	7/19/13	0.0390	8/6/13
G4-L	0.0345	7/18/13	0.0485	7/19/13	0.0610	8/6/13
G5-L	0.0000	7/18/13	0.0140	7/19/13	0.0275	8/7/13
G6-L	0.0020	7/19/13	0.0190	7/20/13	0.0290	8/7/13
G7-L	0.0260	7/19/13	0.0480	7/20/13	0.0680	8/8/13
G8-L	0.0155	7/19/13	0.0390	7/20/13	0.0515	8/8/13
G9-L	0.0270	7/19/13	0.0545	7/20/13	0.0740	8/9/13
G10-L	0.0170	7/19/13	0.0460	7/20/13	0.0610	8/9/13

Table D-2 Strand A End Slip Values

Specimen	Initial End Slip (in) and Date Taken (Immediately after Prestress Release)		1-Day End Slip (in) and Date Taken		End Slip Before Flexural Test (in) and Date Taken	
A1-S	0.0010	7/16/13	0.0385	7/17/13	0.0415	8/5/13
A2-S	0.0360	7/16/13	0.0645	7/17/13	0.0725	8/5/13
A3-S	0.0065	7/16/13	0.0365	7/17/13	0.0365	8/6/13
A4-S	0.0325	7/16/13	0.0605	7/17/13	0.0760	8/6/13
A5-S	0.0480	7/16/13	0.0780	7/17/13	0.0935	8/7/13
A6-S	0.0245	7/18/13	0.0445	7/19/13	0.0670	8/7/13
A7-S	0.0150	7/18/13	0.0435	7/19/13	0.0610	8/8/13
A8-S	0.0360	7/18/13	0.0590	7/19/13	0.0920	8/8/13
A9-S	0.0290	7/18/13	0.0575	7/19/13	0.0840	8/9/13
A10-S	0.0785	7/18/13	0.0945	7/19/13	0.1165	8/9/13
A1-L	0.0200	7/16/13	0.0445	7/17/13	0.0580	8/5/13
A2-L	0.0245	7/16/13	0.0535	7/17/13	0.0640	8/5/13
A3-L	0.0725	7/16/13	0.0890	7/17/13	0.0995	8/6/13
A4-L	0.0255	7/16/13	0.0600	7/17/13	0.0860	8/6/13
A5-L	0.0205	7/16/13	0.0495	7/17/13	0.0660	8/7/13
A6-L	0.0305	7/18/13	0.0465	7/19/13	0.0755	8/7/13
A7-L	0.0310	7/18/13	0.0475	7/19/13	0.0745	8/8/13
A8-L	0.0575	7/18/13	0.0730	7/19/13	0.0975	8/8/13
A9-L	0.0350	7/18/13	0.0585	7/19/13	0.0875	8/9/13
A10-L	0.0275	7/18/13	0.0505	7/19/13	0.0855	8/9/13

Table D-3 Strand I End Slip Values

Specimen	Initial End Slip (in) and Date Taken (Immediately after Prestress Release)		1-Day End Slip (in) and Date Taken		End Slip Before Flexural Test (in) and Date Taken	
I1-S	0.0435	7/16/13	0.0830	7/17/13	0.0905	8/5/13
I2-S	0.0300	7/16/13	0.0725	7/17/13	0.0865	8/5/13
I3-S	0.0325	7/16/13	0.0725	7/17/13	0.0850	8/6/13
I4-S	0.0870	7/16/13	0.1180	7/17/13	0.1225	8/6/13
I5-S	0.0545	7/16/13	0.0930	7/17/13	0.1065	8/7/13
I6-S	0.0335	7/19/13	0.0470	7/20/13	0.0515	8/7/13
I7-S	0.0510	7/19/13	0.0785	7/20/13	0.0950	8/8/13
I8-S	0.0860	7/19/13	0.1095	7/20/13	0.1150	8/8/13
I9-S	0.0735	7/19/13	0.0950	7/20/13	0.1110	8/9/13
I10-S	0.0295	7/19/13	0.0575	7/20/13	0.0580	8/9/13
I1-L	0.0540	7/16/13	0.0900	7/17/13	0.1000	8/5/13
I2-L	0.0150	7/16/13	0.0600	7/17/13	0.0720	8/5/13
I3-L	0.0190	7/16/13	0.0530	7/17/13	0.0625	8/6/13
I4-L	0.0730	7/16/13	0.1045	7/17/13	0.1115	8/6/13
I5-L	0.0635	7/16/13	0.0895	7/17/13	0.0990	8/7/13
I6-L	0.0500	7/19/13	0.0715	7/20/13	0.0830	8/7/13
I7-L	0.0350	7/19/13	0.0655	7/20/13	0.0750	8/8/13
I8-L	0.0635	7/19/13	0.0850	7/20/13	0.0955	8/8/13
I9-L	0.0640	7/19/13	0.0945	7/20/13	0.1055	8/9/13
I10-L	0.0170	7/19/13	0.0460	7/20/13	0.1230	8/9/13

Appendix E - **Rectangular Beam End Actual Dimensions**

Table E-1 Strand A Beam Ends- Actual Dimensions

Beam End	Top Width (in)	Depth to c.g. of Strand (in)	Overall Height (in)
A1-L	6.8435	10.1250	12.1250
A2-L	6.5350	10.0000	12.1250
A3-L	6.6410	9.8750	12.0625
A4-L	6.6010	10.0000	12.1250
A5-L	6.7320	10.0000	12.1875
A6-L	6.7750	10.0625	12.1250
A7-L	6.6000	10.0000	12.1250
A8-L	6.7705	9.9375	12.0625
A9-L	6.7100	10.0000	12.0000
A10-L	6.9545	9.9375	12.0000
A1-S	6.6630	10.0000	12.1250
A2-S	6.4890	9.8750	12.0625
A3-S	6.6050	10.0000	12.1250
A4-S	6.5915	9.9375	12.1250
A5-S	6.6045	9.8750	12.0625
A6-S	6.5820	10.0000	12.0625
A7-S	6.6120	9.9375	12.0625
A8-S	6.6620	10.0000	12.0000
A9-S	6.7000	9.8125	11.9375
A10-S	6.6785	9.8750	11.8750

Table E-2 Strand G Beam Ends- Actual Dimensions

Beam End	Top Width (in)	Depth to c.g. of Strand (in)	Overall Height (in)
G1-L	6.4735	10.1250	12.0625
G2-L	6.5245	10.0000	12.0000
G3-L	6.6340	9.9375	12.1250
G4-L	6.6610	10.0000	12.0000
G5-L	6.5150	10.0000	12.0625
G6-L	6.8360	10.0625	12.1250
G7-L	6.6300	9.8750	12.1250
G8-L	6.9500	9.9375	12.1250
G9-L	7.4090	10.375	12.1875
G10-L	7.1490	9.9375	12.0000
G1-S	6.8620	10.0000	12.0625
G2-S	6.7085	9.9375	12.1250
G3-S	6.7220	10.0000	12.0000
G4-S	6.6510	10.0000	12.0625
G5-S	6.6880	10.0000	12.0625
G6-S	6.5690	9.8750	12.1250
G7-S	6.6170	9.8750	12.1250
G8-S	6.8225	9.9375	11.9375
G9-S	7.1250	9.9375	12.0000
G10-S	6.9390	10.0625	12.0625

Table E-3 Strand I Beam Ends- Actual Dimensions

Beam End	Top Width (in)	Depth to c.g. of Strand (in)	Overall Height (in)
I1-L	6.4760	10.0000	12.0625
I2-L	6.5350	10.0000	12.0625
I3-L	6.6555	9.8750	12.0625
I4-L	6.5910	9.8750	12.0625
I5-L	6.4390	9.8125	12.0625
I6-L	6.5145	9.9375	12.0000
I7-L	6.6480	10.0000	12.1250
I8-L	6.6860	9.9375	12.1875
I9-L	6.7075	10.0625	12.0625
I10-L	6.6220	9.8125	11.8125
I1-S	6.7840	10.0000	12.1250
I2-S	6.7030	9.8750	12.0625
I3-S	6.6890	9.8750	12.0625
I4-S	6.5905	9.8125	12.1250
I5-S	6.7040	10.0000	12.1875
I6-S	6.8790	9.9375	12.0000
I7-S	6.8450	9.9375	12.2500
I8-S	6.7770	10.0000	12.0000
I9-S	6.6910	9.8750	11.8750
I10-S	6.7985	10.1875	12.2500

Appendix F - **Moment Capacity Calculation Example**

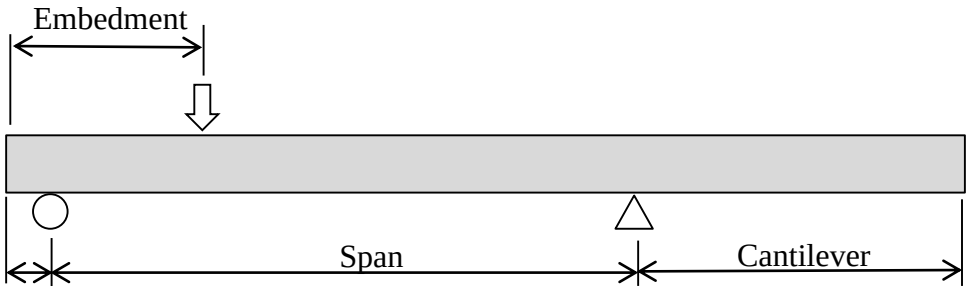

Span= 150 in.

Cantilever= 64.5 in.

End Distance= 1.5 in.

Embedment= 44.5 in. (Short End)

= 59 in. (Long End)

Concrete Section Properties:

w= width= 6.5 in.

h= height= 12 in.

A= cross sectional area= 78 in^2

I= Moment of Inertia= 936 in^4

e= Eccentricity of prestressing force= 4 in.

y_b= Distance from bottom fiber to center of gravity of section= 6 in.

S_b= Section modulus with respect to bottom fiber= I / y_b = 156 in^3

Concrete Material Properties:

f'_c= Concrete Compressive Strength= 6000 psi

f_r= Modulus of rupture of concrete= 7.5 √ (f'_c)= 581 psi

Critical Section Loads (Short End):

At the critical section = 44.5 in. from beam end = 43 in. from roller support:

W_{self}= 150 lb/ft^3 = 81.25 lb/ft

M_{DL}= Dead Load Moment= 15.6 kip-in.

M_{LL}= Live Load Moment= 292.9 kip-in.

M_{total}= M_{DL} + M_{LL}= 308.5 kip-in.

Critical Section Loads (Long End):

Critical Section at 59 in. from beam end = 57.5 in. from roller support

W_{self}= 81.25 lb/ft

M_{DL}= 18.0 kip-in.

M_{LL}= 330.0 kip-in.

M_{total}= 348.0 kip-in.

Cracking Moment Calculations:

(Calculations shown for Standard Beam, No crack former or saw cutting applied)

P_e= Effective prestress force= 28.2 kips

f_r= 581 psi

e= 4 in.

$S_b = I / y_b$ = 156 in^3

M_{cr}= Cracking moment= $[f_r + {Pe}/{Ac} + {(Pe * e)}/{Sb}]$ = 259.8 kip-in.

Appendix G - **Flexural Beam Testing Failure Analysis**

Table G-1 Flexural Beam Testing Failure Analysis for Strand A Beam Ends

Beam End Tested	L_t (in)	M_{exp}/M_n	Slip During Test (in)	Crack Inducing Technique	Failure Mode
A1-S	40	1.37	0.214	Crack Former	Rupture
A2-S	56	1.23	0.108	Crack Former	Shear-Comp
A3-S	40	1.39	0.145	Crack Former	Rupture
A4-S	48	1.41	0.197	Crack Former	Rupture
A5-S	69	1.31	0.267	Crack Former & 1-1.375" Saw Cut on Bottom & Sides	Shear-Comp
A1-L	38	1.23	0.006	Crack Former	Rupture
A2-L	43	1.20	0.033	Crack Former	Shear-Comp
A3-L	42	1.04	0.066	Crack Former	Shear-Comp
A4-L	35	1.12	0.069	Crack Former	Shear-Comp
A5-L	45	1.14	0.032	Crack Former	Shear-Comp
A6-S	47	1.38	0.130	1- 1" Saw Cut	Rupture
A7-S	50	1.31	0.099	NONE	Rupture
A8-S	51	1.17	0.218	2- 1.375" Saw Cuts	Shear-Comp
A9-S	51	1.18	0.286	2- 1.375" Saw Cuts	Shear-Comp
A10-S	52	1.10	0.164	2- 1.375" Saw Cuts	Shear-Comp
A6-L	46	1.24	0.025	3- 1.375" Saw Cuts & 1" Side Cuts	Shear-Comp
A7-L	52	1.18	0.029	NONE	Shear-Comp
A8-L	50	1.21	0.082	3- 1.375" Saw Cuts	Shear-Comp
A9-L	54	1.21	0.091	3- 1.375" Saw Cuts	Shear-Comp
A10-L	61	0.95	0.027	3- 1.375" Saw Cuts	Shear-Comp

Table G-2 Flexural Beam Testing Failure Analysis for Strand G Beam Ends

Beam End Tested	L_t (in)	M_{exp}/M_n	Slip During Test (in)	Crack Inducing Technique	Failure Mode
G1-S	33	1.28	0.289	1- 1” Saw Cut	Shear-Comp
G2-S	36	1.30	0.126	1- 1” Saw Cut	Shear-Comp
G3-S	31	1.40	0.038	1- 1” Saw Cut	Rupture
G4-S	42	1.21	0.092	1- 1” Saw Cut	Shear-Comp
G5-S	38	1.37	0.148	2- 1.375” Saw Cuts & 1” Side Cuts	Shear-Comp
G1-L	34	1.23	0.002	1- 1” Saw Cut	Rupture
G2-L	37	1.22	0.003	1- 1” Saw Cut	Rupture
G3-L	38	1.24	0.007	1- 1” Saw Cut	Rupture
G4-L	43	1.16	0.057	1- 1” Saw Cut	Shear-Comp
G5-L	40	1.23	0.022	1- 1” Saw Cut	Rupture
G6-S	29	1.34	0.104	1- 1” Saw Cut	Shear-Comp
G7-S	30	1.34	0.056	NONE	Shear-Comp
G8-S	47	1.16	0.304	2- 1.375” Saw Cuts	Shear-Comp
G9-S	49	1.38	0.787	2- 1.375” Saw Cuts	Rupture
G10-S	33	1.40	0.260	2- 1.375” Saw Cuts	Rupture
G6-L	31	1.23	0.002	3- 1.375” Saw Cuts & 1” Side Cuts	Rupture
G7-L	44	1.19	0.020	NONE	Rupture
G8-L	42	1.22	0.022	3- 1.375” Saw Cuts	Shear-Comp
G9-L	41	1.15	0.172	3- 1.375” Saw Cuts	Shear-Comp
G10-L	34	1.26	0.022	3- 1.375” Saw Cuts	Shear-Comp

Table G-3 Flexural Beam Testing Failure Analysis for Strand I Beam Ends

Beam End Tested	L_t (in)	M_{exp}/M_n	Slip During Test (in)	Crack Inducing Technique	Failure Mode
I1-S	51	1.30	1.030	Crack Former	Rupture
I2-S	47	1.31	1.098	Crack Former	Rupture
I3-S	56	1.38	0.702	Crack Former	Rupture
I4-S	72	1.35	1.140	Crack Former	Rupture
I5-S	73	1.29	> 0.5	Crack Former	Rupture
I1-L	53	1.17	0.295	Crack Former	Rupture
I2-L	49	1.11	0.046	Crack Former	Shear-Comp
I3-L	41	1.09	0.185	Crack Former	Shear-Comp
I4-L	66	1.14	0.533	Crack Former	Rupture
I5-L	44	0.88	0.059	Crack Former & 2-1.375" Saw Cut on Bottom & Sides	Shear-Comp
I6-S	34	1.12	0.257	2- 1.375" Saw Cuts & 1" Side Cuts	Shear-Comp
I7-S	46	1.28	0.957	NONE	Shear-Comp
I8-S	65	1.01	0.257	2- 1.375" Saw Cuts	Shear-Comp
I9-S	58	0.93	0.216	2- 1.375" Saw Cuts	Shear-Comp
I10-S	32	1.16	0.525	2- 1.375" Saw Cuts	Shear-Comp
I6-L	48	1.22	0.256	1- 1" Saw Cut	Rupture
I7-L	56	1.21	0.177	NONE	Rupture
I8-L	54	1.16	0.231	3- 1.375" Saw Cuts	Shear-Comp
I9-L	66	0.97	0.213	3- 1.375" Saw Cuts	Shear-Comp
I10-L	83	0.94	0.270	3- 1.375" Saw Cuts	Shear-Comp

Appendix H - **Flexural Beam Test Results Summary Charts**

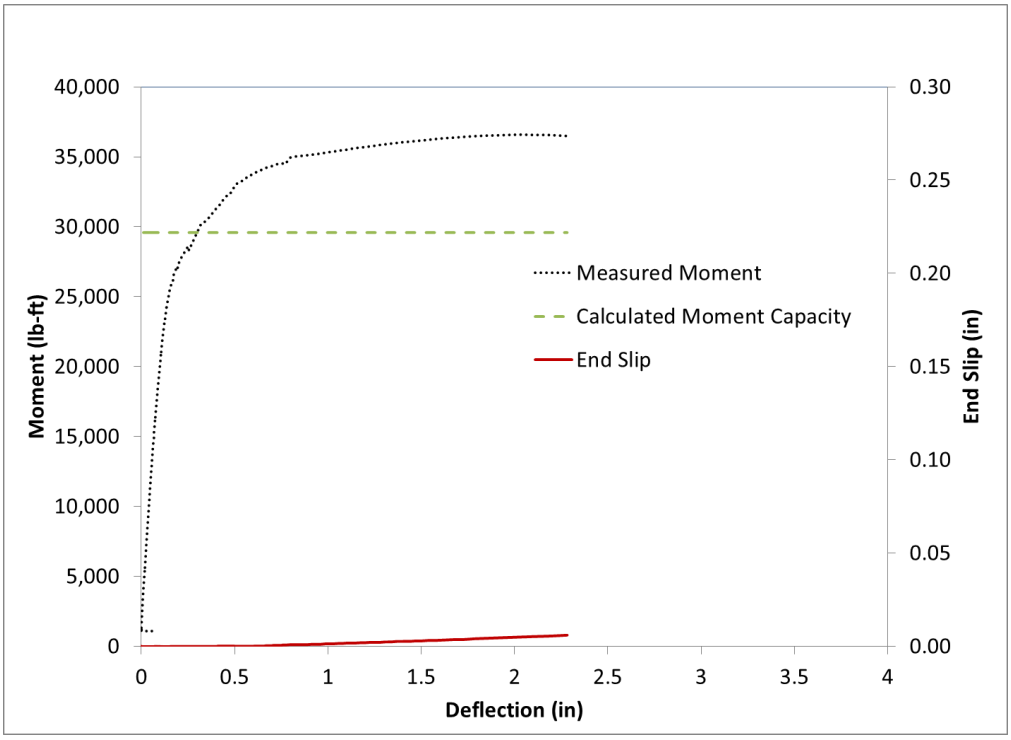

Figure H.1 Beam End A1-L Flexural Test Results Summary Chart A

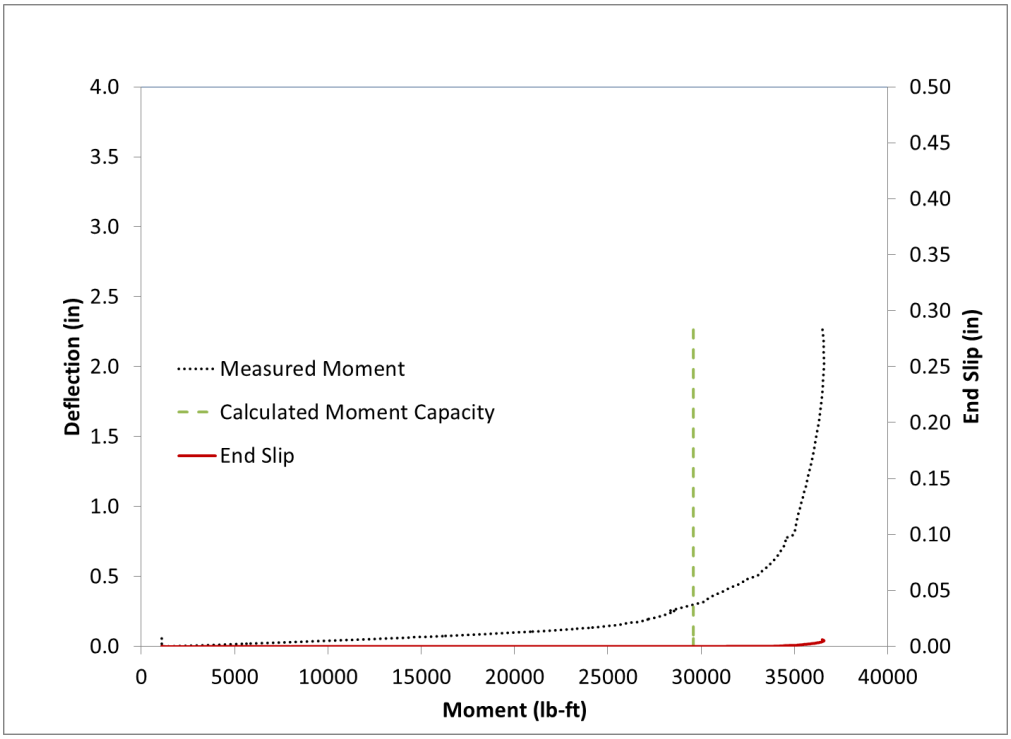

Figure H.2 Beam End A1-L Flexural Test Results Summary Chart B

Figure H.3 Beam End A1-L Failure

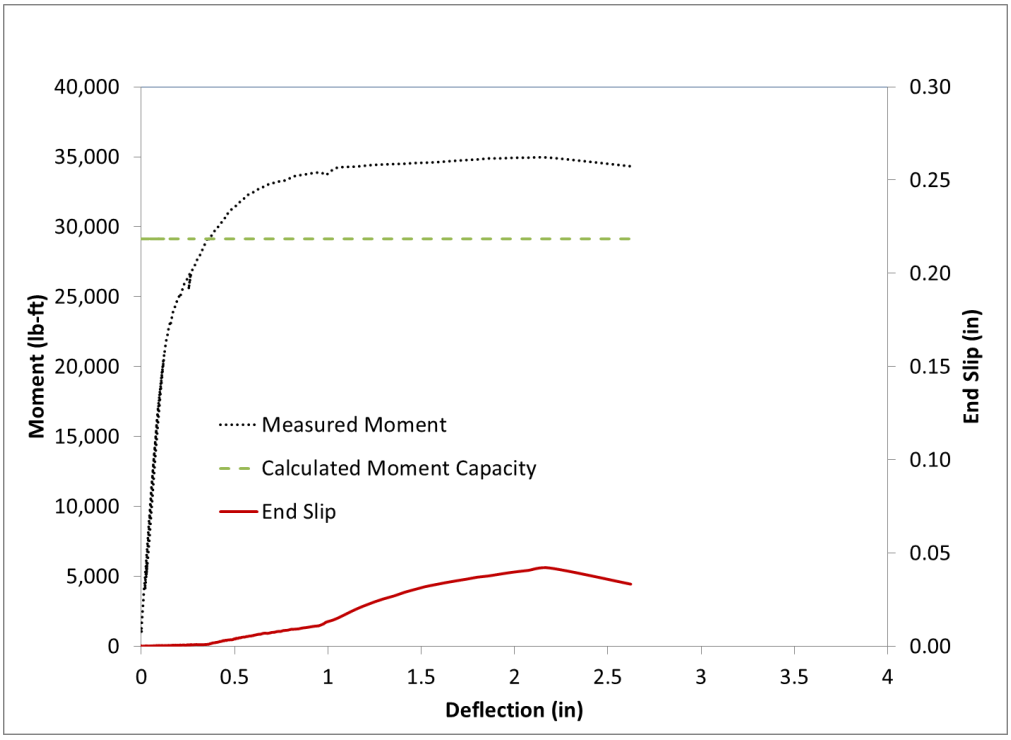

Figure H.4 Beam End A2-L Flexural Test Results Summary Chart A

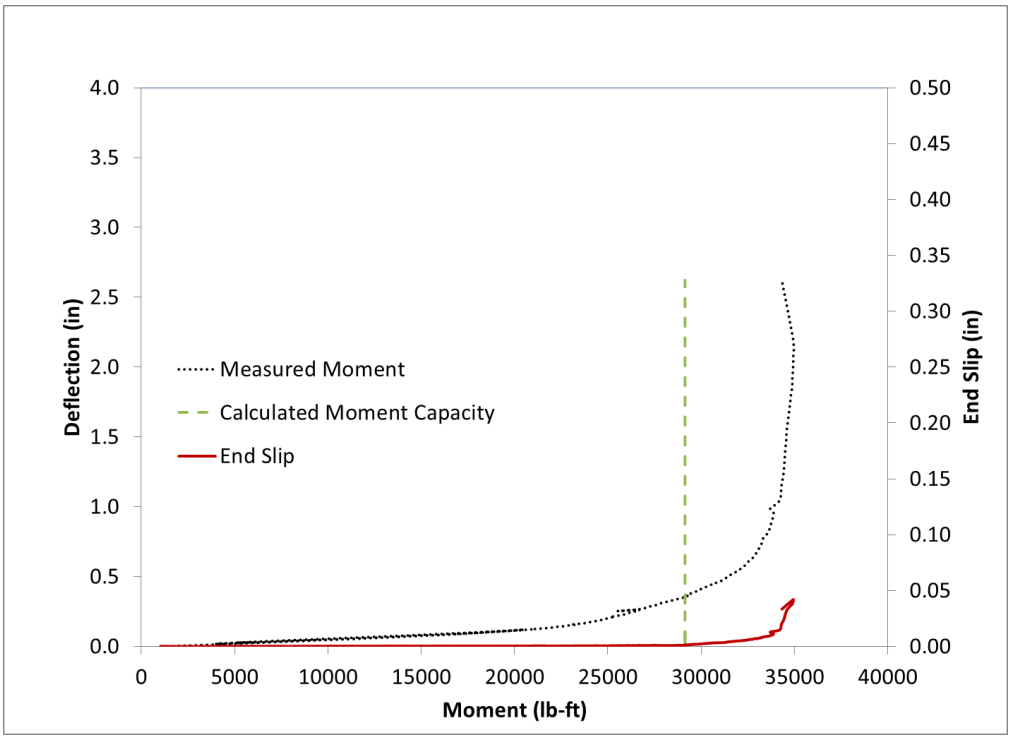

Figure H.5 Beam End A2-L Flexural Test Results Summary Chart B

Figure H.6 Beam End A2-L Failure

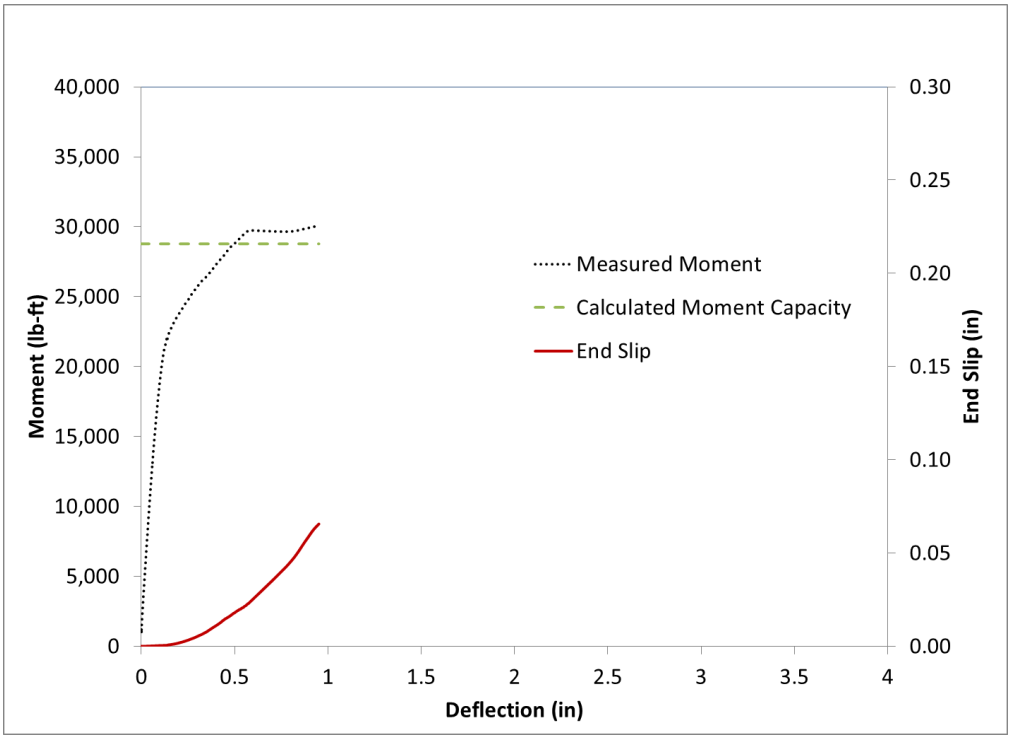

Figure H.7 Beam End A3-L Flexural Test Results Summary Chart A

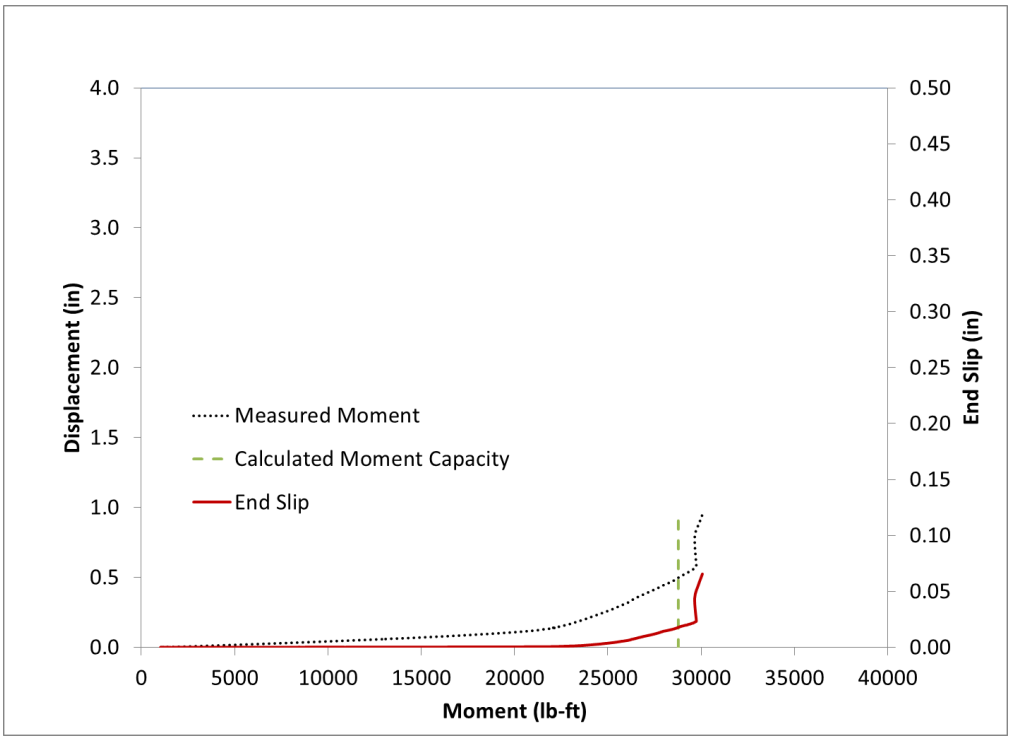

Figure H.8 Beam End A3-L Flexural Test Results Summary Chart B

Figure H.9 Beam End A3-L Failure

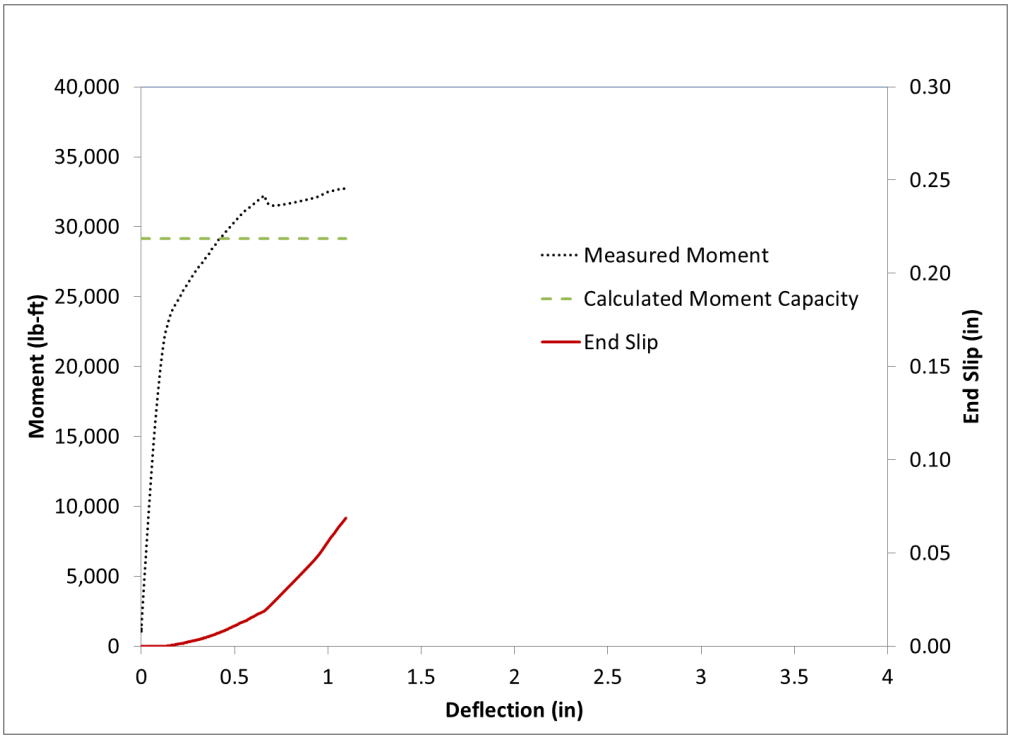

Figure H.10 Beam End A4-L Flexural Test Results Summary Chart A

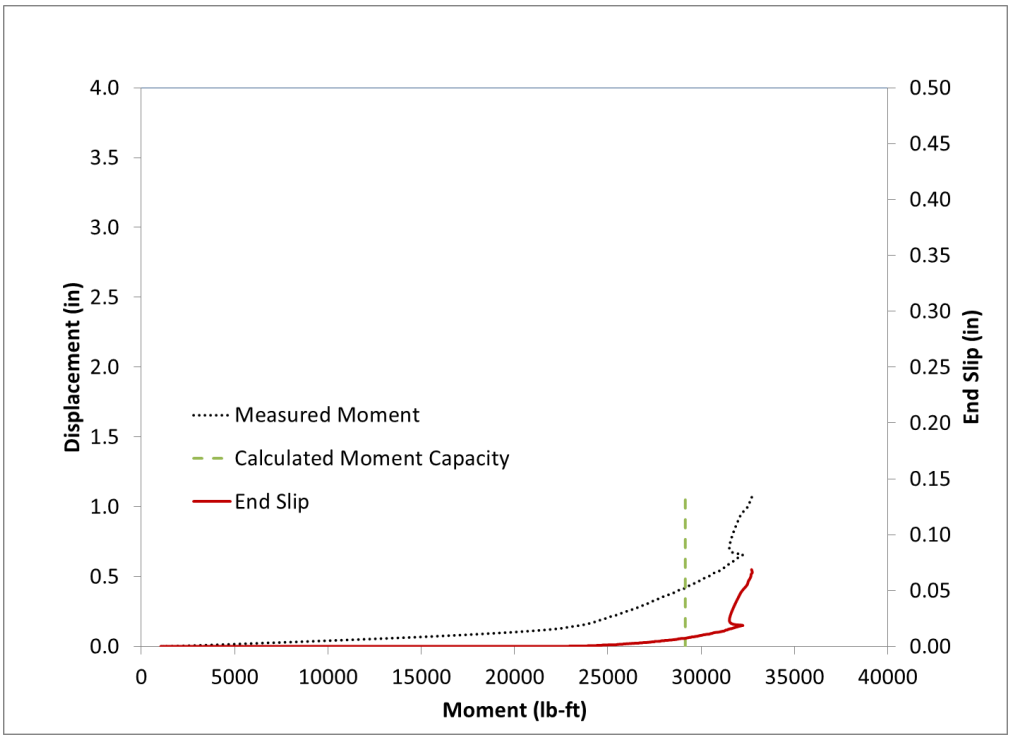

Figure H.11 Beam End A4-L Flexural Test Results Summary Chart B

Figure H.12 Beam End A4-L Failure

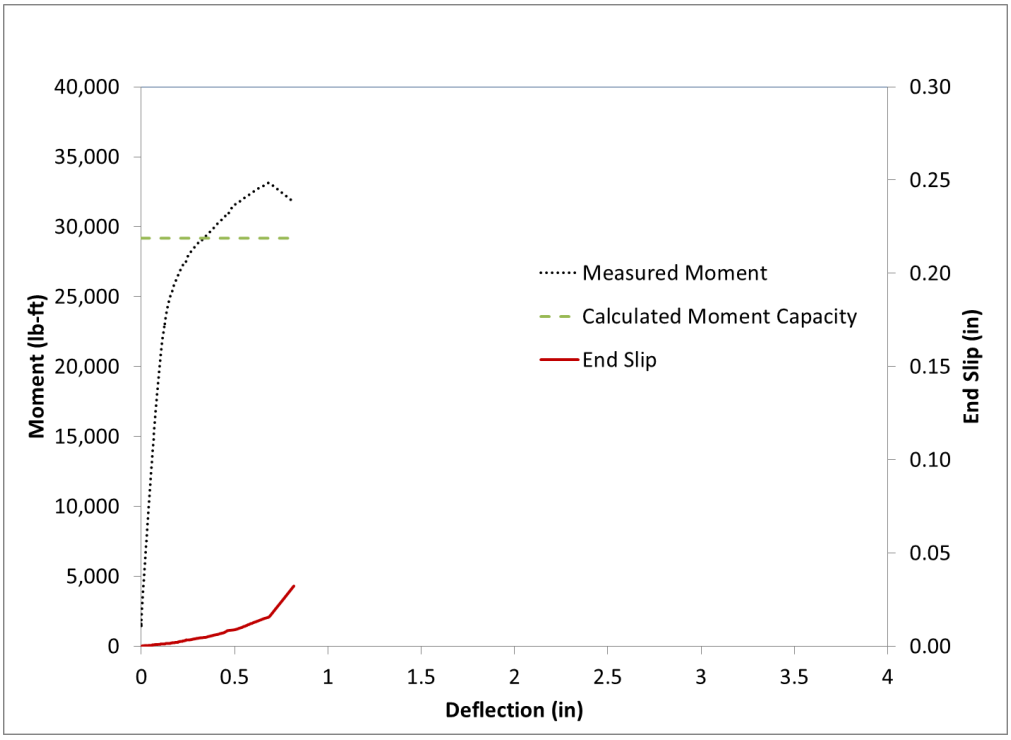

Figure H.13 Beam End A5-L Flexural Test Results Summary Chart A

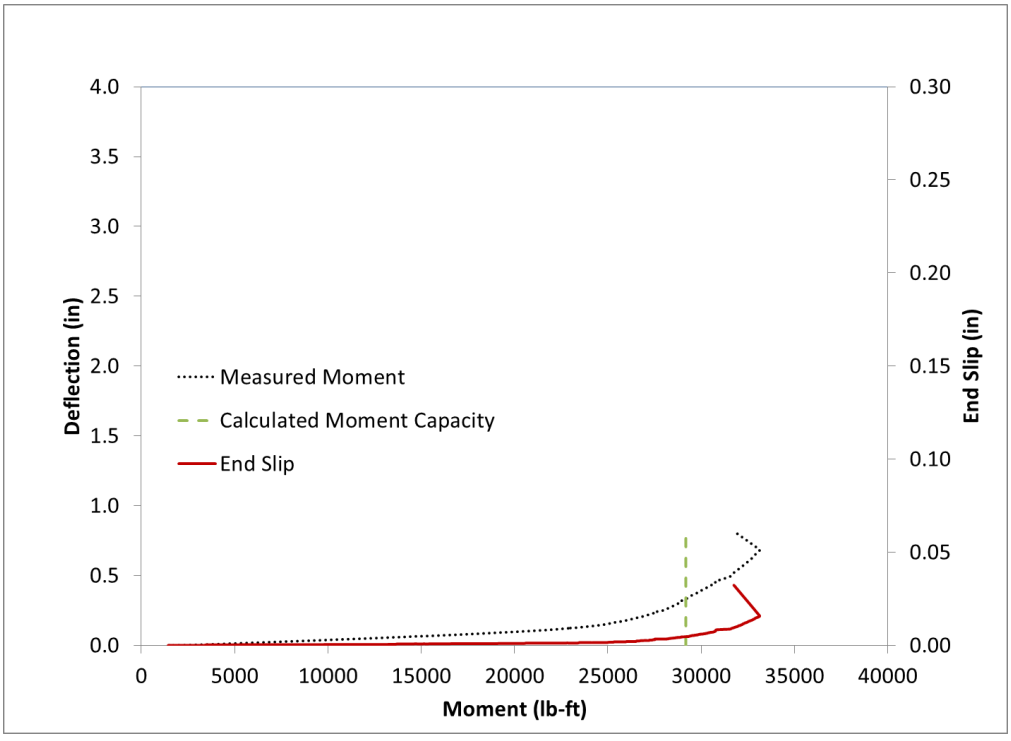

Figure H.14 Beam End A5-L Flexural Test Results Summary Chart B

Figure H.15 Beam End A5-L Failure

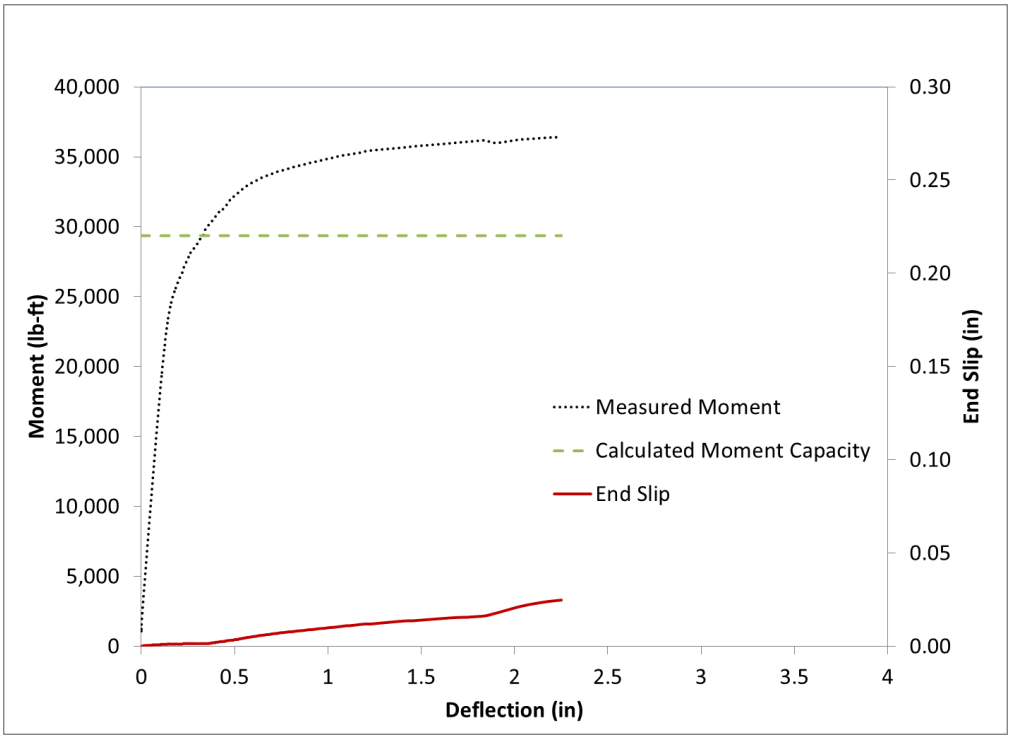

Figure H.16 Beam End A6-L Flexural Test Results Summary Chart A

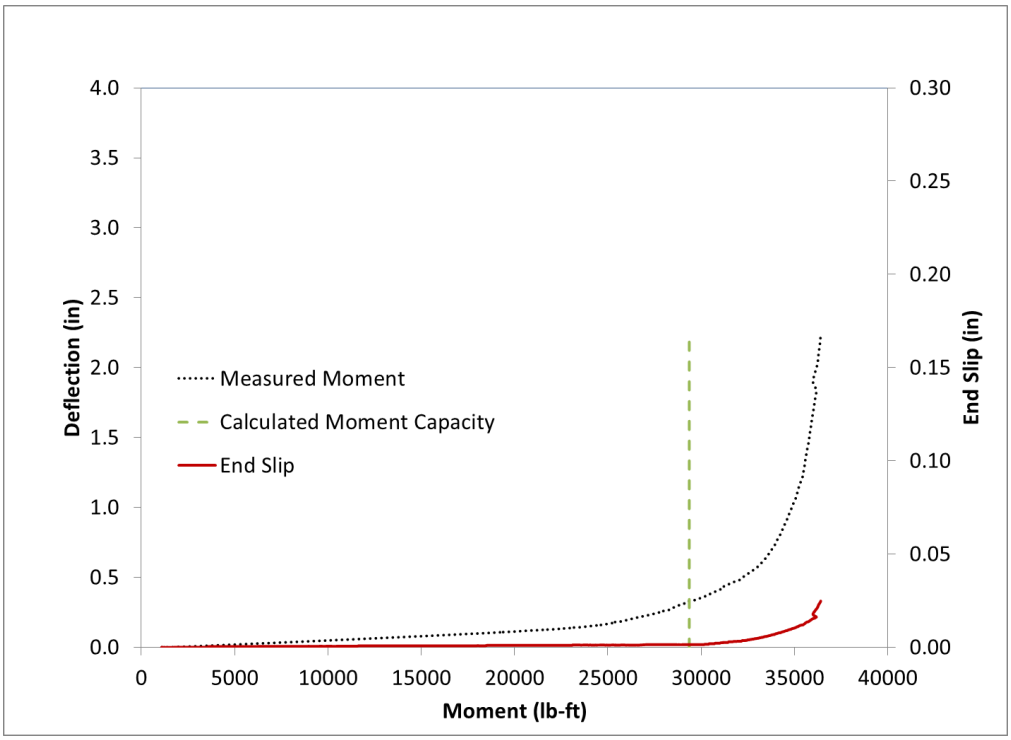

Figure H.17 Beam End A6-L Flexural Test Results Summary Chart B

Figure H.18 Beam End A6-L Failure

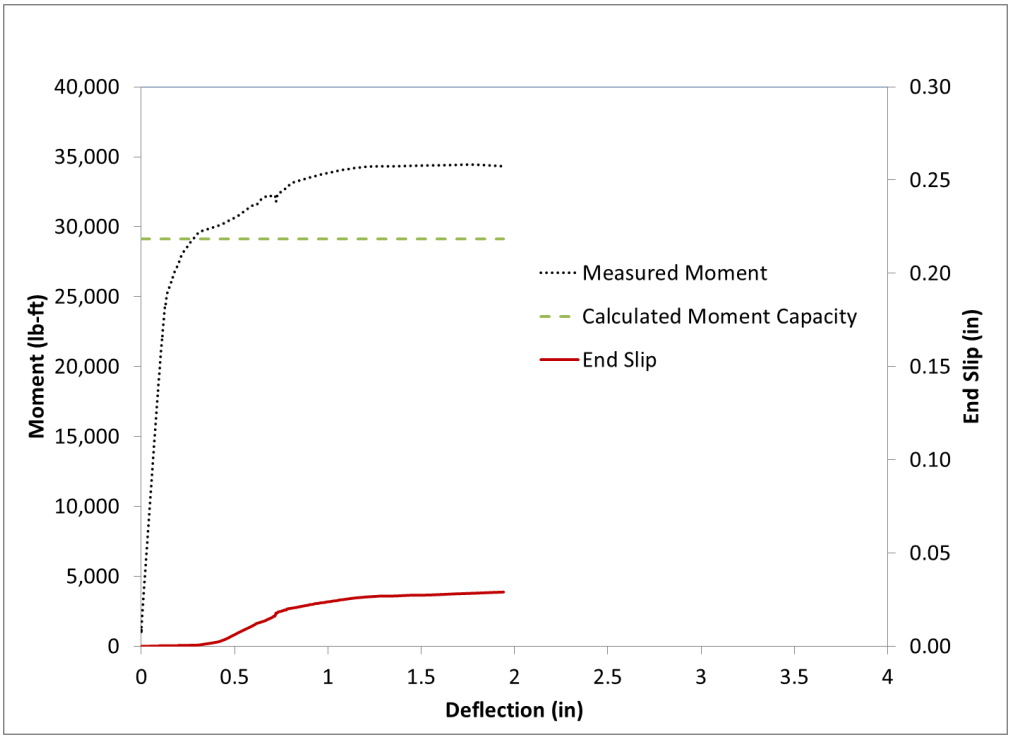

Figure H.19 Beam End A7-L Flexural Test Results Summary Chart A

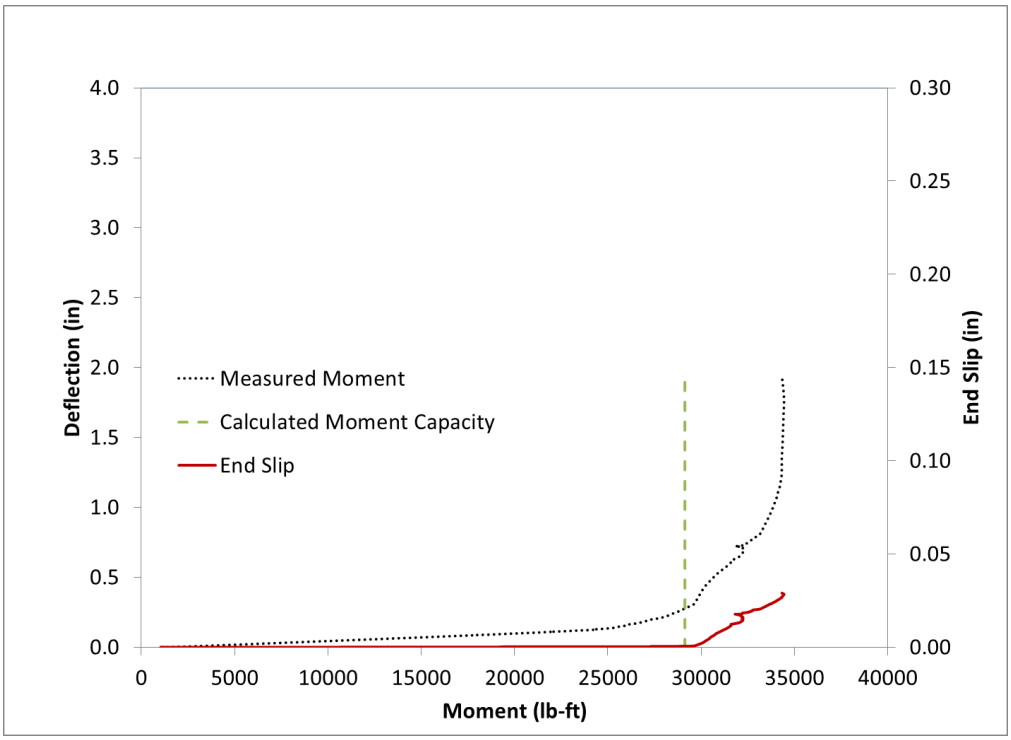

Figure H.20 Beam End A7-L Flexural Test Results Summary Chart B

Figure H.21 Beam End A7-L Failure

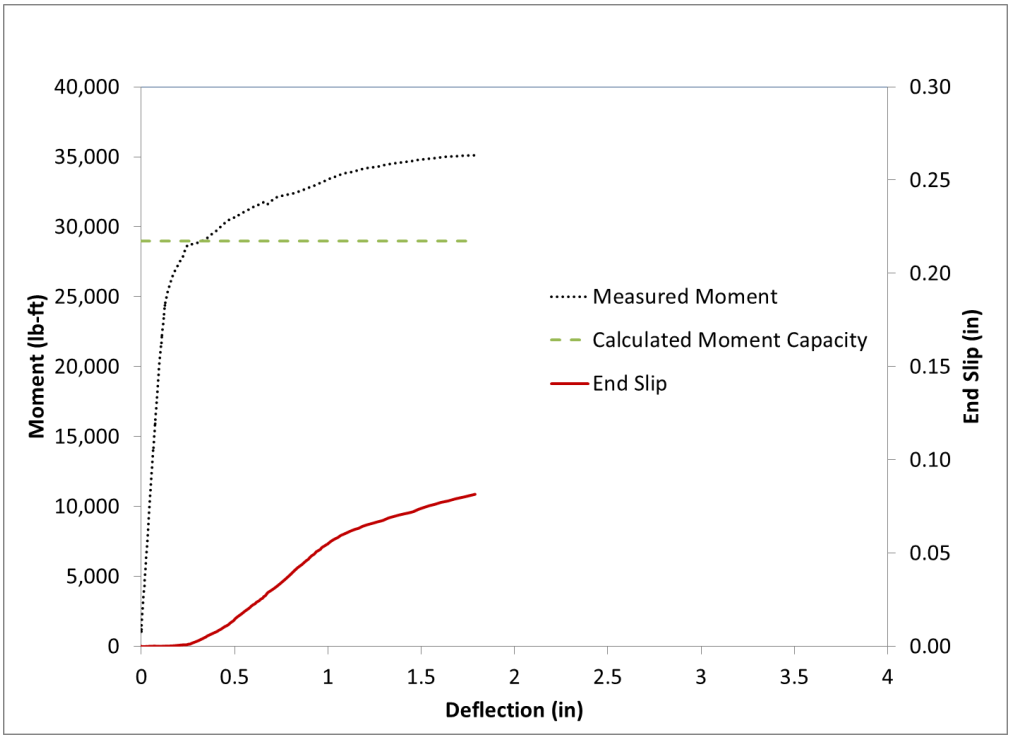

Figure H.22 Beam End A8-L Flexural Test Results Summary Chart A

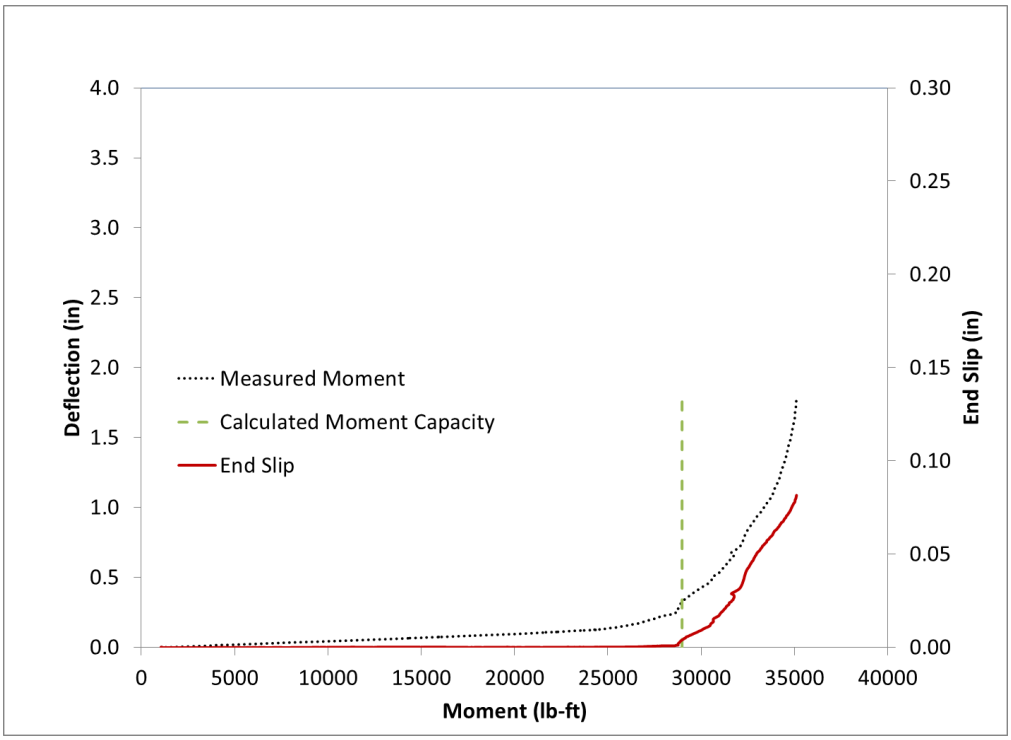

Figure H.23 Beam End A8-L Flexural Test Results Summary Chart B

Figure H.24 Beam End A8-L Failure

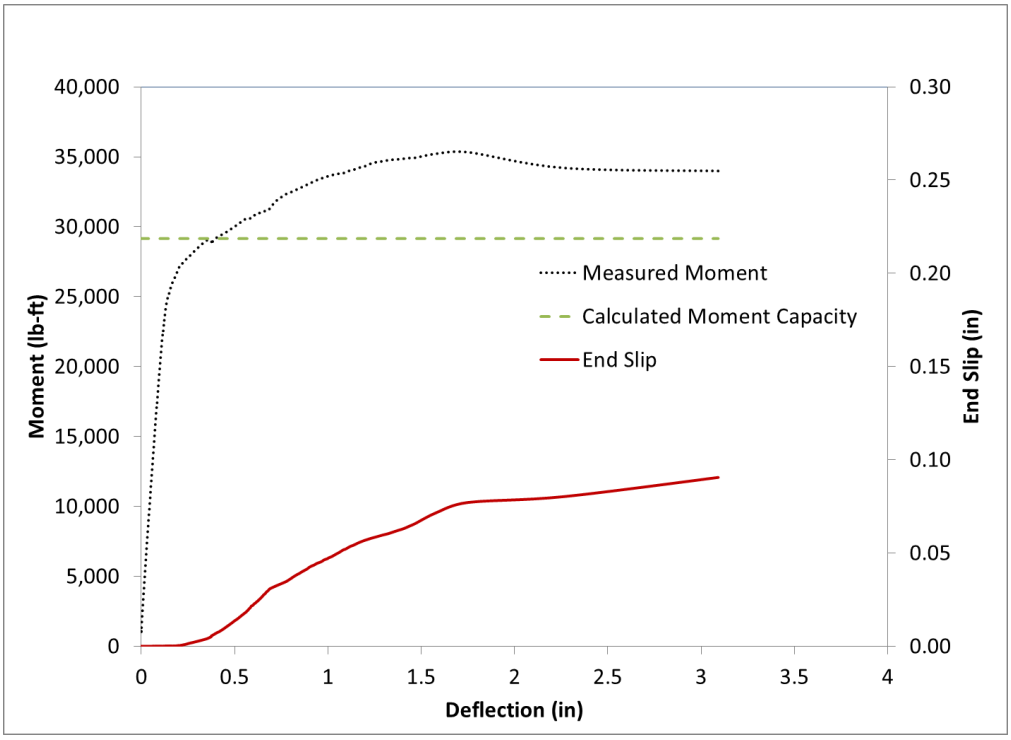

Figure H.25 Beam End A9-L Flexural Test Results Summary Chart A

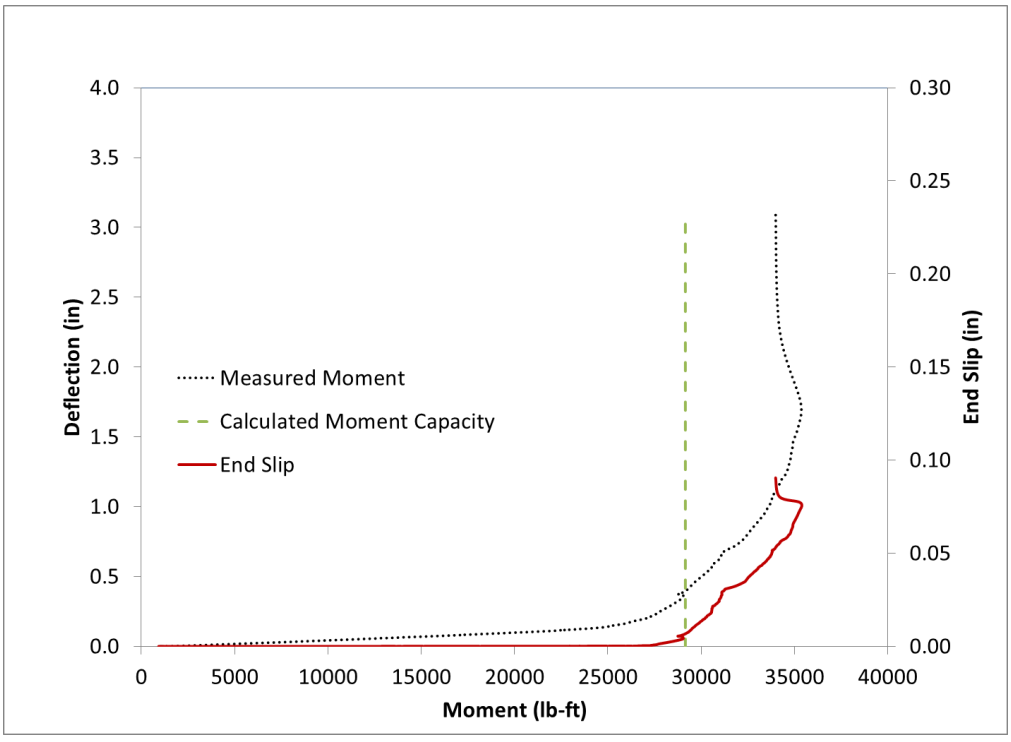

Figure H.26 Beam End A9-L Flexural Test Results Summary Chart B

Figure H.27 Beam End A9-L Failure

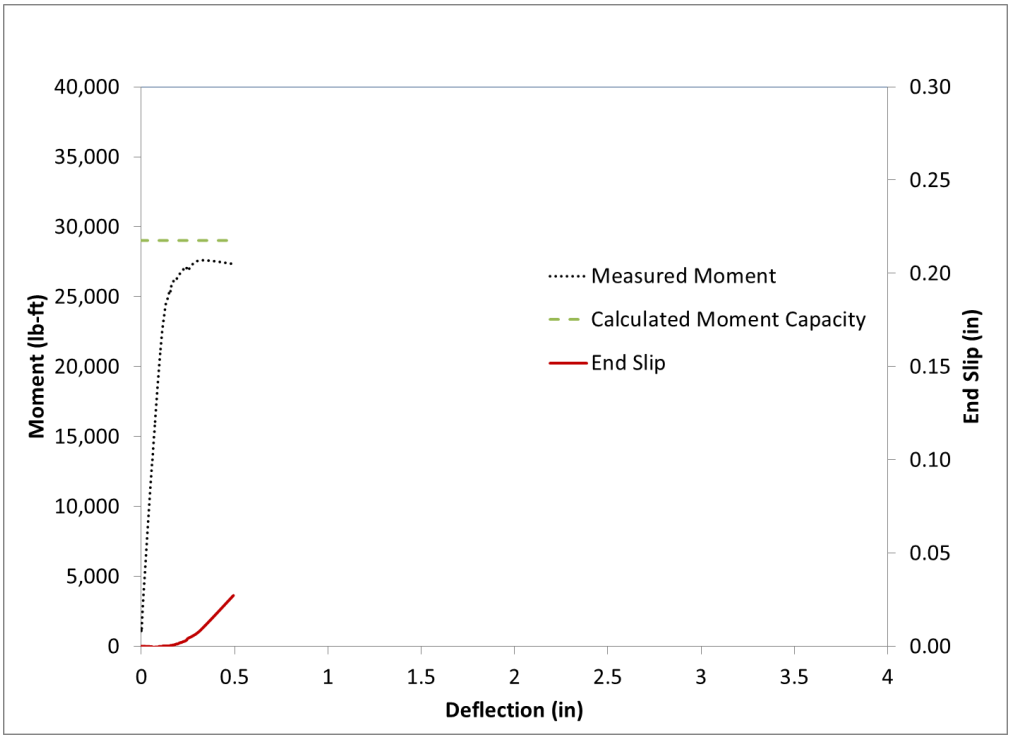

Figure H.28 Beam End A10-L Flexural Test Results Summary Chart A

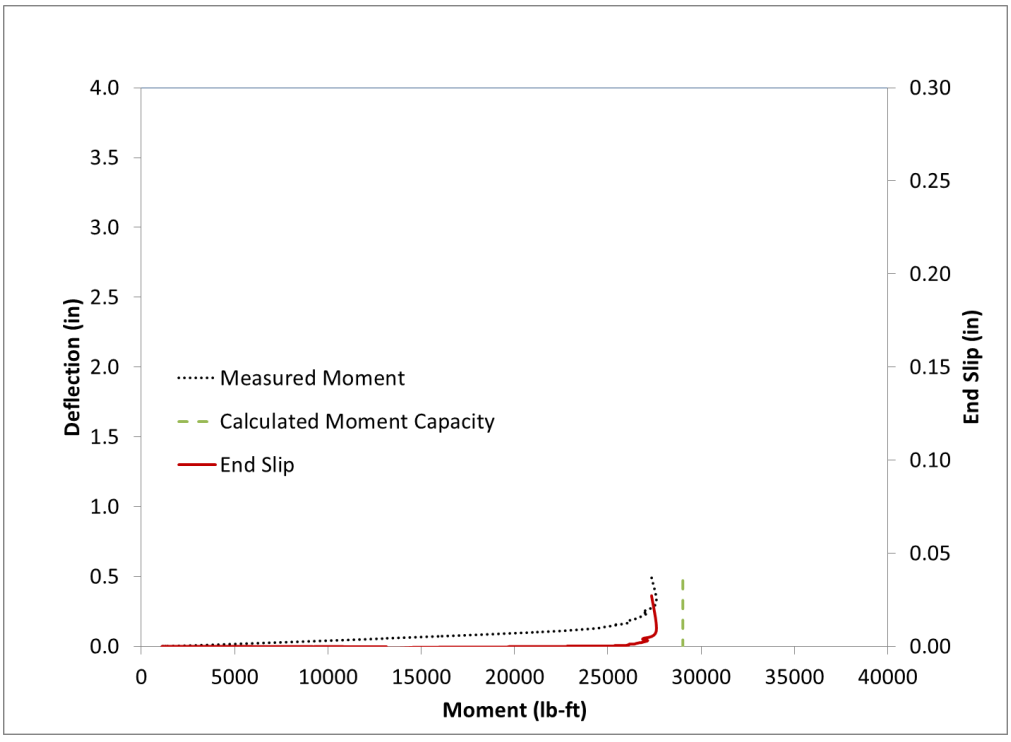

Figure H.29 Beam End A10-L Flexural Test Results Summary Chart B

Figure H.30 Beam End A10-L Failure

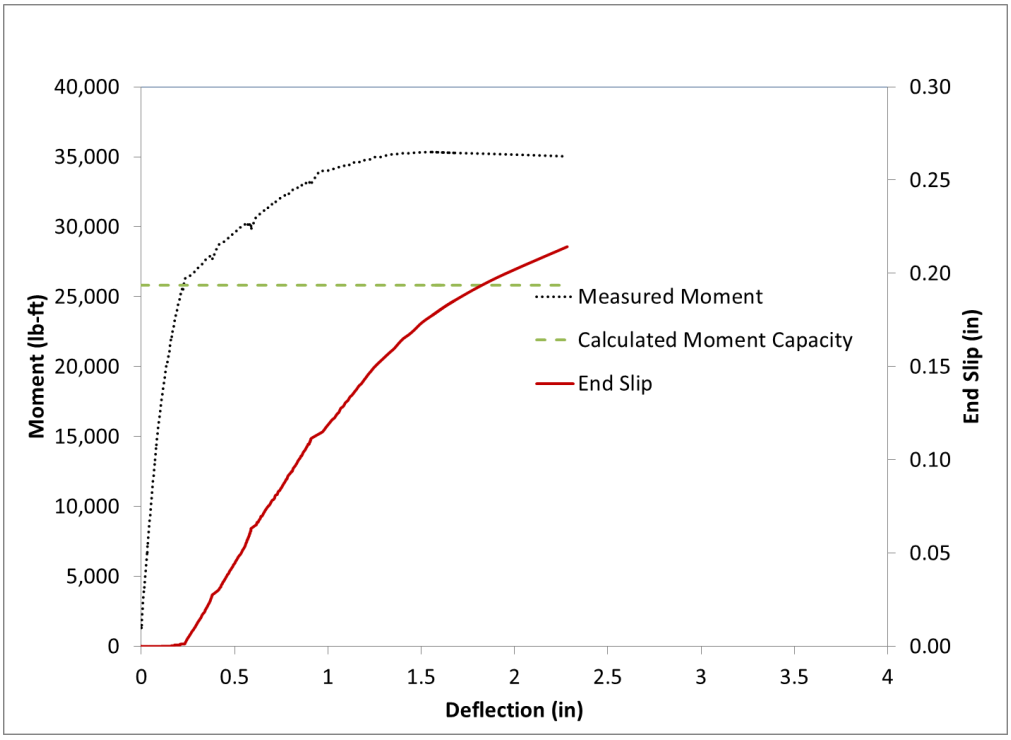

Figure H.31 Beam End A1-S Flexural Test Results Summary Chart A

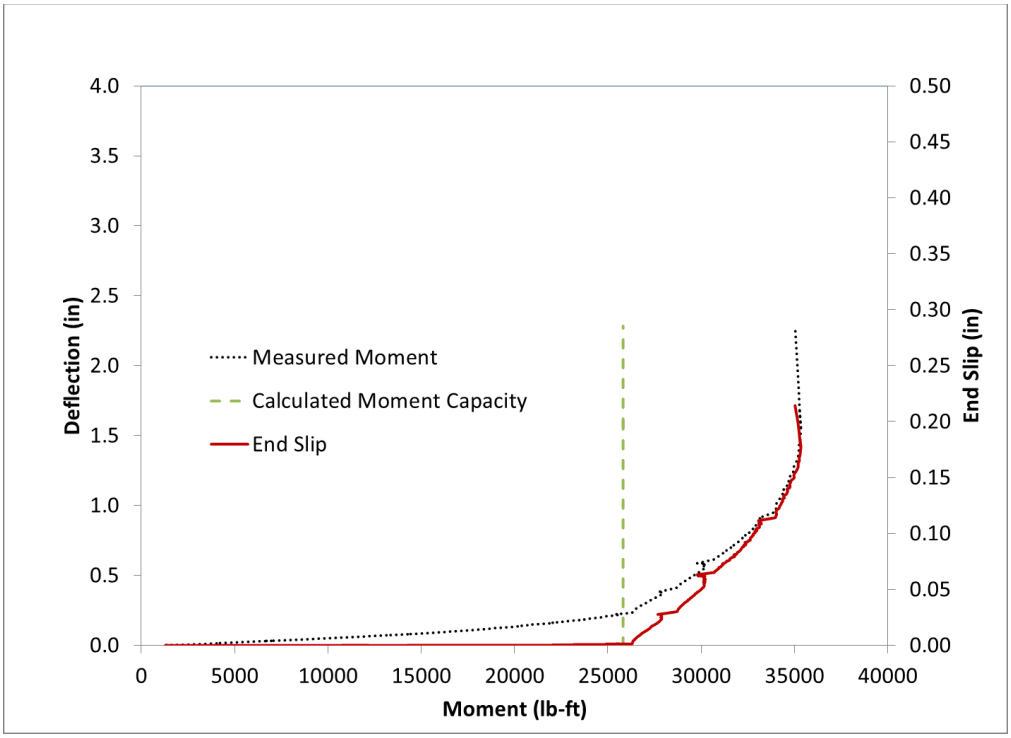

Figure H.32 Beam End A1-S Flexural Test Results Summary Chart B

Figure H.33 Beam End A1-S Failure

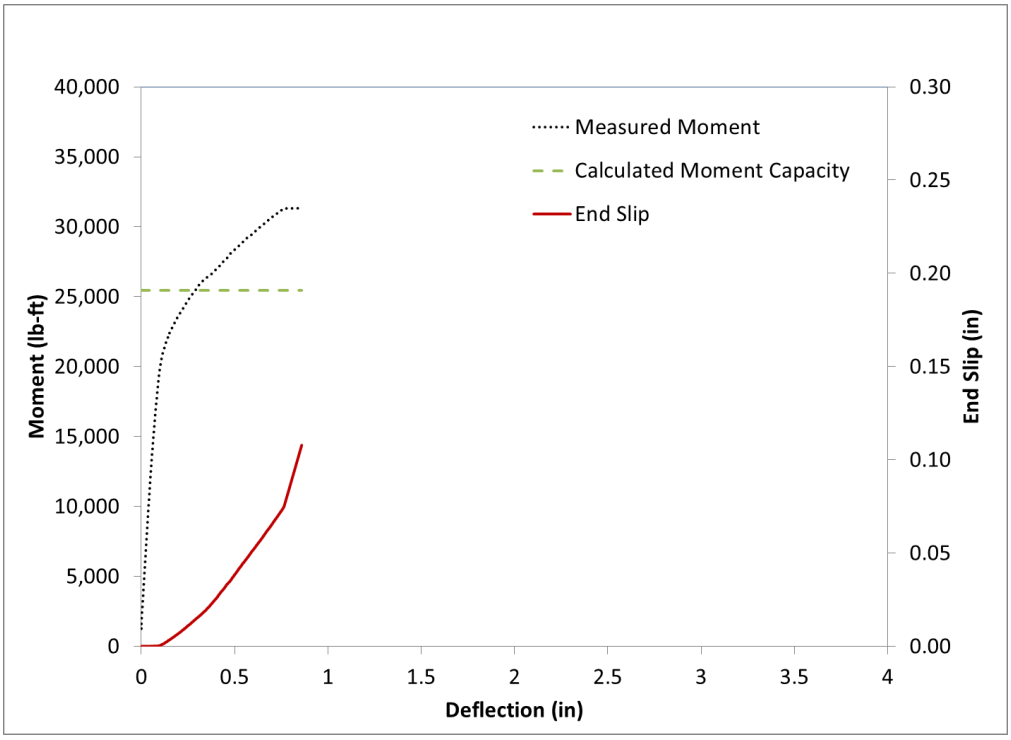

Figure H.34 Beam End A2-S Flexural Test Results Summary Chart A

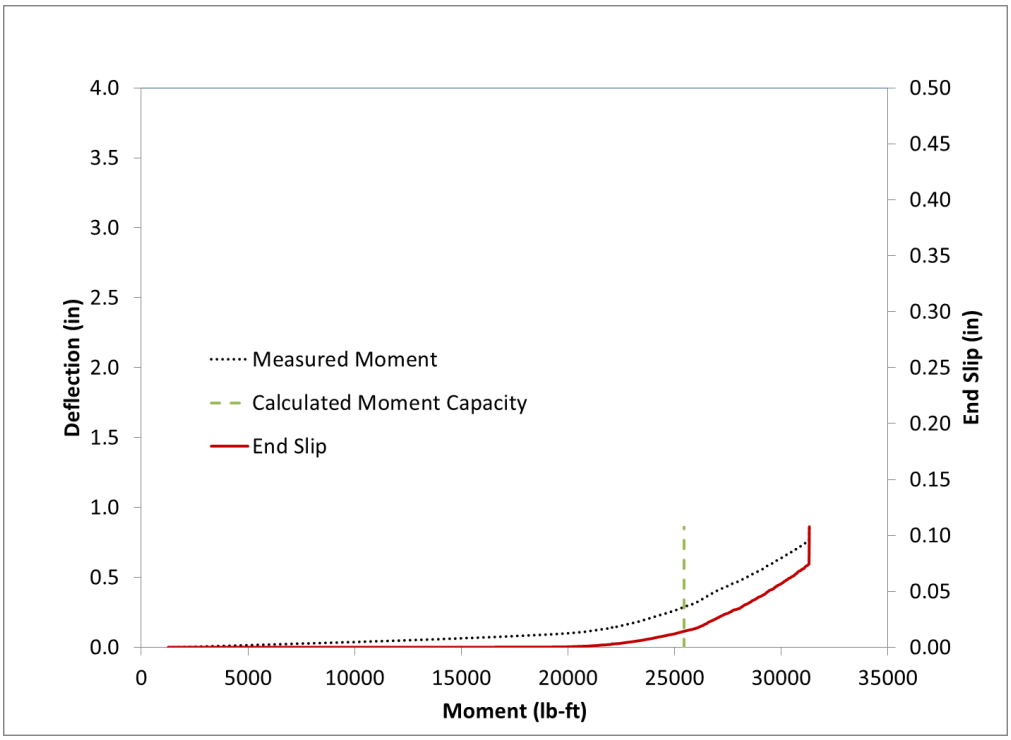

Figure H.35 Beam End A2-S Flexural Test Results Summary Chart B

Figure H.36 Beam End A2-S Failure

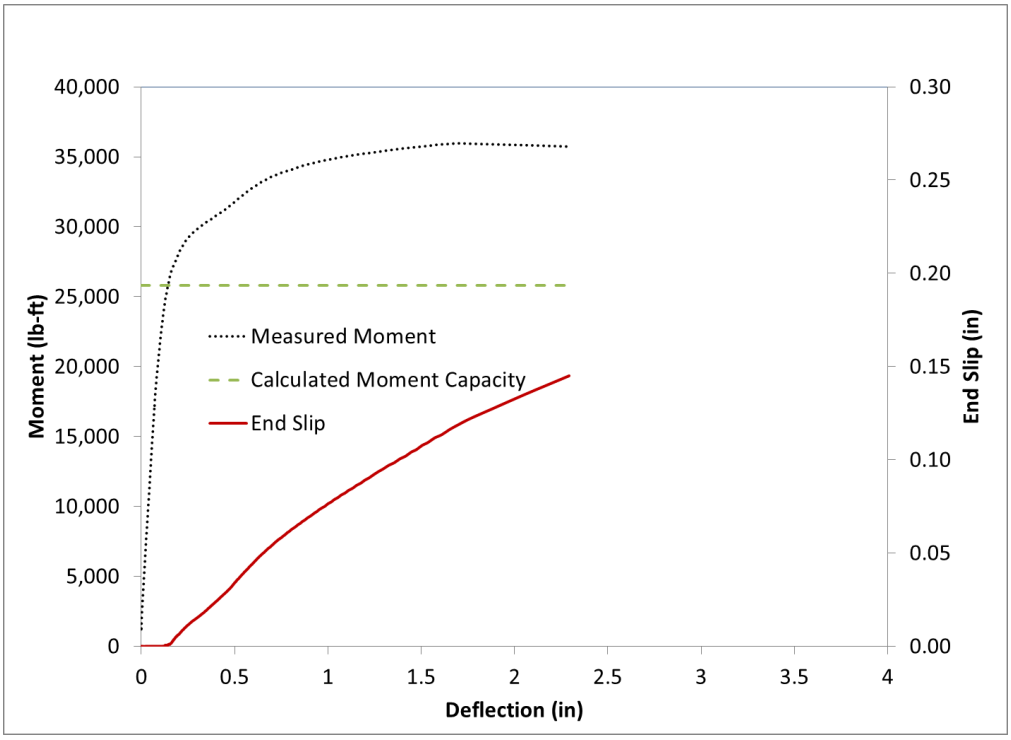

Figure H.37 Beam End A3-S Flexural Test Results Summary Chart A

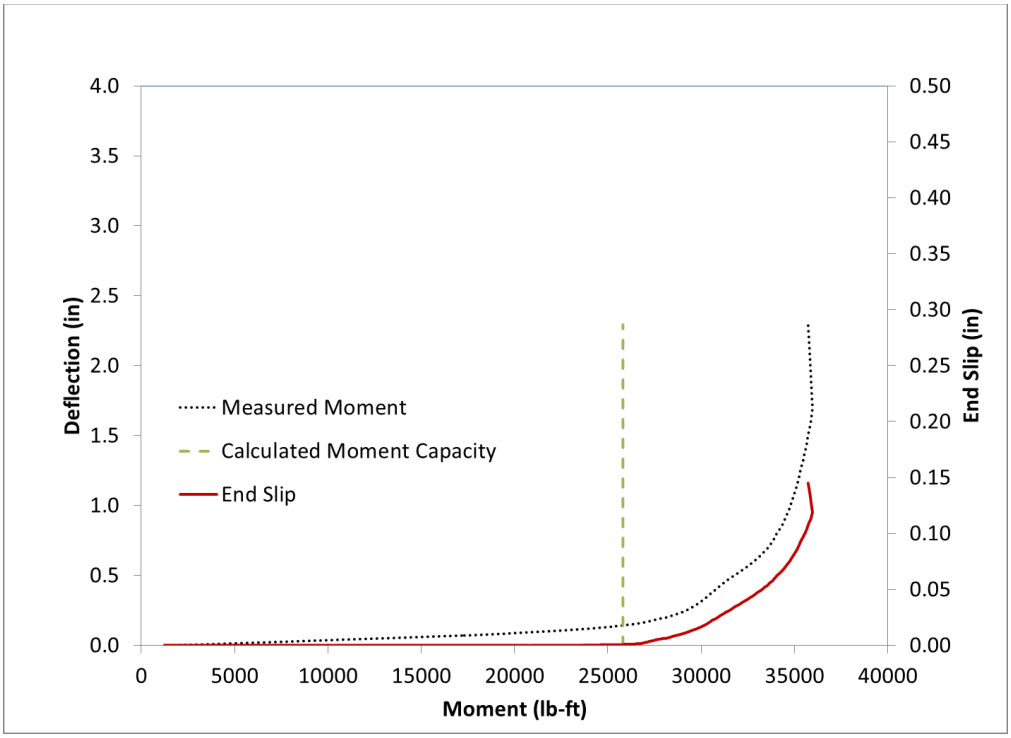

Figure H.38 Beam End A3-S Flexural Test Results Summary Chart B

Figure H.39 Beam End A3-S Failure

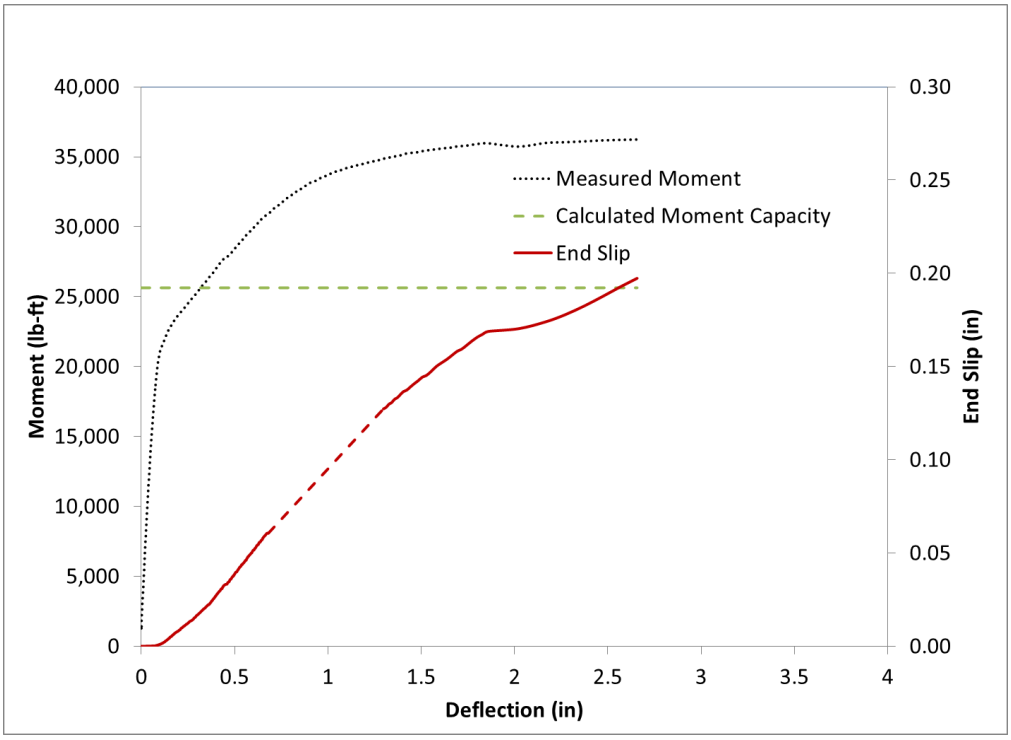

Figure H.40 Beam End A4-S Flexural Test Results Summary Chart A

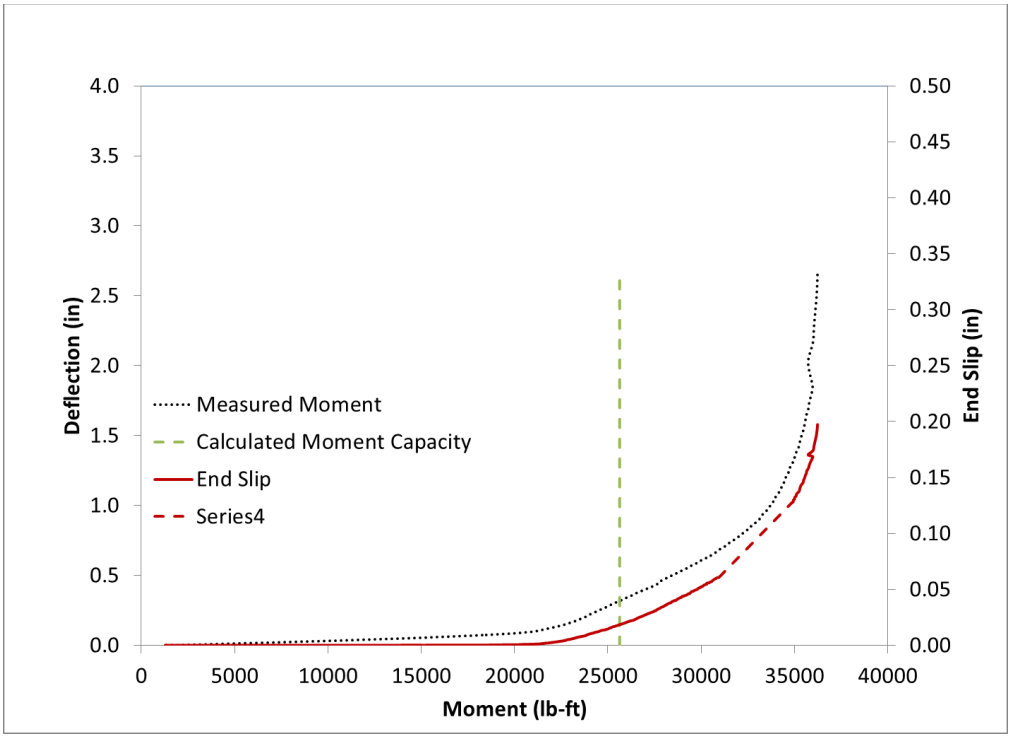

Figure H.41 Beam End A4-S Flexural Test Results Summary Chart B

Figure H.42 Beam End A4-S Failure

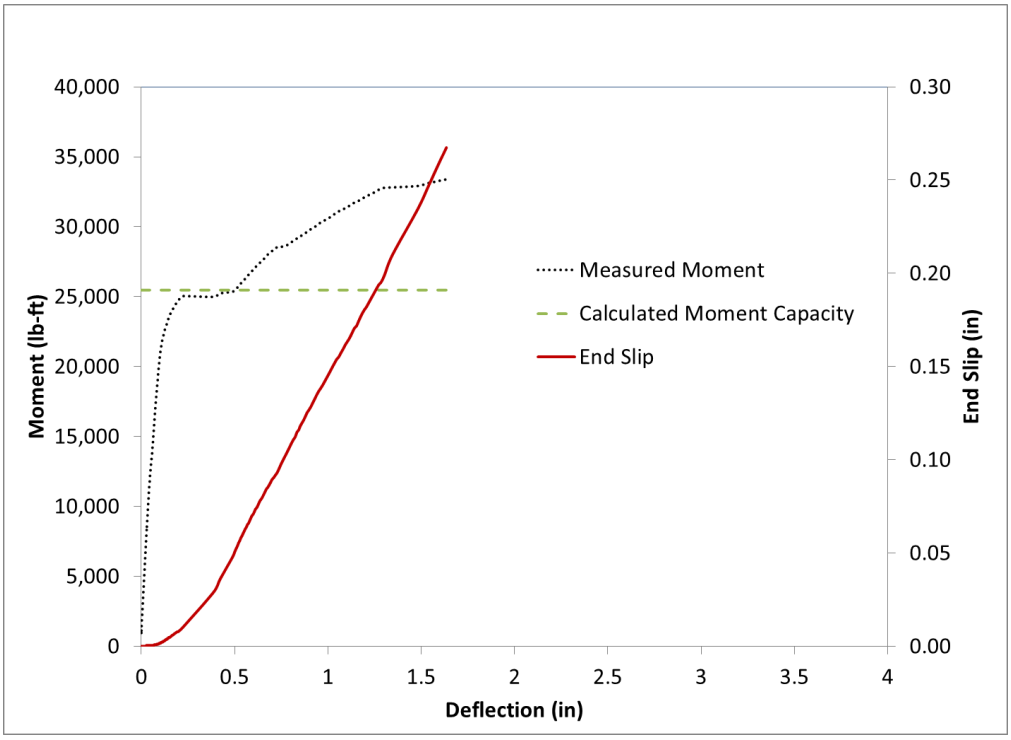

Figure H.43 Beam End A5-S Flexural Test Results Summary Chart A

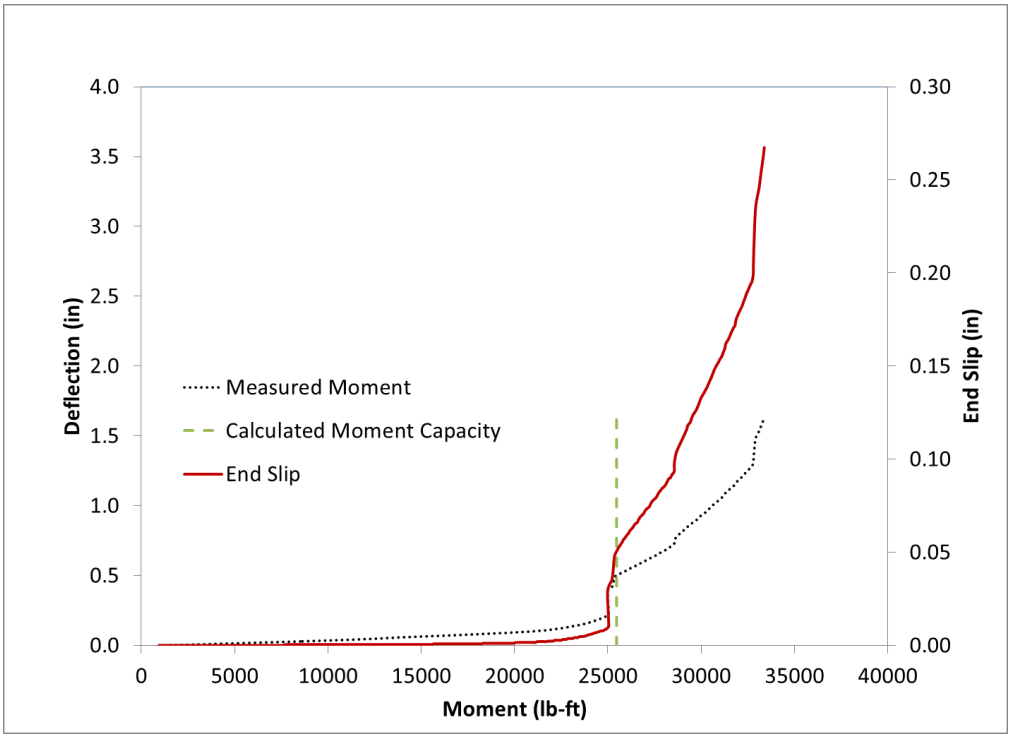

Figure H.44 Beam End A5-S Flexural Test Results Summary Chart B

Figure H.45 Beam End A5-S Failure

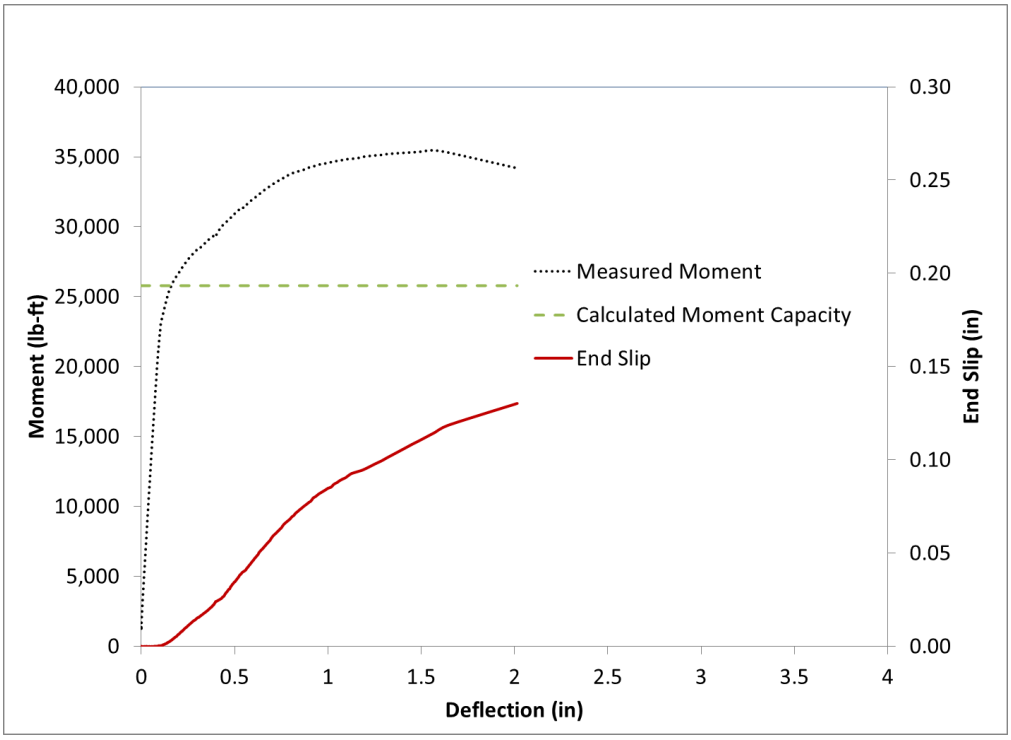

Figure H.46 Beam End A6-S Flexural Test Results Summary Chart A

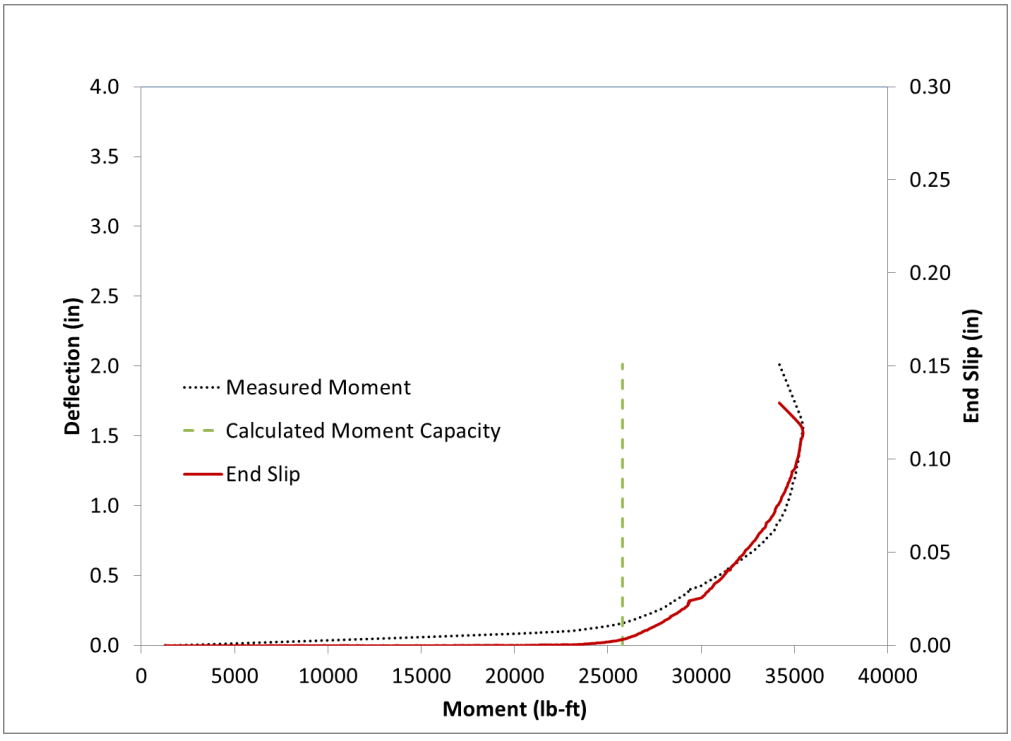

Figure H.47 Beam End A6-S Flexural Test Results Summary Chart B

Figure H.48 Beam End A6-S Failure

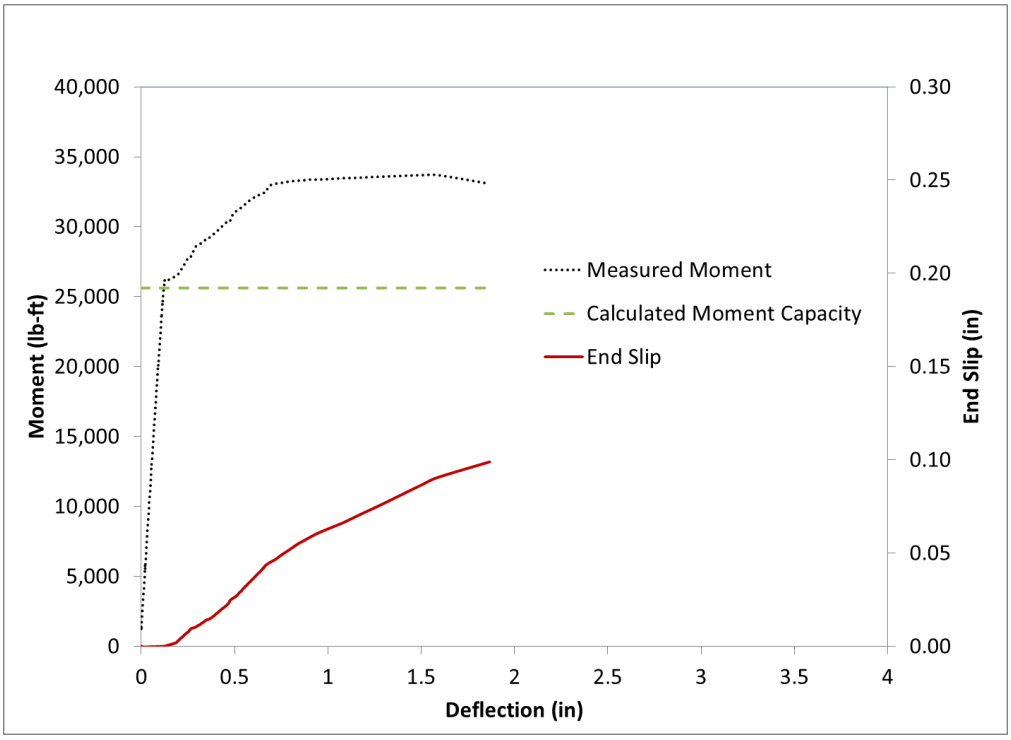

Figure H.49 Beam End A7-S Flexural Test Results Summary Chart A

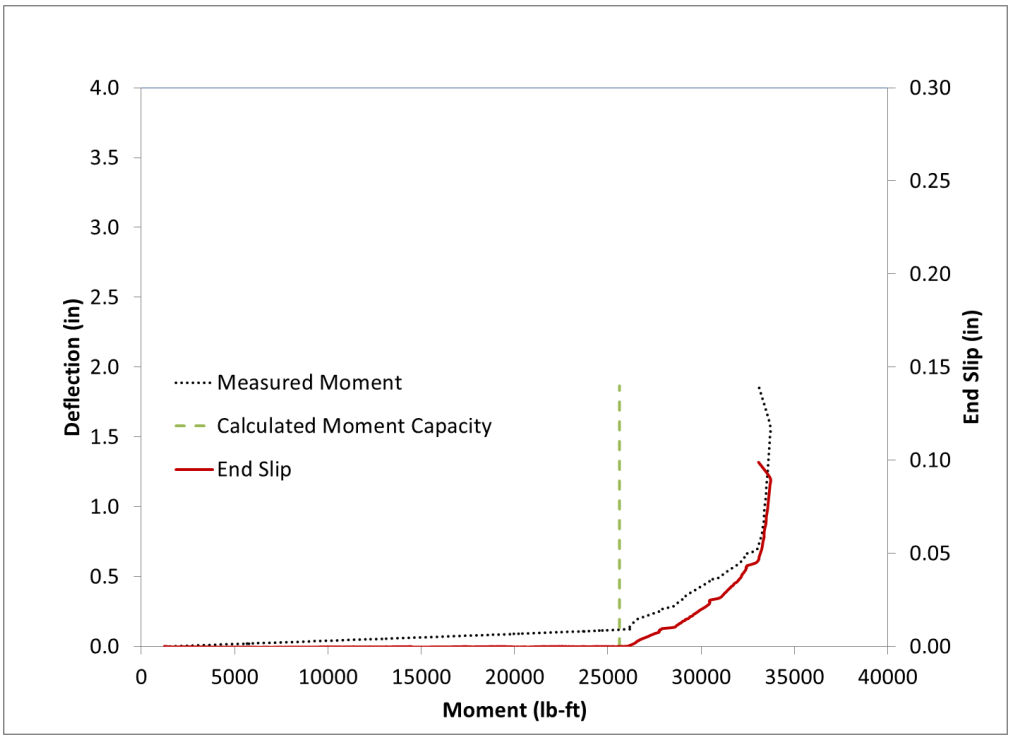

Figure H.50 Beam End A7-S Flexural Test Results Summary Chart B

Figure H.51 Beam End A7-S Failure

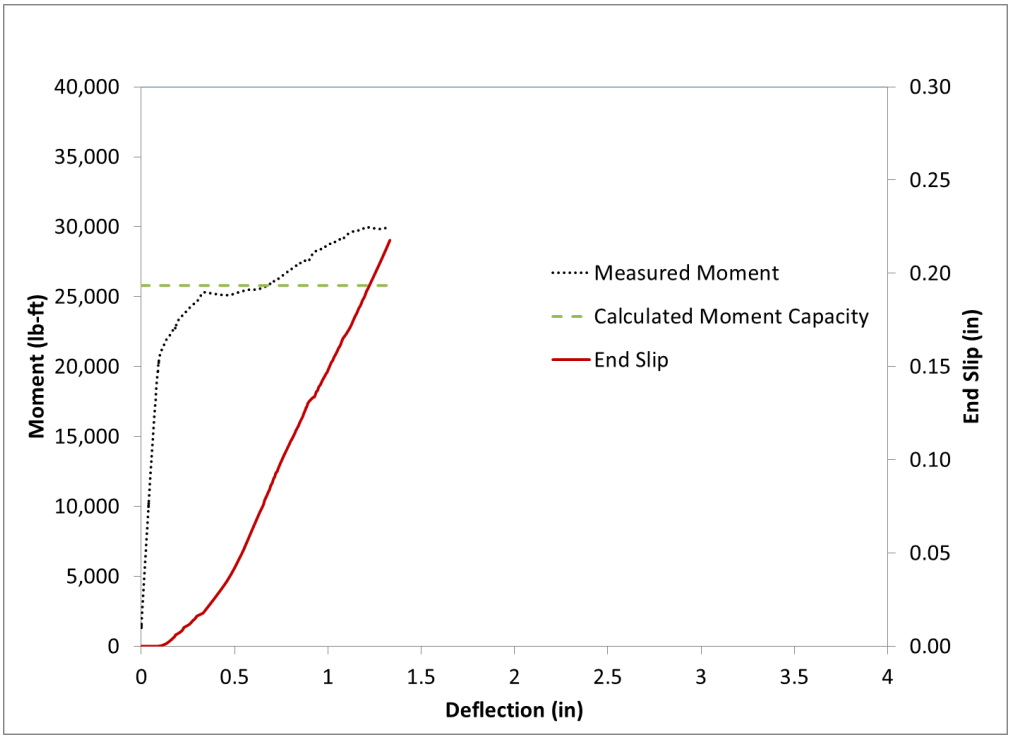

Figure H.52 Beam End A8-S Flexural Test Results Summary Chart A

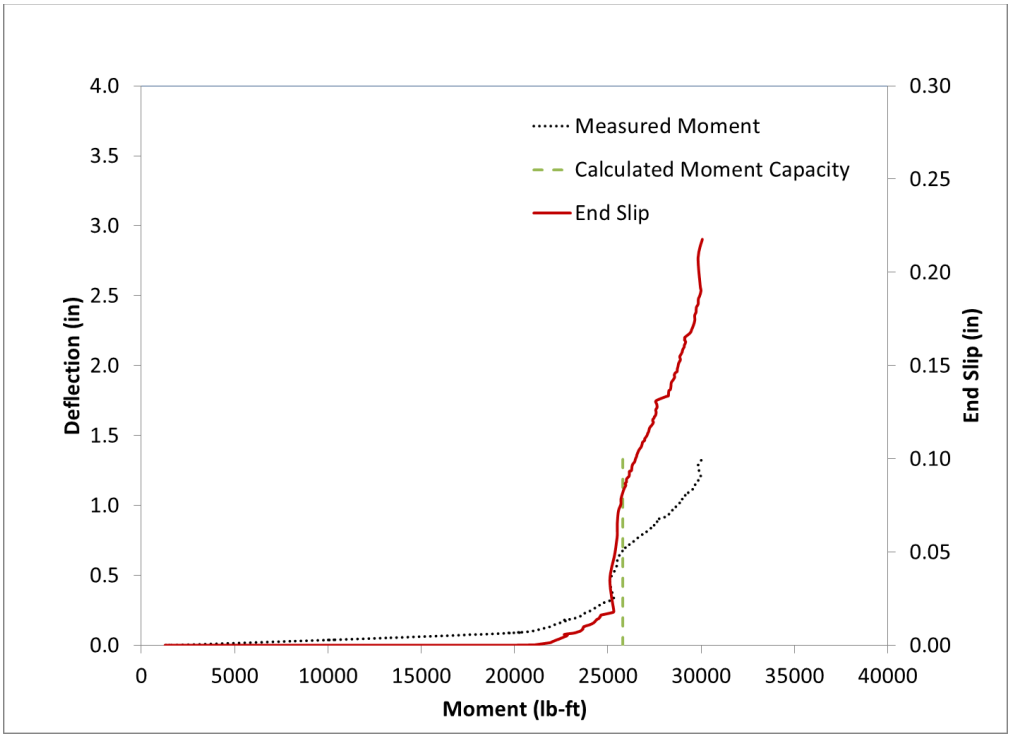

Figure H.53 Beam End A8-S Flexural Test Results Summary Chart B

Figure H.54 Beam End A8-S Failure

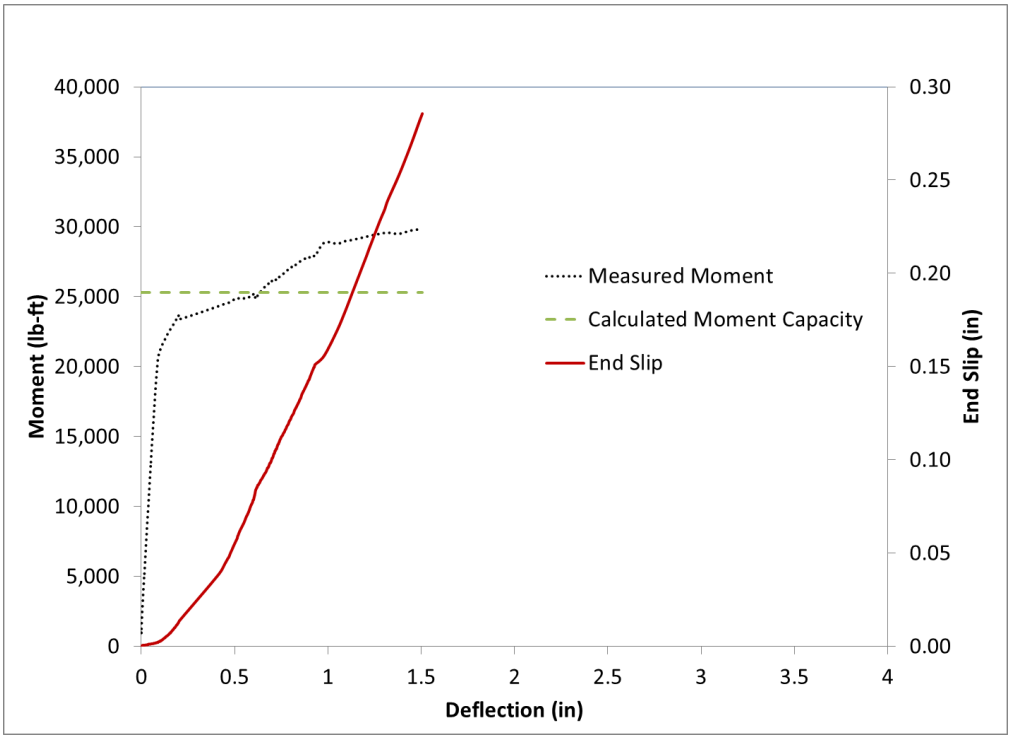

Figure H.55 Beam End A9-S Flexural Test Results Summary Chart A

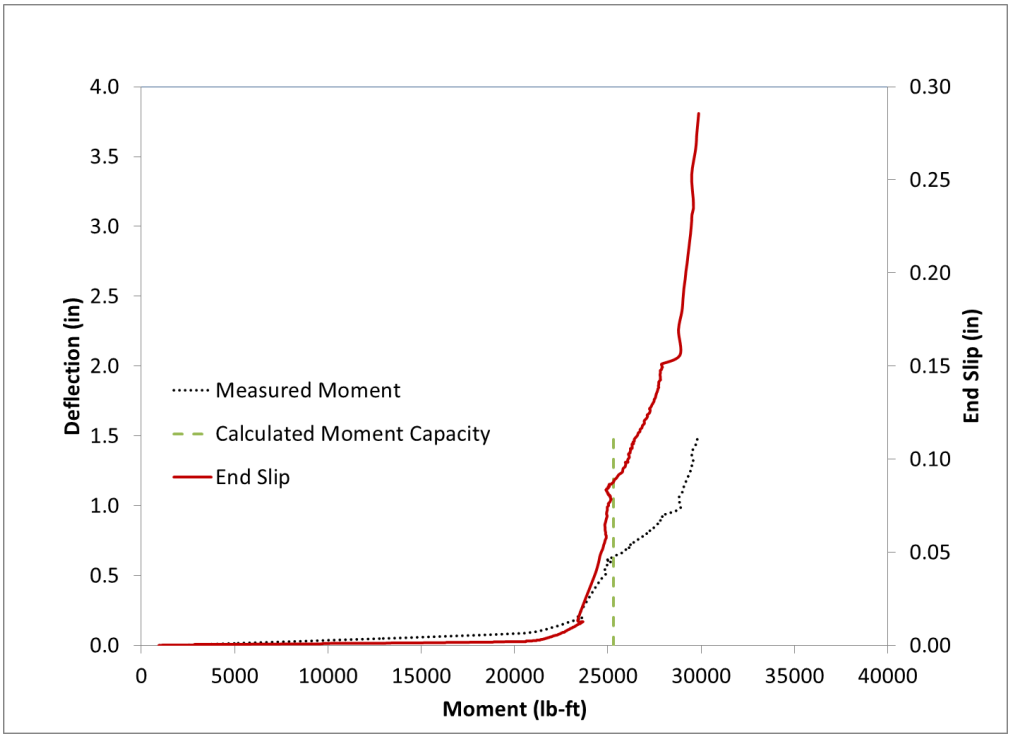

Figure H.56 Beam End A9-S Flexural Test Results Summary Chart B

Figure H.57 Beam End A9-S Failure

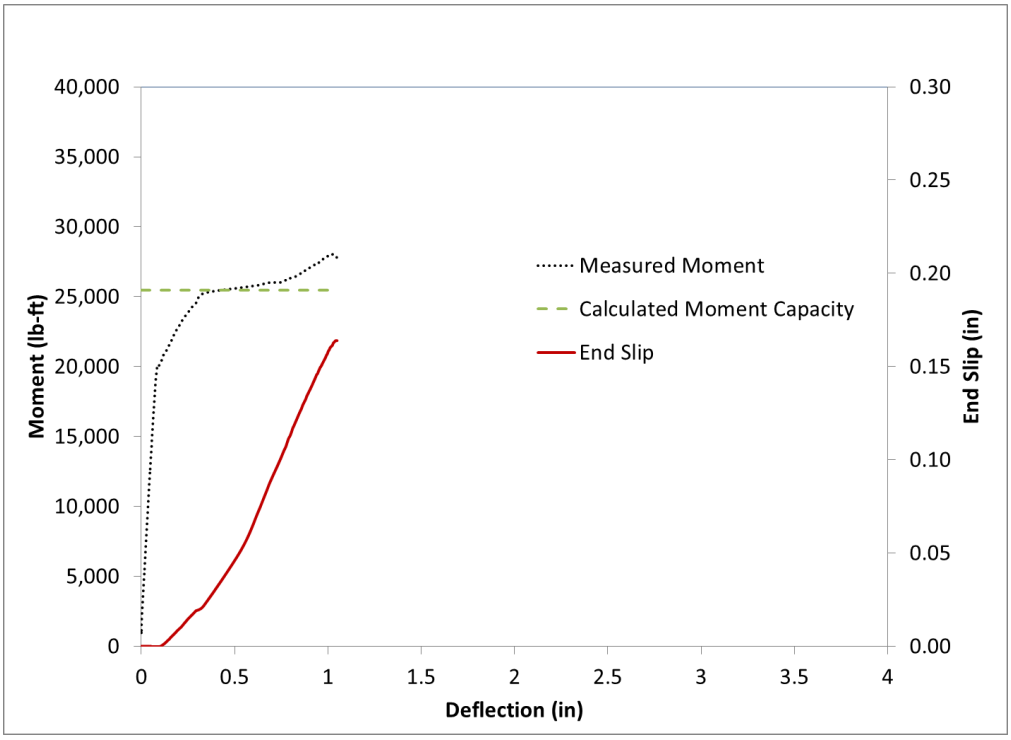

Figure H.58 Beam End A10-S Flexural Test Results Summary Chart A

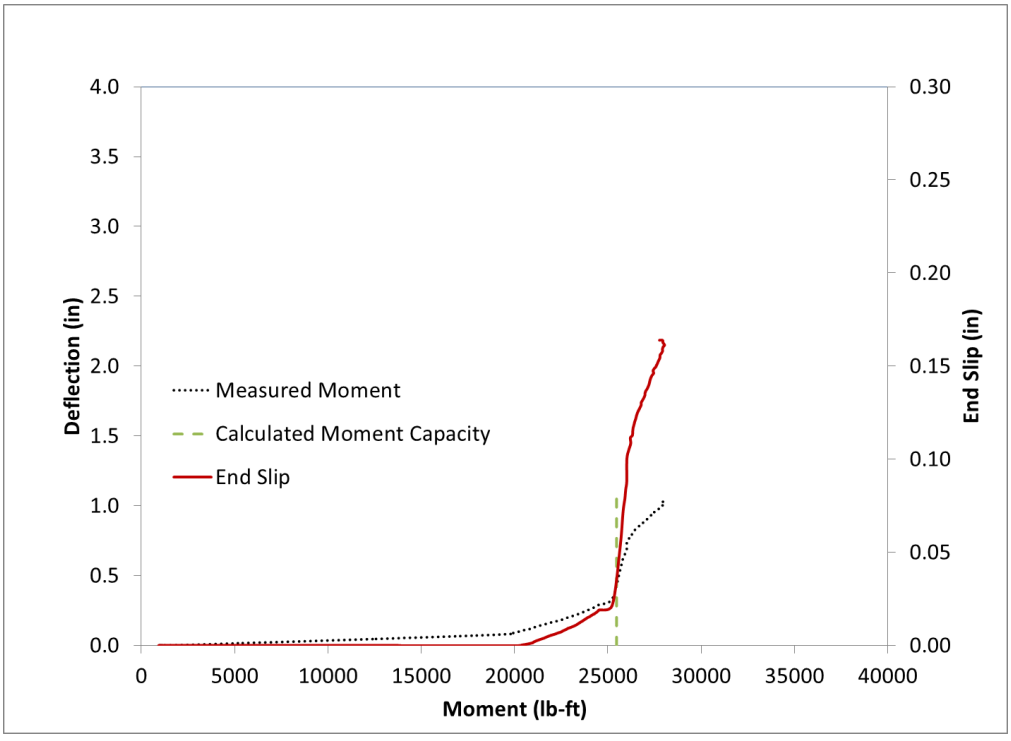

Figure H.59 Beam End A10-S Flexural Test Results Summary Chart B

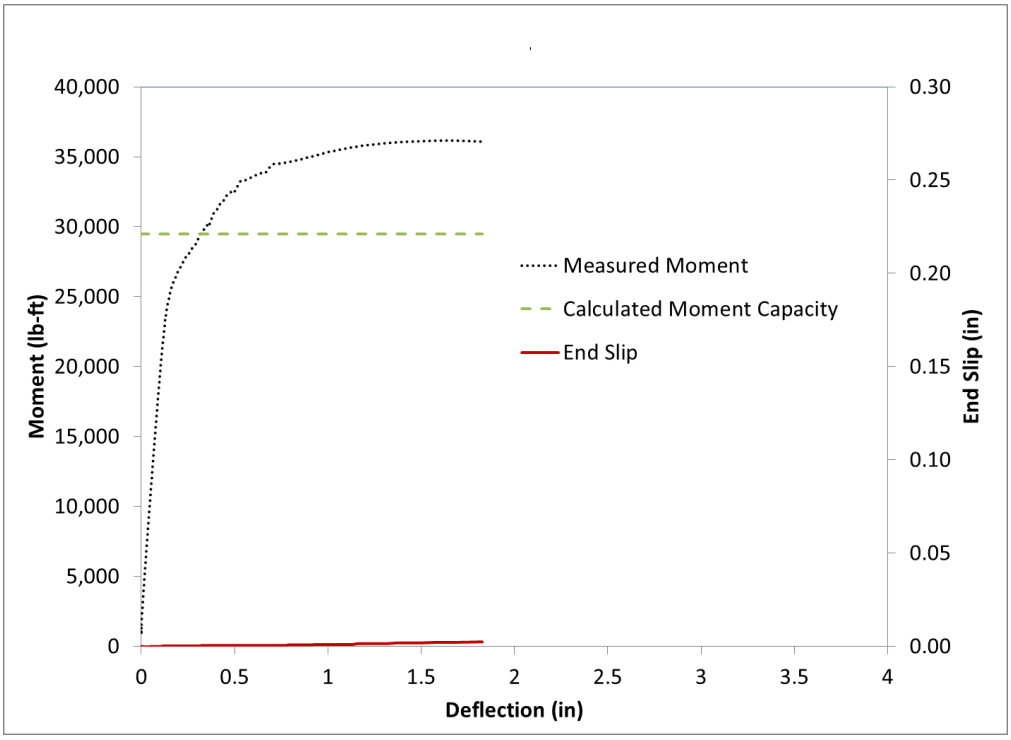

Figure H.60 Beam End G1-L Flexural Test Results Summary Chart A

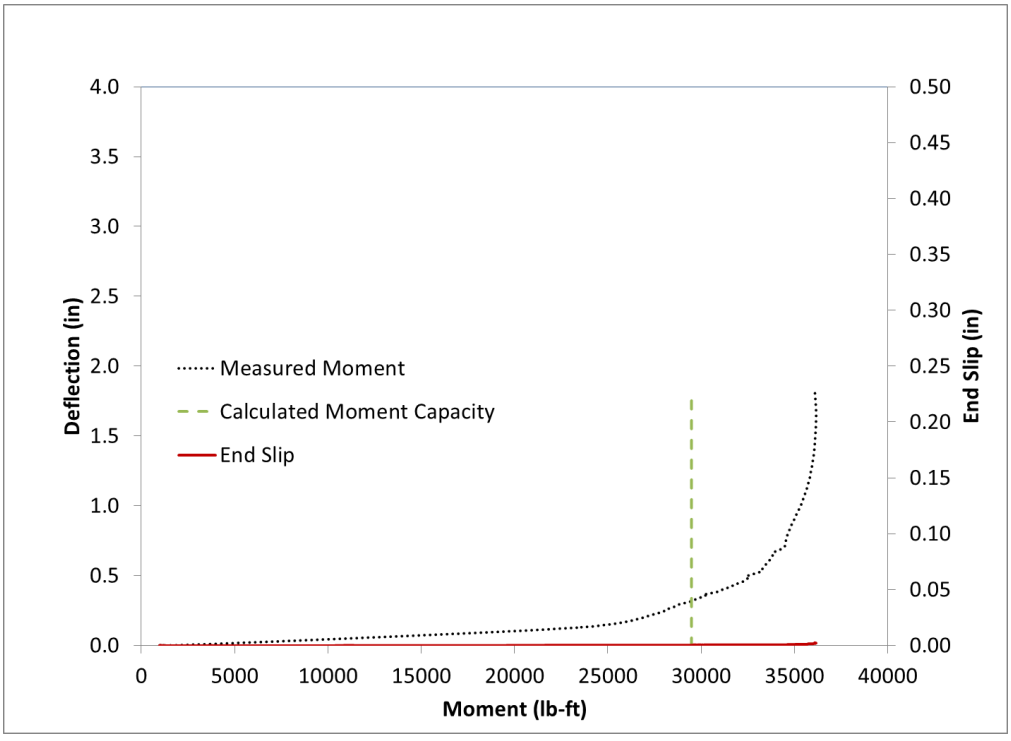

Figure H.61 Beam End G1-L Flexural Test Results Summary Chart B

Figure H.62 Beam End G1-L Failure

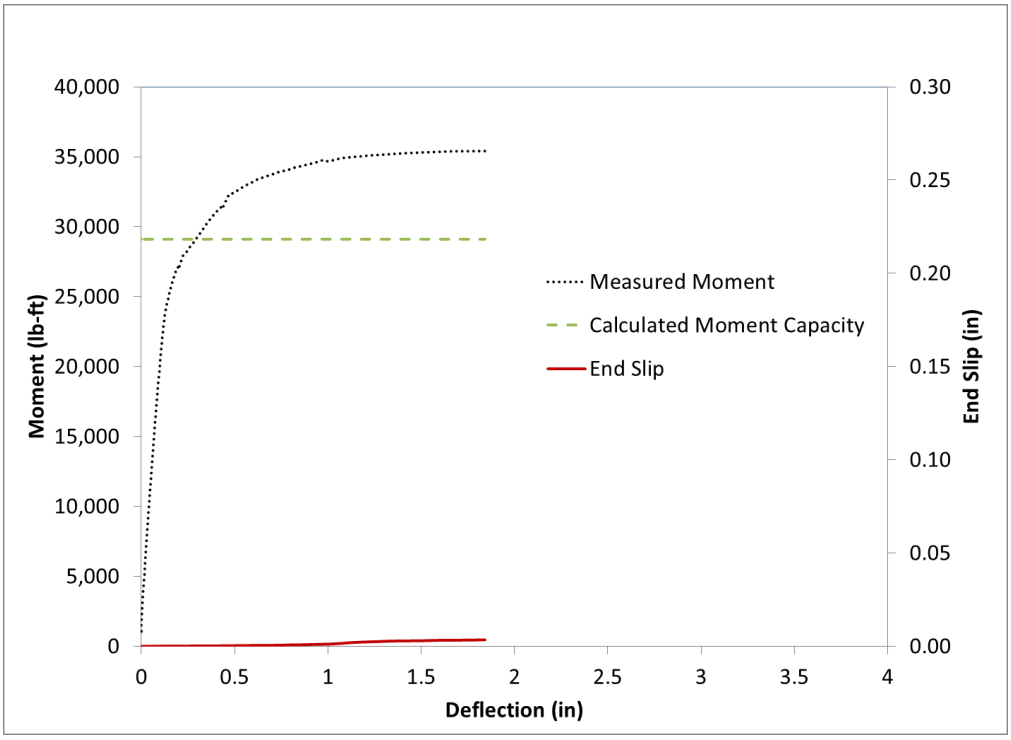

Figure H.63 Beam End G2-L Flexural Test Results Summary Chart A

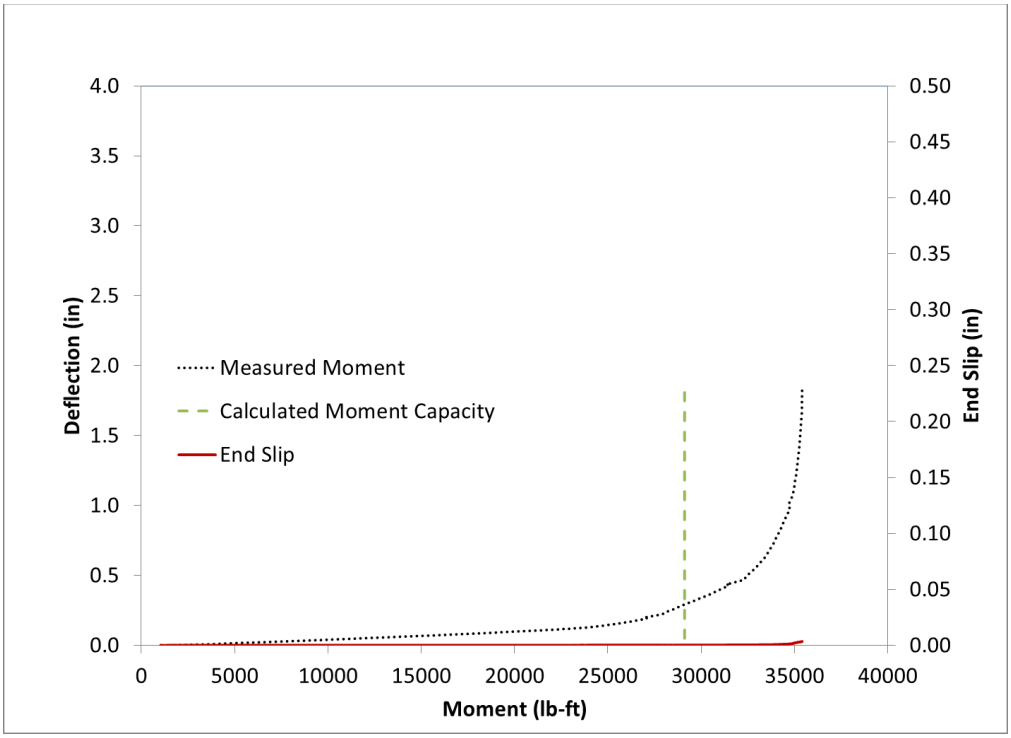

Figure H.64 Beam End G2-L Flexural Test Results Summary Chart B

Figure H.65 Beam End G2-L Failure

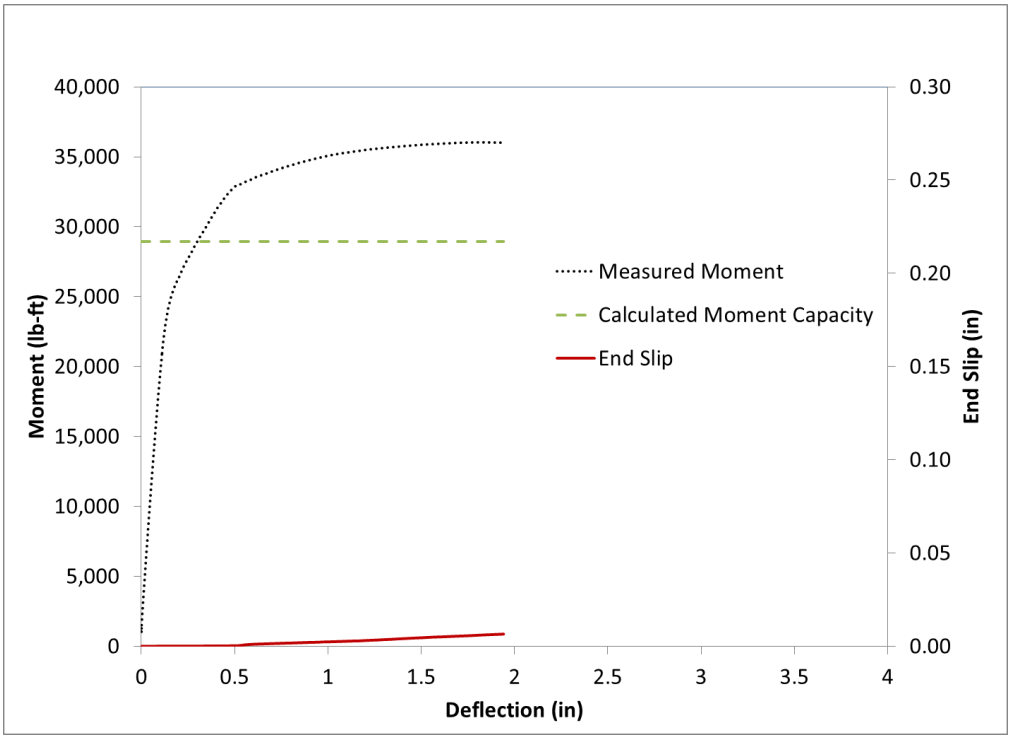

Figure H.66 Beam End G3-L Flexural Test Results Summary Chart A

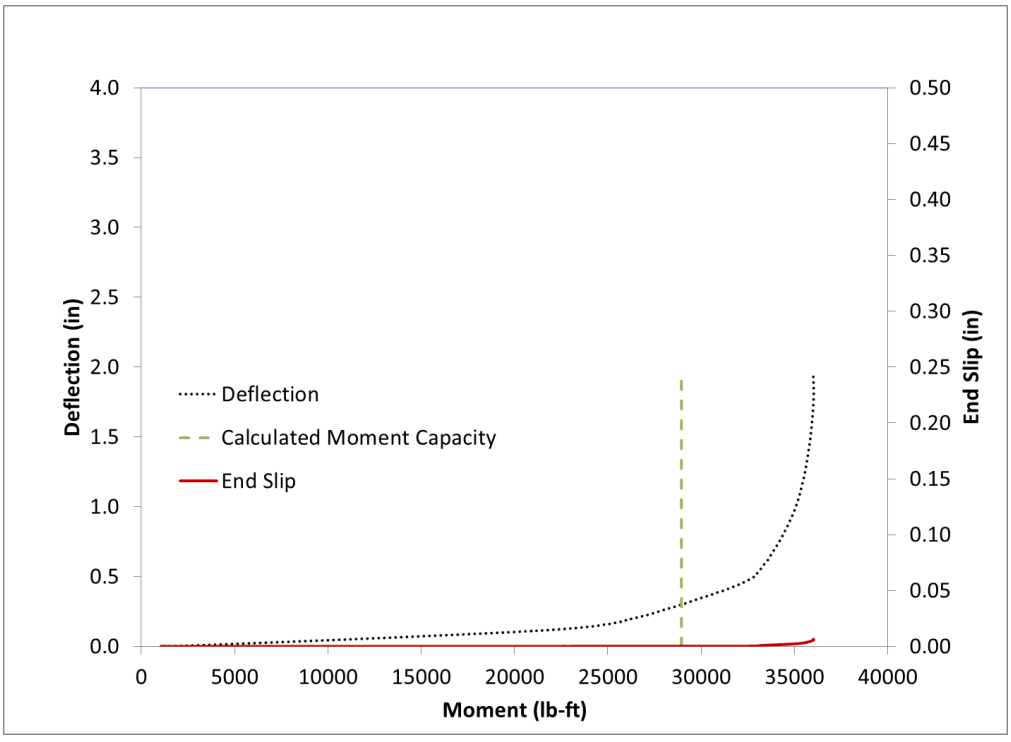

Figure H.67 Beam End G3-L Flexural Test Results Summary Chart B

Figure H.68 Beam End G3-L Failure

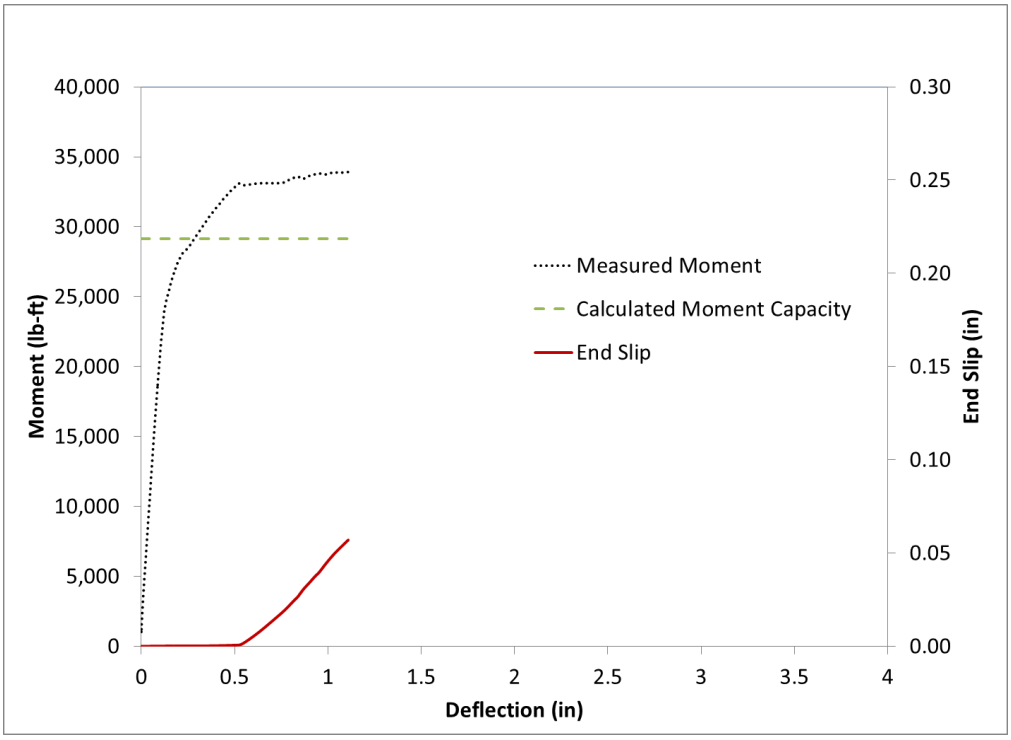

Figure H.69 Beam End G4-L Flexural Test Results Summary Chart A

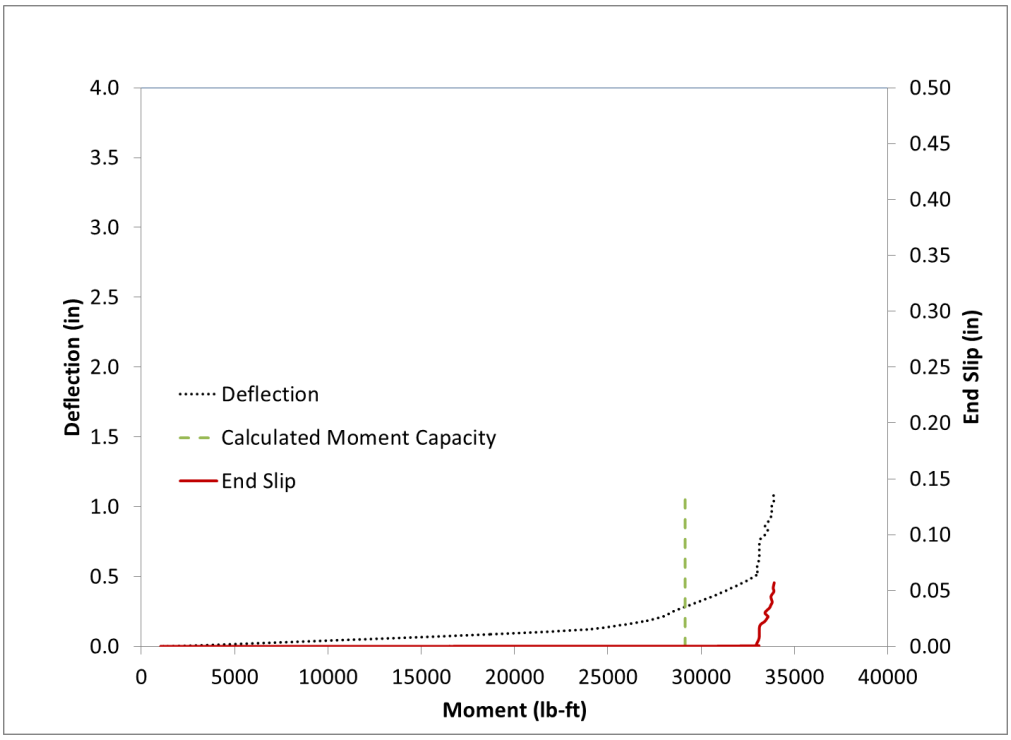

Figure H.70 Beam End G4-L Flexural Test Results Summary Chart B

Figure H.71 Beam End G4-L Failure

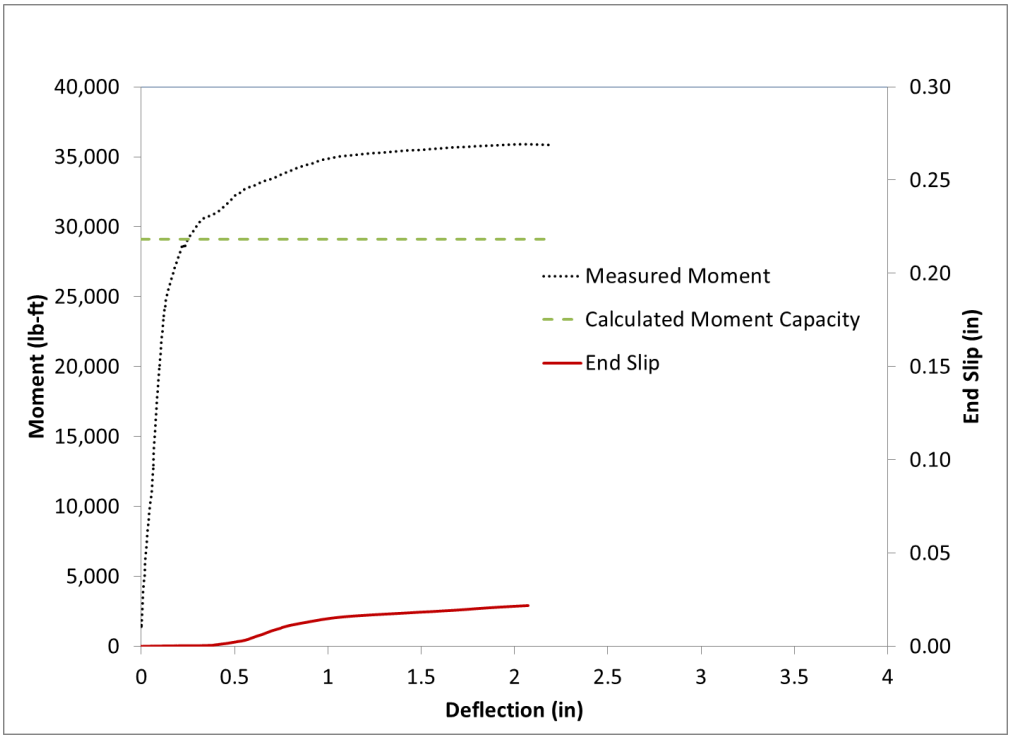

Figure H.72 Beam End G5-L Flexural Test Results Summary Chart A

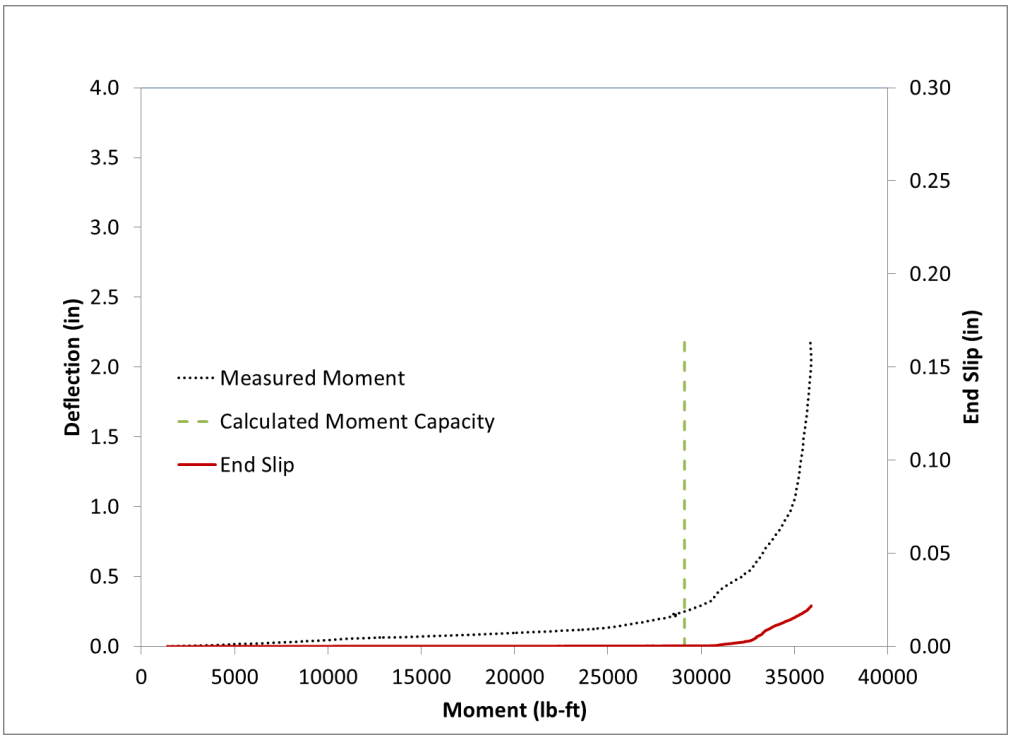

Figure H.73 Beam End G5-L Flexural Test Results Summary Chart B

Figure H.74 Beam End G5-L Failure

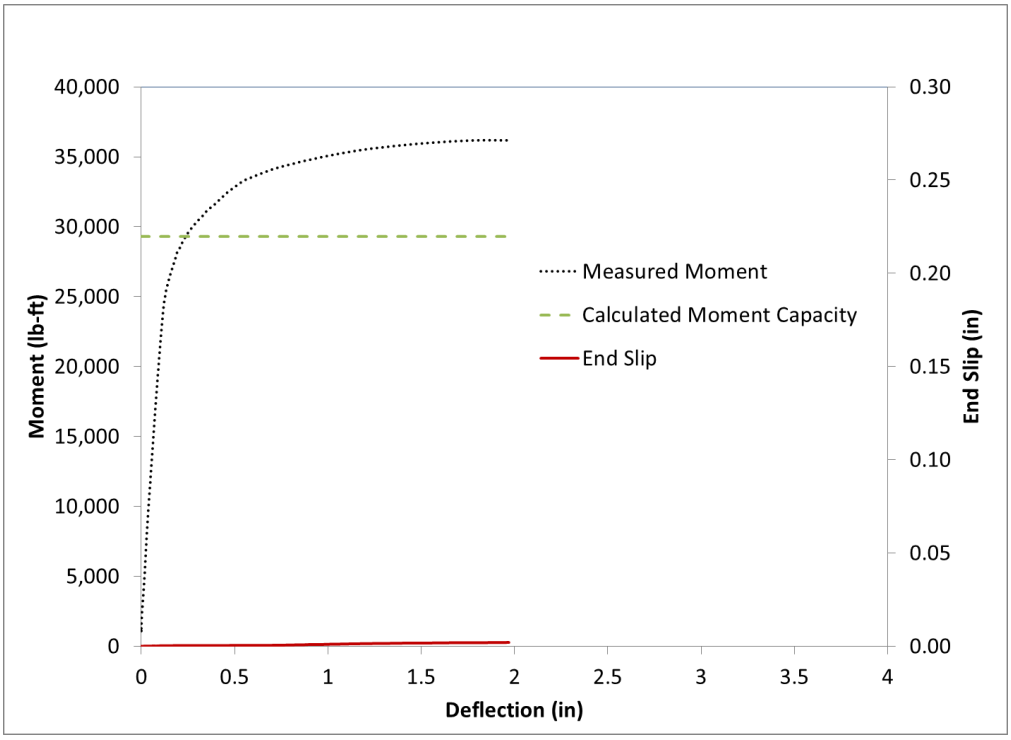

Figure H.75 Beam End G6-L Flexural Test Results Summary Chart A

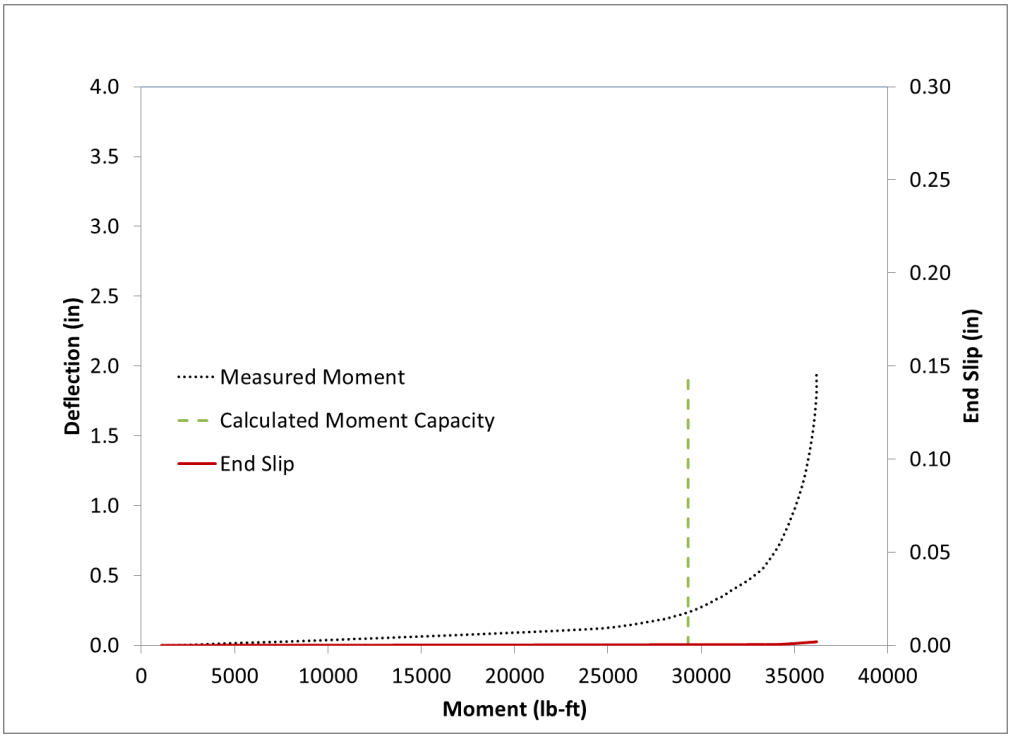

Figure H.76 Beam End G6-L Flexural Test Results Summary Chart B

Figure H.77 Beam End G6-L Failure

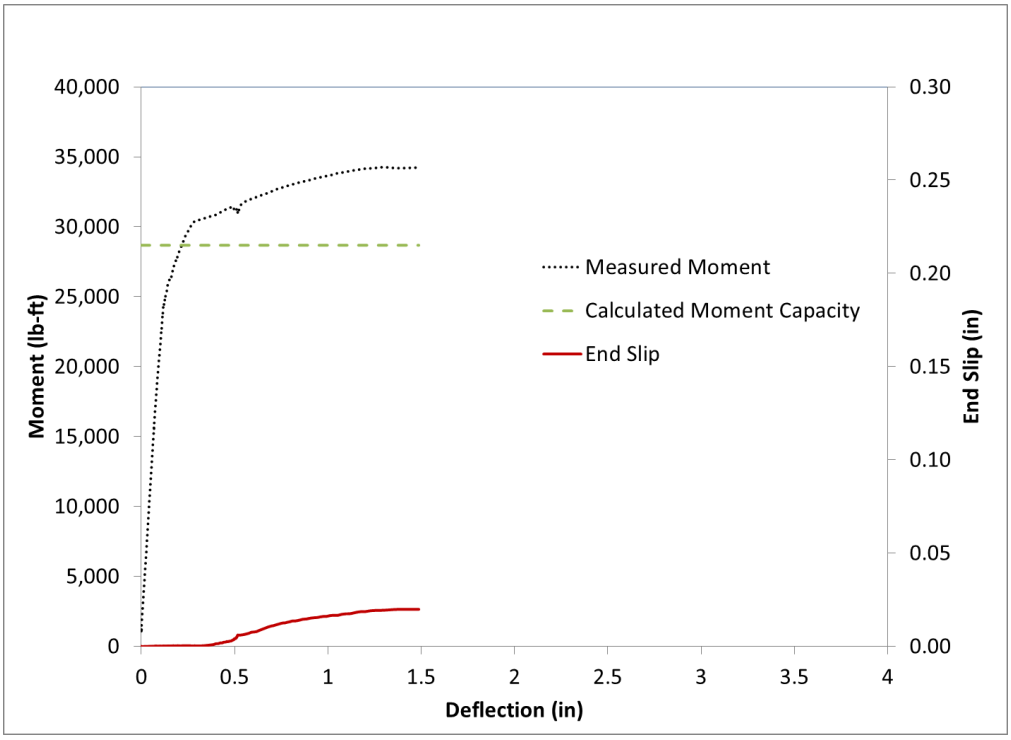

Figure H.78 Beam End G7-L Flexural Test Results Summary Chart A

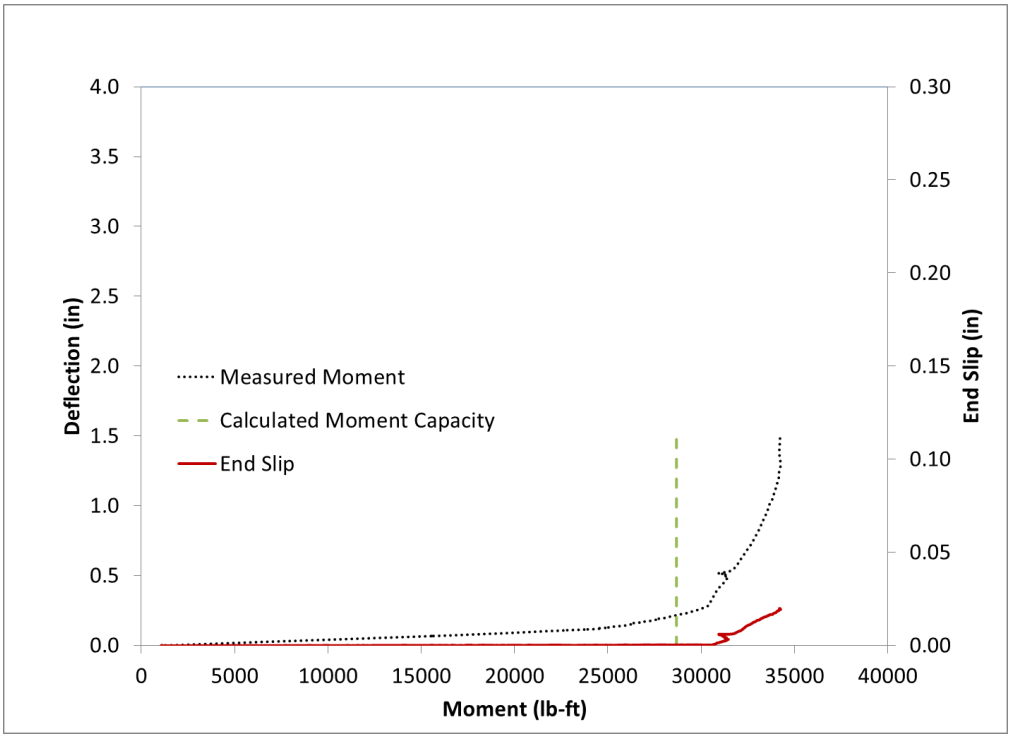

Figure H.79 Beam End G7-L Flexural Test Results Summary Chart B

Figure H.80 Beam End G7-L Failure

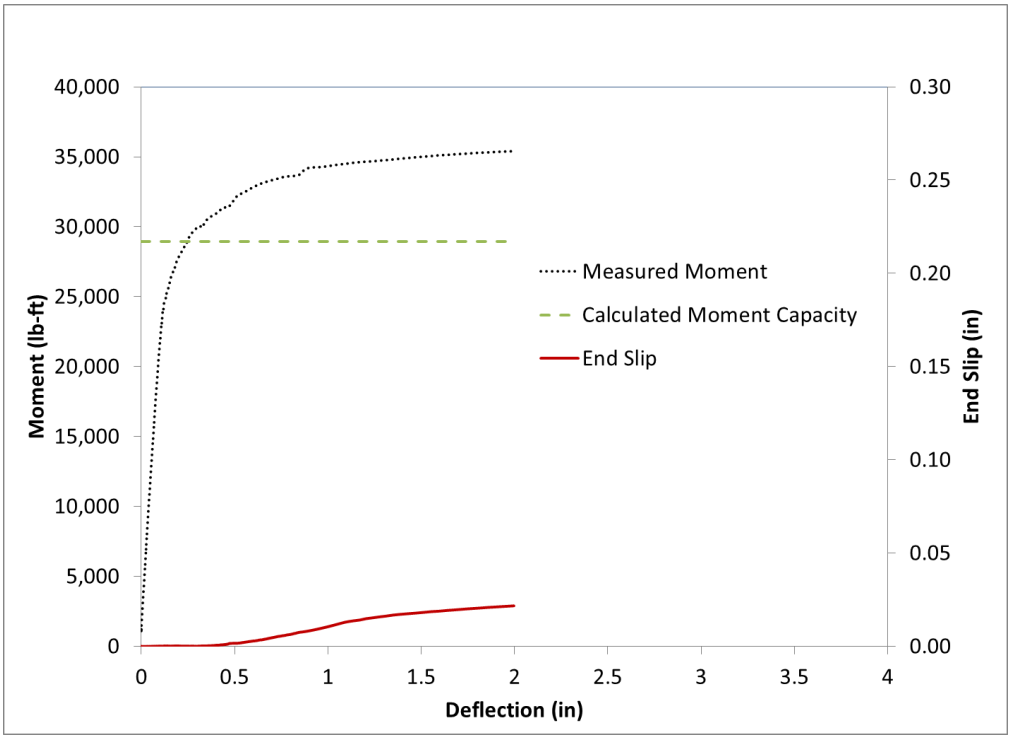

Figure H.81 Beam End G8-L Flexural Test Results Summary Chart A

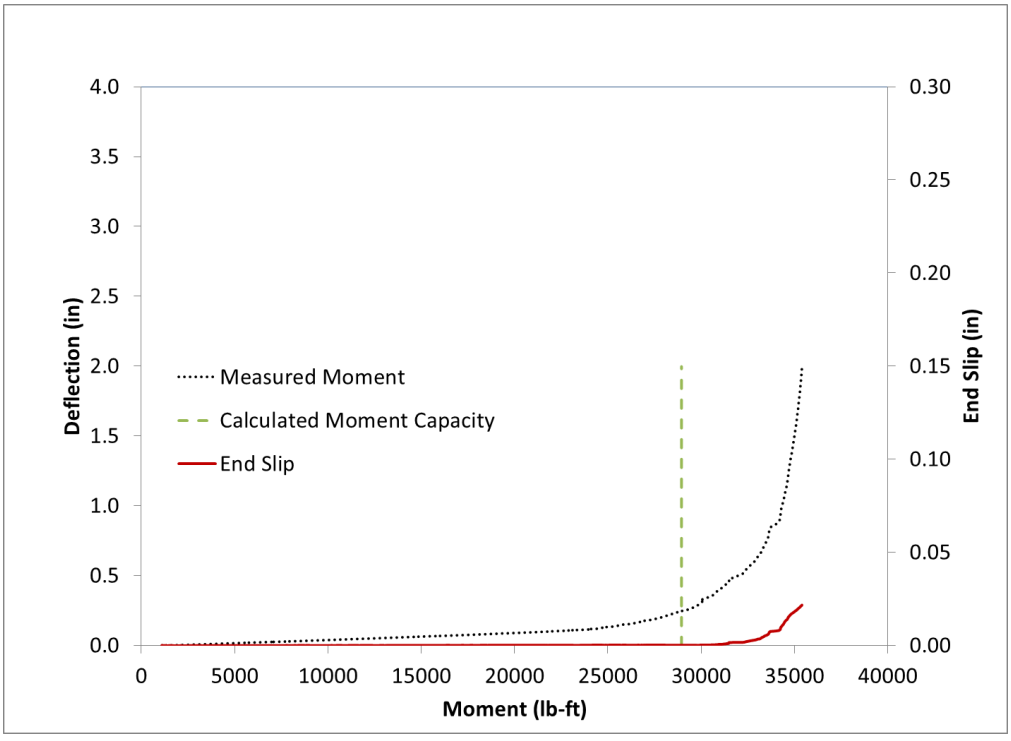

Figure H.82 Beam End G8-L Flexural Test Results Summary Chart B

Figure H.83 Beam End G8-L Failure

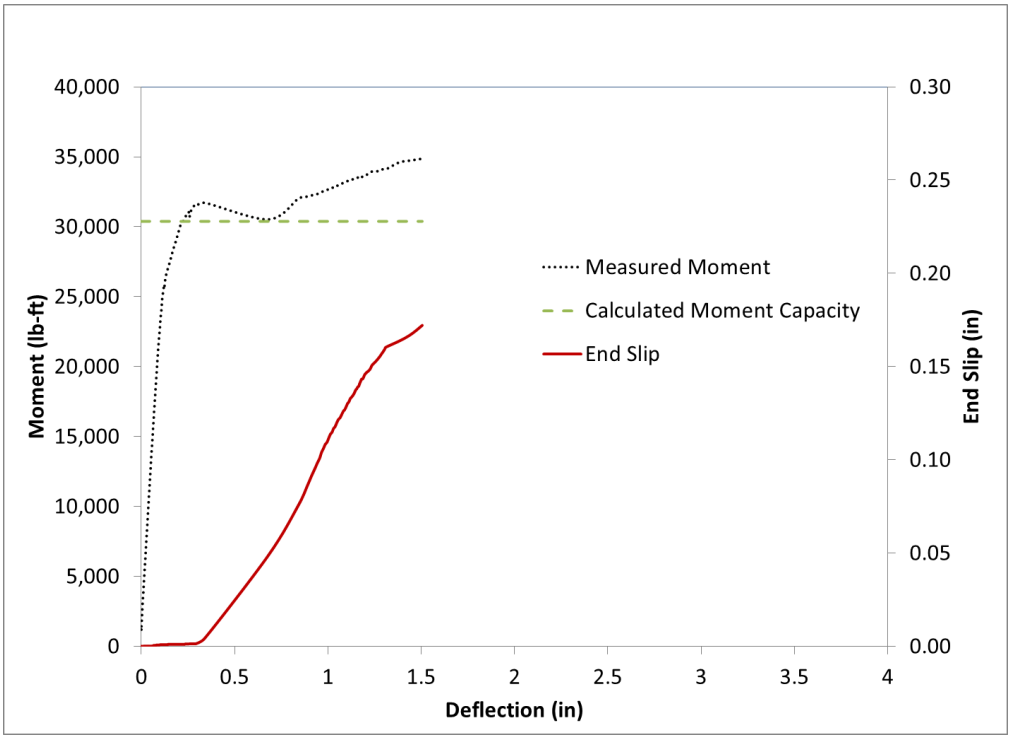

Figure H.84 Beam End G9-L Flexural Test Results Summary Chart A

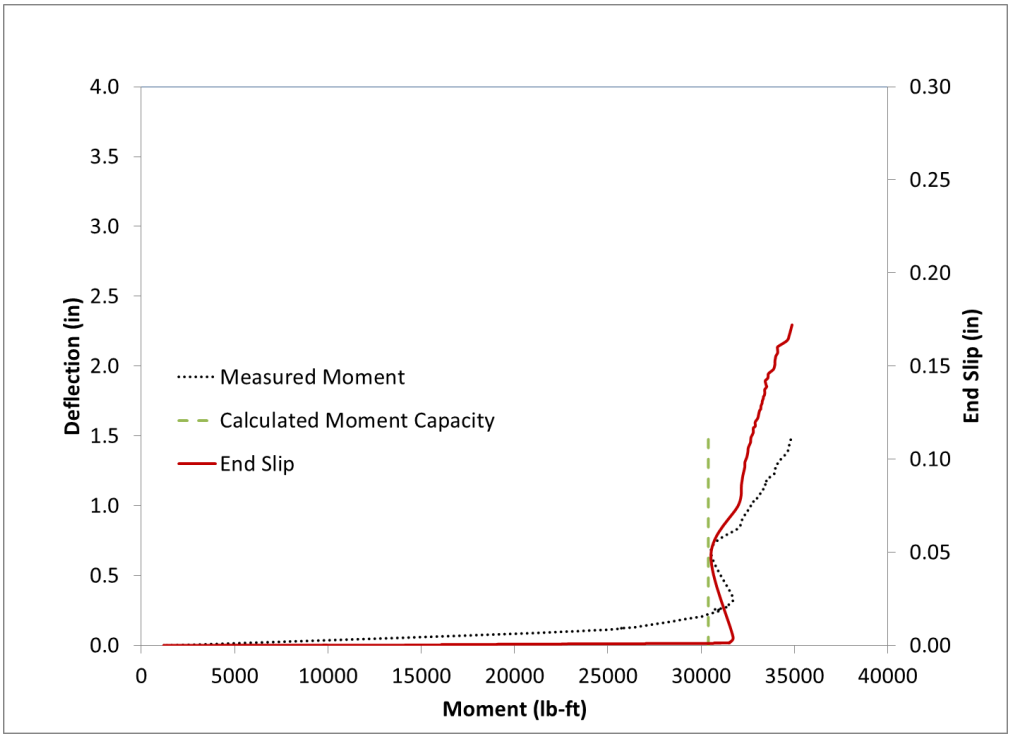

Figure H.85 Beam End G9-L Flexural Test Results Summary Chart B

Figure H.86 Beam End G9-L Failure

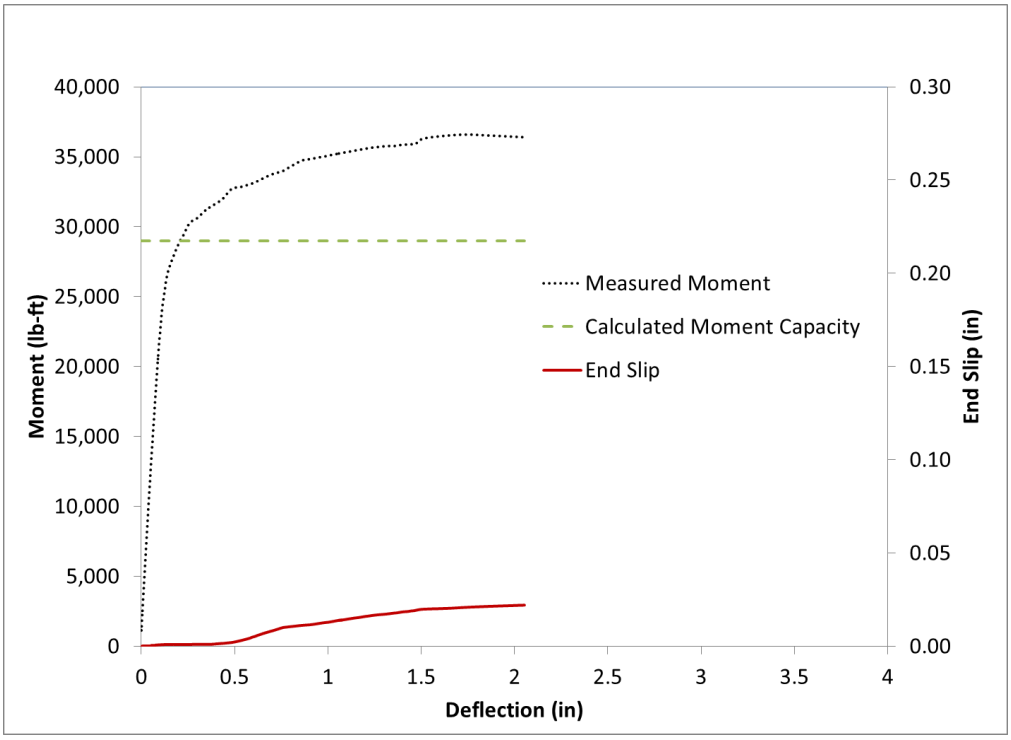

Figure H.87 Beam End G10-L Flexural Test Results Summary Chart A

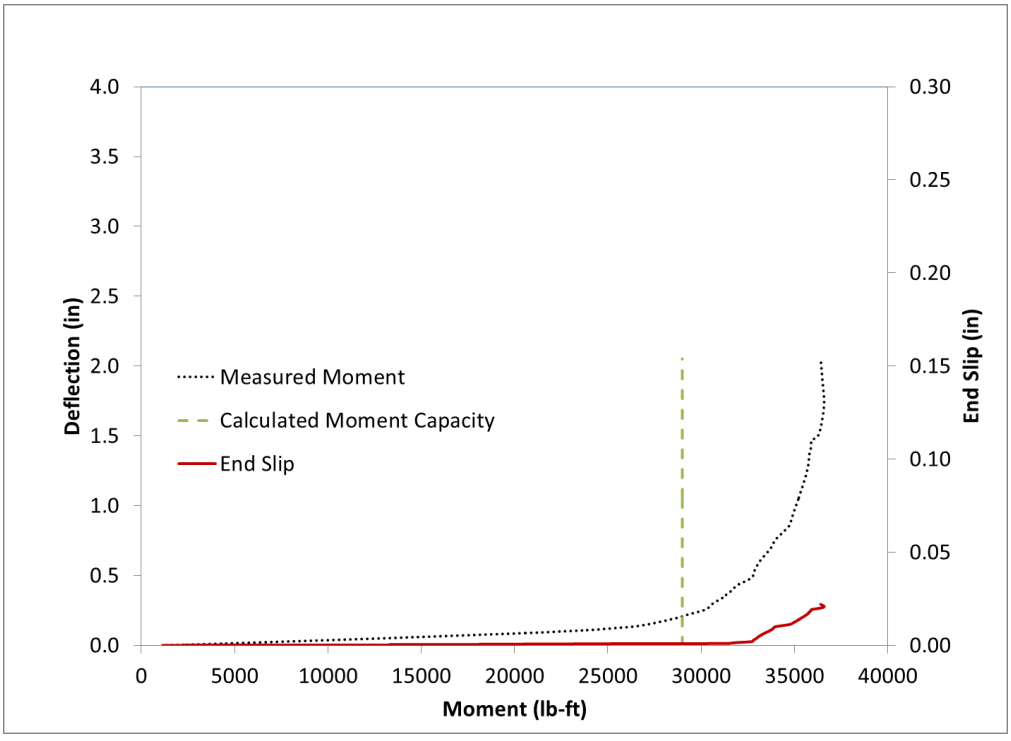

Figure H.88 Beam End G10-L Flexural Test Results Summary Chart B

Figure H.89 Beam End G10-L Failure

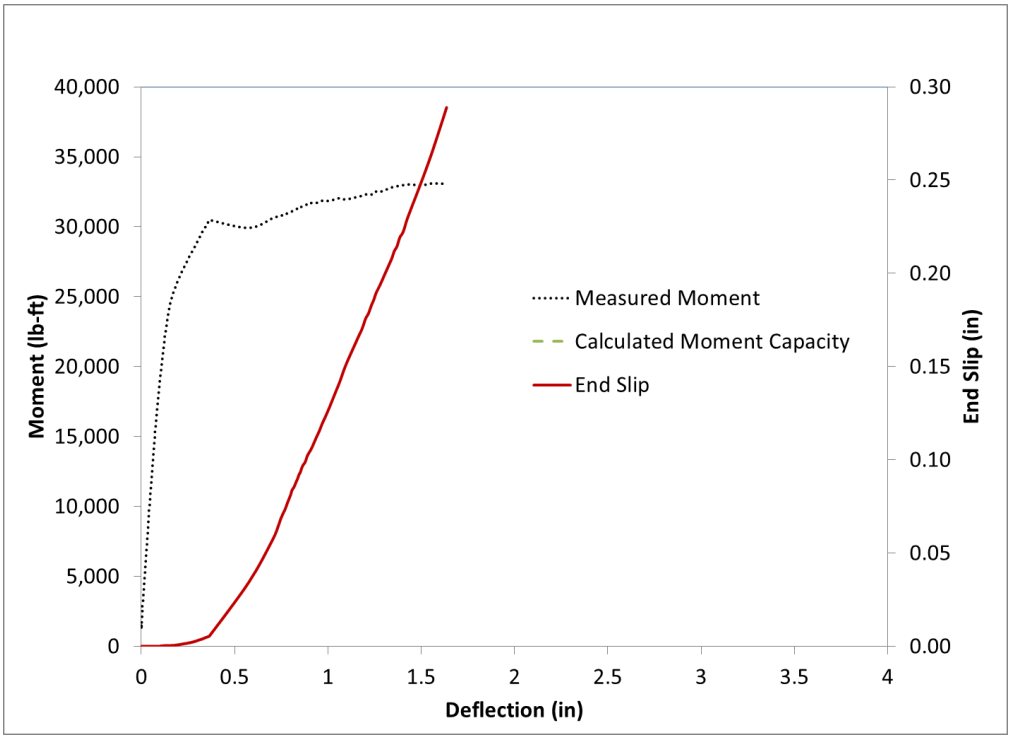

Figure H.90 Beam End G1-S Flexural Test Results Summary Chart A

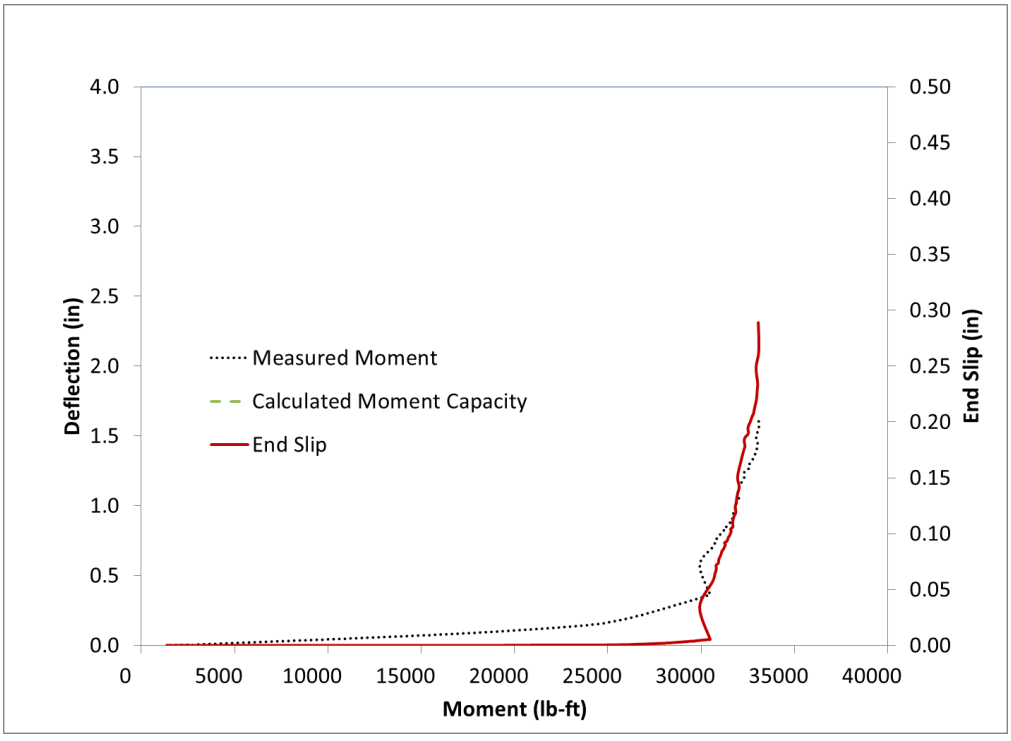

Figure H.91 Beam End G1-S Flexural Test Results Summary Chart B

Figure H.92 Beam End G1-S Failure

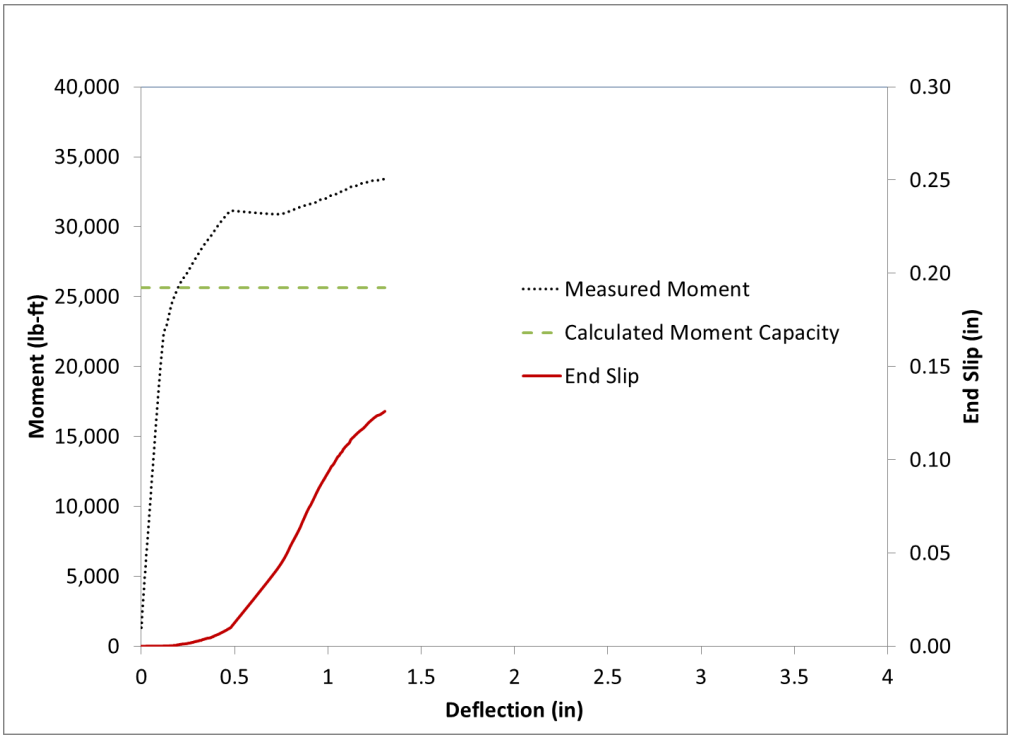

Figure H.93 Beam End G2-S Flexural Test Results Summary Chart A

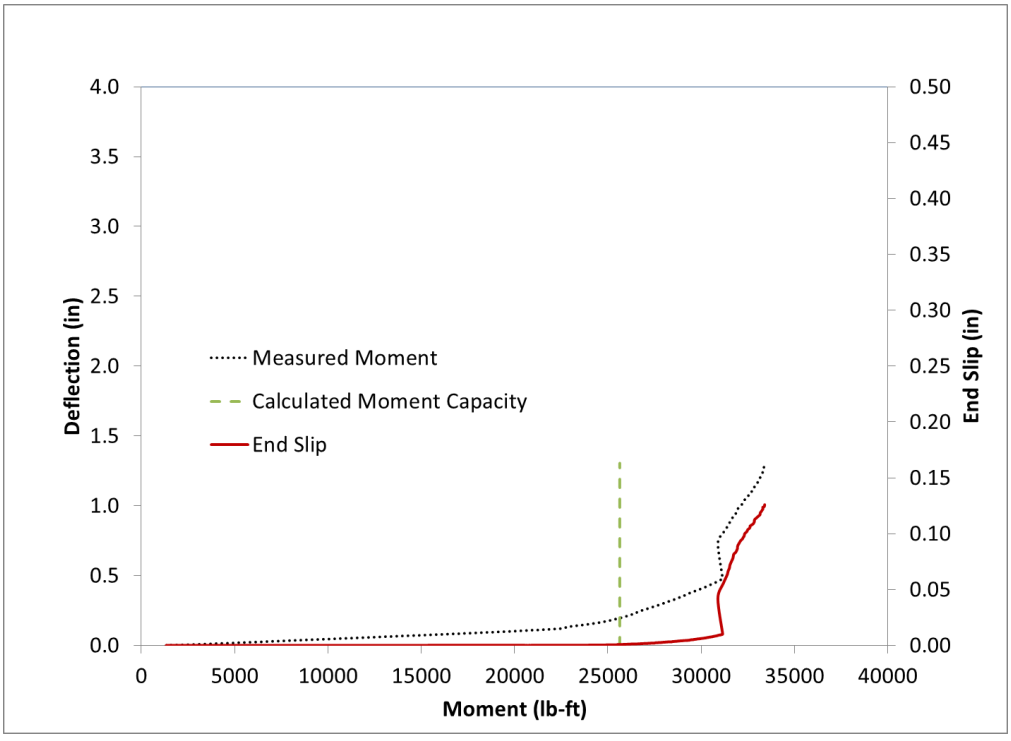

Figure H.94 Beam End G2-S Flexural Test Results Summary Chart B

Figure H.95 Beam End G2-S Failure

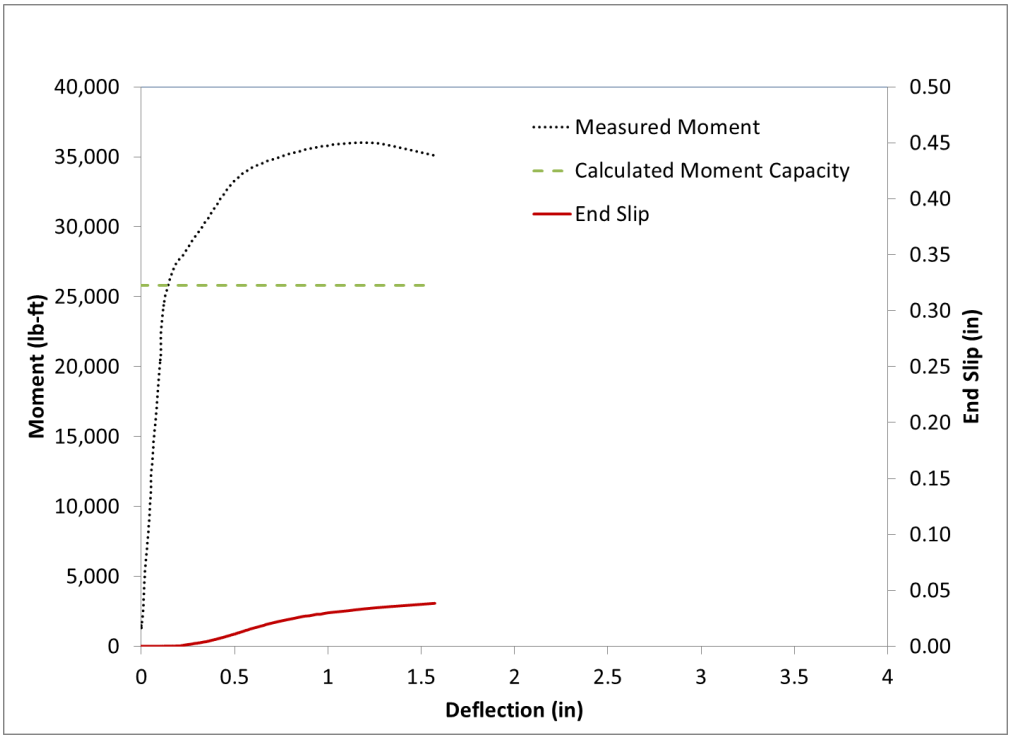

Figure H.96 Beam End G3-S Flexural Test Results Summary Chart A

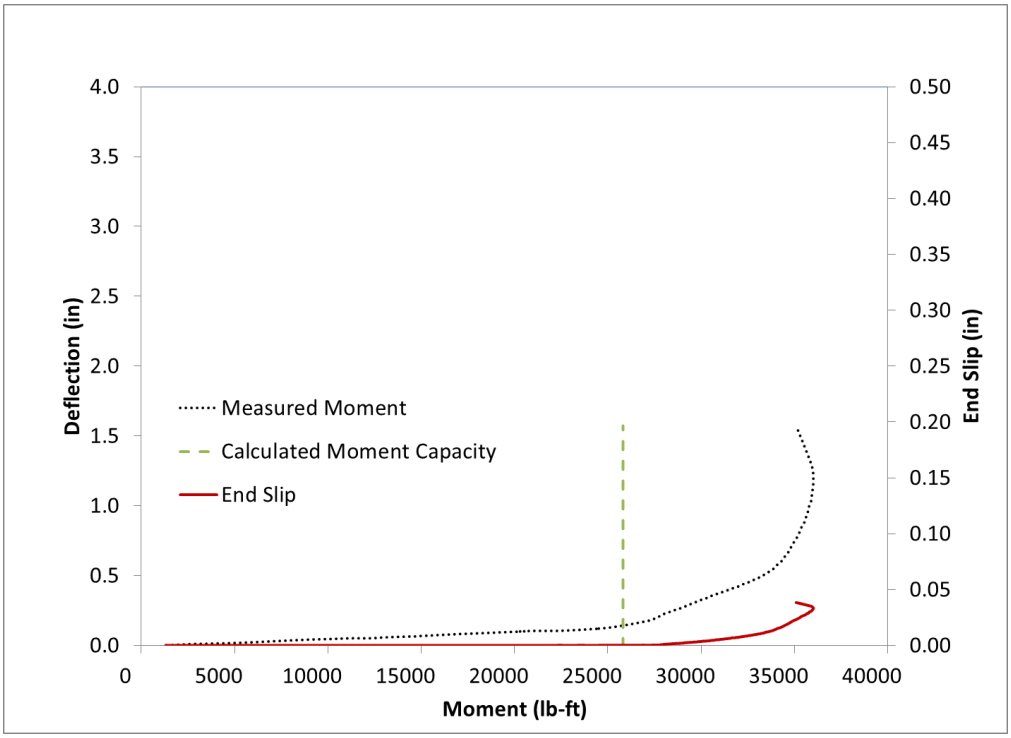

Figure H.97 Beam End G3-S Flexural Test Results Summary Chart B

Figure H.98 Beam End G3-S Failure

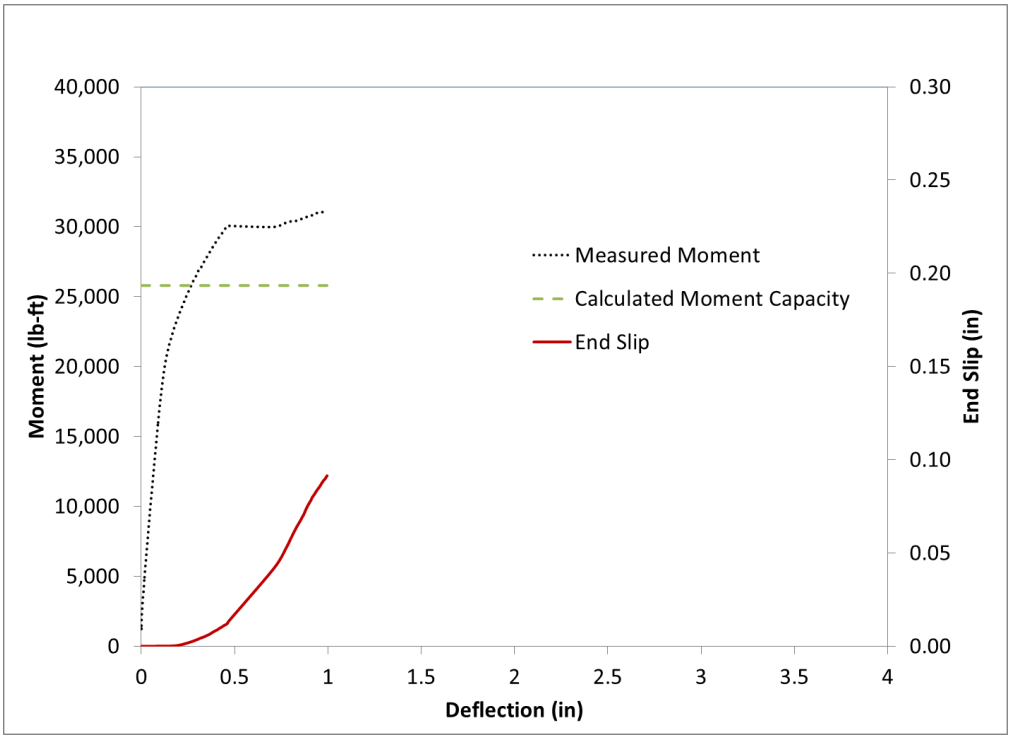

Figure H.99 Beam End G4-S Flexural Test Results Summary Chart A

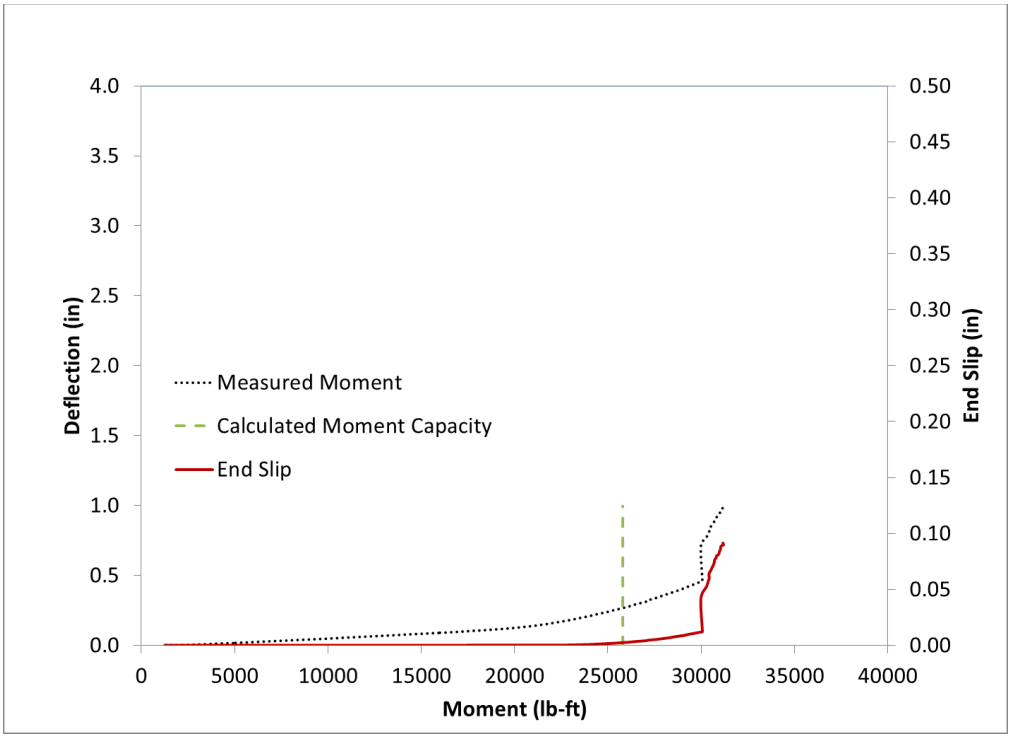

Figure H.100 Beam End G4-S Flexural Test Results Summary Chart B

Figure H.101 Beam End G4-S Failure

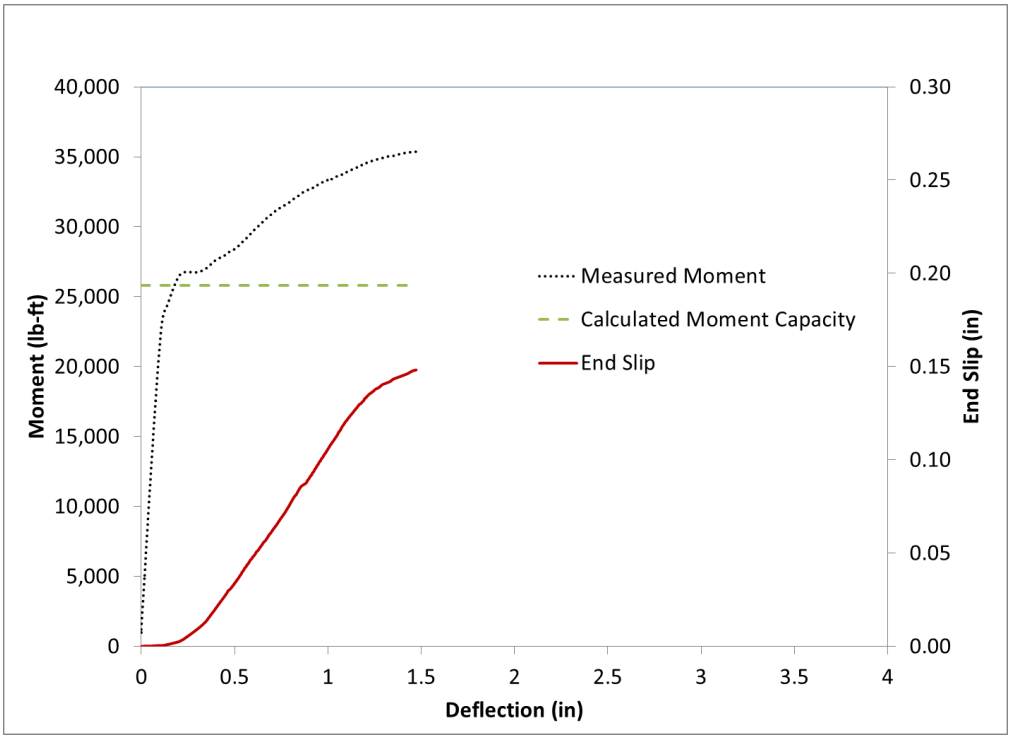

Figure H.102 Beam End G5-S Flexural Test Results Summary Chart A

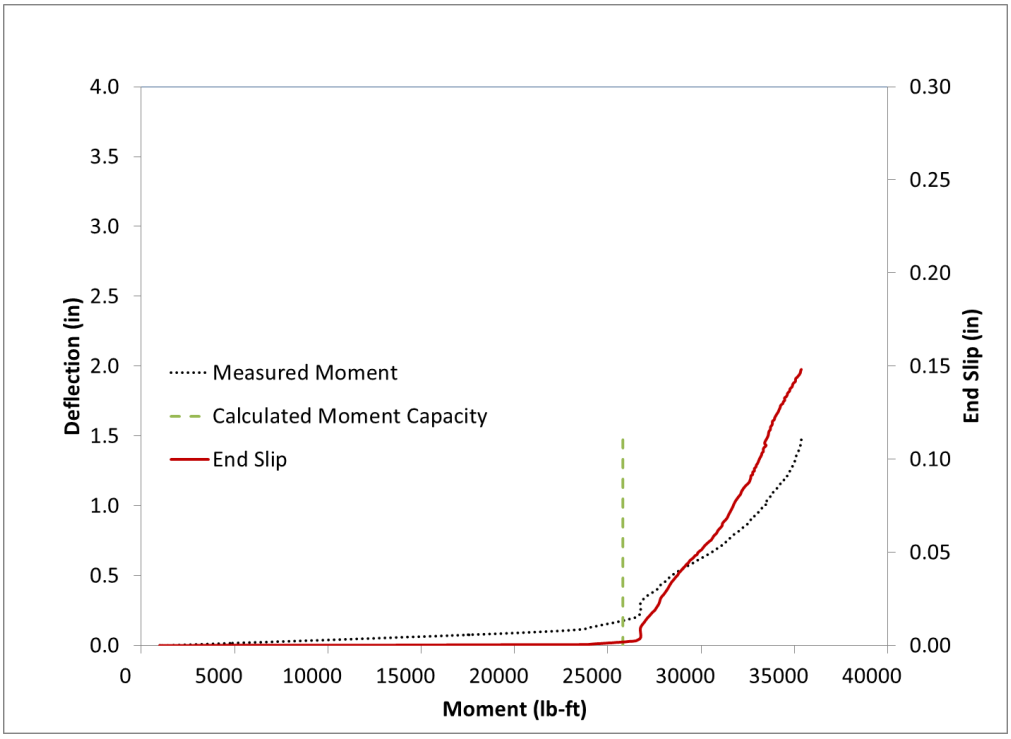

Figure H.103 Beam End G5-S Flexural Test Results Summary Chart B

Figure H.104 Beam End G5-S Failure

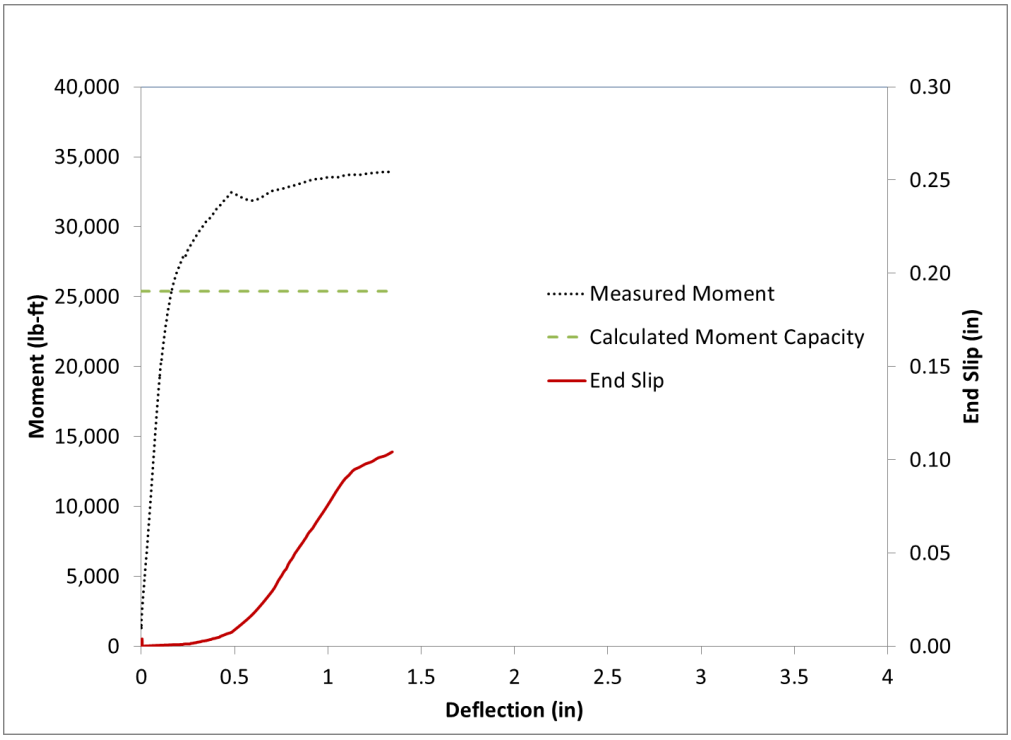

Figure H.105 Beam End G6-S Flexural Test Results Summary Chart A

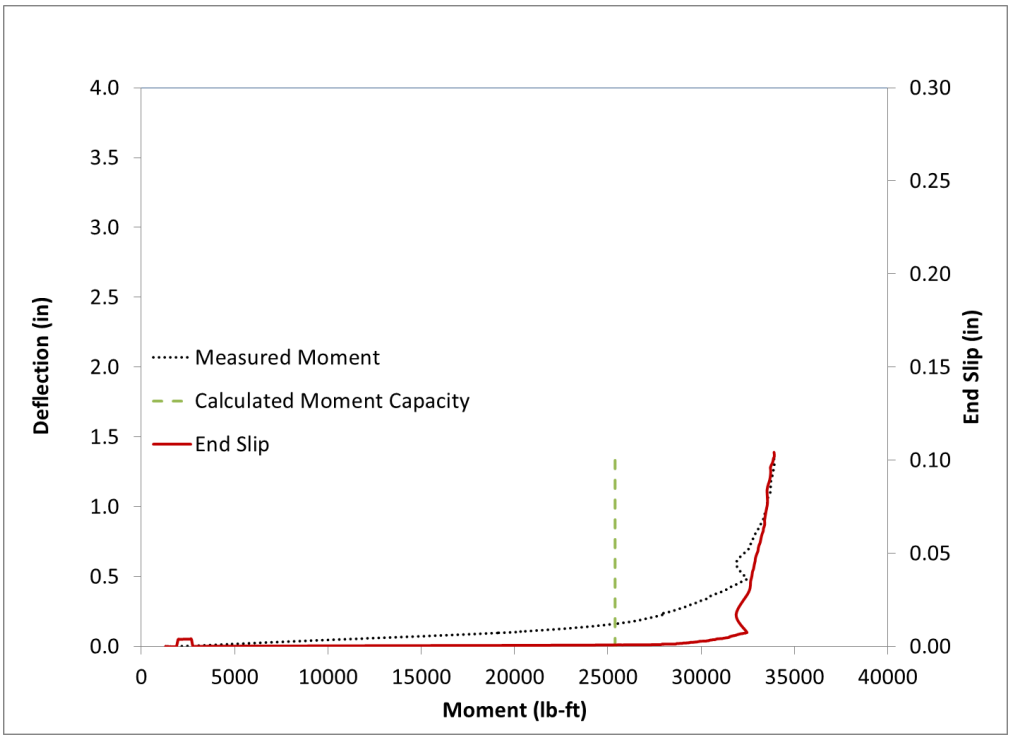

Figure H.106 Beam End G6-S Flexural Test Results Summary Chart B

Figure H.107 Beam End G6-S Failure

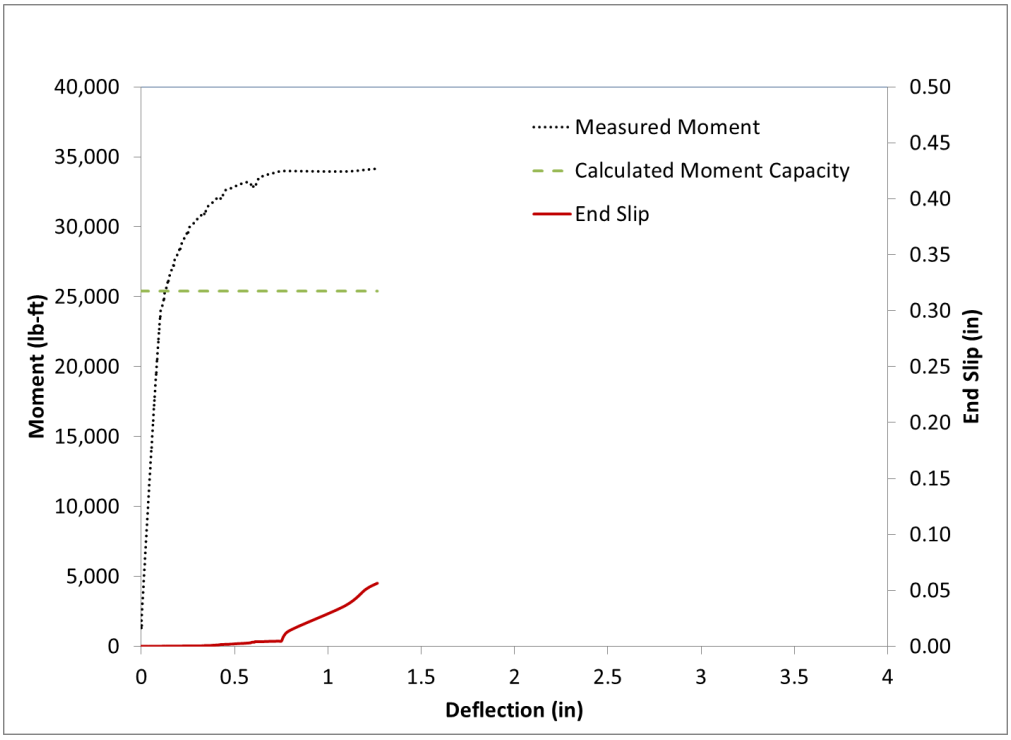

Figure H.108 Beam End G7-S Flexural Test Results Summary Chart A

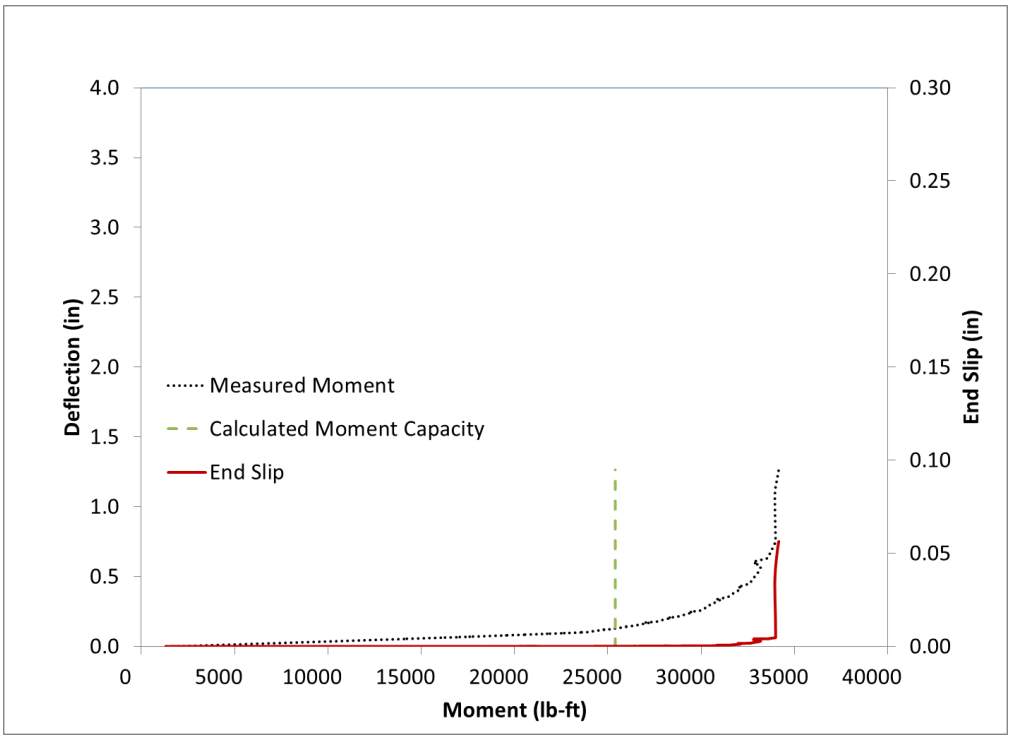

Figure H.109 Beam End G7-S Flexural Test Results Summary Chart B

Figure H.110 Beam End G7-S Failure

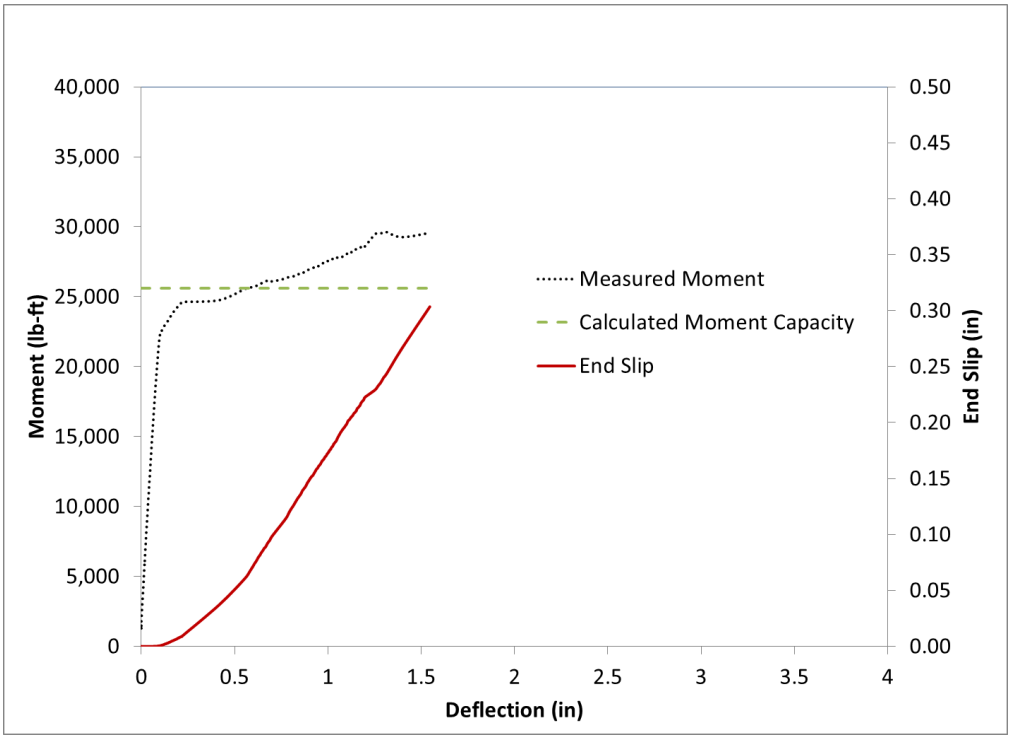

Figure H.111 Beam End G8-S Flexural Test Results Summary Chart A

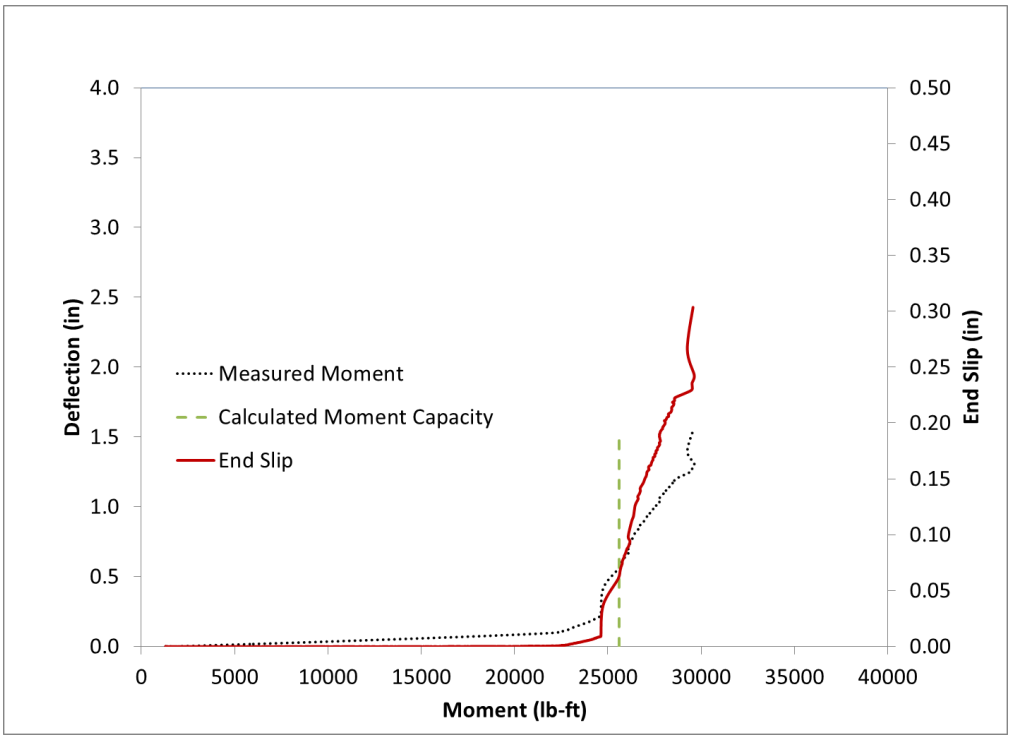

Figure H.112 Beam End G8-S Flexural Test Results Summary Chart B

Figure H.113 Beam End G8-S Failure

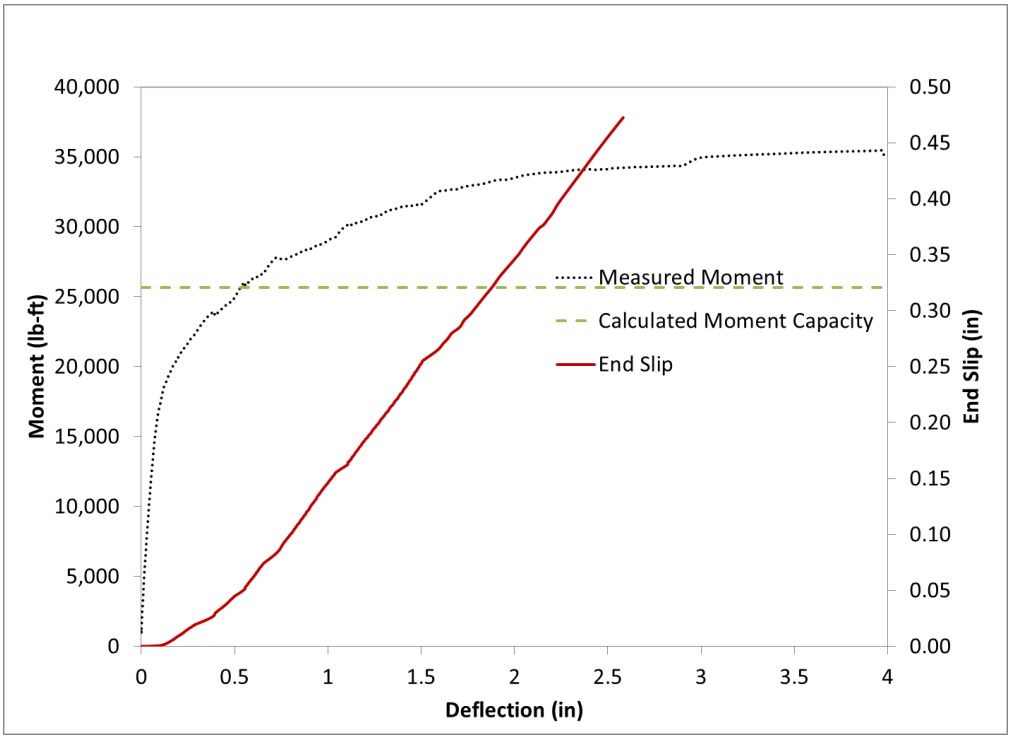

Figure H.114 Beam End G9-S Flexural Test Results Summary Chart A

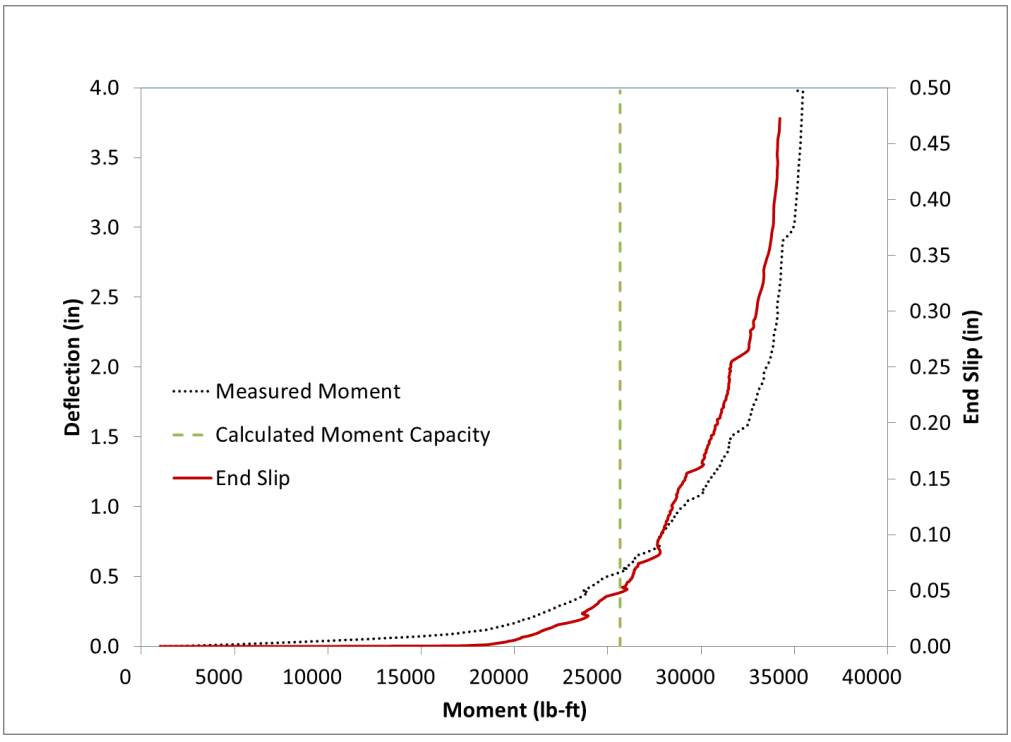

Figure H.115 Beam End G9-S Flexural Test Results Summary Chart B

Figure H.116 Beam End G9-S Failure

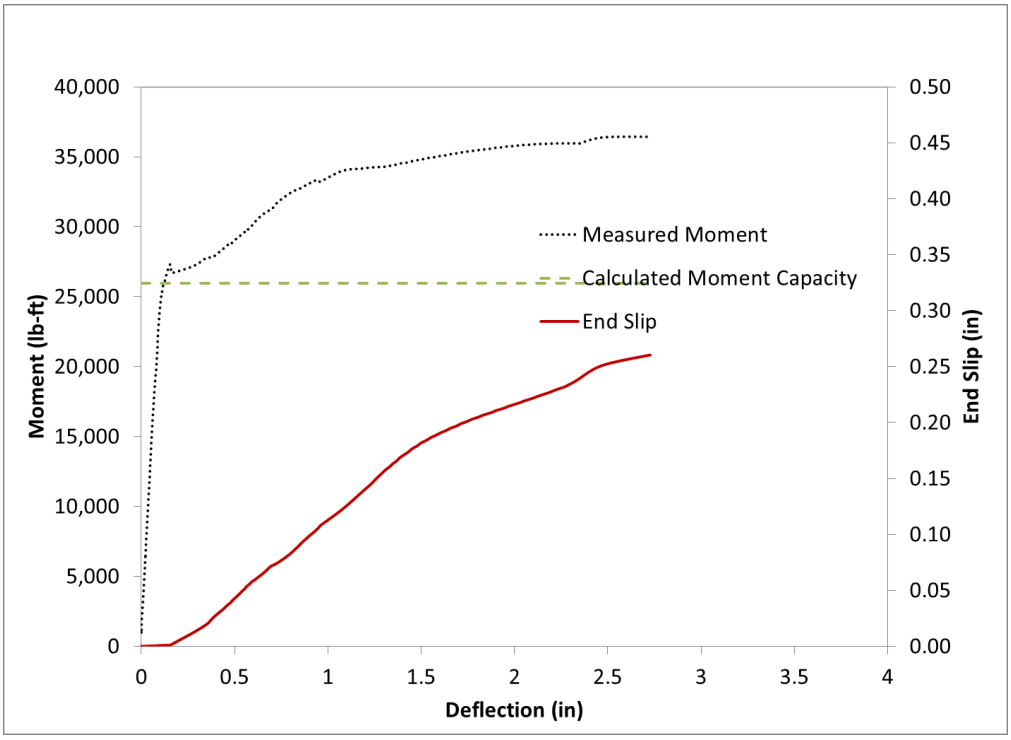

Figure H.117 Beam End G10-S Flexural Test Results Summary Chart A

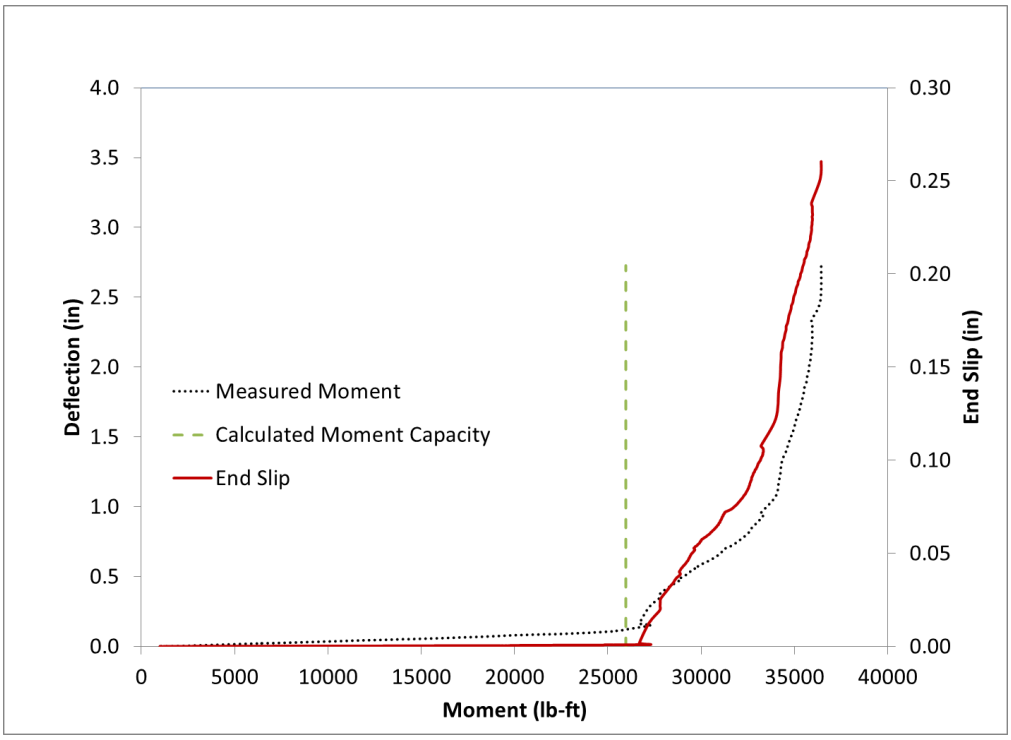

Figure H.118 Beam End G10-S Flexural Test Results Summary Chart B

Figure H.119 Beam End G10-S Failure

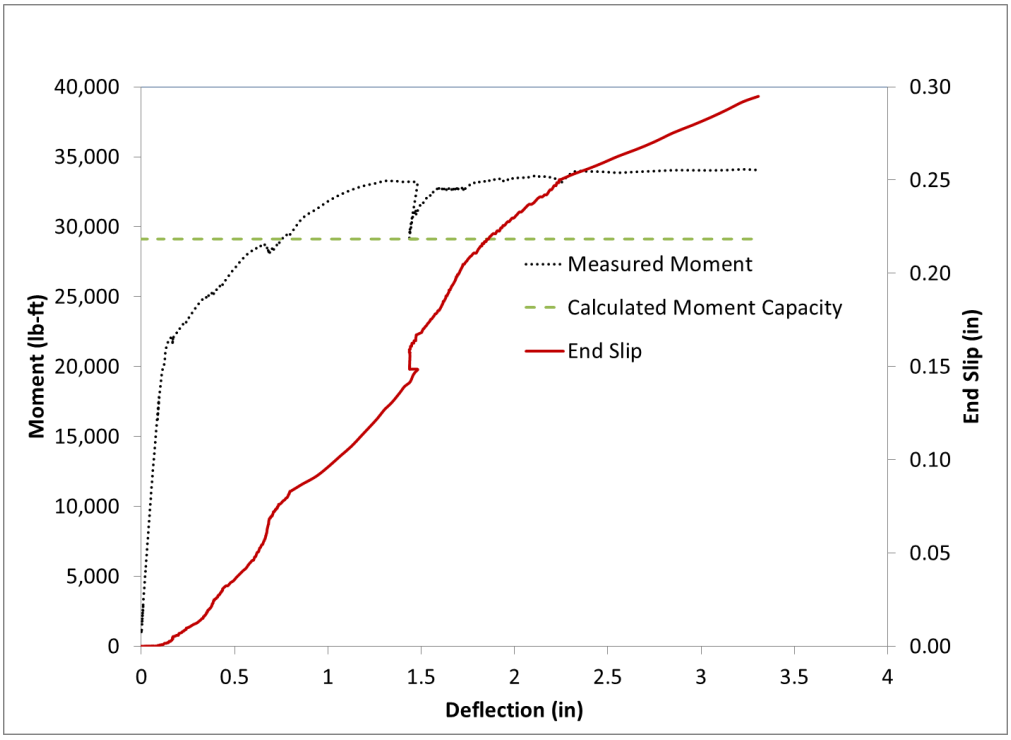

Figure H.120 Beam End I1-L Flexural Test Results Summary Chart A

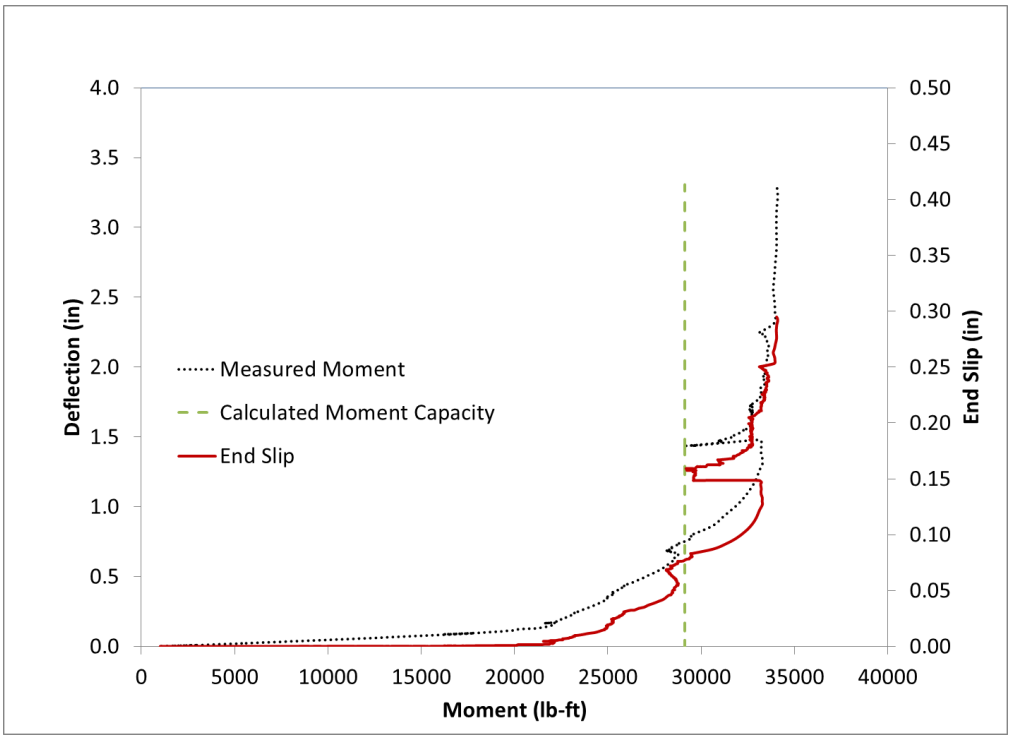

Figure H.121 Beam End I1-L Flexural Test Results Summary Chart B

Figure H.122 Beam End I1-L Failure

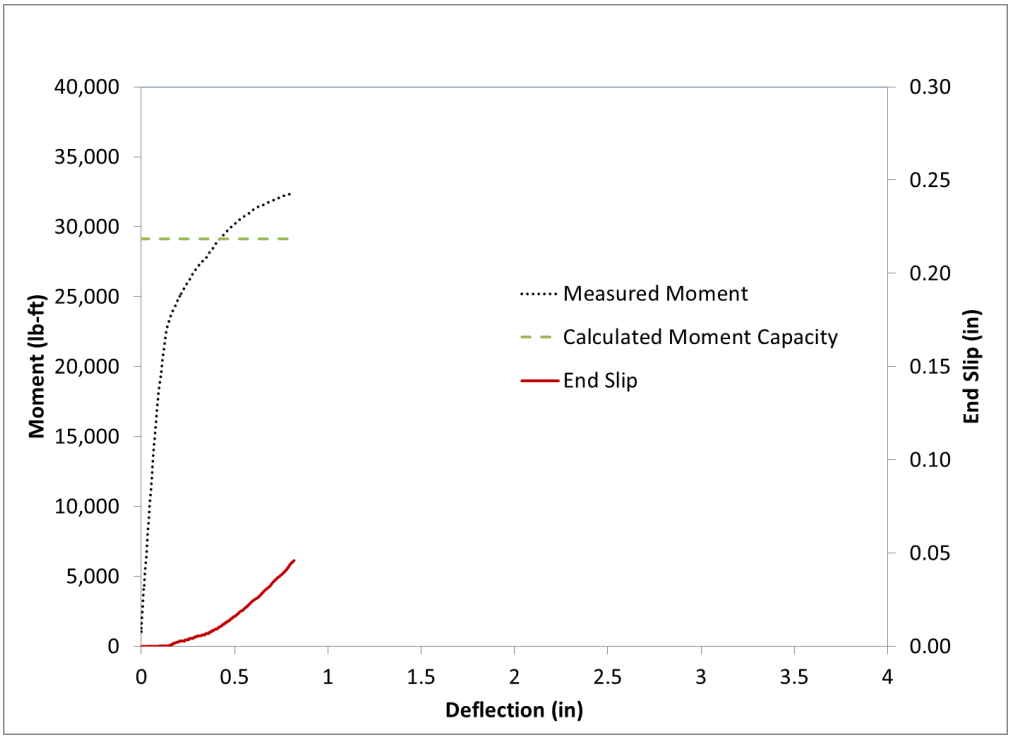

Figure H.123 Beam End I2-L Flexural Test Results Summary Chart A

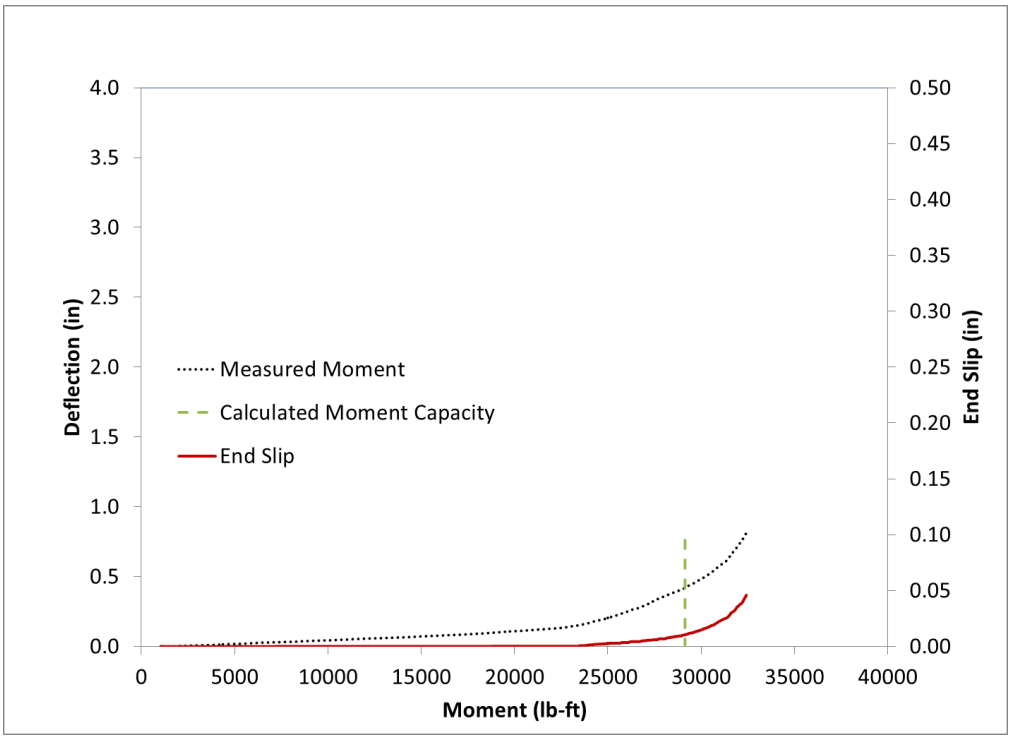

Figure H.124 Beam End I2-L Flexural Test Results Summary Chart B

Figure H.125 Beam End I2-L Failure

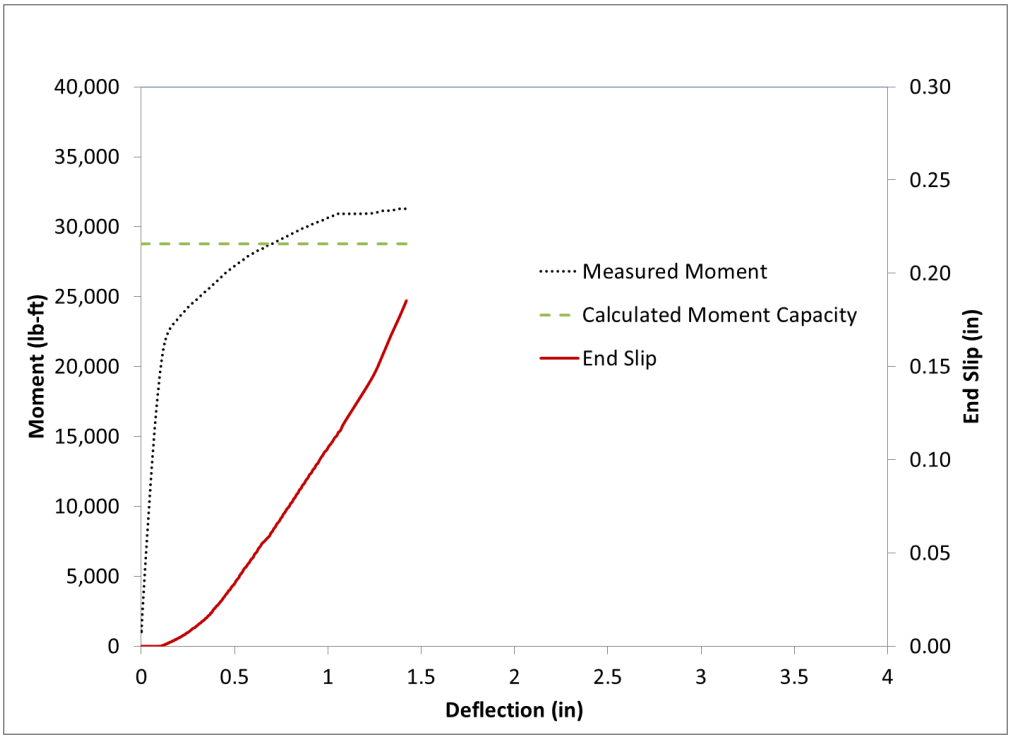

Figure H.126 Beam End I3-L Flexural Test Results Summary Chart A

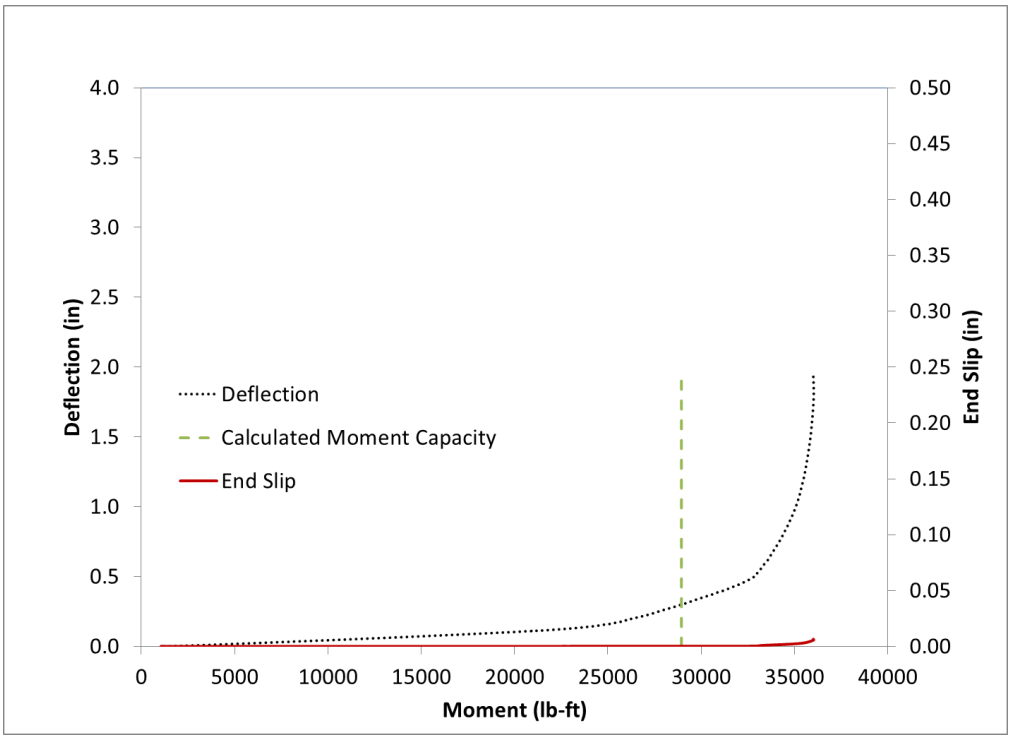

Figure H.127 Beam End I3-L Flexural Test Results Summary Chart B

Figure H.128 Beam End I3-L Failure

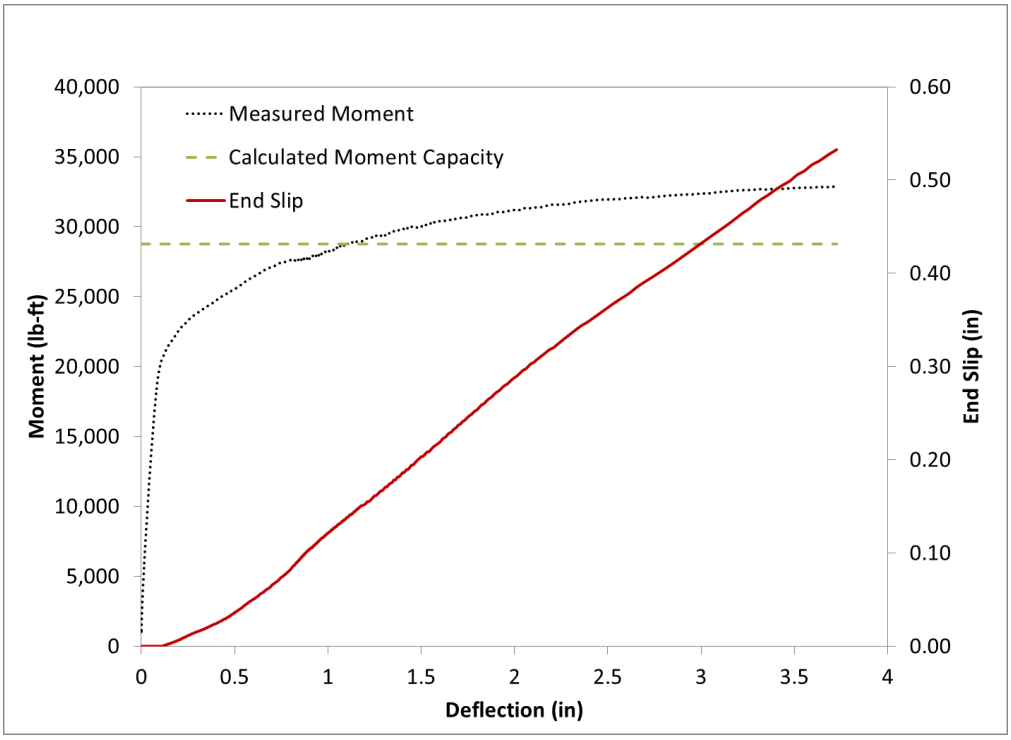

Figure H.129 Beam End I4-L Flexural Test Results Summary Chart A

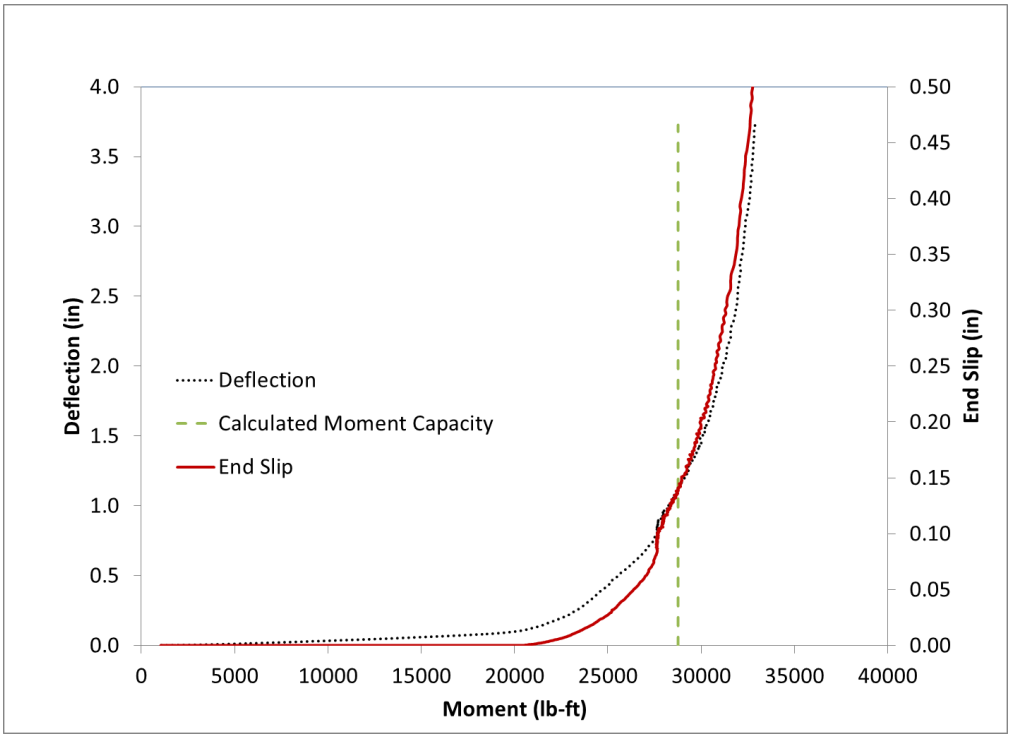

Figure H.130 Beam End I4-L Flexural Test Results Summary Chart B

Figure H.131 Beam End I4-L Failure

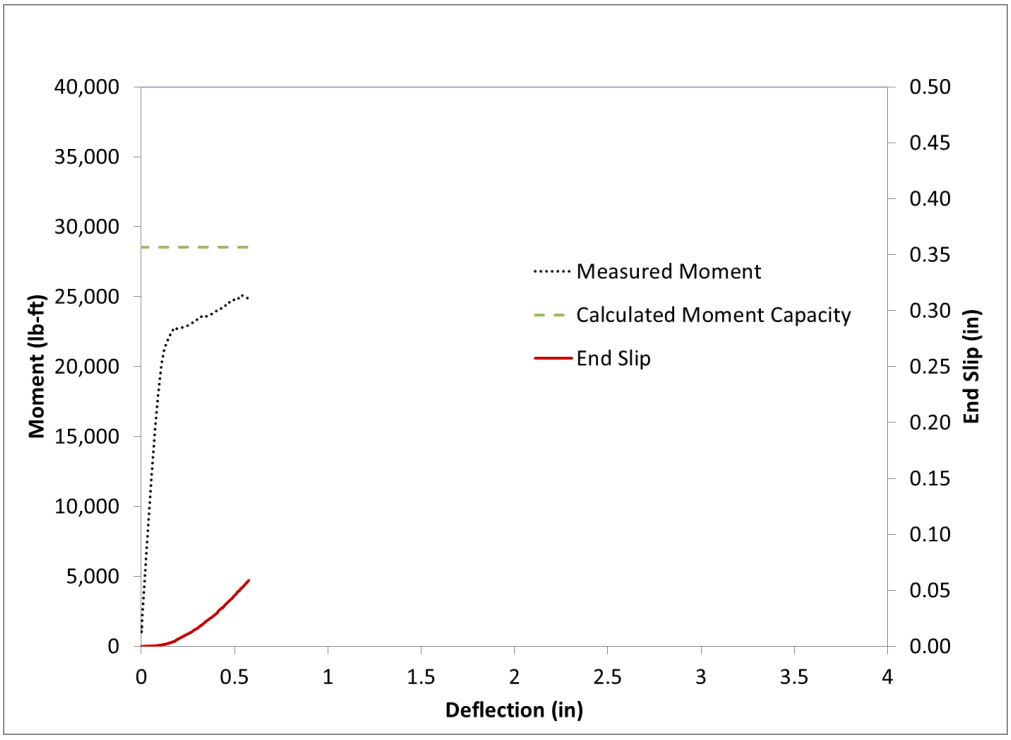

Figure H.132 Beam End I5-L Flexural Test Results Summary Chart A

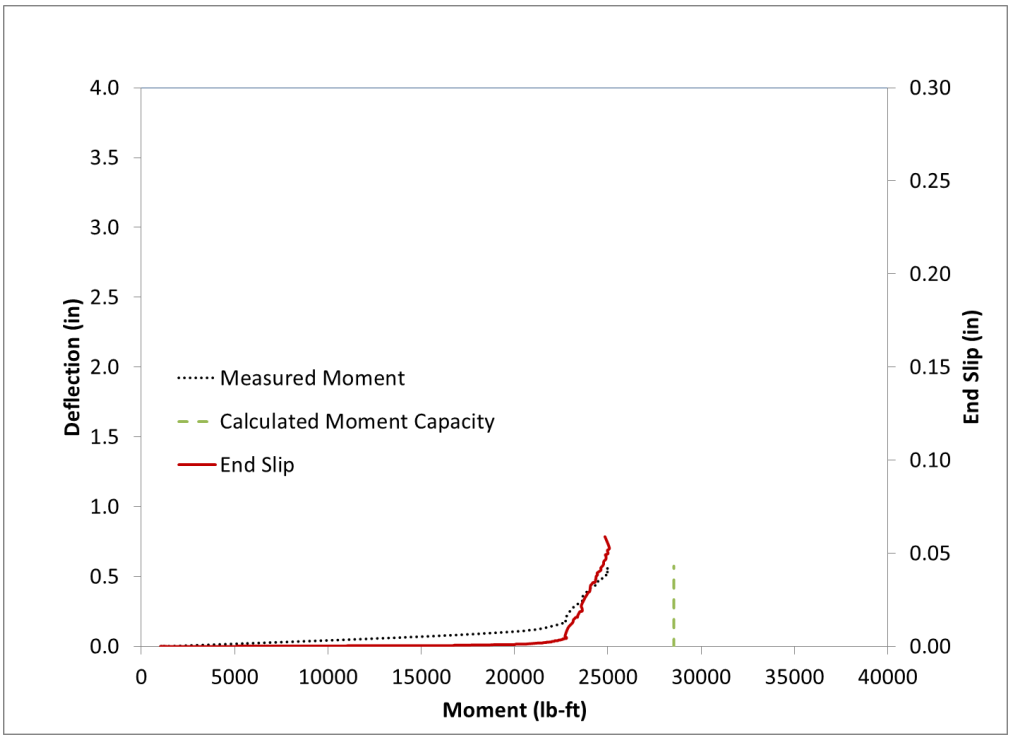

Figure H.133 Beam End I5-L Flexural Test Results Summary Chart B

Figure H.134 Beam End I5-L Failure

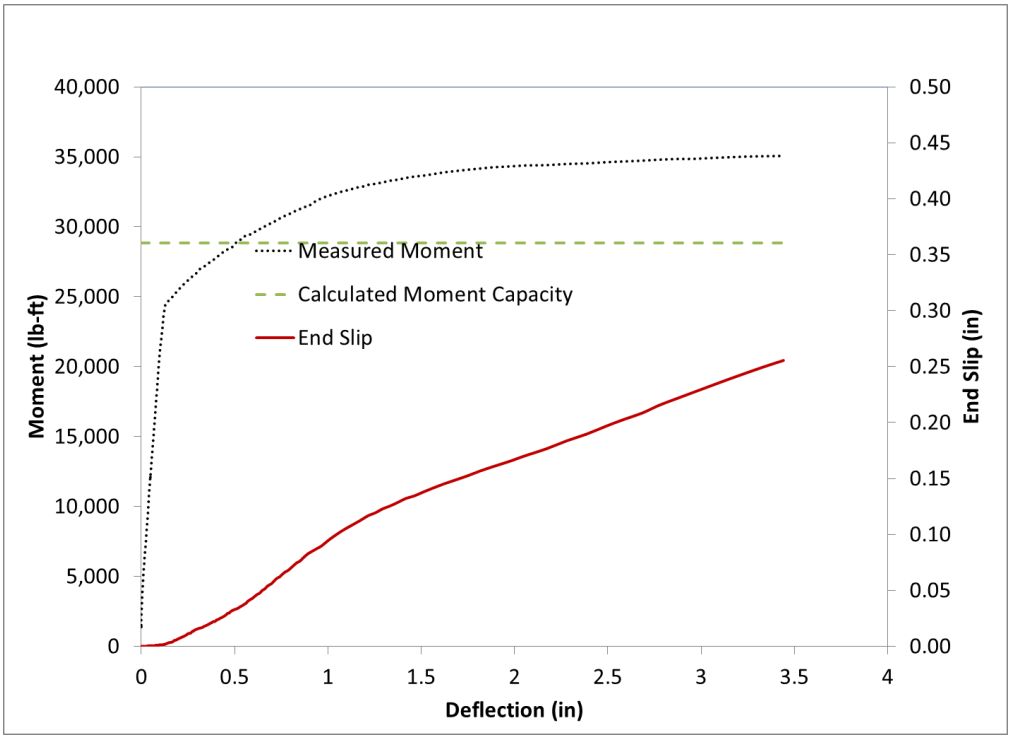

Figure H.135 Beam End I6-L Flexural Test Results Summary Chart A

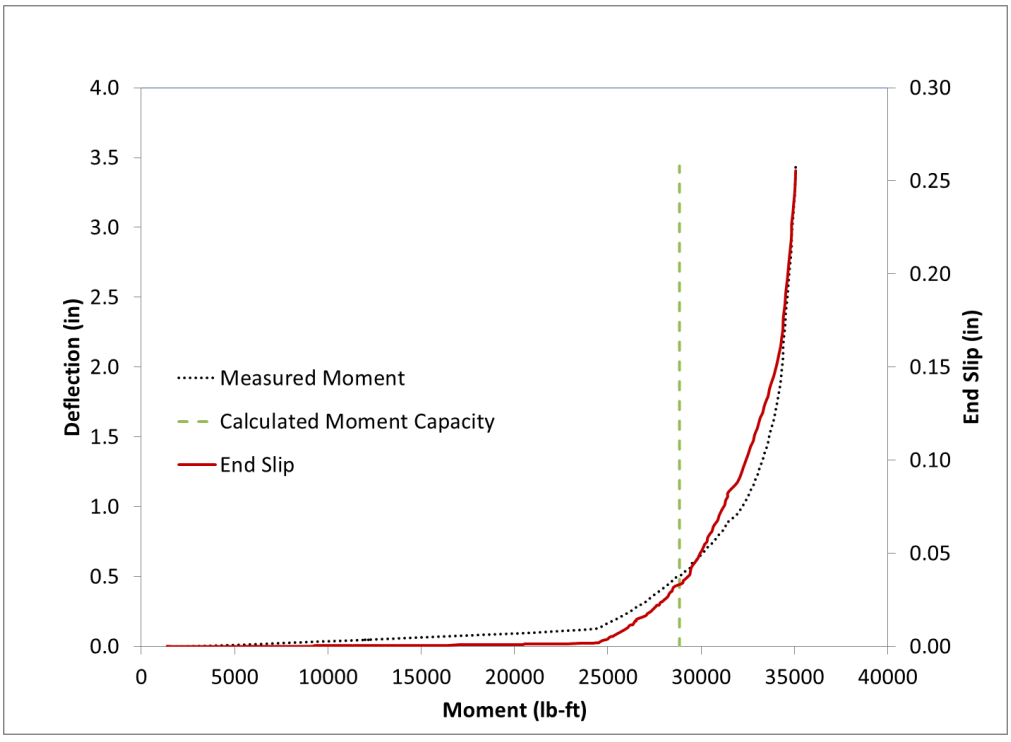

Figure H.136 Beam End I6-L Flexural Test Results Summary Chart B

Figure H.137 Beam End I6-L Failure

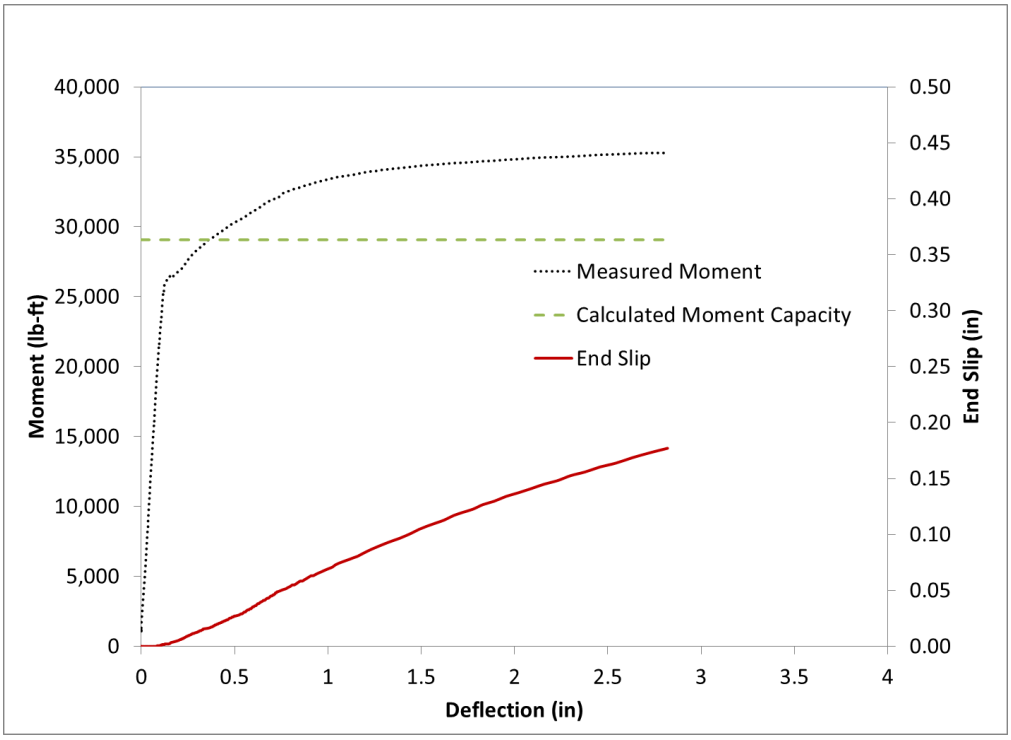

Figure H.138 Beam End I7-L Flexural Test Results Summary Chart A

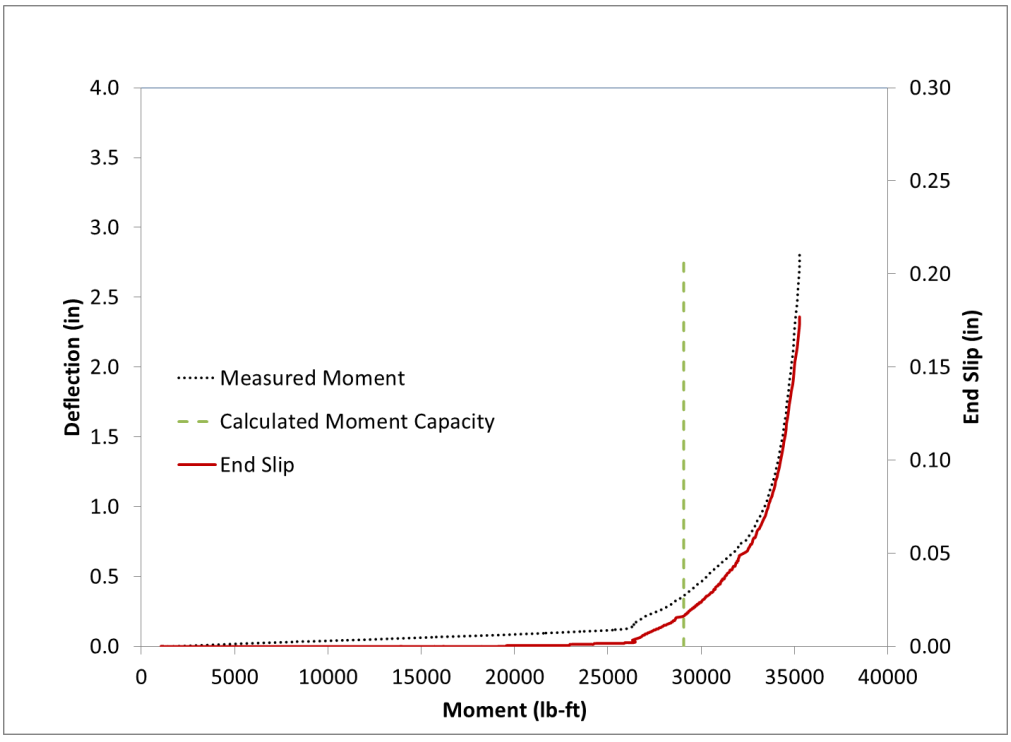

Figure H.139 Beam End I7-L Flexural Test Results Summary Chart B

Figure H.140 Beam End I7-L Failure

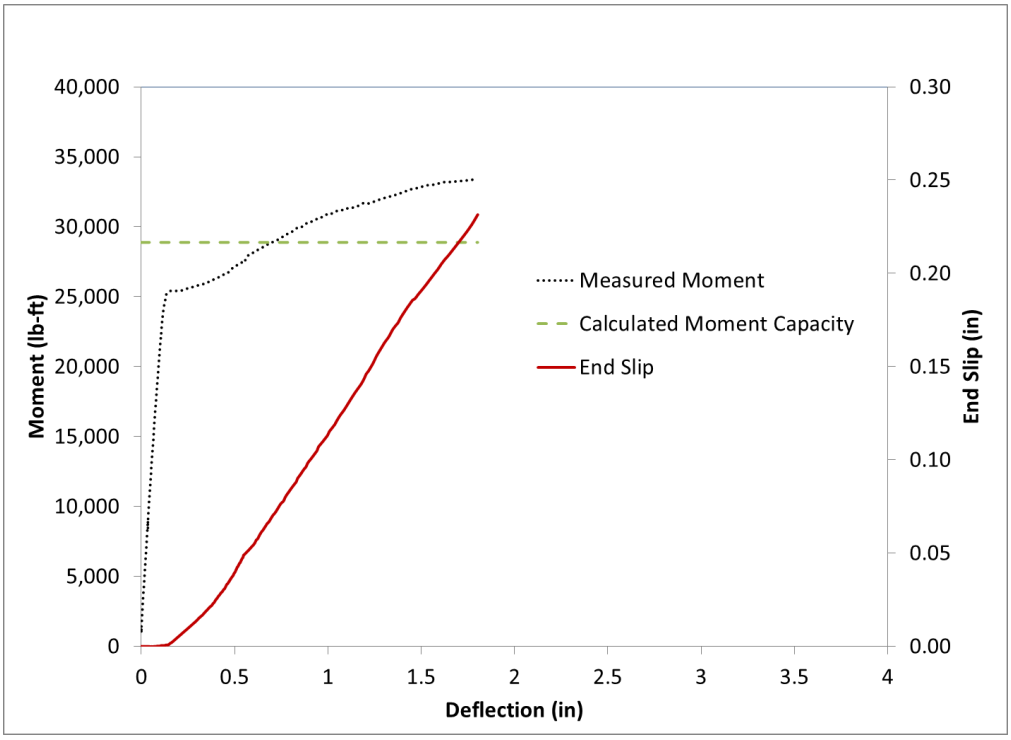

Figure H.141 Beam End I8-L Flexural Test Results Summary Chart A

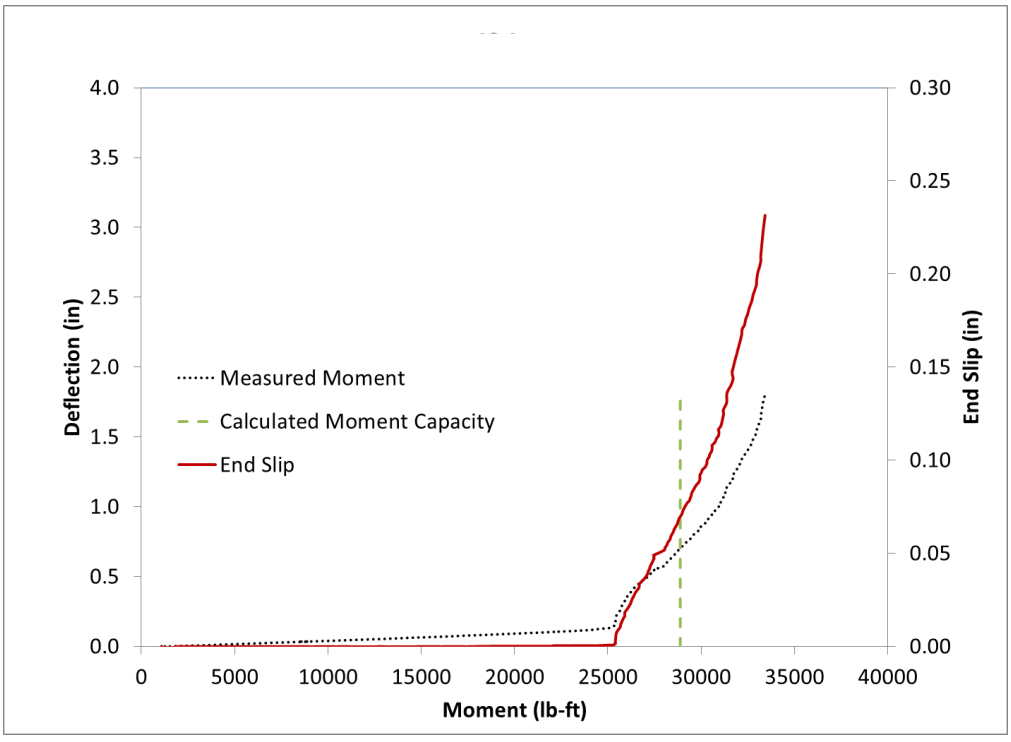

Figure H.142 Beam End I8-L Flexural Test Results Summary Chart B

Figure H.143 Beam End I8-L Failure

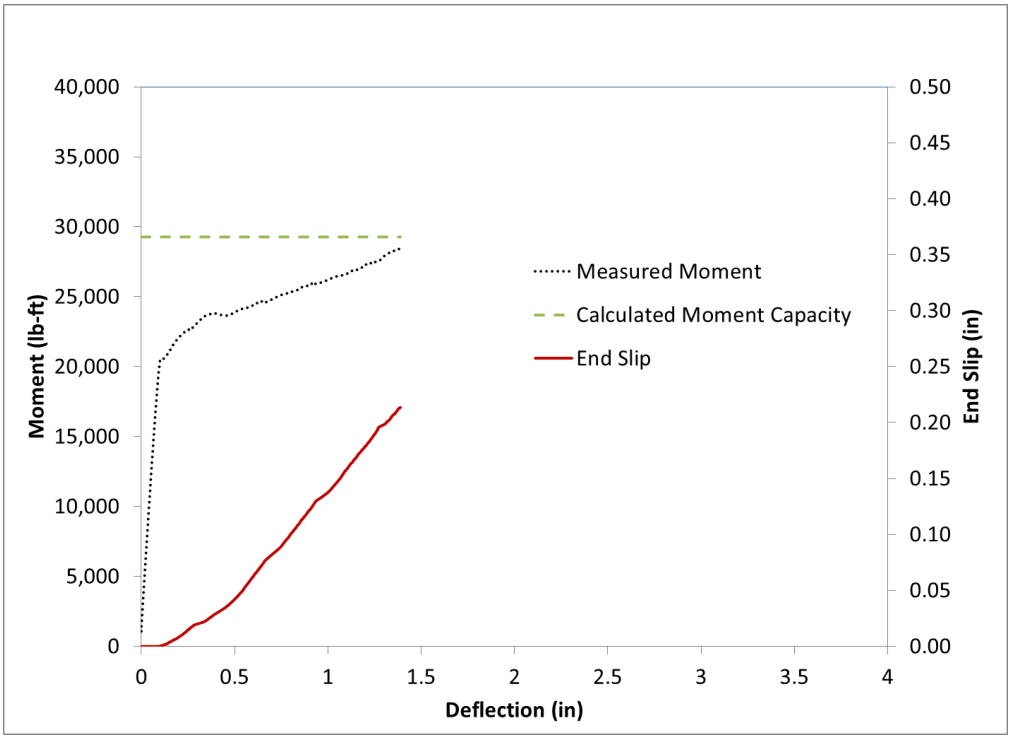

Figure H.144 Beam End I9-L Flexural Test Results Summary Chart A

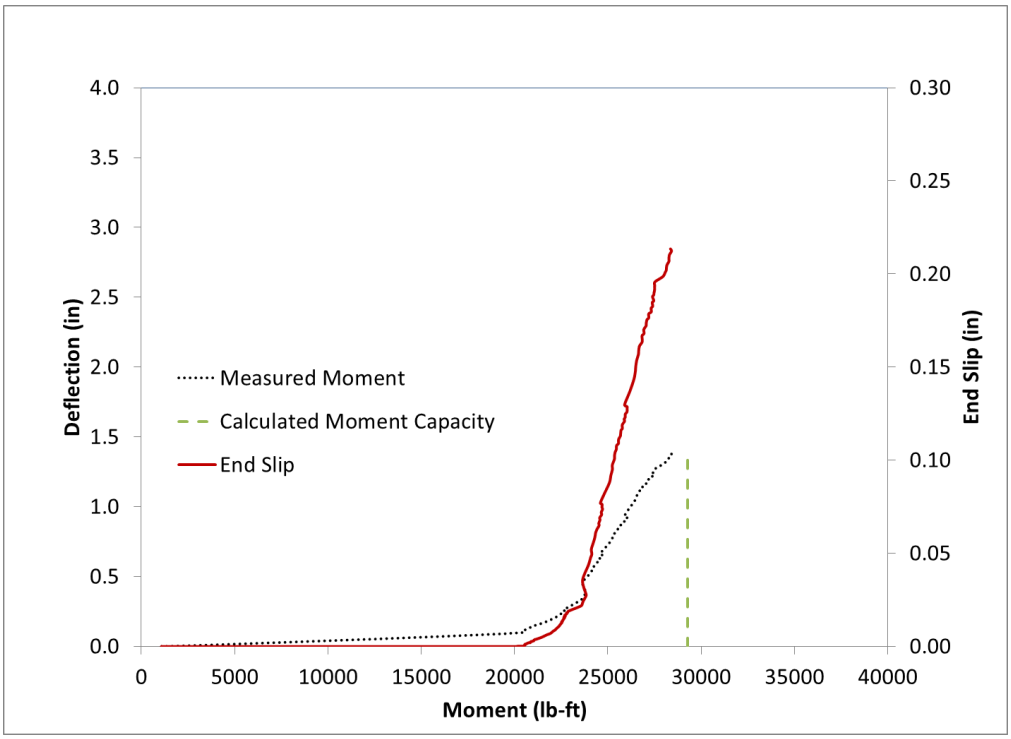

Figure H.145 Beam End I9-L Flexural Test Results Summary Chart B

Figure H.146 Beam End I9-L Failure

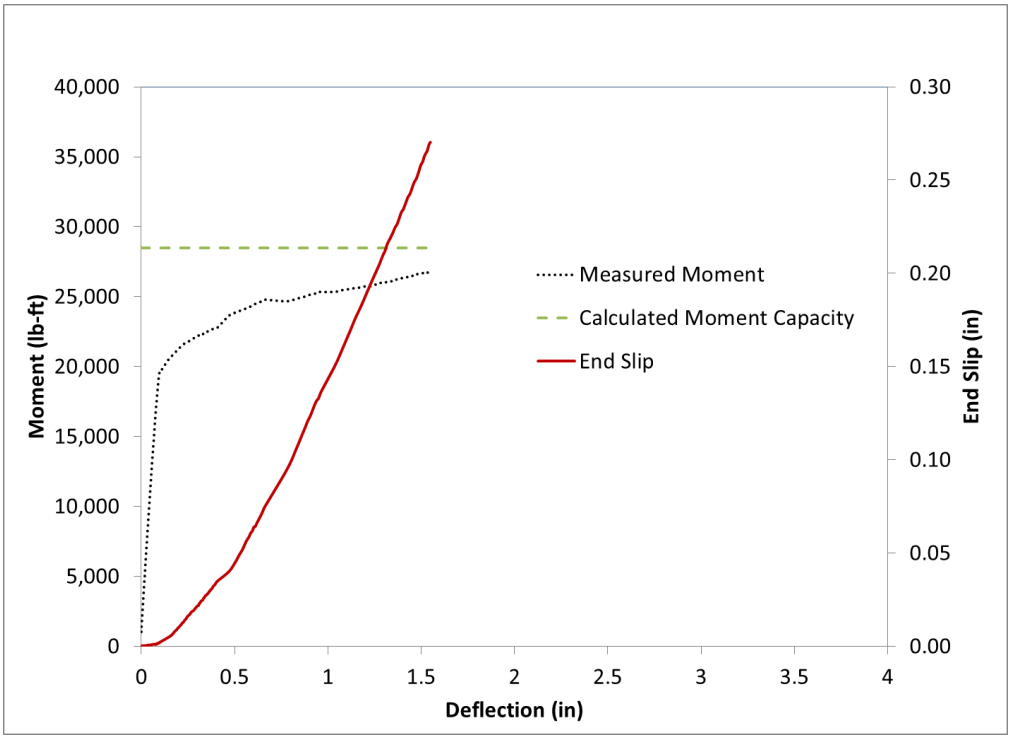

Figure H.147 Beam End I10-L Flexural Test Results Summary Chart A

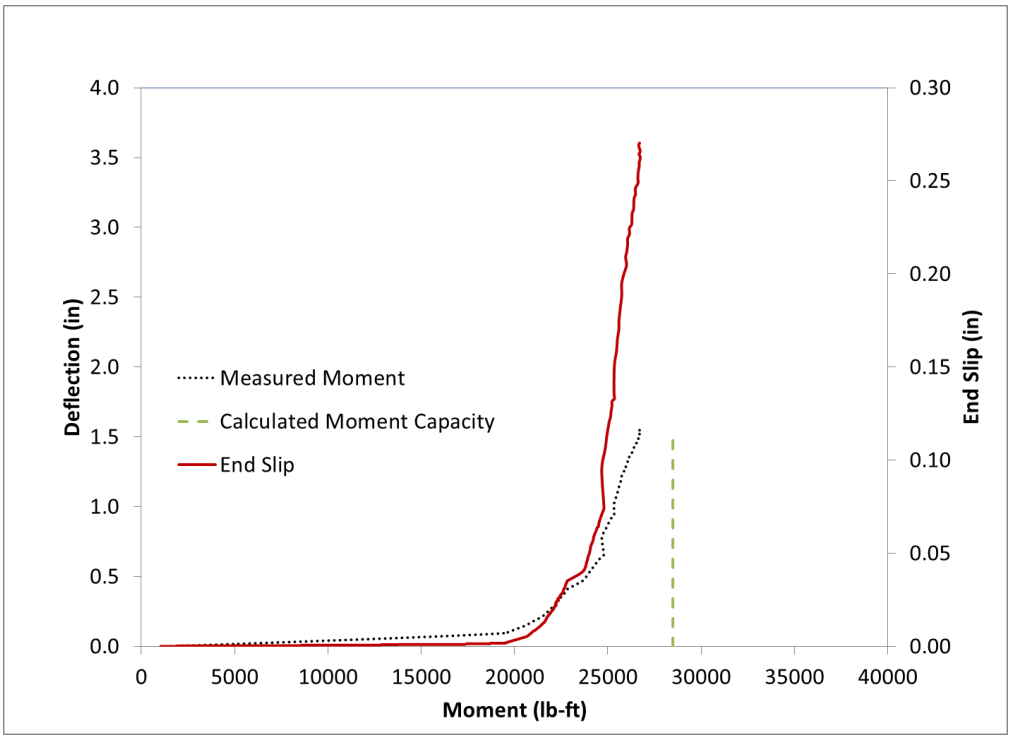

Figure H.148 Beam End I10-L Flexural Test Results Summary Chart B

Figure H.149 Beam End I10-L Failure

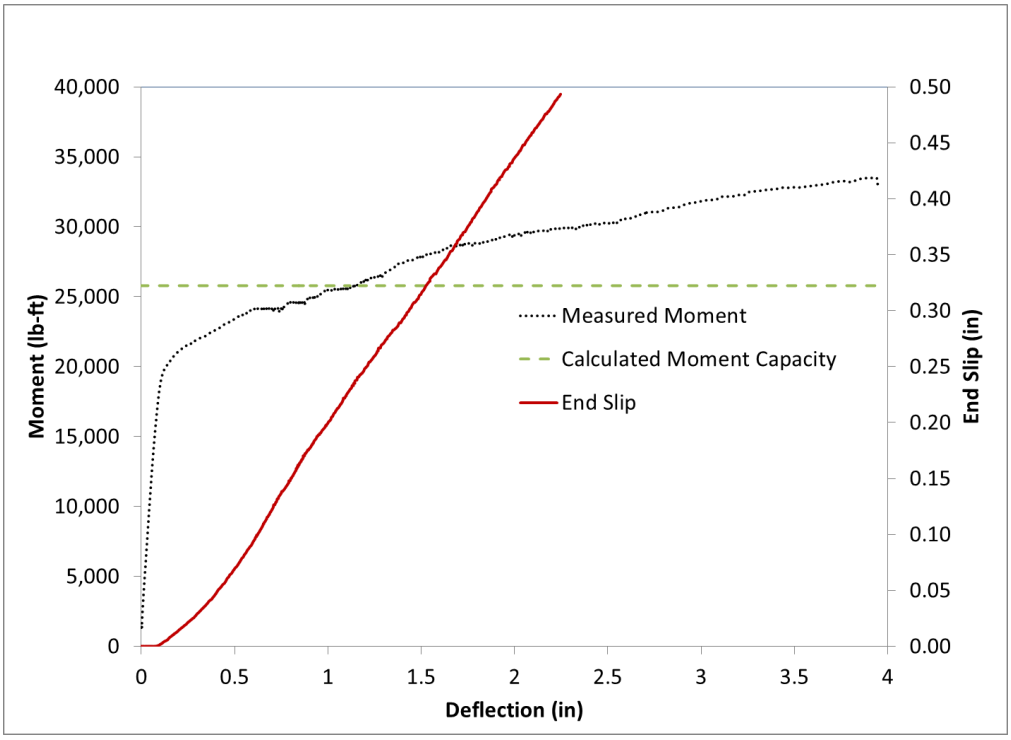

Figure H.150 Beam End I1-S Flexural Test Results Summary Chart A

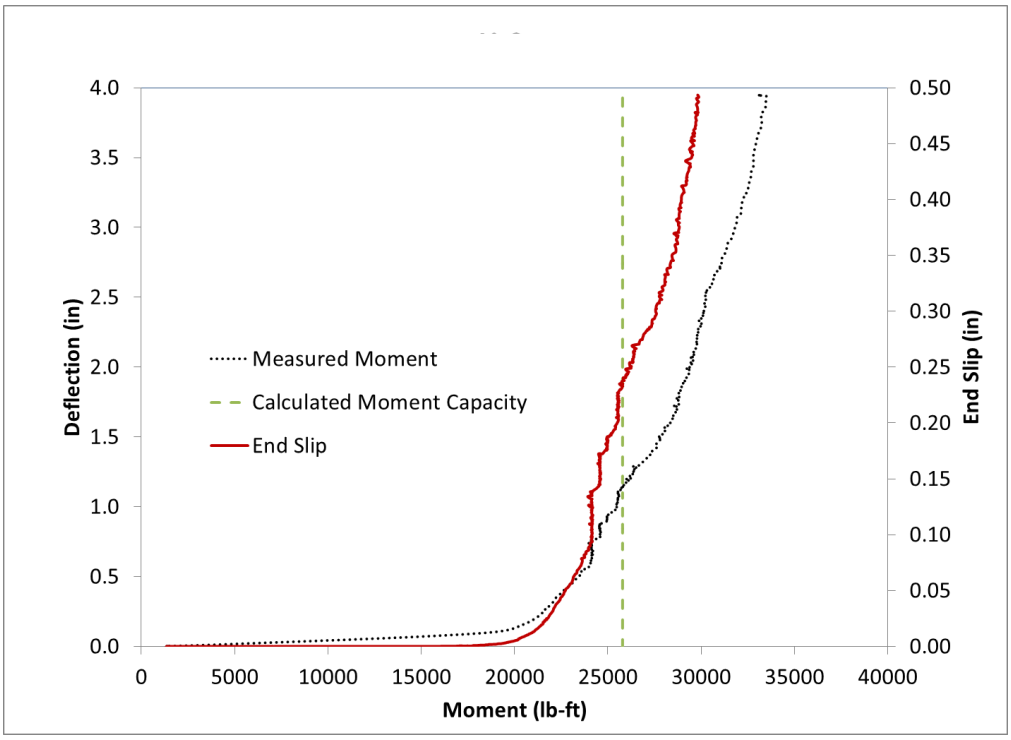

Figure H.151 Beam End I1-S Flexural Test Results Summary Chart B

Figure H.152 Beam End I1-S Failure

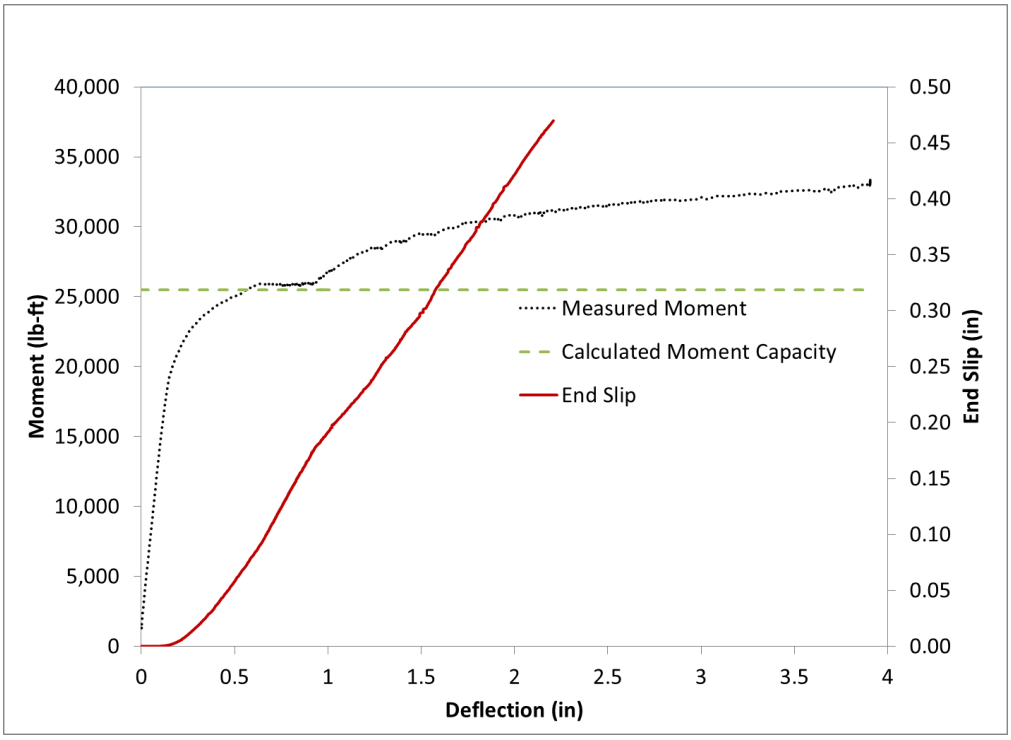

Figure H.153 Beam End I2-S Flexural Test Results Summary Chart A

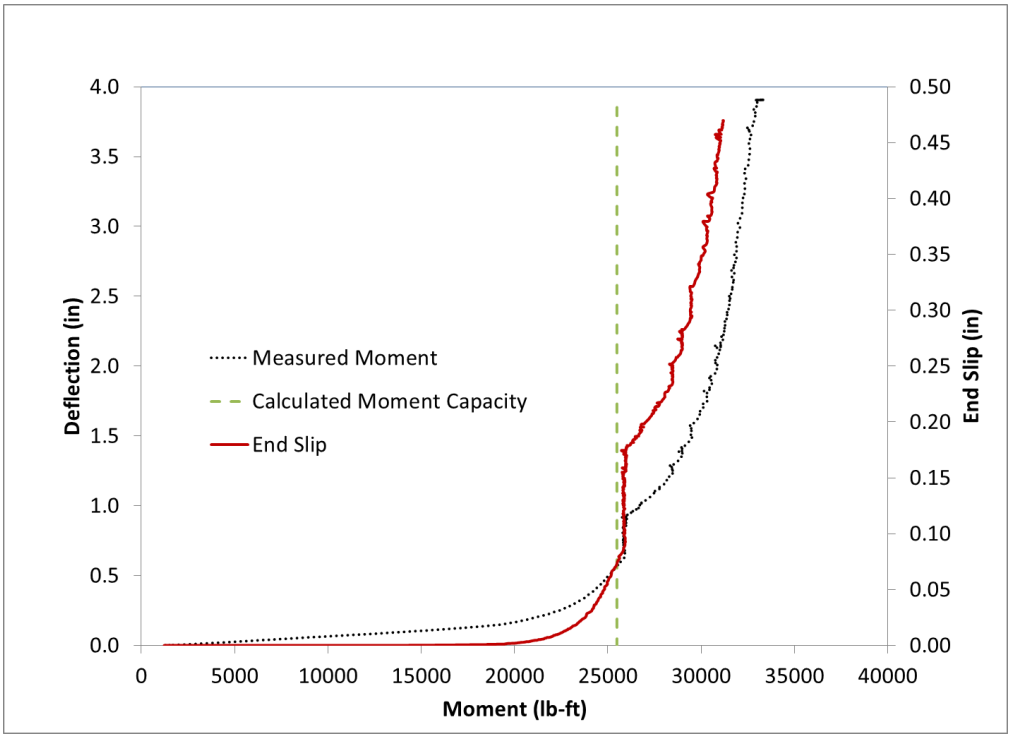

Figure H.154 Beam End I2-S Flexural Test Results Summary Chart B

Figure H.155 Beam End I2-S Failure

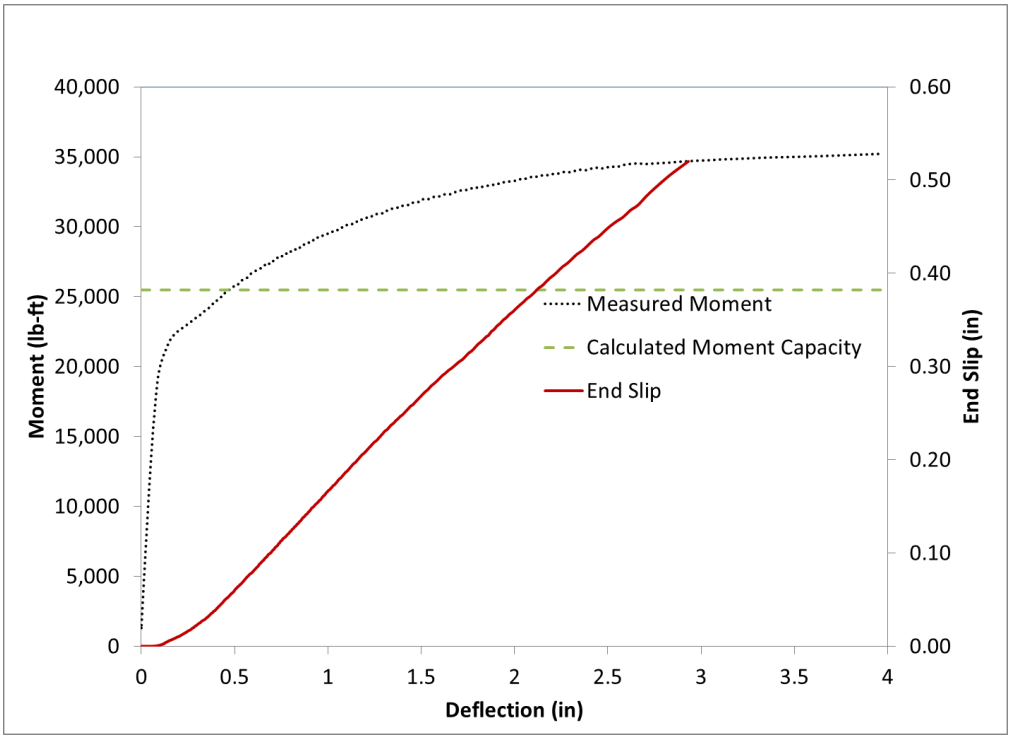

Figure H.156 Beam End I3-S Flexural Test Results Summary Chart A

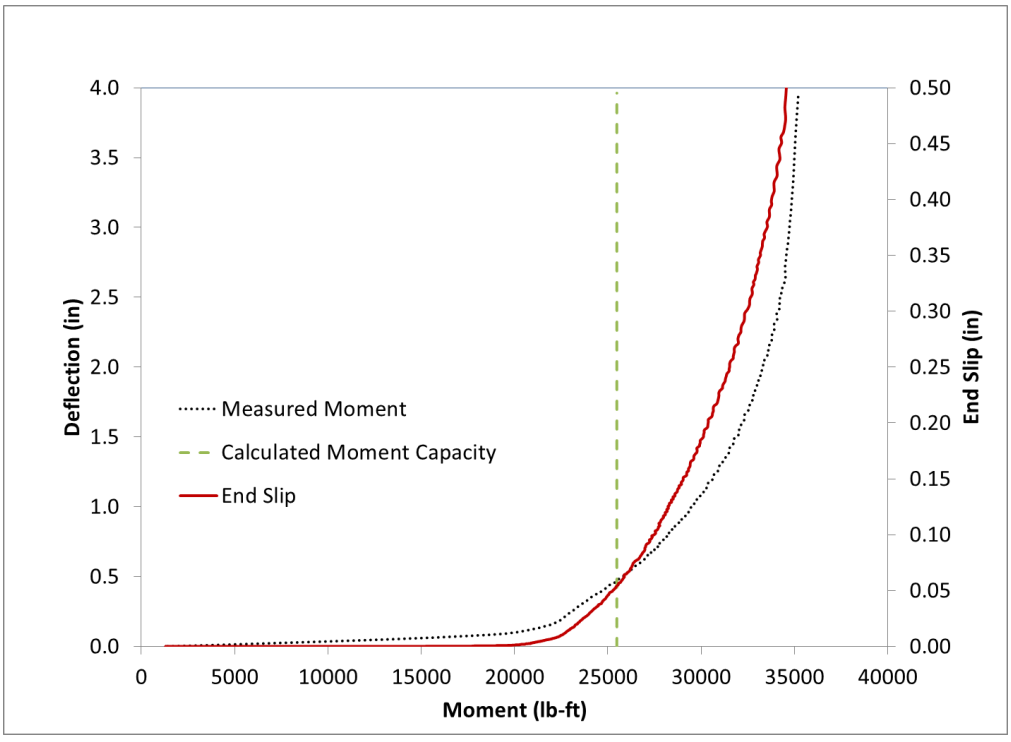

Figure H.157 Beam End I3-S Flexural Test Results Summary Chart B

Figure H.158 Beam End I3-S Failure

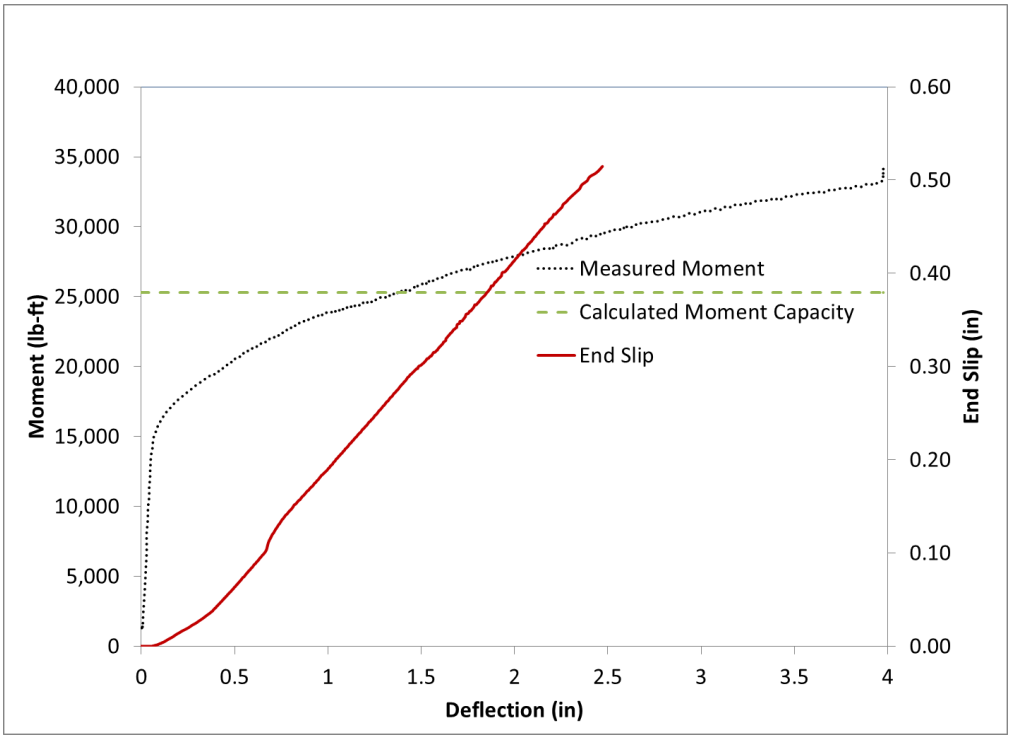

Figure H.159 Beam End I4-S Flexural Test Results Summary Chart A

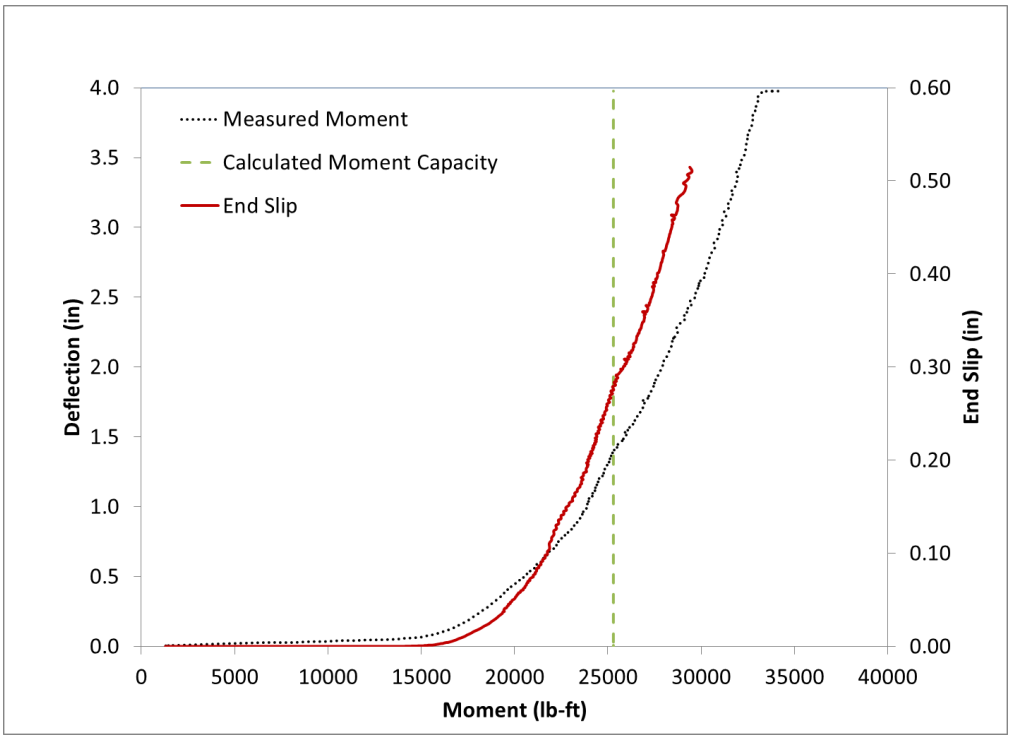

Figure H.160 Beam End I4-S Flexural Test Results Summary Chart B

Figure H.161 Beam End I4-S Failure

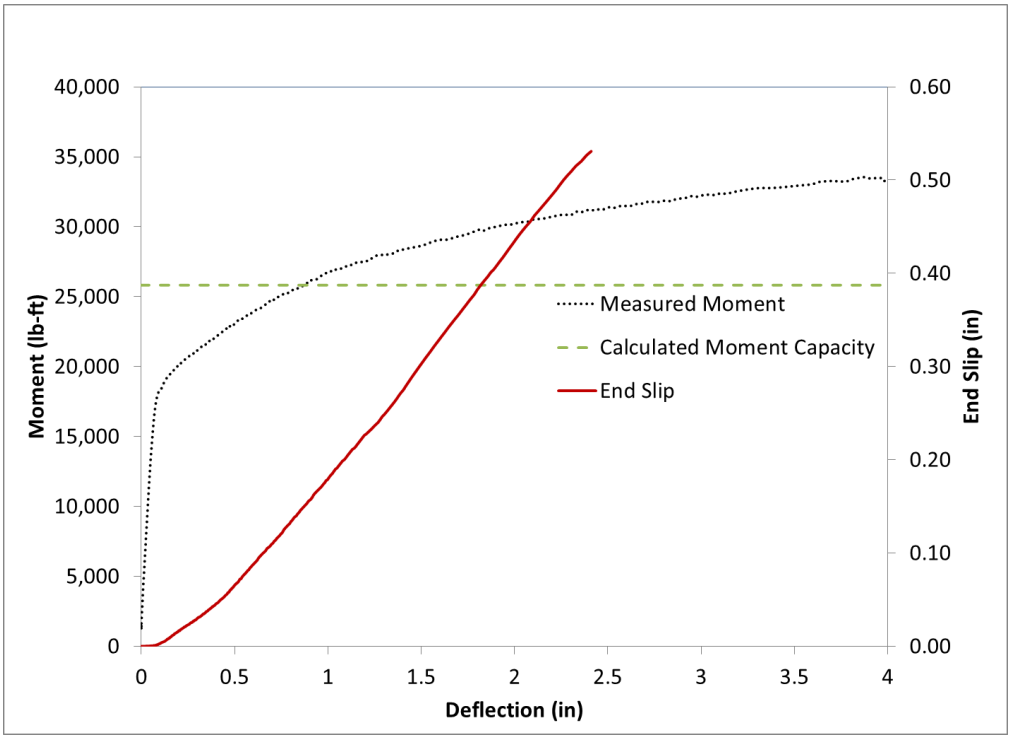

Figure H.162 Beam End I5-S Flexural Test Results Summary Chart A

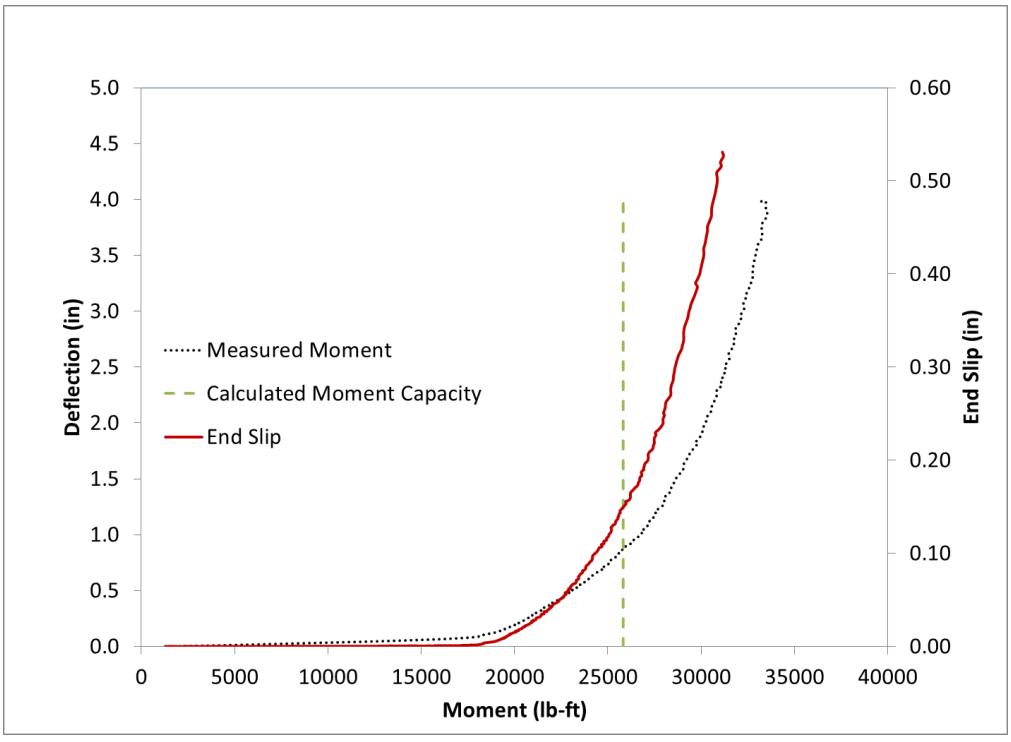

Figure H.163 Beam End I5-S Flexural Test Results Summary Chart B

Figure H.164 Beam End I5-S Failure

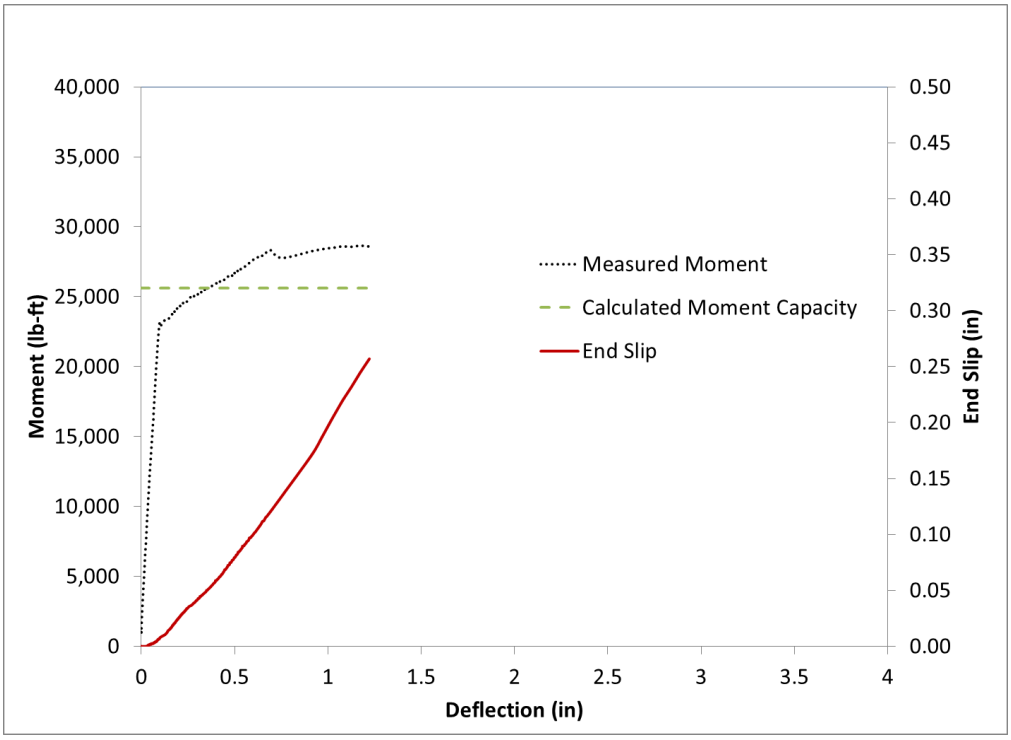

Figure H.165 Beam End I6-S Flexural Test Results Summary Chart A

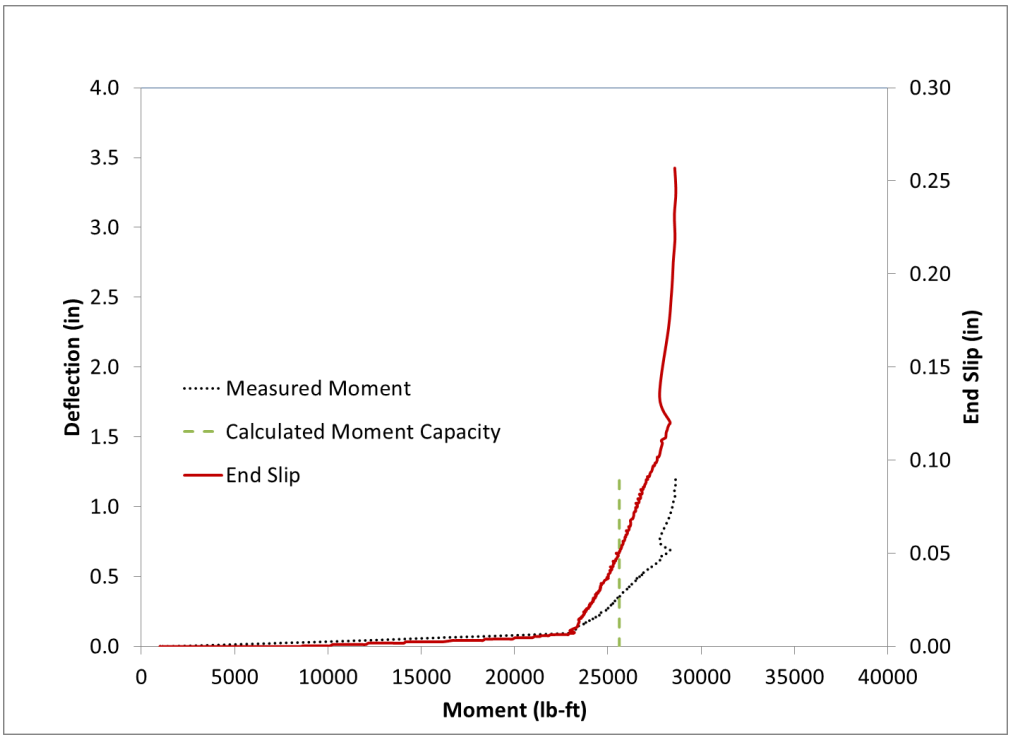

Figure H.166 Beam End I5-S Flexural Test Results Summary Chart B

Figure H.167 Beam End I5-S Failure

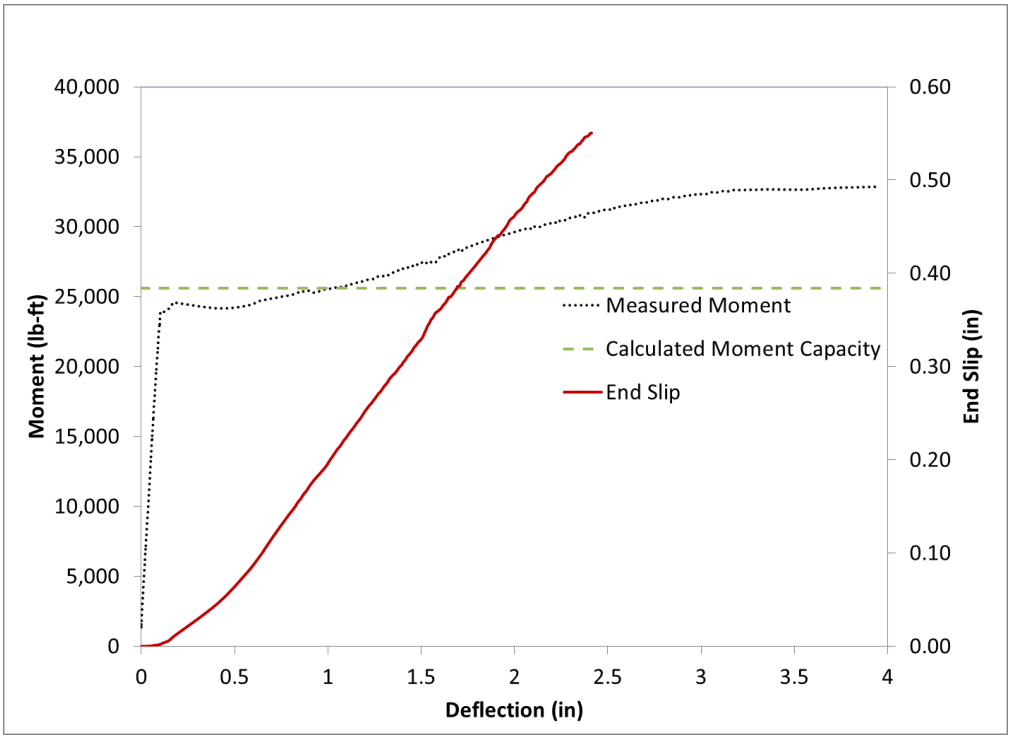

Figure H.168 Beam End I7-S Flexural Test Results Summary Chart A

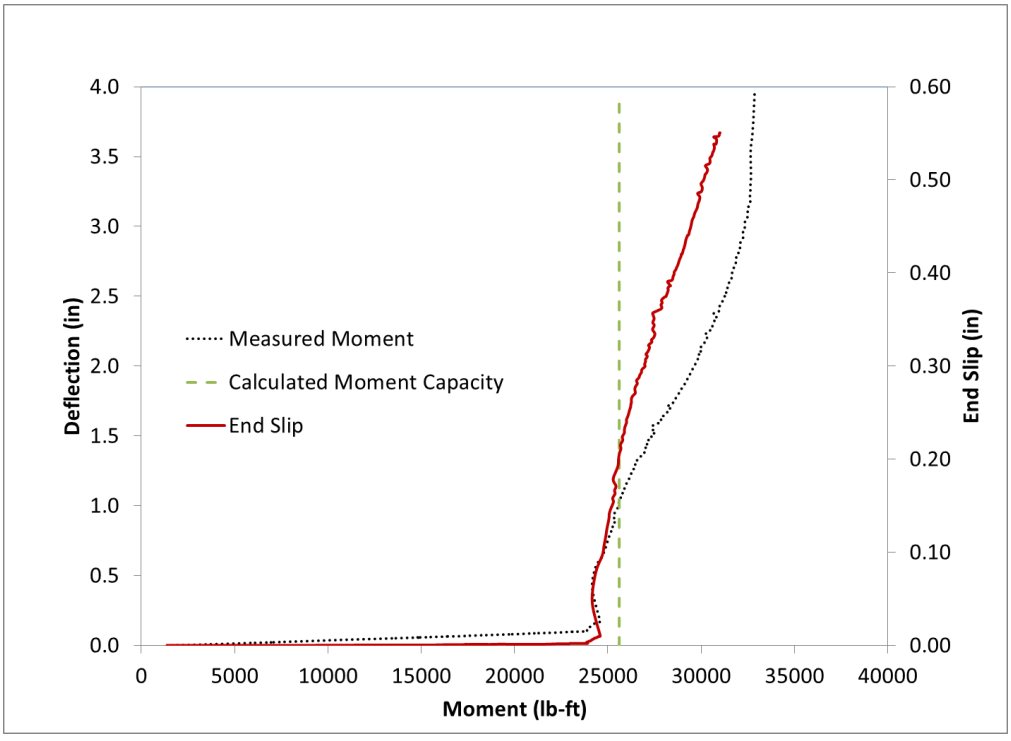

Figure H.169 Beam End I7-S Flexural Test Results Summary Chart B

Figure H.170 Beam End I7-S Failure

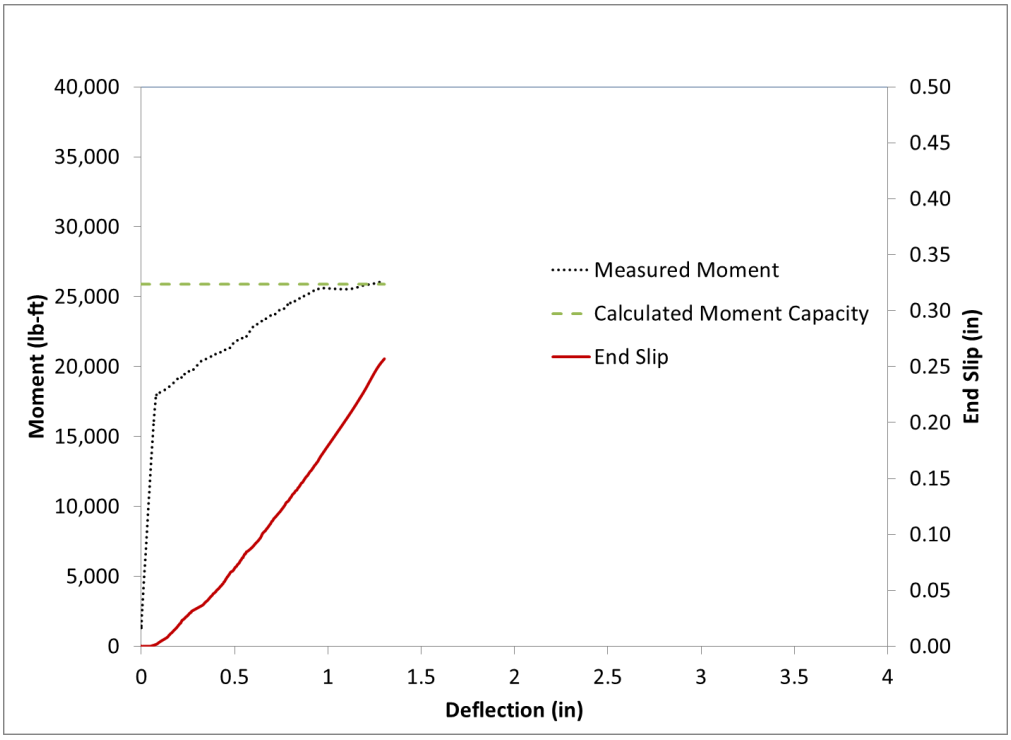

Figure H.171 Beam End I8-S Flexural Test Results Summary Chart A

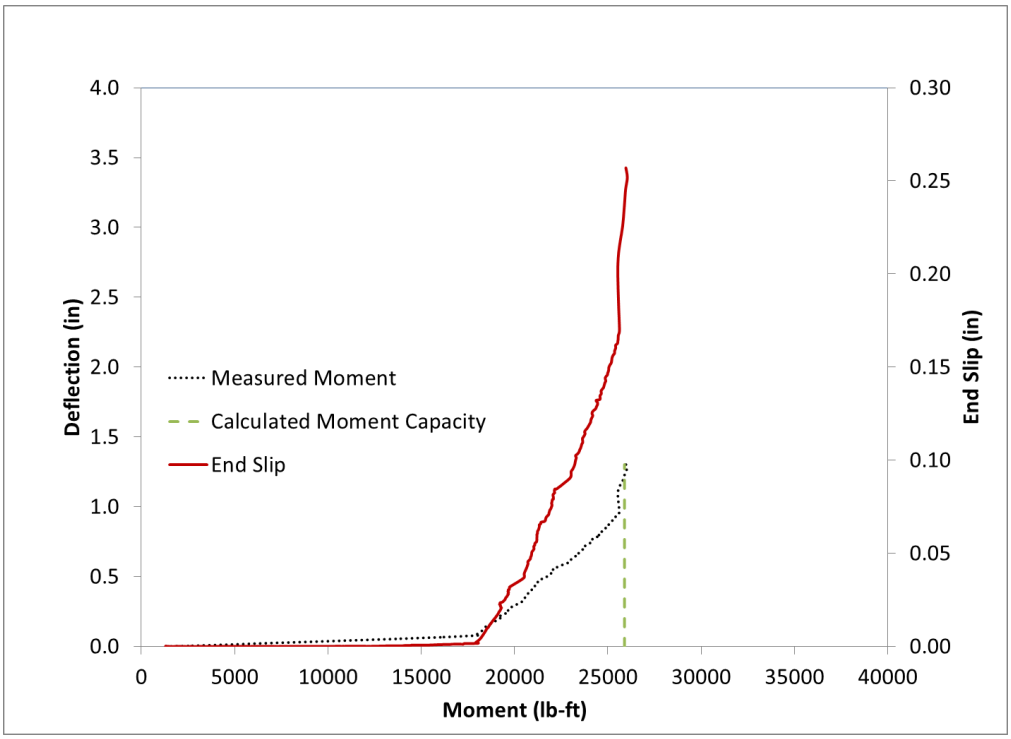

Figure H.172 Beam End I8-S Flexural Test Results Summary Chart B

Figure H.173 Beam End I8-S Failure

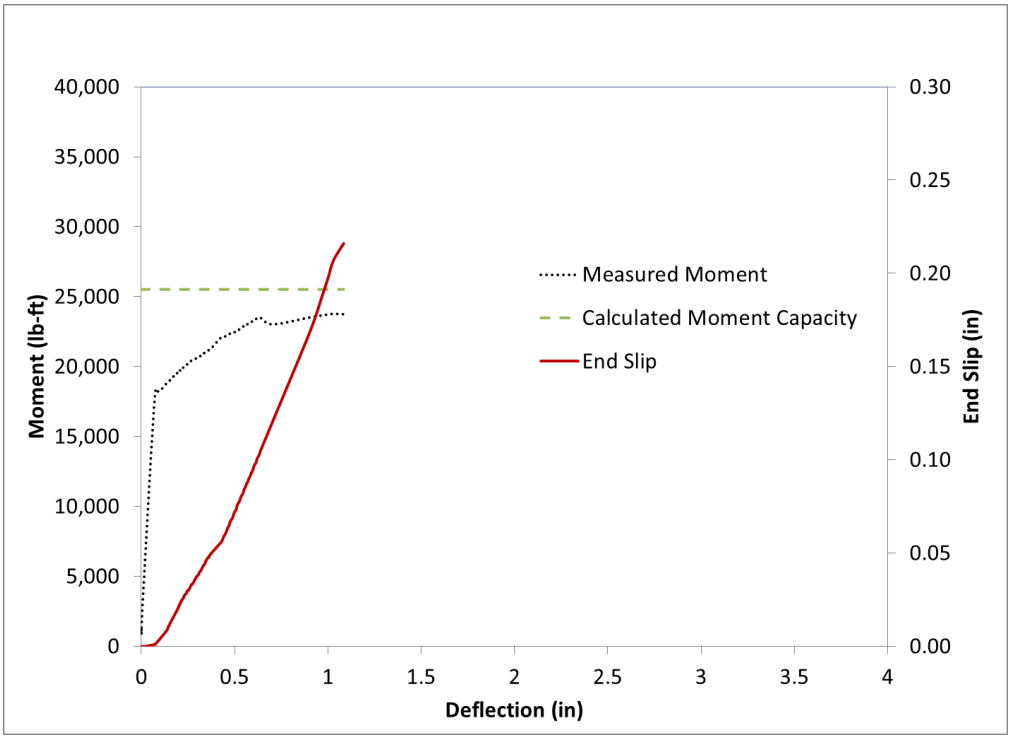

Figure H.174 Beam End I9-S Flexural Test Results Summary Chart A

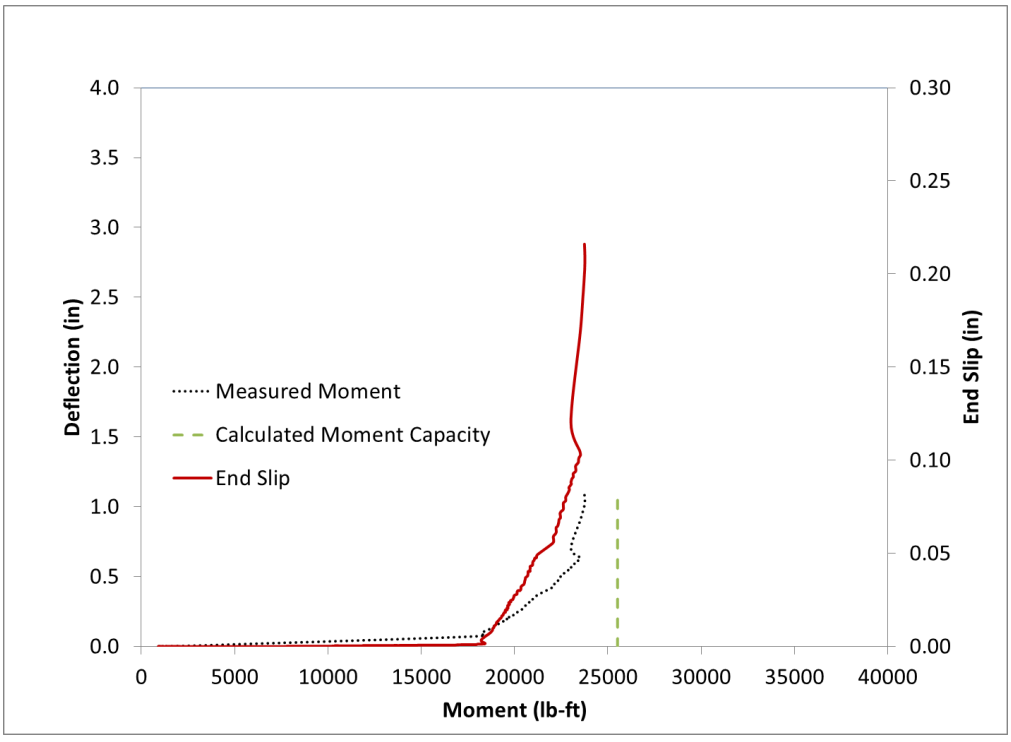

Figure H.175 Beam End I9-S Flexural Test Results Summary Chart B

Figure H.176 Beam End I9-S Failure

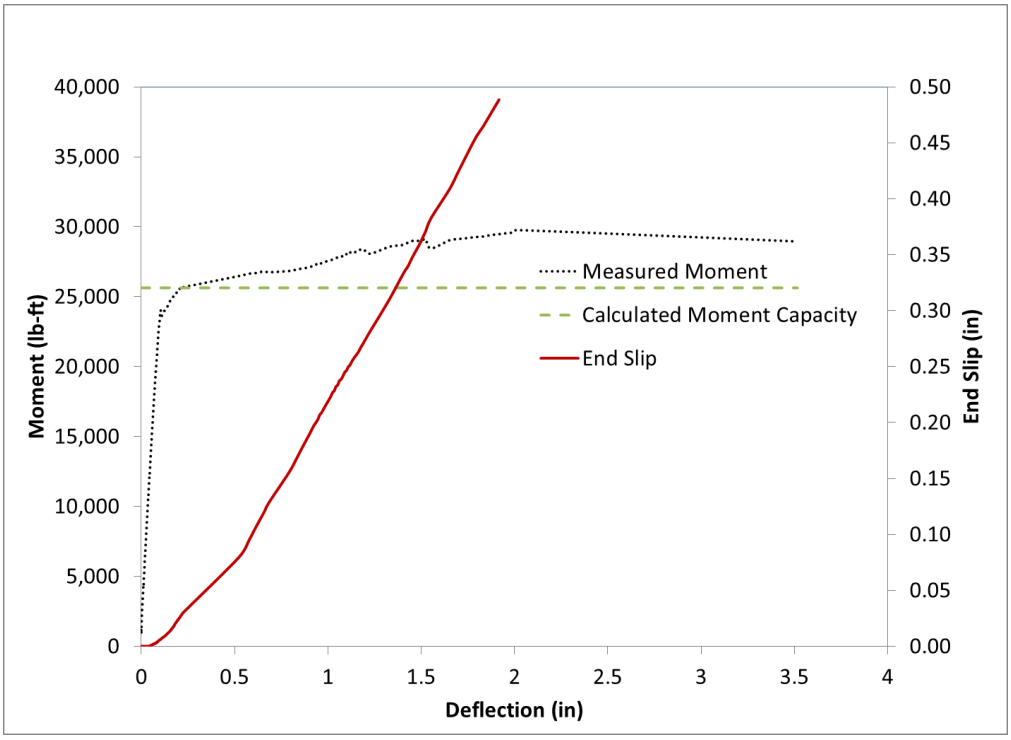

Figure H.177 Beam End I10-S Flexural Test Results Summary Chart A

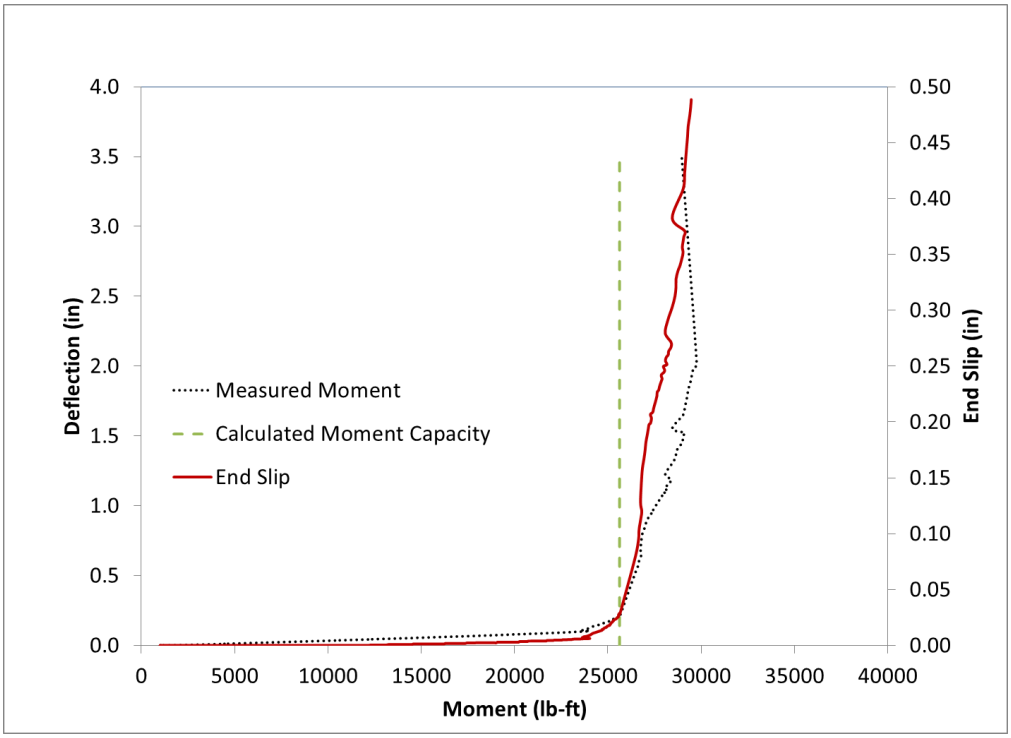

Figure H.178 Beam End I10-S Flexural Test Results Summary Chart B

Figure H.179 Beam End I10-S Failure

Appendix I - **Simple Quality Assurance Test for Strand Bond Summary Charts**

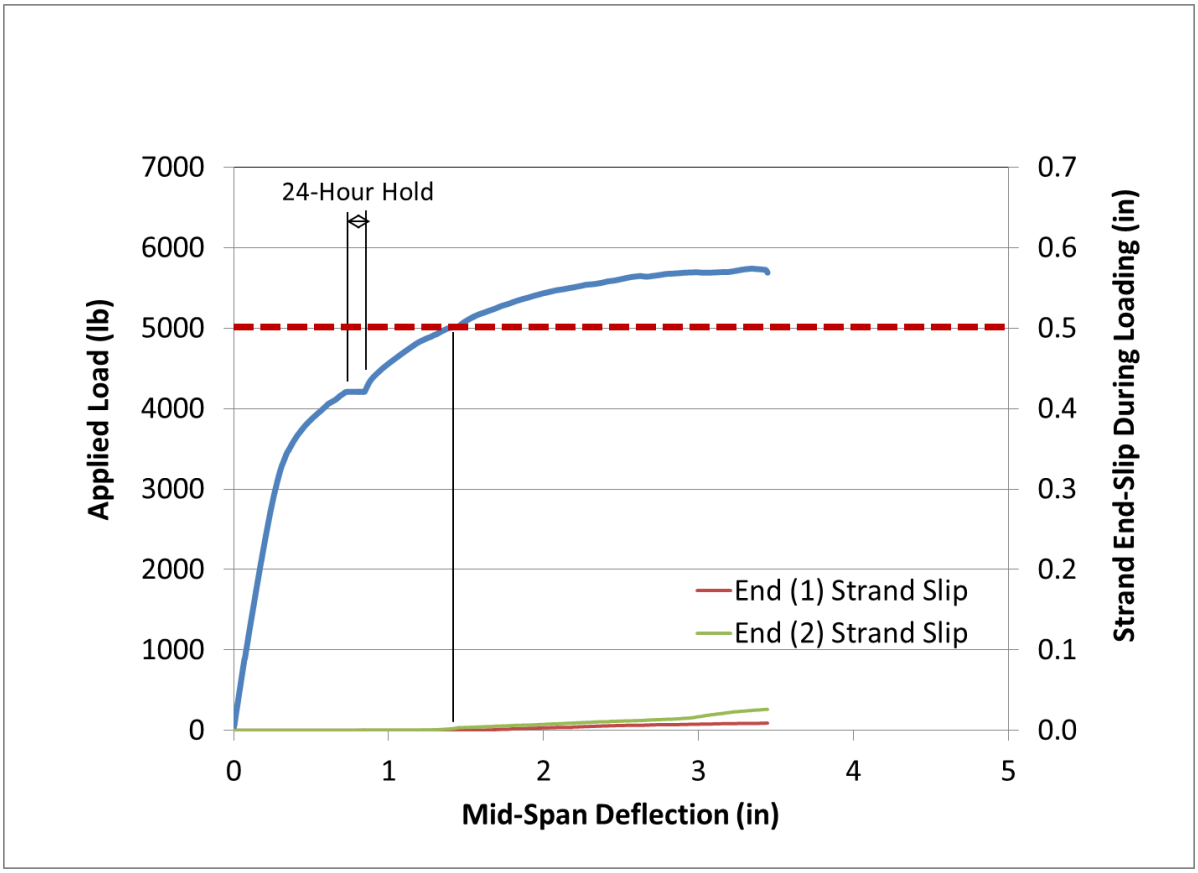

Figure I.1 Simple Quality Assurance Test for Strand Bond Specimen A1 Summary Chart

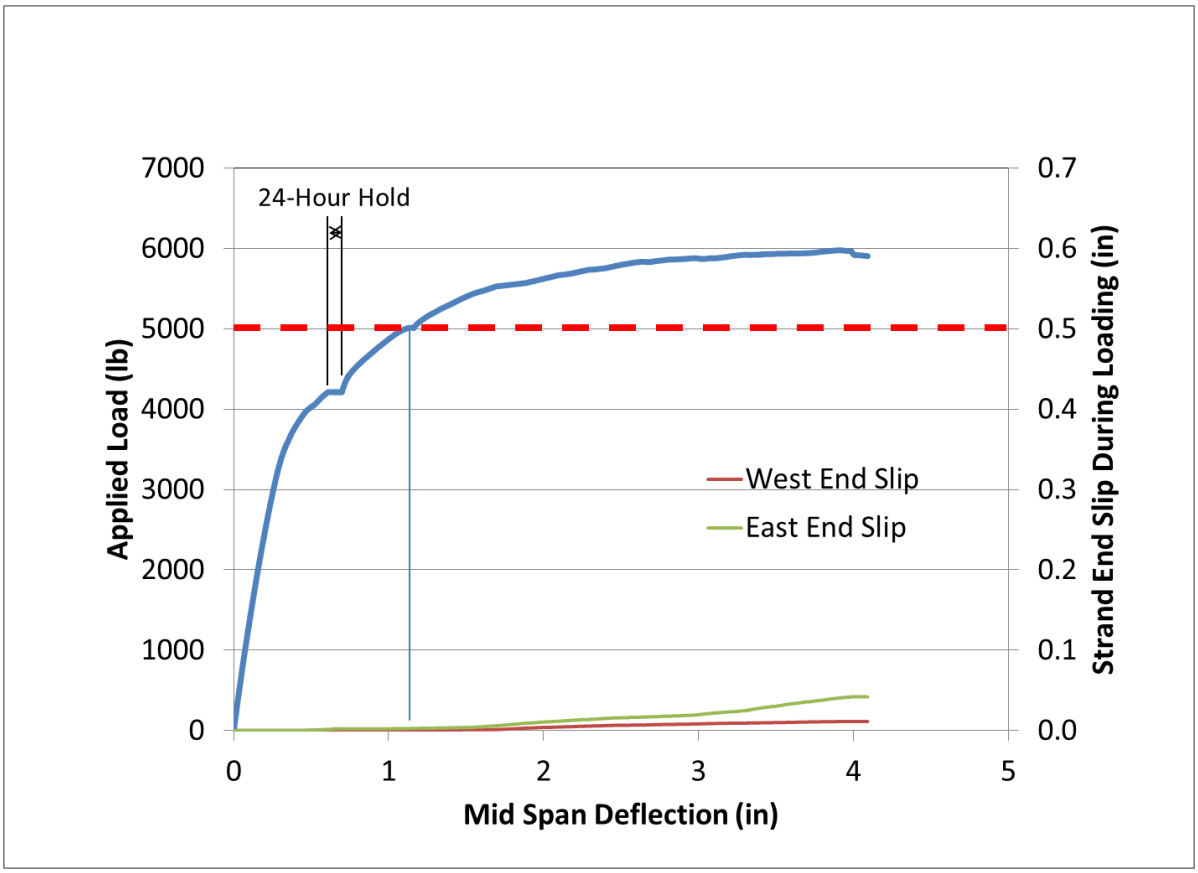

Figure I.2 Simple Quality Assurance Test for Strand Bond Specimen A2 Summary Chart

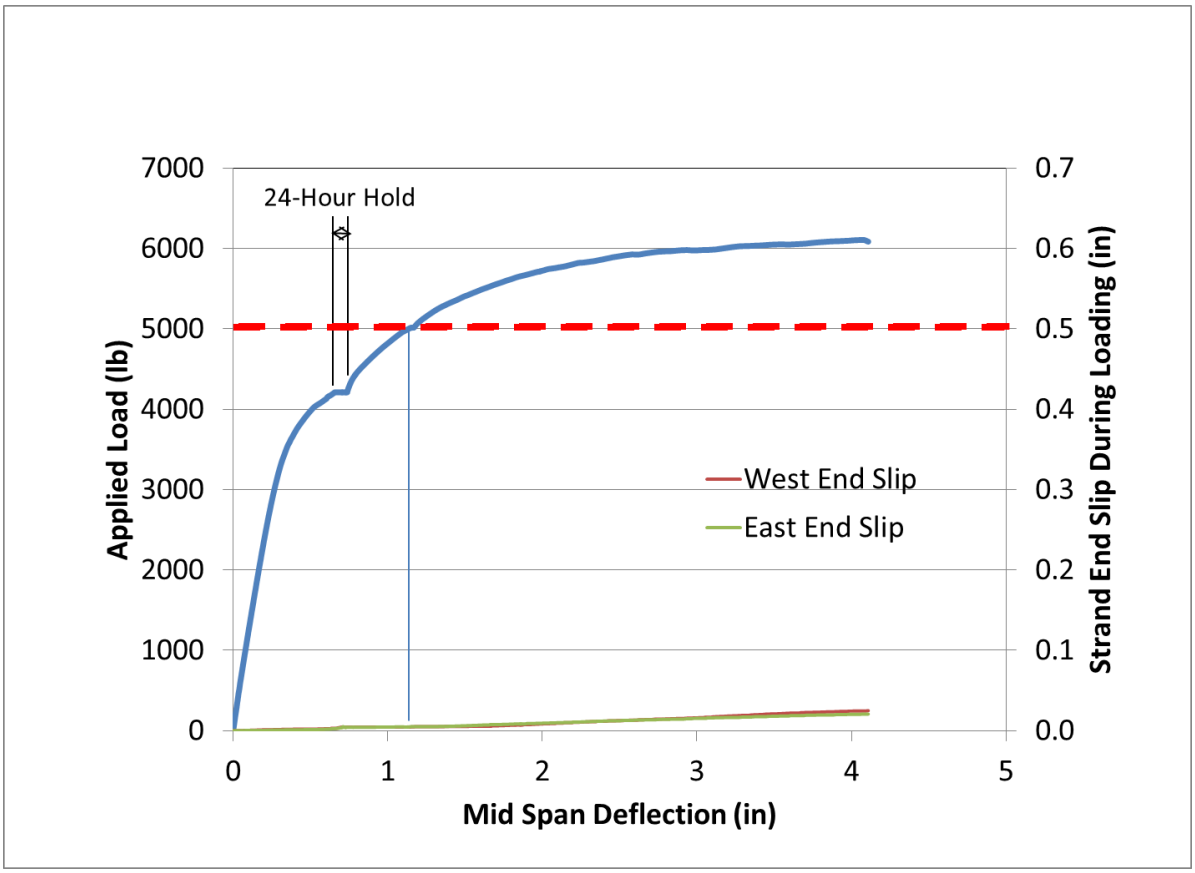

Figure I.3 Simple Quality Assurance Test for Strand Bond Specimen A3 Summary Chart

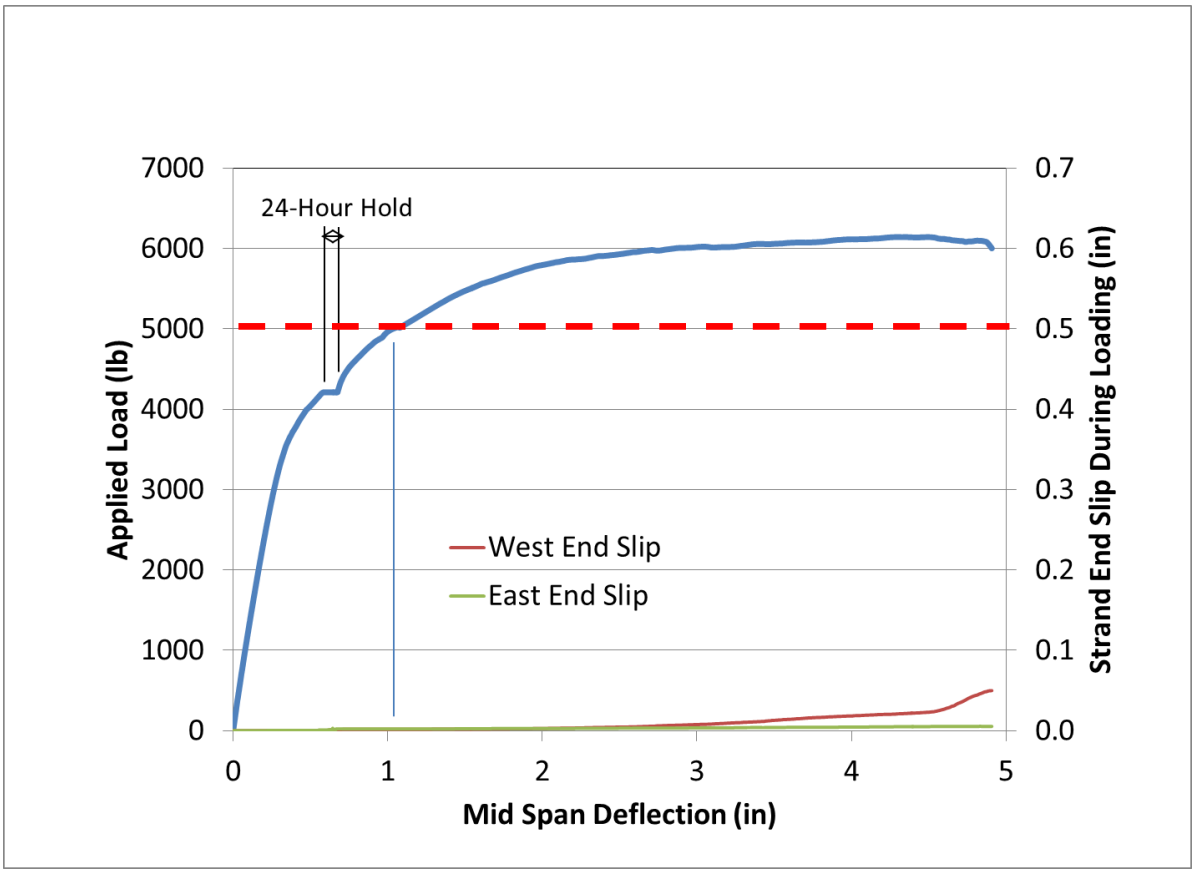

Figure I.4 Simple Quality Assurance Test for Strand Bond Specimen G1 Summary Chart

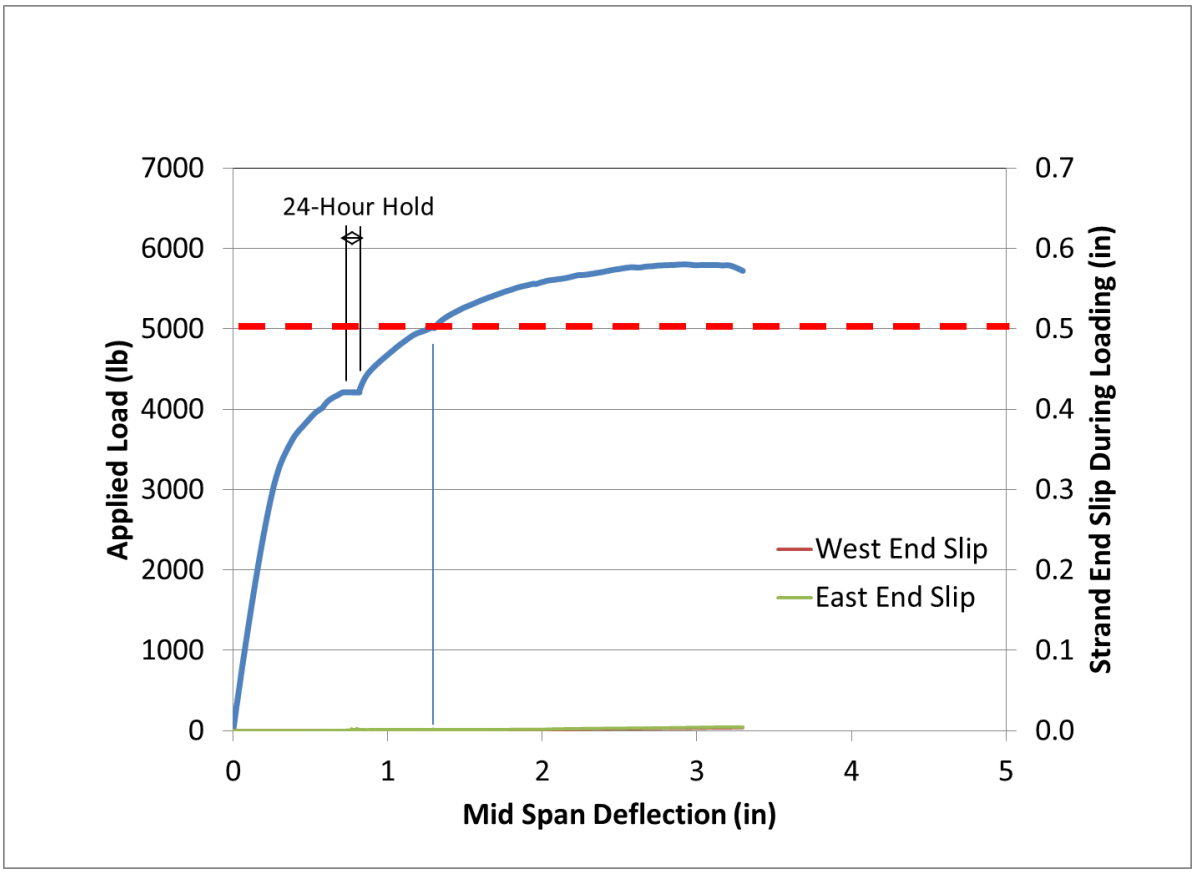

Figure I.5 Simple Quality Assurance Test for Strand Bond Specimen G2 Summary Chart

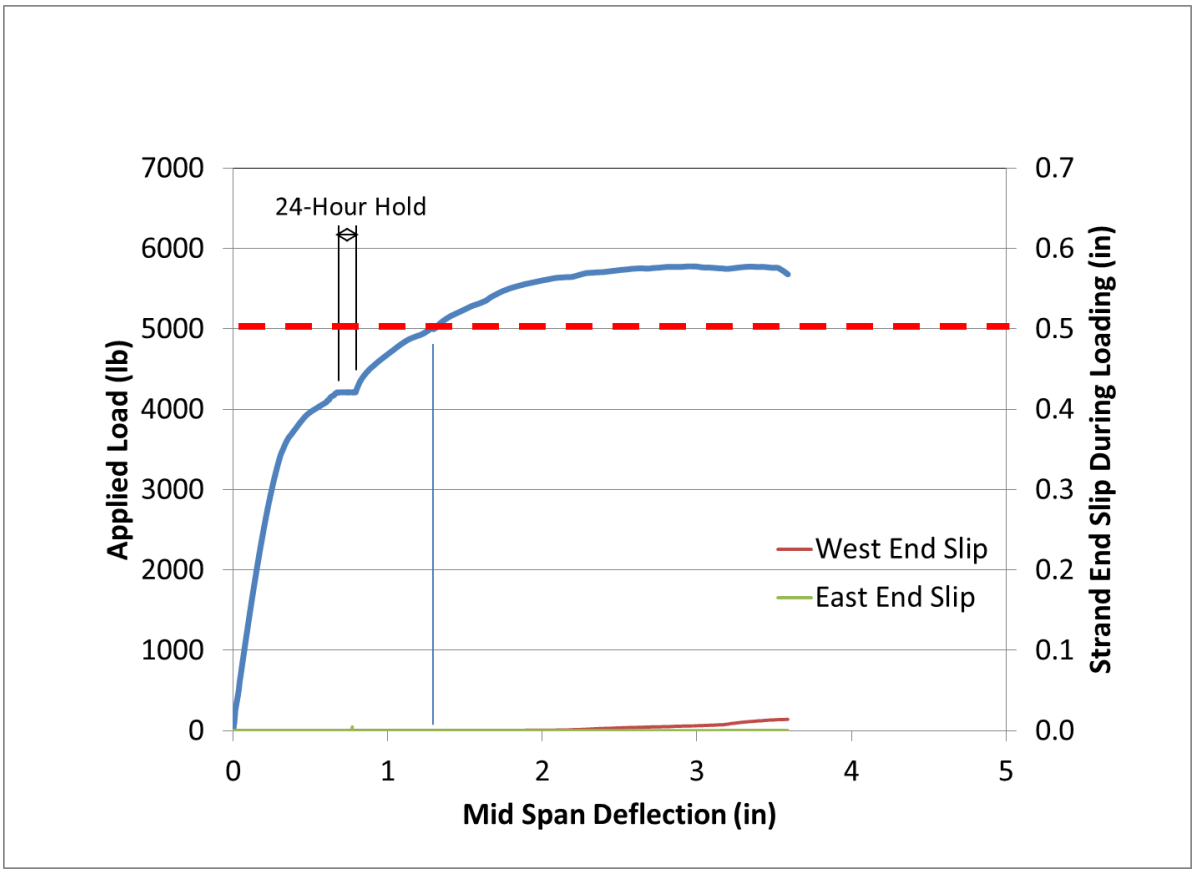

Figure I.6 Simple Quality Assurance Test for Strand Bond Specimen G3 Summary Chart

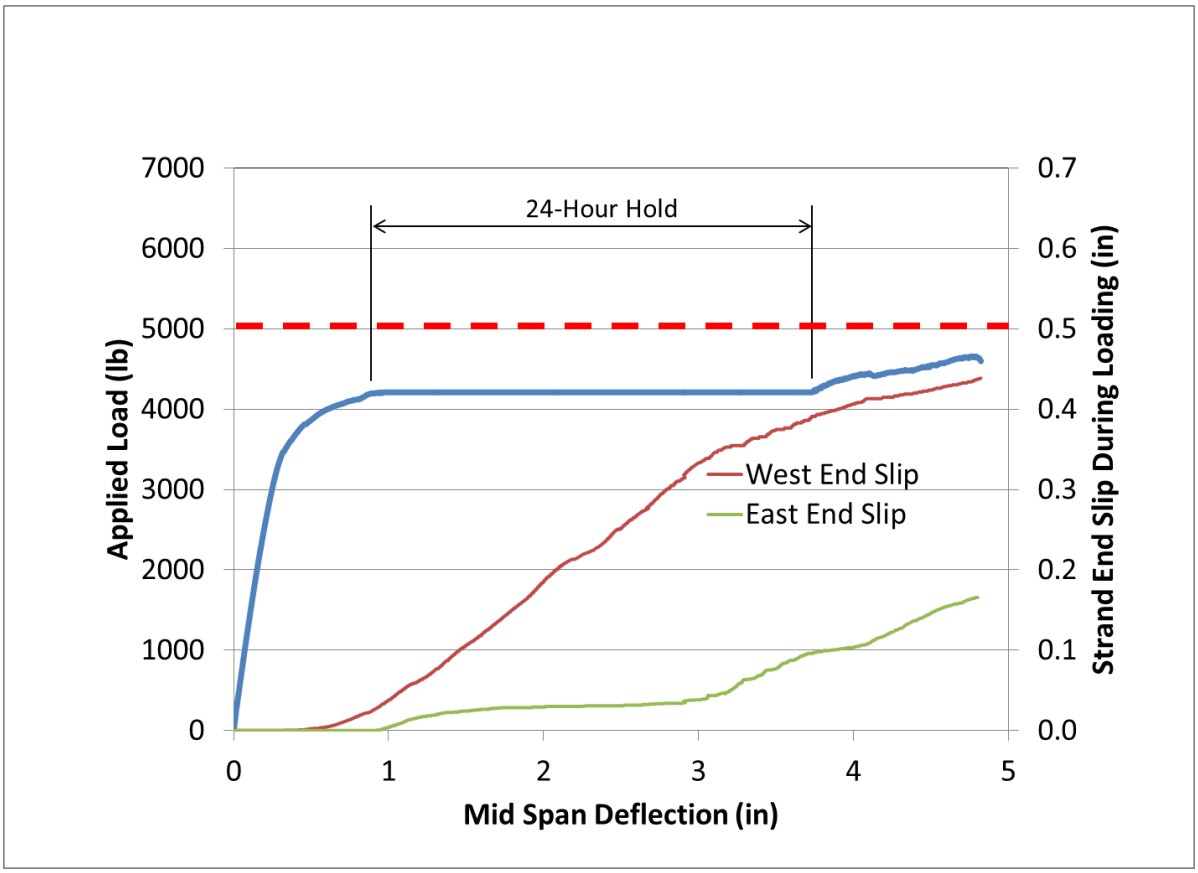

Figure I.7 Simple Quality Assurance Test for Strand Bond Specimen I1 Summary Chart

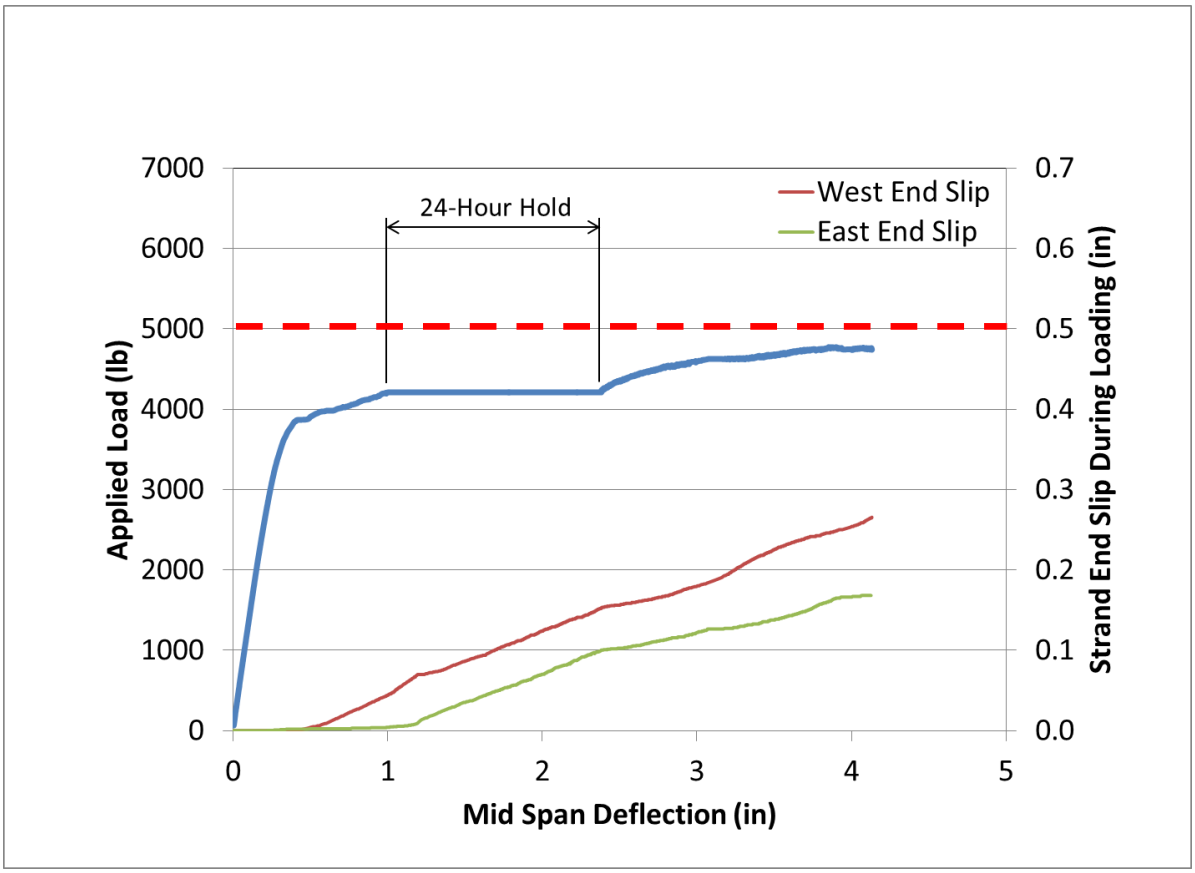

Figure I.8 Simple Quality Assurance Test for Strand Bond Specimen I2 Summary Chart

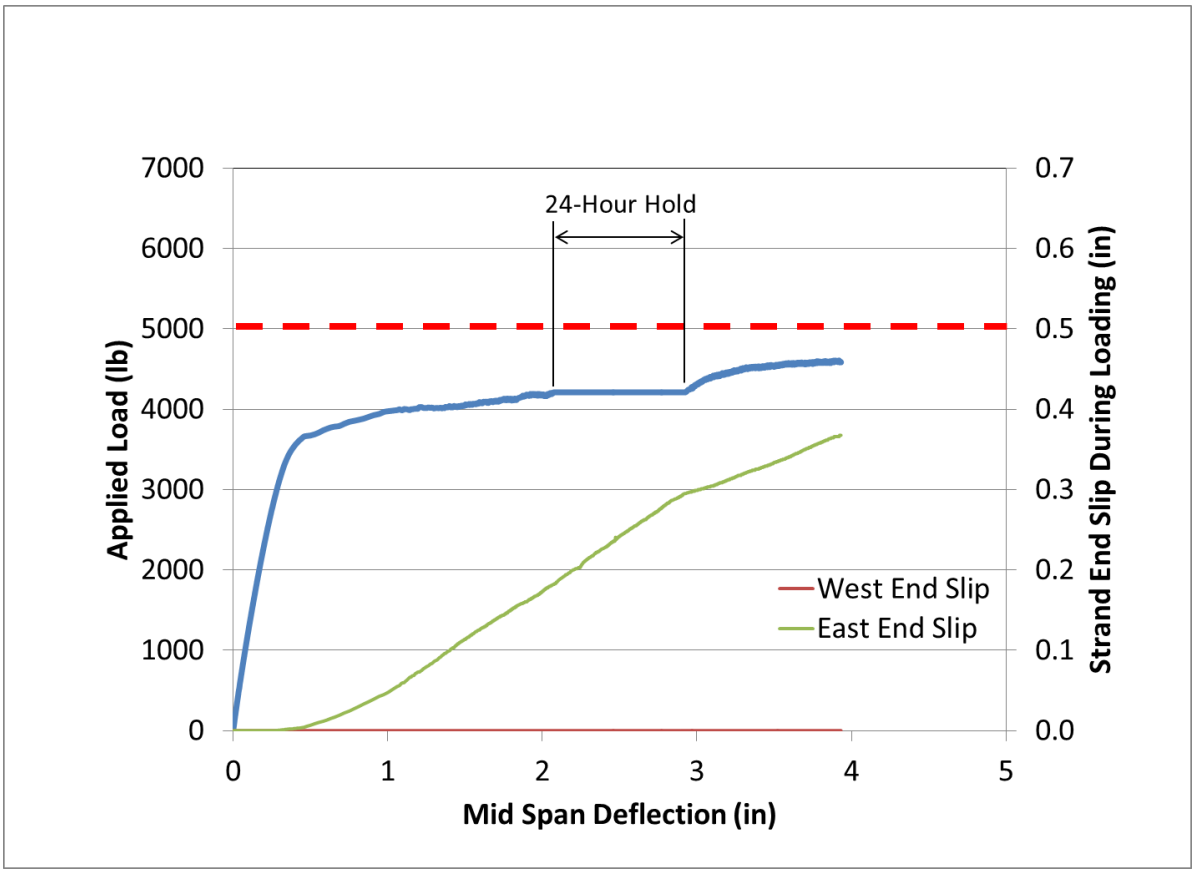

Figure I.9 Simple Quality Assurance Test for Strand Bond Specimen I3 Summary Chart